THE

LONDON, EDINBURGH, AND DUBLIN

PHILOSOPHICAL MAGAZINE

AND

JOURNAL OF SCIENCE.

[SEVENTH SERIES.]

JULY 1937.

I. *The Eddy-Current Heating of Composite Cylindrical Systems.* By D. A. Wright, *M.Sc.*, *F.R.A.S.* (Communication from the Research Staff of the M.O. Valve Co., Ltd., at the G.E.C. Research Laboratories, Wembley, England *.)

Introduction.

1. IN the manufacture of thermionic valves having glass envelopes it is a common practice to utilize eddy-current heating for degassing the valve electrodes and for volatilization of the getter. It is of interest to consider whether this method of heating could be adapted to the production of valves having metal envelopes. The problem may be resolved into a consideration of the eddy-current heating of a composite system consisting of a long hollow cylindrical tube representing the valve envelope, and inside it a coaxial cylinder, hollow or solid, representing a valve electrode. The variables in such a system would be the radius, wall-thickness, and composition of each cylinder. It is the purpose of the present paper to consider theoretically the eddy-current heating of such composite systems, to apply the theory to one or two systems of practical interest, and to describe briefly experiments which confirm the conclusions in the case

* Communicated by C. C. Paterson, M.I.E.E.

of one of these systems. It is necessary to derive expressions for the penetration of field through the outer cylinder, and for the heat developed in the inner cylinder when unit magnetic field-strength is applied to its surface. Combining these results gives the heat developed in the inner cylinder when unit magnetic field-strength is applied to the outer one, while the heat developed in the outer cylinder in these circumstances can also be calculated. Then by studying the variation of the heat developed with frequency, and the ratio of the heat in the inner to that in the outer cylinder, it becomes possible to deduce the practicability of eddy-current heating the inner cylinder, the optimum frequency range, and the magnitude of magnetic field necessary for the purpose.

2. The general theory of eddy-current heating of solid cylinders has been given by a number of writers, selected references being given [(1), (2), (3)]. The case of a single hollow cylindrical tube has also been treated [(3), (4), (5), (6)]. When we have a composite system, as in the present case, the essential modification to the theory is in the consideration of the inner boundary condition for the envelope, since this condition is modified by the presence of an inner charge.

3. We assume, as usual in these problems, an eddy-current heating coil, the "inductor," in the form of a long single-layer close-wound solenoid carrying a sinusoidal alternating current with amplitude I_0 E.M.U. and frequency f. Then the "charge" consists of the coaxial cylinders, which are also coaxial with the inductor.

Let number of turns per cm. of inductor	$= n$
outer radius of envelope	$= a$ cm.
inner ,, ,, ,,	$= b$ cm.
permeability * of envelope	$= \mu$
resistivity of ,,	$= \rho$ E.M.U.
outer radius of inner cylinder	$= a_1$ cm.
inner ,, ,, ,, ,,	$= b_1$ cm.
permeability * of inner cylinder	$= \mu_1$
resistivity ,, ,, ,,	$= \rho_1$ E.M.U.

* The value of permeability to be employed here is, of course, the actual or "intrinsic" permeability of the material. The value of this quantity in a ferromagnetic material varies with field-strength, and

The field produced by the inductor has amplitude $H_0 = 4\pi n I_0$, and at any instant the field-strength is given by

$$H_I = H_0 \cos 2\pi ft.$$

This is the field-strength at the outer surface of the envelope. We require to know the field-strength at the inner boundary of the envelope, H_b; the field will then be constant with this value over the cross-section between radius b and the outer boundary of the inner cylinder. In the material of the inner cylinder there will be a further decrease in the field owing to the eddy-currents in the cylinder.

General Solution.

4. For the field-strength at radius r in a cylindrical charge we have in general [1], [2], [4], [5]

$$\frac{\partial^2 H}{\partial r^2} + \frac{1}{r}\frac{\partial H}{\partial r} - \frac{4\pi\mu}{\rho}\frac{\partial H}{\partial t} = 0. \quad . \quad . \quad . \quad (1)$$

The solution of this is fully treated in the references, being given in terms of Bessel functions of the quantity (mr), where

$$m^2 = \frac{8\pi^2\mu f}{\rho}. \quad . \quad . \quad . \quad . \quad . \quad . \quad . \quad (2)$$

The arbitrary constants are determined from the boundary conditions, which are discussed in [1] and [2] when the charge is a solid cylinder, and in [4] and [5] when the charge is a hollow empty cylinder.

Simplified Solution.

5. When the charge consists of a hollow empty tube with wall-thickness small compared with the radius, then the radius may be taken as constant for all points in the tube [6]. With this assumption the equations are simplified and Bessel functions are avoided. Taking a new

---

probably with frequency. It will therefore vary with depth in the material, since field-strength varies with depth, and it will also vary during a cycle. The theory assumes a constant value of μ, and is, therefore, far from accurate. The question of what value is best employed for μ for a ferromagnetic material is discussed later.

coordinate system with $x=0$ at $r=b$, then for H in the tube at distance x from the inner boundary we have

$$\frac{\partial^2 H}{\partial x^2}-\frac{4\pi\mu}{\rho}\frac{\partial H}{\partial t}=0. \quad . \quad . \quad . \quad . \quad . \quad . \quad (3)$$

It is necessary to consider the solution of this equation as given in [6] for application in the present investigation.

If we write

$$H=A' \cos 2\pi ft+B' \sin 2\pi ft \quad . \quad . \quad . \quad . \quad (4)$$

and

$$\left.\begin{aligned} A'&=\cos px(B_1e^{px}+B_3e^{-px})+\sin px(B_2e^{px}+B_4e^{-px}),\\ B'&=\cos px(B_2e^{px}-B_4e^{-px})+\sin px(-B_1e^{px}+B_3e^{-px}),\end{aligned}\right\} \quad (5)$$

where $p=m/\sqrt{2}$, m being given by (2), then (5) is the solution of (3), and we require to determine the arbitrary constants from the boundary conditions.

(1) At the external boundary

$$x=(a-b) \quad \text{and} \quad H=H_0 \cos 2\pi ft.$$

Putting $p(a-b)=s$,

$$\left.\begin{aligned} H_0&=\cos s(B_1e^{s}+B_3e^{-s})+\sin s(B_2e^{s}+B_4e^{-s}),\\ 0&=\cos s(B_2e^{s}-B_3e^{-s})+\sin s(-B_1e^{s}+B_3e^{-s}).\end{aligned}\right\} \quad . \quad (6)$$

(2) At the inner boundary we can derive and equate two expressions for the current density in a shell of thickness dx. In general,

$$\text{Current density}=i=-\frac{1}{4\pi}\frac{\partial H}{\partial x}. \quad . \quad . \quad . \quad . \quad (7)$$

$\therefore$ we have

$$i_b=-\frac{1}{4\pi}\left(\frac{\partial H}{\partial x}\right)_b \quad . \quad . \quad . \quad . \quad . \quad . \quad . \quad (8)$$

But at the inner boundary $x=0$;

$$\therefore \quad i_b=-\frac{p}{4\pi}[(B_1+B_2-B_3+B_4) \cos 2\pi ft$$
$$+(-B_1+B_2+B_3+B_4) \sin 2\pi ft]. \quad (9)$$

We know also that the flux inside the charge when empty is $\pi b^2 H_b$, and there is, therefore, at the boundary an E.M.F. given by the time-derivative of this quantity.

$$\therefore \quad \text{E.M.F.}=-\pi b^2\frac{\partial H_b}{\partial t}. \quad . \quad . \quad . \quad . \quad . \quad (10)$$

The resistance of a shell of thickness dx is given by

$$\text{Resistance} = \frac{2\pi b\rho}{dx}. \quad . \quad . \quad . \quad . \quad (11)$$

$$\therefore \quad i_b = -\frac{b}{2\rho}\frac{\partial H_b}{\partial t}. \quad . \quad . \quad . \quad . \quad . \quad . \quad (12)$$

But at $x=0$ we have

$$H_b = (B_1+B_3)\cos 2\pi ft + (B_2-B_4)\sin 2\pi ft \quad . \quad . \quad (13)$$

$$\therefore \quad i_b = \frac{\pi fb}{\rho}[(B_1+B_3)\sin 2\pi ft - (B_2-B_4)\cos 2\pi ft]. \quad (14)$$

Equating the values of i_b in equations (9) and (14) gives two equations for B_1, B_2, B_3, B_4 which, combined with equations (6), enable these coefficients to be determined.

The solution is given in [6], enabling the field-strength and current at any radius to be calculated. Important quantities in the equations are

$$\left.\begin{aligned} s &= p(a-b) = \frac{m(a-b)}{\sqrt{2}}, \\ k &= \frac{m\rho}{4\pi^2 af\sqrt{2}}, \\ \Delta &= 2[(\cosh 2s - \cos 2s) + 2k^2(\cosh 2s + \cos 2s) \\ &\qquad + 2k(\sinh 2s - \sin 2s)]. \end{aligned}\right\} \quad (15)$$

The total watts in the charge and the ratio H_b/H_0 are given in [6] in terms of s, k, and Δ. We shall describe the amplitude of the field H_b found in this way for an empty envelope as H_1. We can now proceed to the case of an envelope containing an inner cylinder, and shall require the watts in the envelope under the new conditions and the new value of H_b/H_0. We shall describe the amplitude of H_b found under the new conditions as H_2. Then H_2 will be the amplitude of the field at the surface of the inner charge, and we shall be able to determine the watts developed in this charge also.

Case of a Composite Charge.

6. The treatment of paragraph 5 gives in equation (13) the amplitude and phase of H_b in terms of the as yet known coefficients introduced in equation (5). Knowing the

amplitude of H_b, we can determine the flux developed in the inner charge; if this is solid, then the necessary equations are given in (1) or (2); if hollow, then the equations of (5) or (6) may be utilized. This flux will be given in terms of H_b and the relevant constants of the inner charge, and will be out of phase with H_b. Suppose the area of cross-section between the inner boundary of the outer charge and the outer boundary of the inner one is $d.\pi b^2$. Then the total flux in that region is $d.\pi b^2 H_b$. We have to add to this vectorially the total flux in and inside the inner charge. Suppose we can express this flux as $g\pi b^2 H_2$ in phase with H_b, and $h\pi b^2 H_2$ 90° out of phase with H_b. This can readily be done if the inner charge is either solid or, if hollow, has a wall-thickness so large that the field is reduced to zero inside it. If the inner charge is hollow, with a wall-thickness less than this limit, then this becomes more difficult. If the inner charge has a very thin wall, however, the field inside it will be nearly enough equal to that outside, and there will be very little flux in it, so that its presence will have a negligible effect on the boundary conditions for the envelope, and the equations of paragraph 5 will apply. Reverting to the general case, we obtain the total flux inside radius b by taking the vector sum of $\pi b^2 d H_b$, $g\pi b^2 H_2$, and $h\pi b^2 H_2$. Then, as in paragraph 5, the time-derivative of this total flux gives the E.M.F., from which equations may be obtained giving the values of the coefficients.

Solution for Composite Charge.

7. In valve construction the ratio of envelope wall-thickness $(a-b)$ to radius a is usually small, so that the solution of paragraph 5 may be used. Then from equation (13) we may write alternatively

$$H_b=\sqrt{(B_1+B_3)^2+(B_2-B_4)^2}\cos(2\pi ft-\theta), \quad . \quad (16)$$

where
$$\tan\theta=\frac{B_2-B_4}{B_1+B_3}.$$

or
$$H_b=H_2\cos(2\pi ft-\theta). \quad . \quad . \quad . \quad . \quad (17)$$

Then we have a total flux inside the envelope given by

$$\pi b^2[(d+g)H_2\cos(2\pi ft-\theta)+hH_2\sin(2\pi ft-\theta)]$$

$$=\pi b^2(d+g)\Big[(B_1+B_3)\cos 2\pi ft+(B_2-B_4)\sin 2\pi ft$$

$$+\frac{h}{d+g}\{(\mathrm{B}_1+\mathrm{B}_3)\sin 2\pi ft-(\mathrm{B}_2-\mathrm{B}_4)\cos 2\pi ft\}\Big]. \quad (18)$$

The E.M.F. at the inner boundary of the envelope is then the time-derivative of this expression, *i. e.*,

$$\text{E.M.F.}=-2\pi^2fb^2(d+g)$$

$$\times\Big[-(\mathrm{B}_1+\mathrm{B}_3)\sin 2\pi ft+(\mathrm{B}_2-\mathrm{B}_4)\cos 2\pi ft$$

$$+\frac{h}{d+g}\{(\mathrm{B}_1+\mathrm{B}_3)\cos 2\pi ft+(\mathrm{B}_2-\mathrm{B}_4)\sin 2\pi ft\}\Big].$$

Put
$$\frac{h}{d+g}=v;$$

$\therefore$ current density $=i_b$

$$=-\frac{\pi bf(d+g)}{\rho}\big[(v\overline{\mathrm{B}_2-\mathrm{B}_4}-\overline{\mathrm{B}_1+\mathrm{B}_3})\sin 2\pi ft$$

$$+(\overline{\mathrm{B}_2-\mathrm{B}_4}+v\overline{\mathrm{B}_1+\mathrm{B}_3})\cos 2\pi ft\big]. \quad (19)$$

We also had the expressions for i_b given in equation (9), which is equally true in this case. Now if we write

$$\frac{p\rho}{4\pi^2bf(d+g)}=\frac{m\rho}{4\pi^2\sqrt{2}bf(d+g)}=k_1, \quad . \quad . \quad (20)$$

then we can combine equations (9) and (19) and obtain

$$\left.\begin{aligned}&\mathrm{B}_1(1-k_1)+\mathrm{B}_2(k_1-v)+\mathrm{B}_3(1+k_1)+\mathrm{B}_4(k_1+v)=0,\\&\mathrm{B}_1(k_1-v)-\mathrm{B}_2(1-k_1)-\mathrm{B}_3(k_1+v)+\mathrm{B}_4(1+k_1)=0.\end{aligned}\right\} \quad (21)$$

We have now to combine equations (6) and (21) to obtain the values of the coefficients.

We define

$$s=p(a-b)=\frac{m(a-b)}{\sqrt{2}}. \quad . \quad . \quad . \quad . \quad (22)$$

Then we write

$$\Delta_1=e^{2s}(2k_1{}^2+2k_1+1+v^2+2k_1v)+e^{-2s}(2k_1{}^2-2k_1+1$$

$$+v^2-2k_1v)-2(1+v^2-2k_1{}^2)\cos 2s-4k_1\sin 2s, \quad (23)$$

or, written differently,

$$\Delta_1=2[(1+v^2)(\cosh 2s-\cos 2s)+2k_1{}^2(\cosh 2s+\cos 2s)$$

$$+2k_1(\sinh 2s-\sin 2s)+2k_1v\sinh 2s]. \quad . \quad . \quad . \quad (24)$$

We then find the values of the coefficients are given by

$$\left.\begin{aligned}
B_1 &= \frac{H_0}{\Delta_1}[(2k_1^2+2k_1+1+v^2+2k_1v)e^s \cos s \\
&\qquad -2k_1(1+v)e^{-s}\sin s-(1-2k_1^2+v^2)e^{-s}\cos s], \\
B_2 &= \frac{H_0}{\Delta_1}[(2k_1^2+2k_1+1+v^2+2k_1v)e^s \sin s \\
&\qquad -2k_1(1-v)e^{-s}\cos s+(1-2k_1^2+v^2)e^{-s}\sin s], \\
B_3 &= \frac{H_0}{\Delta_1}[(2k_1^2-2k_1+1+v^2-2k_1v)e^{-s}\cos s \\
&\qquad -2k_1(1+v)e^{s}\sin s-(1-2k_1^2+v^2)e^{s}\cos s], \\
B_4 &= \frac{H_0}{\Delta_1}[(2k_1^2-2k_1+1+v^2-2k_1v)e^{-s}\sin s \\
&\qquad -2k_1(1-v)e^{s}\cos s+(1-2k_1^2+v^2)e^{s}\sin s].
\end{aligned}\right\} \quad . \quad . \quad (25)$$

From these coefficients we can determine the field at radius r in the charge using equations (4) and (5), and the current density at radius r using (7). It is then possible to determine the ratio H_b/H_0 and the watts developed per cm. length of the envelope.

As pointed out in [(5)], the power developed per unit length of the envelope is given by

$$2\pi a\left(-\frac{1}{8\pi}\right)R(H_0E_0), \quad . \quad . \quad . \quad . \quad (26)$$

which follows from Poynting's Theorem, and in which R indicates the real part of (H_0E_0). Now E_0 is simply ρi_a, and the real part of this involves use of the term in $\cos 2\pi ft$ only. Thus we have power/unit length$=$W given in absolute units by

$$\begin{aligned}
W &= -\tfrac{1}{4}aH_0\rho R(i_a) \\
&= \frac{a}{16\pi}\rho H_0^2\frac{P}{\Delta_1}[(B_1e^s-B_3e^{-s}+B_2e^s+B_4e^{-s})\cos s \\
&\qquad +(B_2e^s-B_4e^{-s}-B_1e^s-B_3e^{-s})\sin s] \\
&= \frac{H_0^2 a\rho m}{16\pi\sqrt{2}\Delta_1}[e^{2s}(2k_1^2+2k_1+1+v^2+2k_1v) \\
&\qquad -e^{-2s}(2k_1^2-2k_1+1+v^2-2k_1v) \\
&\qquad -4k_1\cos 2s+4k_1v+2(1-2k_1^2+v^2)\sin 2s]
\end{aligned}$$

$$=\frac{H_0^2\rho ma}{16\pi\sqrt{2}}\left[\frac{\begin{array}{c}(1+v^2)(\sinh 2s+\sin 2s)+2k_1^2(\sinh 2s-\sin 2s)\\ +2k_1(\cosh 2s-\cos 2s)+2k_1v(1+\cosh 2s)\end{array}}{\begin{array}{c}(1+v^2)(\cosh 2s-\cos 2s)+2k_1^2(\cosh 2s+\cos 2s)\\ +2k_1(\sinh 2s-\sin 2s)+2k_1v\sinh 2s\end{array}}\right]. \quad . \quad . \quad . \quad (27)$$

The amplitude of H_2 was given by

$$H_2=[(B_1+B_3)^2+(B_2-B_4)^2]^{1/2}$$

$$=\frac{4k_1H_0}{\Delta_1}\sqrt{\begin{array}{l}2k_1^2(\cosh 2s+\cos 2s)\\ \quad +(1+v^2)(\cosh 2s-\cos 2s)\\ \quad +2k_1(\sinh 2s-\sin 2s)+2k_1v\sinh 2s\\ \quad +v[(1+\cosh 2s)(1-\cos 2s)\\ \quad -2k_1\sin 2s\cosh 2s-(1+v)\sin 2s\sinh 2s]\end{array}}$$

$$=\frac{2k_1H_0}{D}\sqrt{\begin{array}{l}D+v[(1+\cosh 2s)(1-\cos 2s)\\ \quad -2k_1\sin 2s\cosh 2s\\ \quad -(1+v)\sin 2s\sinh 2s],\end{array}} \quad . \quad . \quad . \quad (28)$$

where $D=\frac{\Delta_1}{2}$, Δ_1 being given by equation (24).

From (28) we have at once the ratio H_2/H_0.

8. As in [6], equations (27) and (28) may be simplified according to the value of the quantity s. Thus, if $s<0{\cdot}15$, we have

$$W=\frac{H_0^2\rho ma}{16\pi\sqrt{2}}\left[\frac{s(1+v^2)+k_1v}{(1+v^2)s^2+k_1^2+k_1vs}\right]. \quad . \quad (27_1)$$

when $0{\cdot}4>s>0{\cdot}15$; then

$$W=\frac{H_0^2\rho ma}{16\pi\sqrt{2}}\,\frac{(1+v^2)s+2k_1s^2+\frac{4}{3}k_1^2s^3+k_1v(1+s^2)}{(1+v^2)s^2+k_1^2+\frac{4}{3}k_1s^3+k_1vs\left(1+\frac{2s^2}{3}\right)}. \quad (27_2)$$

When, with $0{\cdot}4>s>0{\cdot}15$, we have also k_1 small compared with s, then

$$W=\frac{H_0^2\rho ma}{16\pi\sqrt{2}}\,\frac{1}{s}=\frac{H_0^2\rho a}{16\pi(a-b)}. \quad . \quad . \quad . \quad (27_3)$$

When $1{\cdot}5>s>0{\cdot}4$, we must employ the full expression (27). Then when $s>1{\cdot}7$ we have

$$W=\frac{H_0^2\rho ma}{16\pi\sqrt{2}}. \quad . \quad . \quad . \quad . \quad . \quad (27_4)$$

In each of the equations (27) the power in watts is obtained by multiplying the value of W by 10^{-7}.

9. Simplifying H_2/H_0 similarly, we have:
If $s<0{\cdot}15$,

$$H_2/H_0=\frac{k_1\sqrt{s^2+k_1{}^2}}{(1+v^2)s^2+k_1{}^2+k_1vs}. \quad . \quad . \quad (28_1)$$

If $0{\cdot}4>s>0{\cdot}15$,

$$H_2/H_0=k_1\frac{\sqrt{s^2+k_1{}^2+\frac{4}{3}k_1s^3-\frac{2}{3}k_13vs^3}}{(1+v^2)s^2+k_1{}^2+\frac{4}{3}k_1s^3+k_1vs\left(1+\frac{2s^2}{3}\right)}. \quad (28_2)$$

If $s>0{\cdot}4$, the full expression (28) must be used.

It should be noted that if the inner charge is absent or has negligible effect on the flux in the envelope, then $d=1$ and $g=h=0$, in which case $v=0$ and k_1 takes the value

$$\frac{mp}{4\pi^2\sqrt{2bf}}=k, \quad . \quad . \quad . \quad . \quad . \quad . \quad (20_1)$$

which is as in (15).

Putting this value of k for k_1, together with $v=0$, in the equations (27) and (28) reproduces the results of [6].

Solid Cylinder as Inner Charge.

10. We have assumed it possible to determine the flux in the inner charge when the field at its surface is H_b, and to express this flux in terms of two multiples of H_b, one in phase and one in quadrature with H_b. Now if the inner charge is a solid cylinder, then the flux in it is given by [2]

$$\phi=H_2\frac{2\pi\mu_1a_1}{m_1}\left[\frac{\operatorname{ber} m_1a_1\operatorname{bei}' m_1a_1-\operatorname{bei} m_1a_1\operatorname{ber}' m_1a_1}{\operatorname{ber}^2 m_1a_2+\operatorname{bei}^2 m_1a_1}\times\cos(2\pi ft-\theta)+\frac{\operatorname{ber} m_1a_1\operatorname{ber}' m_1a_1+\operatorname{bei} m_1a_1\operatorname{bei}' m_1a_1}{\operatorname{ber}^2 m_1a_1+\operatorname{bei}^2 m_1a_1}\times\sin(2\pi ft-\theta)\right]. \quad . \quad . \quad . \quad (29)$$

Writing
$$W(x)=\operatorname{ber} x\operatorname{bei}' x-\operatorname{bei} x\operatorname{ber}' x,$$
$$Z(x)=\operatorname{ber} x\operatorname{ber}' x+\operatorname{bei} x\operatorname{bei}' x,$$
$$X(x)=\operatorname{ber}^2 x+\operatorname{bei}^2 x.$$

$\therefore$ the component of flux in phase with H_b has amplitude $H_2 \dfrac{2\pi\mu_1 a_1}{m_1} \dfrac{W(m_1a_1)}{X(m_1a_1)}$, and the component in quadrature has amplitude $H_2 \dfrac{2\pi\mu_1 a_1}{m_1} \dfrac{Z(m_1a_1)}{X(m_1a_1)}$. Thus to find g and h, paragraph 6, we write

$$\left.\begin{aligned} \pi b^2 g H_2 &= H_2 \frac{2\pi\mu_1 a_1}{m_1} \frac{W(m_1a_1)}{X(m_1a_1)}, \\ \pi b^2 h H_2 &= H_2 \frac{2\pi\mu_1 a_1}{m_1} \frac{Z(m_1a_1)}{X(m_1a_1)}. \end{aligned}\right\} \quad . \quad . \quad . \quad (30)$$

Graph 1.

Components of Flux in Solid Cylinder of Radius a.

Components given by $\dfrac{2\pi\mu a}{m} \dfrac{W(ma)}{X(ma)}$ and $\dfrac{2\pi\mu a}{m} \dfrac{Z(ma)}{X(ma)}$.

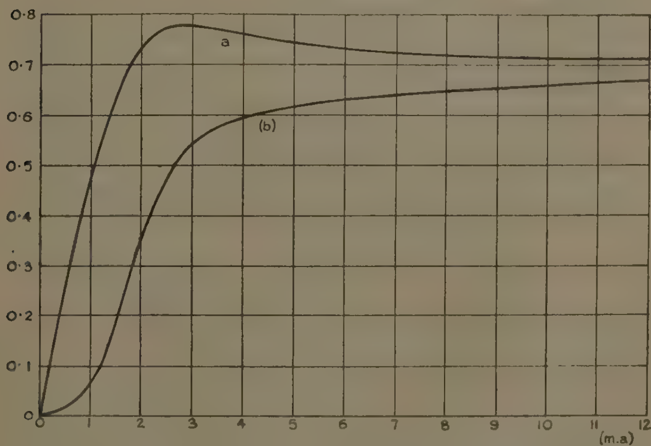

(a) $\dfrac{\text{ber } ma \text{ bei}' ma - \text{bei } ma \text{ ber}' ma}{\text{ber}^2 ma + \text{bei}^2 ma} = \dfrac{W(ma)}{X(ma)}$.

(b) $\dfrac{\text{ber } ma \text{ ber}' ma + \text{bei } ma \text{ bei}' ma}{\text{ber}^2 ma + \text{bei}^2 ma} = \dfrac{Z(ma)}{X(ma)}$.

The functions $\dfrac{W(x)}{X(x)}$ and $\dfrac{Z(x)}{X(x)}$ both have values near $1/\sqrt{2}$ when $(x) > 7$. In cases therefore when $m_1a_1 > 7$, the two components of flux have equal magnitude and we have $g = h$. The functions are plotted in graph 1.

Hollow Cylinder as Inner Charge.

11. When the inner charge takes the form of a hollow cylinder, then if $m_1a_1>7$, and if the value of s_1 corresponding to s for the envelope (equation (22)) is also greater than 1·5, then the flux inside the inner charge is negligible, and the flux in the charge itself is given by equation (29). Thus g and h are found again from equation (30), and will have equal values.

12. When on the other hand, the hollow cylinder has a wall so thin that it does not disturb the flux inside the envelope, which will be the case when its value of s_1 is less than 0·15, then, as noted in paragraph 6, the inner charge will have no effect on the envelope behaviour, and the equations of [6] will apply, *i. e.*, the equations (27) and (28) with $d=1$, $g=h=v=0$.

13. When s_1 lies between 0·15 and 1·5, then the effect of an inner charge of given radius a_1 will be intermediate between that of paragraph 11 and the negligible effect of paragraph 12. Assuming that the wall-thickness for the inner charge remains small compared with its radius, calculations of flux may be made, using the equations given in [6], since the inner charge is assumed empty. That is to say, the equations of paragraph 5 are applicable, and the solutions are as in paragraph 7 if we write $g=h=v=0$, and write for k_1, $k\doteq\dfrac{m_1\rho_1}{4\pi^2\sqrt{2a_1f}}$, putting in the constants for the inner charge. Thus, corresponding to (25), we have for the inner charge

$$\Delta_i=2[(\cosh 2s_1-\cos 2s_1)+2k^2(\cosh 2s_1+\cos 2s_1)$$
$$+2k(\sinh 2s_1-\sin 2s_1)]. \quad (31)$$

The calculation of flux was not made in [6]. The determination is made as follows :—

Total flux in the material of the inner charge is

$$\phi=2\pi\mu_1a_1\int_0^{(a_1-b_1)}\mathrm{H}\,dx. \quad . \quad . \quad . \quad . \quad (31)$$

The component of flux in phase with H_b is

$$\phi_1=2\pi\mu_1a_1\int_0^{(a_1-b_1)}\mathrm{A}'\,dx,$$

and component of flux in quadrature with H_b is

$$\phi_2 = 2\pi a_1 \mu_1 \int_0^{(a_1-b_1)} B'\,dx.$$

A′ and B′ being as defined in (4) and (5).

Integrating, we obtain

$$\left.\begin{aligned}
\phi_1 = \frac{2\pi a_1\mu_1 H_2\sqrt{2}}{m_1\Delta_i}\Big[2k^2 &(\sinh 2s_1+\sin 2s_1)\\
&+2k(\cosh 2s_1+\cos 2s_1)\\
&+(\sinh 2s_1-\sin 2s_1)\\
&+2(\sin s_1\cosh s_1-\cos s_1\sinh s_1\\
&\qquad -2k\cos s_1\cosh s_1)\Big],\\
\phi_2 = \frac{2\pi a_1\mu_1 H_2\sqrt{2}}{m_1\Delta_i}\Big[2k^2 &(\sinh 2s_1-\sin 2s_1)\\
&+2k(\cosh 2s_1-\cos 2s_1)\\
&+(\sinh 2s_1+\sin 2s_1)\\
&-2(\sin s_1\cosh s_1+\cos s_1\sinh s_1\\
&\qquad +2k\sin s_1\sinh s_1)\Big].
\end{aligned}\right\} \quad . \quad . \quad . \quad (32)$$

When $0{\cdot}4 > s_1 > 0{\cdot}15$ these become

$$\left.\begin{aligned}
\phi_1 &= H_2\frac{\pi a_1\mu_1\sqrt{2}}{m_1}\,\frac{s_1(2k^2+s_1^2)}{k^2+s_1^2+\frac{4}{3}ks_1^3},\\
\phi_2 &= H_2\frac{\pi a_1\mu_1\sqrt{2}}{m_1}\,\frac{k_1^2(1+\frac{4}{3}ks)}{k^2+s_1^2+\frac{4}{3}ks_1^3},
\end{aligned}\right\} \quad . \quad . \quad (32_1)$$

and when $s_1 < 0{\cdot}15$,

$$\left.\begin{aligned}
\phi_1 &= H_2\frac{\pi a_1\mu_1\sqrt{2}}{m_1}\,2s_1(1+s_1^2/k^2)^{-1},\\
\phi_2 &= H_2\frac{\pi a_1\mu_1\sqrt{2}}{m_1}\,\frac{s_1^2}{k}\,(1+s_1^2/k^2)^{-1}.
\end{aligned}\right\} \quad . \quad (32_2)$$

We require also the flux inside the inner charge, which is $\pi b_1^2 H_{b_1}$. This has two components, the amplitude of the component in phase with H_b being

$$\left.\begin{aligned}
\theta_1 = \pi b_1^2(B_1+B_3)_1 = \frac{4\pi b_1^2 H_2}{\Delta_i}\,(2k^2 &\cos s_1\cosh s_1\\
&+k\cos s_1\sinh s_1-k\sin s_1\cosh s_1),\\
\theta_2 = \pi b_1^2(B_2-B_4)_1 = \frac{4\pi b_1^2 H_2}{\Delta_i}\,(2k^2 &\sin s_1\sinh s_1\\
&+k\sin s_1\cosh s_1+k\cos s_1\sinh s_1).
\end{aligned}\right\} \quad . \quad . \quad . \quad (33)$$

If $0{\cdot}8 > s_1 > 0{\cdot}3$, this becomes

$$\left.\begin{aligned} \theta_1 &= \pi b_1{}^2 \mathrm{H}_2 \frac{k(k-s_1{}^3/3)}{k^2+s_1{}^2+\frac{4}{3}ks_1{}^3}, \\ \theta_2 &= \pi b_1{}^2 \mathrm{H}_2 \frac{ks_1(1+ks_1)}{k^2+s_1{}^2+\frac{4}{3}ks_1{}^3}, \end{aligned}\right\} \quad . \quad . \quad . \quad (33_1)$$

and if $s_1 < 0{\cdot}3$,

$$\left.\begin{aligned} \theta_1 &= \pi b_1{}^2 \mathrm{H}_2 (1+s_1{}^2/k_2)^{-1}, \\ \theta_2 &= \pi b_1{}^2 \mathrm{H}_2 \frac{s_1}{k}(1+ks_1)(1+s_1{}^2/k^2)^{-1}. \end{aligned}\right\} \quad . \quad . \quad (33_2)$$

To complete our solution we thus write

$$\left.\begin{aligned} \theta_1+\phi_1 &= \pi b^2 g \mathrm{H}_2, \\ \theta_2+\phi_2 &= \pi b^2 h \mathrm{H}_2 \end{aligned}\right\}$$

to give g and h of paragraph 6, and then proceed, as in paragraph 7, to find the watts in the envelope, the value of $\mathrm{H}_2/\mathrm{H}_0$, and hence, knowing H_2, the watts in the inner charge.

14. Equations are now available which will allow any particular system to be studied in detail. It is of interest to consider qualitatively conditions at the inner boundary of an envelope in order to determine what type of systems might be of special interest. Suppose firstly a solid cylinder of radius a, that of the envelope, and composed of the material of the envelope, and let the same field H_0 be applied to its surface. Then at radius b in this cylinder there is a field H_s with amplitude H_3. In the case of a non-ferromagnetic material it is clear that at radius b in a hollow empty cylinder H_1 must always be less than H_3; for if $\mathrm{H}_1 \geqslant \mathrm{H}_3$, then the flux inside radius b would be greater for the hollow than for the solid cylinder, and if this were true then there would be a greater E.M.F. at radius b in the former case, which would only be consistent with a smaller penetration through the hollow than through the solid cylinder. In the case of a ferromagnetic material the reverse might well occur, $\mathrm{H}_1 > \mathrm{H}_3$, particularly with material of high permeability. Now considering the field H_2 at the inner boundary of the envelope when there is an inner charge, it is possible to compare H_2 with H_1 and H_3 in a similar manner. We

suppose for convenience an inner charge with outer radius a_1 equal to b the inner radius of the envelope, in which case for a given thickness the effect of the inner charge is a maximum. We have the following cases :—

(a) *Inner Charge and Envelope of Identical Composition.*

In this case it is clear that H_2 will be intermediate between H_1 and H_3, the value depending on the inner charge-wall thickness (a_1-b_1).

(b) *Inner Charge and Envelope both Non-ferromagnetic.*

(i.) If the resistivity ρ_1 of the inner charge is greater than the resistivity ρ of the envelope, then the result would be as in (*a*), but a greater wall-thickness (a_1-b_1) would be necessary to give the same reduction of H_2 as compared with H_3.

(ii.) If ρ_1 is less than ρ, then we have the important cases where, with a sufficiently high value of (a_1-b_1), H_2 may become greater than H_3.

(c) *Inner Charge Ferromagnetic, Envelope Non-ferromagnetic.*

In this case considerations of flux inside radius b show that H_2 may now become less than H_1.

(d) *Envelope Ferromagnetic.*

(i.) A non-ferromagnetic inner charge would lead, as in (*a*), to a value of H_2 greater than H_1, which may, however, in this case be greater than H_3.

(ii.) If both envelope and inner charge were ferromagnetic, the behaviour would depend similarly on the relative values of both resistivity and permeability.

15. The case (*d*) is not of great practical importance, since the heating of such an envelope would always be large compared with that of the inner charge. Now values of H_3 may be found using formulæ in [(1)] or [(2)], and values of H_1 may be found using formulæ from [(6)]. If for a particular envelope H_1 and H_3 are widely different, then calculation of H_2 for all the cases (*a*), (*b*). and (*c*) of composite charges will be justified in considering in detail a particular system. If, however, H_1 and H_3 are similar in value throughout the frequency range considered, then since in cases (*a*) and (*b*) (i.) H_2 is intermediate between H_1 and H_3, interest is concentrated on cases *b* (ii.) and (*c*), where H_2 is outside the range H_1-H_3.

Application to Particular Systems.

16. We shall consider in particular envelopes of copper (low resistivity) and of a copper-nickel alloy with about 20 per cent. Ni (high resistivity). We suppose that during the eddy-current heating the envelope temperature is maintained at about 500° C., which is an upper limit if glass is present. The inner electrode may consist of Ni, Mo, Cu, or Fe, these metals being typical of normal valve production. We suppose that at the start of eddy-current

Graph 2.

Envelope of Cu at 500° C. $\mu=1$. $\rho=5000$ E.M.U.
$a=1$ cm. $(a-b)=0{\cdot}5$ mm.

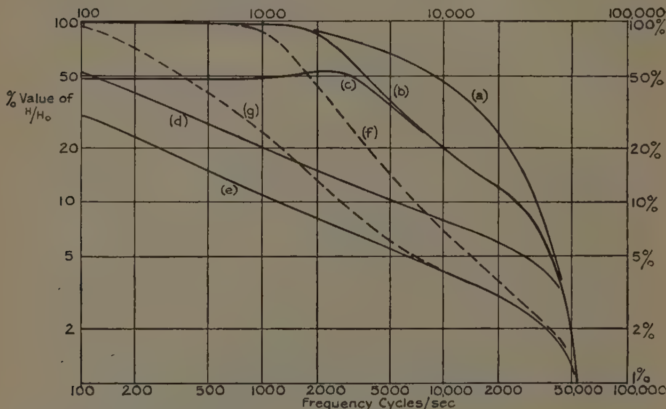

heating the temperature of this electrode is also 500° C. We will take a particular case of an envelope of radius $b=1$ cm. and wall-thickness $(a-b)=0{\cdot}5$ mm. The resistivities of the metals at 500° C. may be found from tables, the values used here being shown on the graphs. The permeability of iron is not readily determined; in order to illustrate case (*c*), paragraph 14, a value of 100 will be assumed as a basis for calculations. Large variations from this value are of course possible, though some justification for the use of a value of this order appears later (paragraph 27).

17. Graphs 2 and 3 show the "penetration" of the field through the two envelopes under various conditions.

Curve (*a*) shows H_3/H_0, the ratio of the field at depth 0·5 mm. to that at the surface when the cylinder is solid, deduced from the equations of [1] and [2]. Curve (*b*) shows H_1/H_0, the ratio of the field inside to that outside when the envelope is empty, or, paragraph 12, when it contains a hollow inner charge whose value of s_1 at all frequencies considered is less than 0·15. This curve is calculated from the equations of [6]. It will also apply

Graph 3.

Envelope of Cu–Ni Alloy at 500° C.

$\mu=1$. $\rho=35{,}000$ E.M.U. $a=1$ cm. $(a-b)=0{\cdot}5$ mm.

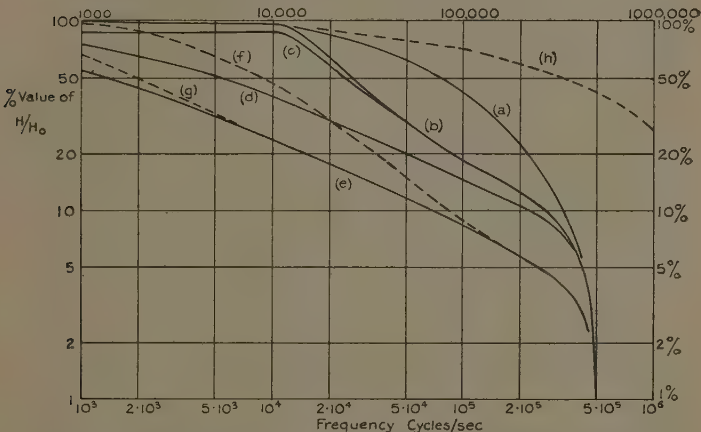

(*a*) H_3/H_0. H_3=field at depth 0·5 mm. in solid cylinder of radius 1 cm.

(*b*) H_1/H_0. H_1=field at inner boundary of empty envelope.

(*c*) H_2/H_0. H_2=field at inner boundary of envelope when inner charge is a solid iron cylinder with radius to give $m_1a_1=2{\cdot}5$.

(*d*) H_2/H_0. H_2=field at inner boundary of envelope when inner charge is an iron tube, radius 0·5 mm., wall-thickness $\geqslant 2{\cdot}5/m_1$.

(*e*) H_2/H_0. H_2 as for (*d*), but iron tube having a radius of 1 cm.

(*f*) H_2/H_0. H_2=field at inner boundary of envelope when inner charge is an iron tube, radius 1 cm., wall-thickness 0·1 mm.

(*g*) H_2/H_0. H_2 as for (*f*), but iron tube with a 0·5 mm. wall.

(*h*) [graph 3 only] H_2/H_0. H_2=field at inner boundary of envelope when inner charge is a Cu tube, radius 1 cm., wall-thickness 0·5 mm.

when the envelope contains solid cylinders of non-ferromagnetic material of radius small compared with that

of the envelope, since such cylinders will have only a small effect on the total flux. It will be seen that curves (*a*) and (*b*) are not widely separated, so that no detailed study will be made here of cases (*a*) and (*b*) (i.), paragraph 14; these would include Cu, Ni, and Mo inside Cu envelopes, and Ni inside Cu–Ni envelopes.

18. Considering in some detail case (*c*) of paragraph 14, we take the case of an iron inner electrode. Now if this is solid it may have quite a small radius, and yet influence the total flux inside the envelope; we consider, therefore, a solid iron cylinder whose radius a_1 is chosen at any frequency to give $m_1a_1=2{\cdot}5$; then, as in [(1)] and [(2)], the watts/c.c. in such a cylinder are a maximum; at 10^4 cycles/second the radius, to fulfil this condition, is 2 mm., while it is proportional to $1/\sqrt{f}$. Curve (*c*) supposes such a cylinder inside the envelope, and gives the value of H_2/H_0. If the iron is in the form of a hollow cylinder, calculation is easiest (paragraph 11) when at any frequency the wall-thickness is chosen to be equal to or greater than this radius for maximum watts/c.c., $m_1(a_1-b_1)\geqslant 2{\cdot}5$. Curves (*d*) and (*e*) deal with this case, showing the maximum effect when the inner cylinder has outer radius 1 cm., that of the envelope, and the case also of radius 0·5 cm. If we consider a cylinder of radius 1 cm. and a fixed wall-thickness at all frequencies, then over part of the frequency range the formulæ of paragraph 13 must be used to determine the flux inside the envelope. At the higher frequencies where $s_1>1{\cdot}5$, the curves will coincide with (*e*), and at the lower frequencies, where $s_1<0{\cdot}15$, with (*b*). Complete curves are shown dotted in graphs (2) and (3), curve (*f*) giving H_2/H_0 for the envelope when the inner charge has a 0·1 mm. wall, curve (*g*) when it has a 0·5 mm. wall. In all the cases of a composite charge, but particularly with the large radius tubes, the curves are very different from (*a*) and (*b*), and the results of applying the theory of the present paper have great practical significance.

19. To illustrate case (*b*) (ii.) of paragraph 14, we consider a copper inner charge inside Cu–Ni, the copper having radius equal to the inner envelope radius and wall-thickness 0·5 mm. A similar, but less marked, effect would be observed with Mo inside Cu–Ni. Then the

values of H_2/H_0 are as plotted in curve (*h*), graph 3. Again the variation from (*a*) and (*b*) is large, and would have practical importance.

20. To illustrate the application of the results of graphs 2 and 3 to the complete investigation of a particular problem, we consider further the case of iron inner charges with wall-thickness 0·1 or 0·5 mm., curves (*f*) and (*g*). If unit field exists at the surface of such charges, then the watts produced vary with frequency as in graph 4, these curves being derived from the equations of [6], since the iron tubes are empty. But if the iron tubes form inner charges inside the Cu or Cu–Ni envelope, then unit field at the envelope surface is reduced in the ratio H_2/H_0 given by curves (*f*) or (*g*) of graphs 2 or 3. The watts in a tube depend on the square of the field at the tube surface. Thus the watts in the iron tube are reduced in the ratio $(H_2/H_0)^2$. Multiplying curves (*a*) and (*b*), graph 4 by values of $(H_2/H_0)^2$ from curves (*f*) or (*g*) of graphs 2, and 3 gives the dotted curves (a'), (a''), (b'), (b''), showing the variation of watts in the inner iron tubes with frequency per unit field at the outer envelope surface, *i. e.*, per unit inductor field. The optimum frequency ranges are clearly indicated.

21. We require also the watts in the envelope. Now, disregarding the presence of the iron tubes, the watts/unit field in the envelope tubes vary with frequency as in graph 5, the curves (*a*) and (*b*) again being obtained from the formulæ of [6]. When the iron inner tubes are present, however, the envelope watts are raised, and are given by equation (27). In the Cu envelope the watts are raised from curve (*a*) to (*e*) by 0·1 mm. Fe, to (*c*) by 0·5 mm. Fe, while curve (*b*) for Cu–Ni is raised to (*f*) by 0·1 mm. Fe and to (*d*) by 0·5 mm. Fe. Comparison of the dotted curves of graphs 4 and 5 shows how the watts in the inner charge compare with those in the envelope, and hence enable the practicability of eddy-current heating the iron to be deduced.

22. Similarly, if the Cu inner charge of paragraph 19 has unit field at its surface, the watts are given by curve (*a*), graph 5. Inside a Cu–Ni envelope the watts are reduced in the ratio $(H_2/H_0)^2$ for unit field at the Cu–Ni surface,

H_2/H_0 being given by curve (h) of graph 3. The resulting curve is shown dotted as curve (g), graph 5. It remains at an almost constant level for frequencies up to 10^3

Graph 4.

Watts in Iron Tubes.

Radius 1 cm. Wall-thickness $\begin{cases} (a)\ 0{\cdot}1 \text{ mm.} \\ (b)\ 0{\cdot}5 \text{ mm.} \end{cases}$

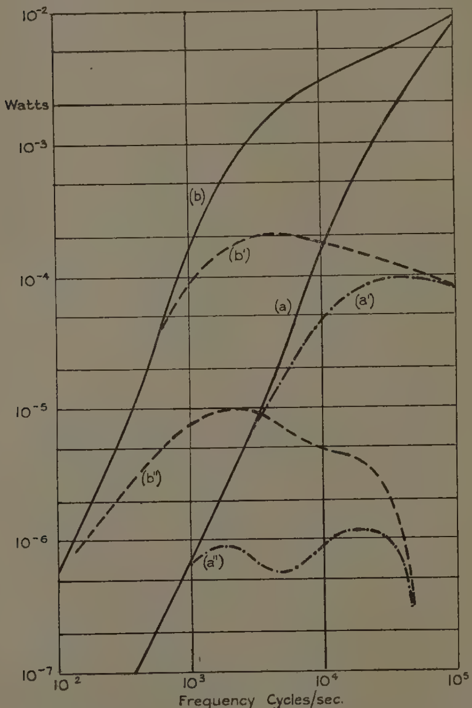

(a'), (b'). Tubes (a) and (b) inside a Cu–Ni envelope. Radius 1 cm., 0·5 mm. wall.

(a''), (b''). Tubes (a) and (b) inside a Cu envelope. Radius 1 cm., 0·5 mm. wall.

cycles/second, giving a very wide optimum frequency range. This is in great contrast with the results which would be obtained using (H_1/H_0) as given by curve (b),

graph 3, which would indicate a negligible heating of the Cu above 10^5 cycles/second.

Graph 5.

Watts in Cu and Ni tubes. Radius 1 cm. Wall-thickness 0·5 mm.

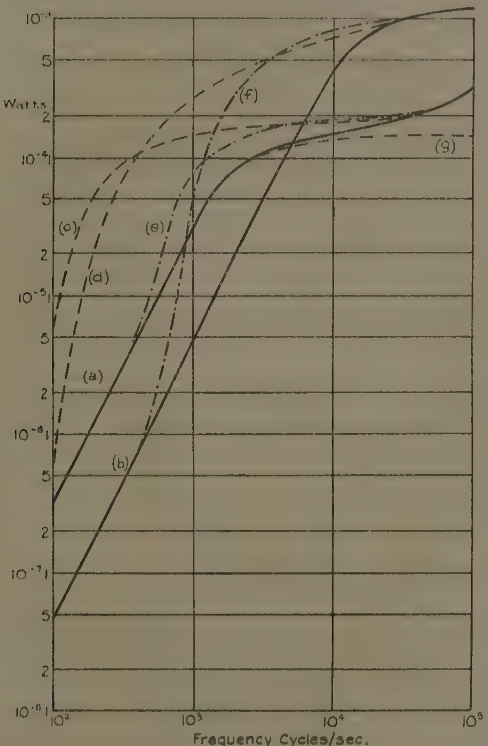

(*a*) Watts in Cu tube when empty.

(*b*) Watts in Cu–Ni tube when empty.

(*c*) Watts in Cu tube containing an iron tube, radius 1 c.m., 0·5 mm. wall.

(*d*) Watts in Cu–Ni tube containing an iron tube, radius 1 cm., 0·5 mm. wall.

(*e*) Watts in Cu tube containing an iron tube, radius 1 cm. 1 mm. wall.

(*f*) Watts in Cu Nu tube containing an iron tube, radius 1 cm., 1 mm. wall.

(*g*) Watts in Cu tube when inside a Cu–Ni envelope.

23. We are now able to deduce the possibility of eddy-current heating the internal parts of the systems discussed by comparing the heating of the inner charge with that of the envelope for a given field-strength and frequency. Thus from graphs 4 and 5 it is clear that iron inside copper cannot readily be heated ; high field-strengths and elaborate arrangements for cooling the copper would be necessary. Inside Cu–Ni the possibility is much greater, particularly with the 0·5 mm. Fe tube (curve (b'), graph 4) at frequencies from 10^3 to 5×10^3, where the watts in the iron are almost as great as those in the envelope (curve (f), graph 5). Similarly the 0·5 mm. Cu tube (curve (g), graph 5) could be heated when inside Cu–Ni at frequencies near or below 10^4, since then the watts are similar to those in the Cu–Ni, which, when containing Cu, are given by a curve very slightly lower than curve (b), graph 5. If we know to what temperature the inner charge must be raised, and what is the requirement in watts per sq. cm. of surface in order to attain this temperature, then for the optimum frequency estimated as above, we can estimate the necessary field-strength, and therefore the current in the eddy-current heating coil. The theory applies only to long charges ; if, however, the length of the charges is greater than the diameter, and is similar to that of the heating coil, the results will be in error by a factor of not more than two [3].

Experimental Confirmation.

24. For each of the systems studied the optimum frequency occurs in the neighbourhood of 10^4 cycles/second. A source of power at this frequency was not available, so that no complete experimental check of the conclusions could be made. A brief description will, however, be given of experiments using a frequency of 300 cycles/second, since these experiments gave confirmation of the theory as applied to the behaviour of iron inside copper. The copper envelope was a small cylindrical transmitting valve anode, length 6·8 cm., radius 1·2 cm., wall-thickness 0·5 mm., closed at the top and sealed at the lower edge to a cylindrical glass tube which could be sealed to a pinch. Solid iron cylinders were used, length 6 cm., having two values of radius, one 0·17 cm. and the other 0·5 cm. The cylinder under

examination was mounted on the pinch so that after assembly it was coaxial with the anode, the clearance between the top of the cylinder and that of the anode being 3 mm. Thermocouples of fine wire were welded to the iron and led out through the pinch. The assembly was pumped on a diffusion pump to a pressure of 10^{-6} mm. Hg and baked for one hour at 450° C. It was then sealed off, and could be placed in the eddy-current heating coil. Similar iron cylinders were mounted on pinches which were sealed into envelopes wholly of glass, and these also were pumped, baked, and sealed off. The eddy-current heating coil had internal radius 2·1 cm., length 8 cm., and consisted of 14 turns of 0·4 cm. diameter Cu tubing through which water was allowed to flow. The current was 100 amps. R.M.S.

25. Graph 6 shows the plot of rise of temperature against time for the iron. In a glass envelope the initial rate of rise is about 5° C. per second in each case; in a copper envelope there is an almost identical rate of rise for the 0·17 cm. iron, whereas for the 0·5 cm. Fe the rate is reduced to 2·2° C. per second. The final temperature of the 0·5 cm. Fe is higher in each case than that of the 0·17 cm. Fe, since watts/sq. cm. of surface increase with radius.

Now for Fe a rate of rise of temperature of 1° C. per second corresponds to an input of 3·7 watts. Thus the actual input to the iron in the absence of the Cu envelope is 18·5 watts. When the 0·17 cm. Fe is inside the envelope at least 80 per cent. of these watts remain available, whereas the 0·5 cm. Fe has only 44 per cent. of the watts. The copper temperature after five minutes' heating was 170° C. in the case of the 0·17 cm. Fe, 250° in the case of the 0·5 cm. Fe. Thus the quantity of iron inside the copper does affect both the penetration of the field through the copper and the watts developed in it, as is to be expected from the theory presented.

26. It is not possible, however, to account exactly for the behaviour at 300 cycles/second using the above theory, since it is uncertain what value of μ to write in the equations and to what extent hysteresis loss is important. These matters have been discussed [7], and it appears that hysteresis losses may occur at frequencies below

10^5 cycles/second. Now if all the energy developed in the iron was due to eddy currents, we could predict the

Graph 6.

Temperature of Iron Cylinders heated by Eddy Currents.
$f=300$ cycles/sec.

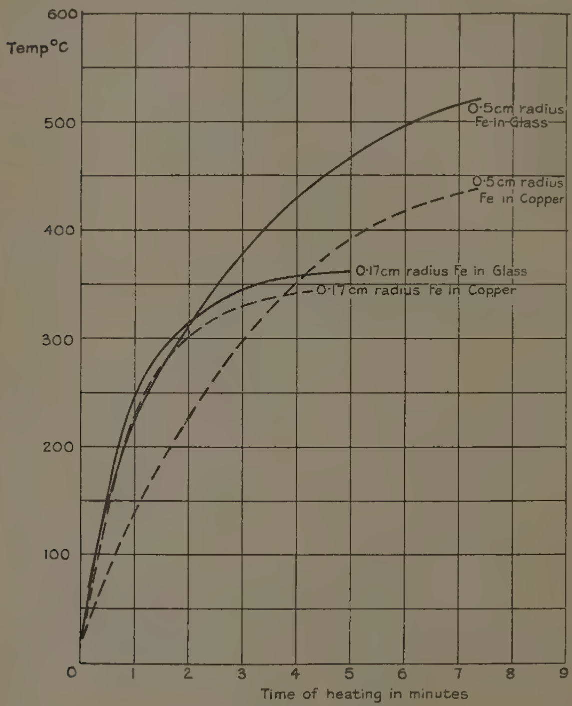

input of 18·5 watts /c.c., assuming $\mu=400$, with resistivity $=10,000$ E.M.U. per cm.³. Since some hysteresis loss will probably be present, the actual value of μ must be less than this for the eddy-current loss to be only a fraction of the total loss. If there were no hysteresis loss, this value of μ would remain too high, since it is well known[7] that observed eddy-current losses are greater than those calculated from a measured flux density. Thus the

actual value of μ to be employed in determining the flux in the iron is unknown, but is certainly much less than 400. The flux itself is therefore smaller than would be estimated with $\mu=400$, being proportional to $\mu^{\frac{1}{2}}$, so that the penetration of field through the copper is greater than would be calculated with $\mu=400$. To account for the observed ratios 80 per cent. and 44 per cent. for the two specimens by means of equations (28) and (29), it is necessary to assume a value of permeability rather less than 100. This value would lead to a calculated eddy-current loss of about half the total observed loss in the iron.

27. This deduction of the value of 100 for intrinsic permeability offers some justification for the use of this value throughout the frequency range in the calculations of paragraphs 18 and 20. It is shown in (7) that intrinsic permeability in weak fields is constant from 0–10^4 cycles/second, and then falls to values of the order of 100 as frequency increases from 10^4–10^7 cycles/second. Thus, since in paragraphs 18 and 20 we are concerned with a temperature of 500° C., the value of 100 is not likely to be too low above 10^4 cycles/second. In a table in (8) the value of $\mu=100$ is assumed throughout the whole range 0–10^8 cycles/second, though no mention is made of the justification for this assumption.

Summary.

28. Expressions are deduced for the penetration of field through the wall of a cylindrical tube carrying eddy currents and containing an inner cylindrical charge, and for the watts developed in the outer tube under these conditions. Knowing the watts developed in the inner charge per unit field at its surface, it is then possible to deduce the watts in the inner charge per unit field outside the outer tube. Comparison of the watts in the two cylinders then indicates the practical possibility of eddy current heating the inner cylinder, while a study of the variations of the two quantities with frequency enables the optimum conditions to be determined. Under certain conditions it is sufficient for practical purposes to use for the watts developed in the outer tube and for penetration through it formulæ as given in (6) for the empty tube. It is shown in what types of system this

is sufficient, and in what types it is important to utilize the present theory. Two examples of the latter type of system are examined in some detail. A brief account is given of practical work which confirms the conclusions regarding the behaviour of one system of this type.

In conclusion, the author desires to tender his acknowledgments to the General Electric Company and the Marconiphone Company, on whose behalf the work was done which has led to this publication.

References.

(1) McLachlan, ' Theory of Bessel Functions for Engineers.' Oxford, 1934, p. 142.
(2) J. Grieg, ' World Power,' vol. xxv. pp. 246 and 315 (1936).
(3) Burch and Davis, ' Introduction to Theory of Eddy-Current Heating.' Benn, 1928.
(4) McLachlan, Phil. Mag. xviii. p. 610 (1934).
(5) McLachlan, Phil. Mag. xix. p. 846 (1935).
(6) Oatley, Phil. Mag. xxii. p. 445 (1936).
(7) Dannatt, J.I.E.E. lxxix. p. 667 (1936).
(8) Schelkunoff, Bell System Techn. Journal, xiii. p. 532 (1934)

II. *Periodic Motion in Functional Dynamics.*

By W. H. Watson, *McGill University, Montreal* *.

THE system of functional dynamics dealt with here is due to Volterra †, and has been discussed by the present writer mainly in connexion with the representation of electromagnetic fields ‡. It is with the same general aim that the application of the equations of motion is attempted now in vibration problems, because of their importance as the basis of a theory of functional optics.

We have to treat the motion of a line represented analytically by giving the coordinates (x, y, z) of any one of its points as functions of the pair of independent variables u and v. To a line L in xyz-space there corresponds a line λ in uv-space, and it is desired to investigate motions in which the functional dependent variables

* Communicated by the Author.
† Volterra, ' Theory of Functionals,' p. 156.
‡ Trans. Roy. Soc. Can. 28, iii. p. 1 (1934), referred to as I; Phil. Trans. A, vol. ccxxxvi. p. 155 (1937), referred to as II.

such as $\iint dy\,dz$ (integrated between L_0 and L_1) depend in some periodic way on the functional independent variable $\iint du\,dv$ (integrated between λ_0 and λ_1).

1. *A Kinematic Analogue of the Simple Harmonic Motion of a Particle.*

Consider the motion of a line on a sphere with constant velocity H. The reader is referred to II for the definition of the notation employed. Let X, Y, Z be the direction cosines of the normal to the sphere at (x, y, z); then

$$H^2=(y, z)^2+(z, x)^2+(x, y)^2, \quad (y, z)=HX \text{ etc.} \quad (1)$$

Let S be the area of the sphere described between the epochs λ_0 and λ_1, and let Ω be the solid angle subtended at the centre of the sphere by that portion of its surface traversed between L_0 and L_1. If R is the radius of the sphere

$$R^2\Omega=S=\iint H\,du\,dv, \quad . \quad . \quad . \quad . \quad (2)$$

i. e.,

$$H=R^2\frac{d\Omega}{d(uv)}=R^2\omega. \quad . \quad . \quad . \quad . \quad . \quad (3)$$

The " angular velocity " ω is therefore constant.

From equation II (38), since H is assumed independent of u and v, the acceleration of the line at (x, y, z) is given by

$$a_x=K_mH^2X, \quad a_y=K_mH^2Y, \quad a_z=K_mH^2Z. \quad . \quad (4)$$

K_m, being the mean curvature of the trajectory of the line, is equal to $1/R$. From (3) and (4) we have, for example,

$$a_z=R^3\omega^2Z, \quad . \quad . \quad . \quad . \quad . \quad . \quad (5)$$

while

$$(y, z)=HX=R^2\omega X. \quad . \quad . \quad . \quad . \quad . \quad (6)$$

Now let the line M move on the yz-plane in such a way as to be the orthogonal projection of L on that plane. The acceleration of M parallel to z at (y, z) is

$$(a_z)_M=((z, y), y)=-H(X, y)=-R^3\omega(X, Y). \quad . \quad (7)$$

Since the acceleration parallel to z must be the same for L and M, we have from (5) and (7)

$$(X, Y)=-\omega Z, \quad . \quad . \quad . \quad . \quad . \quad . \quad (8)$$

and similarly

$$(Z, X) = -\omega Y, \quad . \quad . \quad . \quad . \quad . \quad . \quad (9)$$

while from (6)

$$(Y, Z) = \omega X. \quad . \quad . \quad . \quad . \quad . \quad . \quad . \quad (10)^*$$

We are, of course, interested in the motion of the line M on the yz-plane ; its velocity at (y, z) is given by

$$(y, z) = R\omega x = R^2\omega\sqrt{1-\frac{y^2+z^2}{R^2}}. \quad . \quad . \quad . \quad (11)$$

Integrating, we have

$$\iint\frac{dy\,dz}{\sqrt{1-\frac{y^2+z^2}{R^2}}} = R^2\omega\iint du\,dv = R^2\Omega. \quad . \quad (12)$$

We wish to invert this formula to obtain $\iint dy\,dz$ in terms of the functional Ω. Transforming to spherical polar coordinates (R, θ, ϕ), with x as polar axis, we have from (11) and (3)

$$\left.\begin{aligned} dy\,dz &= R^2\iint\cos\theta\,d\Omega, \\ d\Omega &= \sin\theta\,d\theta\,d\phi. \end{aligned}\right\} \quad . \quad . \quad . \quad . \quad (13)$$

Now the second member of (13) is an integral of the general type,

$$\iint S_n S_m\,d\Omega,$$

where S_n and S_m are surface harmonics, and vanishes when integrated over the whole solid angle. Thus, while $\iint du\,dv$ may increase indefinitely as L moves over the sphere, $\iint dy\,dz$ is always bounded, the line M is confined within the circle of radius R on the yz-plane, and the projection of the yz-plane on the uv-plane is multiple-valued. To one line on the yz-plane correspond a family of lines on the uv-plane such that successive members of the family enclose an area of plane $4\pi/\omega$. This number may be spoken of as the " period " of the motion.

2. *Dynamical Analogue of Simple Pendulum.*

Let us consider the oscillation of a line on a surface of constant mean curvature. In accordance with II (38)

* These equations should be compared with the Poisson bracket relations for angular momentum in dynamics.

the acceleration of the line at one of its points (x, y, z) is

$$a_x = K_m H^2 X + Y(z, H) - Z(y, H), \text{ etc.},$$

and the acceleration in the direction (λ, μ, ν)

$$\begin{aligned} a_{\lambda\mu\nu} &= \lambda a_x + \mu a_y + \nu a_z \\ &= (x, H)(\mu Z - \nu Y) + (y, H)(\nu X - \lambda Z) + (z, H)(\lambda Y - \mu X) \\ &\qquad + K_m H^2(\lambda X + \mu Y + \nu Z). \quad (14) \end{aligned}$$

Suppose that the line, constrained to move on the given surface, does so under the action of a force F parallel to the fixed direction (a, b, c). Equating $\kappa a^{\lambda}{}_{\mu\nu}$ and the component of F in the direction (λ, μ, ν) where κ is the inertial coefficient of the line, we have with $f = F/\kappa$

$$f(a\lambda + b\mu + c\nu) = \Sigma(x, H)(\mu Z - \nu Y) + K_m H^2(\Sigma\lambda X)$$

or

$$\Sigma\lambda[fa - K_m H^2 X - Y(z, H) + Z(y, H)] = 0. \quad . \quad . \quad (15)$$

The equations of motion are given by equating to zero the coefficients of λ, μ, and ν in (15). For small oscillations the motion is considered in the neighbourhood of a point on the surface where f is normal to it. Let us choose the coordinate axes so that $a=1$, $b=0$, $c=0$; the variations in x are small compared with the variations in y and z. The approximate equations are

$$\left.\begin{aligned} f - K_m H^2 X - Y(z, H) + Z(y, H) &= 0, \\ -K_m H^2 Y + X(z, H) &= 0, \\ -K_m H^2 Z - X(y, H) &= 0. \end{aligned}\right\} \quad . \quad . \quad (16)$$

From (16) we immediately deduce

$$Xf = K_m H^2 \quad . \quad . \quad . \quad . \quad . \quad . \quad (17)$$

and

$$\left.\begin{aligned} (z, H) &= fY, \\ (y, H) &= -fZ. \end{aligned}\right\} \quad . \quad . \quad . \quad . \quad . \quad (18)$$

Hence

$$\left.\begin{aligned} (z, \tfrac{1}{2}H^2) &= f(z, x), \\ (y, \tfrac{1}{2}H^2) &= f(y, x). \end{aligned}\right\} \quad . \quad . \quad . \quad . \quad . \quad (19)$$

Since y and z can be varied at will on the surface, we obtain

$$\tfrac{1}{2}H^2 - fx = \text{constant}. \quad . \quad . \quad . \quad . \quad . \quad (20)$$

and since in our approximation $H=(y, z)$,

$$\tfrac{1}{2}(y, z)^2-fx=\text{constant}. \qquad (21)$$

For a *spherical surface* of radius R

$$\tfrac{1}{2}(y, z)^2-f\sqrt{R^2-(y^2+z^2)}=\text{constant},$$

and approximately

$$\tfrac{1}{2}(y,z)^2+\frac{1}{2}\frac{f}{R}(y^2+z^2)=\text{constant}. \qquad (22)$$

The Hamiltonian function for this motion on the yz-plane is

$$\tfrac{1}{2}(y, z)^2+\tfrac{1}{2}n^2(y^2+z^2), \qquad n^2=f/R,$$

or, in polar coordinates,

$$r^2=y^2+z^2, \ \tan\phi=y/z,$$

$$H(p, r, \phi)=\frac{1}{2}\frac{p^2}{r^2}+\tfrac{1}{2}n^2r^2. \qquad (23)$$

The Volterra equations of motion give

$$\left.\begin{aligned} &\text{(i.)} \quad (r, \phi)=\frac{\partial H}{\partial p}=\frac{p}{r^2}, \\ &\text{(ii.)} \quad (p, \phi)=-\frac{\partial H}{\partial r}=\frac{p^2}{r^3}-n^2r, \\ \text{and} \quad &\text{(iii.)} \quad (p, r)=\frac{\partial H}{\partial \phi}=0. \end{aligned}\right\} \qquad (24)$$

From (iii.) $p=\psi(r)$. Substitute in (ii.)

$$\psi'(r)(r, \phi)=\frac{p^2}{r^3}-n^2r,$$

$$\frac{\psi'(r)\psi(r)}{r^2}=\frac{[\psi(r)]^2}{r^3}-n^2r,$$

or

$$\frac{d}{dr}\left[\left(\frac{\psi(r)}{r}\right)^2\right]=-2n^2r.$$

$$\therefore \quad \frac{[\psi(r)]^2}{r^2}=C-n^2r^2, \qquad (25)$$

where C is a constant. Writing $C=n^2B^2$, we have

$$\psi(r)=nr\sqrt{B^2-r^2},$$

and from (24) (i.)

$$r\,dr\,d\phi = n\sqrt{\mathrm{B}^2 - r^2}\,du\,dv \quad . \quad . \quad . \quad . \quad . \qquad (26)$$

Let $r = \mathrm{B}\sin\theta$, then

$$d\Omega = \sin\theta\,d\theta\,d\phi = \frac{n}{\mathrm{B}}\,du\,dv \quad . \quad . \quad . \quad . \qquad (27)$$

and

$$dy\,dz = \mathrm{B}^2\,d\Omega\cos\theta. \quad . \quad . \quad . \quad . \quad . \quad . \qquad (28)$$

This equation is the same as (13); its solution therefore corresponds to the orthogonal projection on the yz-plane of the motion of a line describing a sphere of radius B with constant "angular velocity" $\frac{n}{\mathrm{B}} = \omega$.

[As regards the explicit solution for y and z in terms of u and v, one possible solution is

$$\left.\begin{aligned} y &= \mathrm{B}\sqrt{1-u^2}\cos\omega v, \\ z &= \mathrm{B}\sqrt{1-u^2}\sin\omega v, \end{aligned}\right\} \quad . \quad . \quad . \quad . \quad . \qquad (29)$$

a form which presupposes, of course, that u never exceeds unity. The corresponding value of (y, z) is $\omega\mathrm{B}^2 u$.]

3. *Analogue of the Propagation of Transverse Waves along a Taut Wire.*

In the place of the wire under tension, let us consider a membrane which, when undisturbed, has a constant surface tension T over its area S. The membrane, being free except at its boundary, must have the form of a minimal surface. Following the method of Tait's proof for the wire, let us imagine the membrane to be drawn through the gap between two surfaces Σ and Σ', one of which can be regarded as the mould for producing the other. The membrane will be deformed so that its mean curvature at (x, y, z) is K_m—that of the deforming surfaces at that point. We can regard the lines composing the membrane as moving along the surface Σ. The acceleration normal to Σ at xyz is

$$a_n = \mathrm{K}_m \mathrm{V}^2,$$

where V is the velocity of line at that point on Σ. The normal component of force per unit area due to the distortion of the membrane is $\mathrm{K}_m\mathrm{T}$. If at each point of the membrane

$$\kappa a_n = \mathrm{K}_m \mathrm{T} \quad . \quad . \quad . \quad . \quad . \quad . \quad . \quad . \qquad (30)$$

(where κ is the inertial coefficient per unit area of the membrane), the deforming surfaces Σ and Σ' may be removed, and V becomes the functional velocity with which the deformation is propagated over the membrane, and is given by

$$V=\sqrt{\frac{T}{\kappa}} \quad . \quad . \quad . \quad . \quad . \quad . \quad . \quad (31)$$

In forming the equations of motion for this supposed functional vibration of the membrane, let us in the interest of simplicity dispense with the complicated geometrical questions arising in the case of the general minimal surface and treat the membrane whose equilibrium configuration is the xy-plane. Corresponding to a particular value of u and of v, the point which was at $(x, y, 0)$ is displaced to the point P $(x+\xi, y+\eta, \zeta)$. The acceleration of any line of the membrane passing through P will have as components a_1, a_2, a_3 parallel to the axes of references, where

$$a_1=((\xi, \eta), \eta)+((\xi, \zeta), \zeta), \text{ etc.}$$

Let (X, Y, Z) be the direction cosines of the deformed membrane at P, then

$$\left.\begin{aligned} \kappa a_1 &= -\mathrm{TK}_m\mathrm{X}, \\ \kappa a_2 &= -\mathrm{TK}_m\mathrm{Y}, \\ \kappa a_3 &= -\mathrm{TK}_m\mathrm{Z}. \end{aligned}\right\} \quad . \quad . \quad . \quad . \quad . \quad (32)$$

It is assumed that T remains uniform over the deformed membrane. We have to determine K_m, X, Y, and Z in terms of the deformation, ξ, η, ζ being regarded as functions of x and y. In the expressions a_1, a_2, and a_3 we consider the dependence of ξ, η, and ζ on u and v.

For the deformed surface we have

$$\mathrm{E}=\left(1+\frac{\partial\xi}{\partial x}\right)^2+\left(\frac{\partial\eta}{\partial x}\right)^2+\left(\frac{\partial\zeta}{\partial x}\right)^2,$$

$$\mathrm{G}=\left(\frac{\partial\xi}{\partial y}\right)^2+\left(1+\frac{\partial\eta}{\partial y}\right)^2+\left(\frac{\partial\zeta}{\partial y}\right)^2.$$

$$\mathrm{F}=\left(1+\frac{\partial\xi}{\partial x}\right)\frac{\partial\xi}{\partial y}+\left(1+\frac{\partial\eta}{\partial y}\right)\frac{\partial\eta}{\partial x}+\frac{\partial\zeta}{\partial x}\cdot\frac{\partial\zeta}{\partial y},$$

$$\mathrm{X}=\frac{1}{\mathrm{H}}\left(\frac{\partial(\eta, \zeta)}{\partial(x, y)}-\frac{\partial\zeta}{\partial x}\right),$$

$$Y=\frac{1}{H}\left(\frac{\partial(\zeta,\xi)}{\partial(x,y)}-\frac{\partial\zeta}{\partial y}\right),$$

$$Z=\frac{1}{H}\left(1+\frac{\partial\xi}{\partial x}+\frac{\partial\eta}{\partial y}+\frac{\partial(\xi,\eta)}{\partial(x,y)}\right),$$

$$D=X\frac{\partial^2\xi}{\partial x^2}+Y\frac{\partial^2\eta}{\partial x^2}+Z\frac{\partial^2\zeta}{\partial x^2}.$$

$$D'=X\frac{\partial^2\xi}{\partial x\,\partial y}+Y\frac{\partial^2\eta}{\partial x\,\partial y}+Z\frac{\partial^2\zeta}{\partial x\,\partial y},$$

$$D''=X\frac{\partial^2\xi}{\partial y^2}+Y\frac{\partial^2\eta}{\partial y^2}+Z\frac{\partial^2\zeta}{\partial y^2},$$

E, G, F, H, X, Y, Z, and D, D′, D″ being given their usual meaning in differential geometry.

Finally,

$$K_m=\frac{2FD'-ED''-GD}{H}.$$

Now if the displacements are all small, we take $E=1$, $G=1$, $F=0$, etc., and

$$K_m=-\left(\frac{\partial^2\zeta}{\partial x^2}+\frac{\partial^2\zeta}{\partial y^2}\right) \quad . \quad . \quad . \quad . \quad (33)$$

approximately. In a functional displacement, however, ξ and η need not be small, but ζ is necessarily so, for we have dealt only with a small distortion of the membrane. The formula (33) still gives K_m for the deformed membrane at P provided that in calculating the differential coefficients of ζ we give x and y the values $x+\xi$ and $y+\eta$ respectively.

The principal equation is evidently the third of (32), viz.,

$$\kappa[((\zeta,\eta),\eta)+((\zeta,\xi),\xi)]=T\left(\frac{\partial^2\zeta}{\partial x^2}+\frac{\partial^2\zeta}{\partial y^2}\right) . \quad . \quad (34)$$

If we now require that the motion be a vibration of the type we have discussed in § 2, we have

$$\left.\begin{aligned}(\xi,\eta)&=Rn\left(1-\frac{\xi^2+\eta^2}{R^2}\right)^{\frac{1}{2}},\\ (\eta,\zeta)&=Rn\left(1-\frac{\eta^2+\zeta^2}{R^2}\right)^{\frac{1}{2}},\\ (\zeta,\xi)&=Rn\left(1-\frac{\zeta^2+\xi^2}{R^2}\right)^{\frac{1}{2}},\end{aligned}\right\} \quad . \quad . \quad . \quad . \quad (35)$$

and

$$a_1 = -n^2\xi, \quad a_2 = -n^2\eta, \quad a_3 = -n^2\zeta. \quad . \quad . \quad . \quad (36)$$

Hence (34) becomes

$$-n^2\zeta = \frac{\mathrm{T}}{\kappa}\left(\frac{\partial^2\zeta}{\partial x^2} + \frac{\partial^2\zeta}{\partial y^2}\right), \quad . \quad . \quad . \quad . \quad . \quad (37)$$

which is the form of equation satisfied by the amplitude of the displacement in the ordinary acoustical vibration of a membrane.

The dependence of ξ and η on u and v is given by the first two equations of (32) combined with (36), namely,

$$-\kappa n^2\xi = -\mathrm{TK}_{'''}\mathrm{X} = -\kappa n^2\zeta\mathrm{X}$$

or

$$\xi = \zeta\mathrm{X}. \quad . \quad . \quad . \quad . \quad . \quad . \quad . \quad . \quad . \quad (38)$$

Since X and ζ are both of the first order of small quantities, ξ, and similarly η, is of the second order of smallness.

In consequence of this last deduction we have to admit that although we have employed the equations of functional dynamics in treating the deformation of a membrane, the vibration of lines which is allowed by the equations produces the usual nodal figures for stationary vibration of the membrane. Roughly speaking we may say that the functional problem has degenerated into an ordinary problem, because one of the independent variables of the functional problem has not been allowed to vary except to the first order of smallness.

If we consider longitudinal vibrations of a lamina which we have endowed with elastic properties, as in the theory of vibrations of an elastic solid, we shall find a similar state of affairs. This is because we are dealing with equations of motion which, when transformed by equations of the type (35), degenerate into those of the ordinary dynamical problem. The mathematical barrier we have to surmount is associated with the assumption, inherent in Volterra's equations, that the acceleration is a function of a point only. The possibility of making another assumption which will take us away from linear functionals has been discussed in II. The value of the present investigation lies in showing that the analogue of simple harmonic motion discussed in § 1 of this paper, attractive though it may be, will not do for us what is achieved by the explicit relation of two functionals (namely, the displacement and the analogue of the time) by means of a sine or other harmonic function.

III. *The Potential of a Screen of Circular Wires between two Conducting Planes.* *By* R. C. KNIGHT, *M.Sc., Ph.D., and* B. W. McMULLEN, *B.Sc.**

Introduction.

THE potential problem of an infinite row of circular wires situated between two infinite planes reduces to one in two dimensions, in which the boundaries are a row of circles between two parallel straight lines. In this form it has been previously stated †. It may also be regarded as an extension of an earlier paper by one of the authors ‡. The type of boundary conditions assumed is that of constant potential on the wires and on the planes, but in general the three values are different. The harmonic functions necessary for our problem will be given in the general form when the circles are not symmetrically placed between the lines, but the absence of numerical tables of the elliptic functions used has compelled us to restrict the numerical solution to the case when the line of centres of the circles is midway between the parallel lines. The results obtained enable us to compare the capacity of one of the wires with that of a single wire placed between infinite parallel planes ‡. The variation of potential along a line perpendicular to the planes and passing through the axis of one of the wires will be given and the form of the equipotentials shown.

The method consists in constructing harmonic functions having singularities of the correct type at the centres of the circles and producing zero potential on the straight lines. These functions are multiplied by constants and added to the function which produces the required value on the lines. The constants are then determined by an approximation method ‡ so as to give the desired boundary condition on the circle.

The Potential Functions.

We suppose the plane in which the two-dimensional problem is considered to be that of $z=x+iy=re^{i\theta}$.

* Communicated by the Authors.

† R. C. J. Howland and B. W. McMullen, Proc. Camb. Phil. Soc. xxxii. pp. 402–415 (1936).

‡ R. C. Knight, Proc. Lond. Math. Soc. (2) xxxix. pp. 272–281 (1935).

In this plane let the circles, each of radius b, have their centres at the points $2nai+\xi$, ξ being real and n having all positive and negative integral values including zero. Let the straight boundaries be defined by $x=\pm c$ (fig. 1).

We require a solution of

$$\nabla^2 V=\frac{\partial^2 V}{\partial x^2}+\frac{\partial^2 V}{\partial y^2}=0, \quad . \quad . \quad . \quad . \quad (1)$$

with the following boundary conditions :

(*a*) $V=v_w$ (constant) when $|z-2nai-\xi|=b$,

(*b*) $V=v_p$ (constant) when $z=c$,

$=0$ when $z=-c$.

Fig. 1.

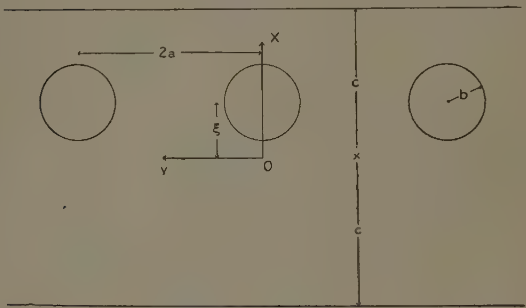

Before satisfying the condition (*b*) we shall construct potential functions having zero value on both the straight lines. To do this we take an image system of line charges along lines perpendicular to the z-plane and passing through the singular points. Without loss of generality we consider the line charges to be of unit strength. The system is composed of

1. Positive line charges at $4mc+2nai+\xi$,
2. Negative line charges at $(2m+1)2c+2nai-\xi$.

The required function is then the real part of the complex function $W(z)$ where, apart from a constant

$$W(z)=-\log(z-\xi)\Pi'(z-\xi-\Omega_{m,n})$$
$$+\log(z-2e+\xi)\Pi'(z-2c+\xi-\Omega_{m,n}),$$

where $\Omega_{m,n}=4mc+2nai=2m\omega_1+2n\omega_2$ and the Π' denotes the infinite product over all positive and negative integral values of m and n except for $m=0$, $n=0$ together.

We have

$$\mathrm{W}(z)=-\log(z-\xi)\Pi'\left\{1-\frac{z-\xi}{\Omega_{m,n}}\right\}$$
$$+\log(z-2c+\xi)\Pi'\left\{1-\frac{z-2c+\xi}{\Omega_{m,n}}\right\}$$
$$=-\log\sigma(z-\xi)+\log\sigma(z-2c+\xi)+4c_1(c-\xi)(z-c), \quad (2)$$

where $\sigma(z)$ is the elliptic function of periods ω_1, ω_2, and

$$c_1=\tfrac{1}{2}\Sigma'\Omega^{-2}_{m,n}. \quad . \quad . \quad . \quad . \quad . \quad . \quad (3)$$

In the above equation (2) we neglected a constant. We may add any constant to W(z) to produce our required value of V on the straight lines. It is easily seen that the constant in this case is zero.

We now transfer our origin to the centre of one of the circles, *i. e.*, define new variables

$$\zeta=z-\xi,\ d=c-\xi. \quad . \quad . \quad . \quad . \quad . \quad . \quad (4)$$

Then

$$\mathrm{W}(\zeta)=-\log\sigma(\zeta)+\log\sigma(\zeta-2d)+4c_1d(\zeta-d). \quad . \quad (5)$$

We require an expansion of W(ζ) valid near $\zeta=0$, and to obtain this we proceed in the following way. For the first term we may use the series *

$$\log\sigma(z)=\log z-\sum_{n=2}^{\infty}c_nz^{2n},$$

where

$$c_n=\frac{1}{2n}\Sigma'\Omega^{-2n}_{m,n} \quad (n>1). \quad . \quad . \quad . \quad . \quad (6)$$

In particular the coefficients c_2 and c_3 are given by

$$c_2=\frac{1}{240}g_2,\ c_3=\frac{1}{840}g_3, \quad . \quad . \quad . \quad . \quad (7)$$

where g_2, g_3 are the invariants of the elliptic functions

* Tannery et Molk, 'Fonctions Elliptiques,' vol. i. p. 178 (Paris, 1893).

with periods ω_1, ω_2. If these are known the other coefficients may be determined from the relation

$$c_n=\{3/(2n)(2n+1)(2n-1)(n-3)\}$$
$$\sum_{r=2}^{n-2} 2r(2r-1)(2n-2r)(2n-2r-1)c_r c_{n-r} \quad (n>3)\ . \quad (8)$$

The same series cannot be used for expanding the secondary term in (5), as it is not convergent for $\zeta=2d$; we therefore use

$$\log \sigma(\zeta-2d)=\sum_{n=0}^{\infty}\frac{1}{n\,!}\frac{d^n}{d\zeta^n}\,[\log \sigma(\zeta-2d)]_{\zeta=0}\zeta^n$$
$$=\sum_{n=0}^{\infty}\frac{a_n}{n\,!}\zeta^n, \quad . \ . \ . \ . \ . \ . \ . \ . \quad (9)$$

where

$$\left.\begin{array}{l} a_0=\log \sigma(-2d),\quad a_1=\zeta(-2d),\quad a_2=-\wp(-2d),\\ \qquad a_n=-\wp^{(n)}(-2d) \quad (n\geqslant 3), \end{array}\right\} \quad (10)$$

and $\zeta(z)$, $\wp(z)$ are the well-known elliptic functions whose periods here are ω_1 and ω_2.

Hence our required complex potential function is

$$W_0(\zeta)=-\log \zeta+\sum_{n=2}^{\infty} c_n\zeta^{2n}+\sum_{n=0}^{\infty}\frac{a_n}{n\,!}\zeta^n+4c_1d(\zeta-d). \quad (11)$$

Further potential functions satisfying the same condition of zero value on the straight lines are defined by

$$W_s(\zeta)=\frac{(-)^s(2d)^s}{(s-1)\,!}\frac{d^s}{d\zeta^s}[W_0(\zeta)]. \quad . \ . \ . \quad (12)$$

The equations (11) and (12) may be formally written

$$W_0(\zeta)=-\log (\zeta/2d)+\sum_{n=0}^{\infty} {}_0A_n(\zeta/2d)^n,$$

$$W_s(\zeta)=(2d/\zeta)^s+\sum_{n=0}^{\infty} {}_sA_n(\zeta/2d)^n,$$

where the new coefficients ${}_sA_n$ depend upon the c_n and d_n and also upon d. They are real, and our required potential functions have the form, given by $V_s=\mathbf{R}\{W_s(\zeta)\}$,

$$V_0=-\log (r/2d)+\sum_{n=0}^{\infty} {}_0A_n(r/2d)^n \cos n\theta,$$

$$V_s=(2d/r)^s \cos s\theta+\sum_{n=0}^{\infty} {}_sA_n(r/2d)^n \cos n\theta.$$

These functions are in the form required for combination to give any desired conditions on the circles which may be produced by potential functions assumed to give values on the lines other than zero. The functions are restricted by a symmetry condition that necessitates the same boundary conditions on each of the circles.

In the general case for any value of $\xi < c$ the evaluation of the coefficients ${}_sA_n$ presents much difficulty. We have been unable to find tables of the elliptic functions suitable for this work, and even in the symmetrical case ($\xi = 0$) the numerical work involved in the calculation of the coefficients has been considerable. We shall now discuss this case.

The Symmetrical Case.

When the centres of the circles are situated midway between the straight lines $\xi = 0$, and hence $\zeta = z$, $d = c$. The coefficients c_n are unaltered, and may be evaluated in the following manner.

We write

$$a/2c = \omega_2/\omega_1 i = \lambda. \quad . \quad . \quad . \quad . \quad . \quad (13)$$

Then

$$\Sigma' \Omega_{m,n}^{-2} = \Sigma' \{4mc + 2nai\}^{-2}$$

$$= \frac{1}{16c^2} \Sigma' \frac{m^2 - n^2\lambda^2}{(m^2 + n^2\lambda^2)^2}$$

$$= \frac{1}{16c^2} \left\{ 2(1 - \lambda^{-2}) \sum_{m=1}^{\infty} \frac{1}{m^2} + 4 \sum_{n=1}^{\infty} \sum_{m=1}^{\infty} \frac{m^2 - n^2\lambda^2}{(m^2 + n^2\lambda^2)^2} \right\}. \quad . \quad . \quad . \quad (14)$$

Consider the series *

$$\sum_{m=1}^{\infty} (m^2 + x^2\lambda^2)^{-1} = -(1/2\lambda^2 x^2) + (\pi/2\lambda x) \coth \lambda\pi x,$$

and differentiate this with respect to x. We obtain

$$\sum_{m=1}^{\infty} (m^2 + x^2\lambda^2)^{-2} = -(1/2\lambda^4 x^4) + (\pi/4\lambda^3 x^3) \coth \lambda\pi x$$
$$+ (\pi/4\lambda^3 x^2) \operatorname{cosech}^2 \lambda\pi x.$$

* Whittaker and Watson, 'Modern Analysis,' p. 136 (Camb., 1920).

If we replace x by n in the above result, and substitute into equation (14), we get, after some reduction,

$$\Sigma'\Omega_{n,\,m}^{-2}=\frac{\pi^2}{(4c)^2}\left\{\frac{1}{3}-2\sum_{n=1}^{\infty}\operatorname{cosech}^2 n\pi\lambda\right\}.$$

In a similar manner we may show that

$$\Sigma'\Omega_{m,\,n}^{-4}=\frac{\pi^4}{(4c)^4}\left\{\frac{1}{45}-\frac{2}{3}\sum_{n=1}^{\infty}(2\operatorname{cosech}^2 n\pi\lambda+3\operatorname{cosech}^4 n\pi\lambda)\right\},$$

$$\Sigma'\Omega_{m,\,n}^{-6}=\frac{\pi^6}{(4c)^6}\left\{\frac{2}{945}-\frac{2}{15}\sum_{n=1}^{\infty}(2\operatorname{cosech}^2 n\pi\lambda+15\operatorname{cosech}^4 n\pi\lambda+15\operatorname{cosech}^6 n\pi\lambda)\right\}. \quad . \; . \; . \quad (15)$$

The series in equations (15) enable us to calculate the coefficients c_1, c_2, and c_3, and hence c_n ($n>3$), using equation (8).

The coefficients a_n are somewhat simplified, since $2d=2c=\omega_1$, which is half the real period of the elliptic functions. We have

$$a_0=\log\sigma(\omega_1)$$

$$=\log\frac{2\omega_1}{\pi}+\frac{\eta_1\omega_1}{2}+\sum_{n=1}^{\infty}\log\coth^2 n\pi\lambda\,{}^{*} \quad . \quad (16.1)$$

$$=\log\frac{4c}{\pi}+4c^2c_1+\sum_{n=1}^{\infty}\log\coth^2 n\pi\lambda,$$

since

$$\eta_1=\zeta(\omega_1)=2c\Sigma'\Omega_{m,\,n}^{-2}=4cc_1.$$

$$a_1=-\zeta(\omega_1)=-\eta_1$$

$$=-4cc_1.$$

$$a_2=-\wp(\omega_1)=e_1$$

$$=-\frac{\eta_1}{2c}+\left(\frac{\pi}{4c}\right)^2-2\left(\frac{\pi}{2c}\right)^2\Sigma(-)^n n\,(\coth n\pi\lambda-1).\;{}^{\dagger}(16.2)$$

$$a_3=\wp'(\omega_1)=0.$$

* *Ibid.* p. 448.

† Whittaker and Watson, p. 460; see also Tannery et Molk, 'Fonctions Elliptiques,' vol. i. p. 198.

The coefficients a_n, $n>3$ can be expressed as polynomials in e_1 when n is even and as $\wp'(\omega_1)$ multiplied by polynomials in e_1 when n is odd. Consequently

$$\begin{aligned} a_{2n+1} &= 0 \quad (n \geqslant 1), \\ a_{2n} &= \text{polynomial in } e_1 \quad (n \geqslant 2). \end{aligned}$$

The coefficient a_n can therefore be evaluated when a_0, a_1, a_2 have been found.

The first potential function is now

$$\begin{aligned} W_0(z) &= -\log z + \sum_{n=2}^{\infty} c_n z^{2n} + \sum_{n=1}^{\infty} \frac{a_n}{n!} z^n + 4c_1 c(z-c) \\ &= -\log \frac{z}{2c} + \sum_{n=0}^{\infty} {}_0\alpha_{2n} \left(\frac{z}{2c}\right)^{2n}, \qquad (17) \end{aligned}$$

where

$$\left.\begin{aligned} {}_0\alpha_0 &= a_0 - \log 2c - 4c_1 c^2 \\ &= \log \frac{\pi}{2} + \sum_{1}^{\infty} \log \coth^2 n\pi\lambda ; \\ {}_0\alpha_{2n} &= \{c_n + a_n/n!\}(2c)^{2n} \quad (n>0). \end{aligned}\right\} \qquad (18)$$

The other potential functions as defined by equation (12) now become,

when s is even,

$$\begin{aligned} W_{2s}(z) &= \left(\frac{z}{2c}\right)^{-2s} + \sum_{n=0}^{\infty} \frac{(2n+2s)!}{(2n)!\,(2s-1)!}\, {}_0\alpha_{2n+2s} \left(\frac{z}{2c}\right)^{2n} \\ &= \left(\frac{z}{2c}\right)^{-2s} + \sum_{n=0}^{\infty} {}_{2s}\alpha_{2n} \left(\frac{z}{2c}\right)^{2n} ; \qquad (19.1) \end{aligned}$$

when s is odd,

$$\begin{aligned} W_{2s+1} &= \left(\frac{z}{2c}\right)^{-2s-1} - \sum_{n=0}^{\infty} \frac{(2n+2s+2)!}{(2n+1)!\,(2s)!}\, {}_0\alpha_{2n+2s+2} \left(\frac{z}{2c}\right)^{2n} \\ &= \left(\frac{z}{2c}\right)^{-2s-1} - \sum_{n=0}^{\infty} {}_{2s+1}\alpha_{2n+1} \left(\frac{z}{2c}\right)^{2n+1}. \qquad (19.2) \end{aligned}$$

The new coefficients being given by

$$\left.\begin{aligned} {}_{2s}\alpha_{2n} &= 2s \binom{2n+2s}{2n} {}_0\alpha_{2n+2s}, \\ {}_{2s+1}\alpha_{2n+1} &= (2s+1) \binom{2n+2s+2}{2n+1} {}_0\alpha_{2n+2s+2}. \end{aligned}\right\} \qquad (20)$$

We note that

$$ {}_{2s}\alpha_{2n} = {}_{2n+1}\alpha_{2s+1}. \quad . \quad . \quad . \quad . \quad . \quad (20.1) $$

Taking the real parts of the complex functions given by (17) and (19) we get the potential functions necessary to our problem. These are

$$ \left. \begin{aligned} V_0 &= -\log \rho + \sum_{n=0}^{\infty} {}_0\alpha_{2n}\rho^{2n} \cos 2n\theta, \\ V_{2s} &= \rho^{-2s} \cos 2s\theta + \sum_{n=0}^{\infty} {}_{2s}\alpha_{2n}\rho^{2n} \cos 2n\theta, \\ V_{2s+1} &= \rho^{-2s-1} \cos (2s+1)\theta - \sum_{n=0}^{\infty} {}_{2s+1}\alpha_{2n+1}\rho^{2n+1} \cos (2n+1)\theta, \end{aligned} \right\} \quad . \quad . \quad . \quad (21) $$

where $\rho = | z | 2c |$.

These functions have the property that they produce zero potential on $z = \pm c$, so that our final potential function will be given by

$$ V = V' + V'', \quad . \quad . \quad . \quad . \quad . \quad . \quad (22) $$

where $V' = v_p(\frac{1}{2} + \rho \cos \theta)$, in order that the boundary conditions (*b*) shall be satisfied ; and

$$ V'' = \sum_{s=0}^{\infty} A_s V_s. $$

The A_s being constants, which have to be determined to satisfy the boundary condition (*a*).

The Determination of the Constants.

Thus, when $r = b$ we have, writing

$$ b/2c = \mu, $$

$$ \begin{aligned} v_u = v_p(\tfrac{1}{2} + \mu \cos \theta) + A_0 \left\{ -\log \mu + \sum_{n=0}^{\infty} {}_0\alpha_{2n}\mu^{2n} \cos 2n\theta \right\} \\ + \sum_{s=1}^{\infty} A_{2s} \left\{ \mu^{-2s} \cos 2s\theta + \sum_{n=0}^{\infty} {}_{2s}\alpha_{2n}\mu^{2n} \cos 2n\theta \right\} \\ + \sum_{s=0}^{\infty} A_{2s+1} \left\{ \mu^{-2s-1} \cos (2s+1)\theta \right. \\ \left. - \sum_{n=0}^{\infty} {}_{2s+1}\alpha_{2n+1}\mu^{2n+1} \cos (2n+1)\theta \right\}. \end{aligned} $$

The equations which the constants must satisfy are therefore

$$\left.\begin{aligned}
v_w-\tfrac{1}{2}v_p&=-A_0\log\mu+\sum_{s=0}{}_{2s}\alpha_0A_{2s}\\
-v_p\mu&=\mu^{-1}A_1-\mu\sum_{s=0}^{\infty}{}_{2s+1}\alpha_1A_{2s+1}\\
0&=\mu^{-2n}A_{2n}+\mu^{2n}\sum_{s=0}^{\infty}{}_{2s}\alpha_{2n}A_{2s}\quad(n\geqslant1),\\
0&=\mu^{-2n-1}A_{2n+1}-\mu^{2n+1}\sum_{s=0}^{\infty}{}_{2s+1}\alpha_{2n+1}A_{2s+1}\quad(n\geqslant1).
\end{aligned}\right\}\quad\ldots\quad(23)$$

A formal solution of these equations is given by assuming

$$A_n=\sum_{r=0}^{\infty}A_n^{(r)},$$

where

$$\left.\begin{aligned}
&A_0^{(0)}=-(v_w-\tfrac{1}{2}v_p)/\log\mu,\quad A_1^{(0)}=-v_p\mu^2,\\
&\qquad A_n^{(0)}=0\quad(n\geqslant2),\\
&\text{and for } r\geqslant1\\
&A_0^{(r)}=\sum_{s=0}^{\infty}{}_{2s}\alpha_0A_{2s}^{(r-1)}/\log\mu,\\
&A_{2n}^{(r)}=-\mu^{4n}\sum_{s=0}^{\infty}{}_{2s}\alpha_{2n}A_{2s}^{(r-1)}\quad(n\geqslant1),\\
&A_{2n+1}^{(r)}=\mu^{4n+2}\sum_{s=0}^{\infty}{}_{s+1}\alpha_{2n+1}A_{2s+1}\quad(n\geqslant0).
\end{aligned}\right\}\quad.\quad(24)$$

This approximation method can be carried out so long as the ratio μ is not too large. In a case of practical interest this ratio is likely to be very small, and in the numerical example given below the values of the A's can be determined to a sufficient degree of approximation by taking the process as far as $r=5$.

Finally, the expression for the potential can be written

$$V=v_w-B_0\log(\rho/\mu)+\sum_{n=0}^{\infty}B_n\{(\mu/\rho)^n-(\rho/\mu)^n\}\cos n\theta,\quad(25)$$

where
$$B_n=A_n\mu^{-n}.\quad\ldots\ldots\quad(26)$$

TABLE I.—Values of $(-)^{n+s}\,{}_{2s}\alpha_{2n}$.

s.	$n=0$.	$n=1$.	$n=2$.	$n=3$.	$n=4$.	$n=5$.	$n=6$.	$n=7$.
0......	$6{\cdot}1056\times10^{-1}$	$6{\cdot}5803$	$8{\cdot}6513$	$2{\cdot}1742\times10$	$6{\cdot}4153\times10$	$2{\cdot}0519\times10^{2}$	$6{\cdot}8261\times10^{2}$	$2{\cdot}3409\times10^{3}$
1......	$1{\cdot}3161\times10$	$1{\cdot}0382\times10^{2}$	$6{\cdot}5225\times10^{2}$	$3{\cdot}5926\times10^{3}$	$1{\cdot}8467\times10^{4}$	$9{\cdot}0104\times10^{4}$	$4{\cdot}2604\times10^{5}$	
2......	$3{\cdot}4605\times10$	$1{\cdot}3045\times10^{3}$	$1{\cdot}7963\times10^{4}$	$1{\cdot}7236\times10^{5}$	$1{\cdot}3516\times10^{6}$	$9{\cdot}373\times10^{6}$		
3......	$1{\cdot}3045\times10^{2}$	$1{\cdot}0778\times10^{4}$	$2{\cdot}5854\times10^{5}$	$3{\cdot}7844\times10^{6}$	$4{\cdot}218\times10^{7}$			
4......	$5{\cdot}1323\times10^{2}$	$7{\cdot}3869\times10^{4}$	$2{\cdot}7031\times10^{6}$	$5{\cdot}624\times10^{7}$				
5......	$2{\cdot}0519\times10^{3}$	$4{\cdot}5052\times10^{5}$	$2{\cdot}343\times10^{7}$					
6......	$8{\cdot}1913\times10^{3}$	$2{\cdot}5563\times10^{6}$						
7......	$3{\cdot}2773\times10^{4}$							

Numerical Solution.

For the purpose of a numerical example we have taken

$$\lambda = a/2c = 1/4, \quad \mu = b/2c = 1/20.$$

The coefficients c_n given by equations (3) and (6) were calculated from the series (15) using tables * of values of the hyperbolic functions, and were determined correct to six or seven figures. The coefficients a_n were evaluated from the series (16) correct to the same number of figures. From these the coefficients ${}_n\alpha_s$ can be found. The even ones are given in Table I., and are correct to five figures. The odd ones are similar, and may be found using the relation (20.1).

TABLE II.

n.	β_n.	γ_n.
0	$-1{\cdot}387\times10^{-1}$	$2{\cdot}773\times10^{-1}$
1	$4{\cdot}807\times10^{-2}$	
2	$-2{\cdot}280\times10^{-3}$	$4{\cdot}560\times10^{-3}$
3	$-1{\cdot}048\times10^{-5}$	
4	$7{\cdot}480\times10^{-6}$	$-1{\cdot}495\times10^{-5}$
5	$9{\cdot}87\times10^{-8}$	
6	$-4{\cdot}68\times10^{-8}$	$9{\cdot}37\times10^{-8}$
7	$-9{\cdot}70\times10^{-10}$	
8	$3{\cdot}43\times10^{-10}$	$-6{\cdot}87\times10^{-10}$
9	$6{\cdot}82\times10^{-12}$	
10	$2{\cdot}73\times10^{-12}$	$5{\cdot}46\times10^{-12}$

The values of the constants A_n can now be determined from equations (23). It is to be noted that the odd and even ones are independent. They were calculated correct to four figures, using the approximation process (24). It is, however, the constants B_n (equation 26) that are required. If we write

$$B_n = \beta_n v_p + \gamma_n v_w,$$

the values of β_n and γ_n are given in Table II.

The values given in Table II. were used to calculate the potential at various points in the plane, near to one of the circles. Fig. 2 shows the variation in the potential

* British Association Tables, vol. i. p. 24 (1931).

Fig. 2.

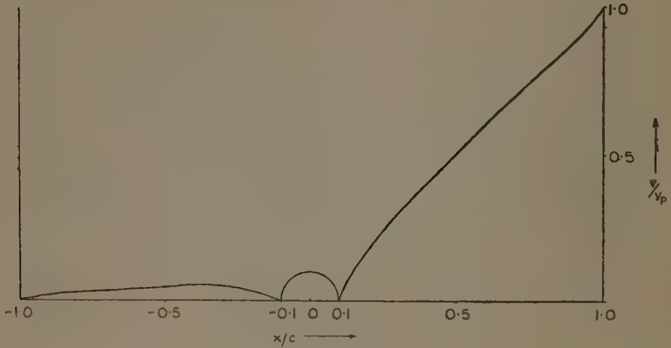

Values of V/v_p along the line $y=0$ when $v_w=0$.

Fig. 3.

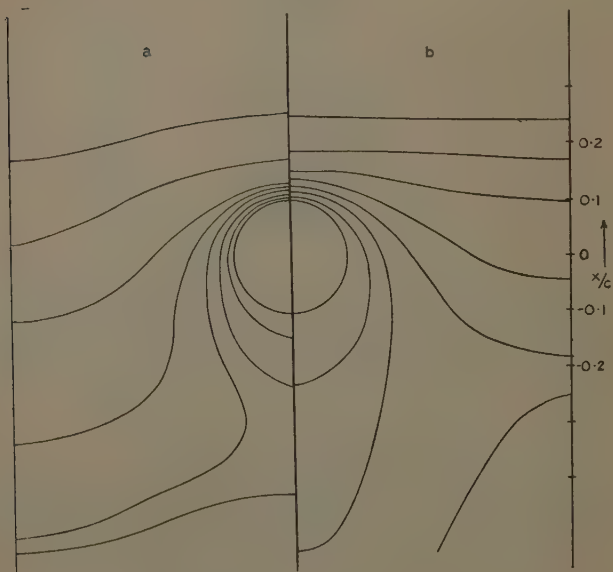

Equipotentials for (a) $v_w=0$, (b) $v_w=-v_p/10$.

along a line, perpendicular to the straight boundaries though the centre of a circle, *e. g.*, along $y=0$. Here we have assumed $v_w=0$. The fall in potential is practically linear between $x/c=0{\cdot}9$ and $x/c=0{\cdot}3$, while behind the circle a maximum of about 0·05 is reached near $x/c=-0{\cdot}4$.

The equipotentials near a circle are shown in fig. 3 in two cases, (*a*) $v_w=0$, (*b*) $v_w=-v_p/20$. In each case the width of the figure corresponds to half the distance between two centres.

The capacity of one of the wires depends only on A_0, and is, in fact, equal to 0·2773 K when both planes are at zero potential, compared with ·3931 K for one wire of the same dimensions situated singly between two parallel planes. K is the specific inductive capacity of the medium between the wires and the plates.

In conclusion, we wish to express our thanks to the Research Committee of University College, Southampton, for the grants that have made possible this work.

IV. *Notes on Two-Dimensional Potential Theory.*—IV. *The Expression for the Fluid Energy and its Application.* *By* ROSA M. MORRIS, *B.Sc.**

1. IN a series of previous notes we have indicated the great simplification in various problems of potential theory in two dimensions which results from the consistent use of the complex potential throughout the discussion. In pursuing these discussions we now proceed to examine the interpretation of the field energy in terms of this complex potential. We shall limit ourselves here to the analytically more general hydrodynamical cases, but many of the results have an obvious and direct application in electrical theory as well.

We calculate then the kinetic energy of incompressible fluid of density ρ in motion due to the presence of a single cylindrical body moving perpendicular to its length. The kinetic energy of the fluid surrounding such a body is given in terms of the velocity potential ϕ by

$$T=\tfrac{1}{2}\rho\int_v\left\{\left(\frac{\partial\phi}{\partial x}\right)^2+\left(\frac{\partial\phi}{\partial y}\right)^2\right\}dv$$

* Communicated by Prof. G. H. Livens.

integrated throughout the volume outside the cylinder, ϕ being the real velocity potential.

2. If we assume now that the motion is acyclic as well as irrotational, we can transform this, in the usual way, into the integral

$$\tfrac{1}{2}\rho\int\phi\frac{\partial\phi}{\partial n}df,$$

integrated over the surface of the body, dn being an element of the normal to the surface drawn into the body. At this point we may notice that in all cases in which the fluid is not at rest at infinity we could not neglect, as we have done, the contribution by a surface at infinity, and the kinetic energy would in that case be infinite. Thus in the case of a moving cylinder

$$T=\tfrac{1}{2}\rho\int_c\phi\left(\frac{\partial\phi}{\partial n}\right)ds$$

integrated round c, the curve of cross-section of the cylinder.

3. In a similar manner, by using the stream function ψ instead of the velocity potential ϕ, we have

$$T=\tfrac{1}{2}\rho\int_v\left\{\left(\frac{\partial\psi}{\partial x}\right)^2+\left(\frac{\partial\psi}{\partial y}\right)^2\right\}dv,$$

$$=\tfrac{1}{2}\rho\int_c\psi\frac{\partial\psi}{\partial n}ds.$$

But in the two-dimensional case we know that

$$\frac{\partial\phi}{\partial n}=+\frac{\partial\psi}{\partial s},\quad\frac{\partial\psi}{\partial n}=-\frac{\partial\phi}{\partial s},$$

so that

$$T=\tfrac{1}{2}\rho\int_c\phi\,d\psi=-\tfrac{1}{2}\rho\int_c\psi\,d\phi.$$

But this means also that

$$T=-\tfrac{1}{4}\rho\int_c(\psi\,d\phi-\phi\,d\psi),$$

which is the imaginary part of the expression

$$T'=-\tfrac{1}{4}\rho\int_c(\phi+i\psi)(d\phi-i\,d\psi),$$

or of the expression

$$T''=\tfrac{1}{4}\rho\int_c(\phi-i\psi)(d\phi+i\,d\psi).$$

Thus we see that the expression for the energy of the liquid can be identified with the imaginary part of the integral

$$-\tfrac{1}{4}\rho\int \Omega\, d\bar{\Omega}=\tfrac{1}{4}\rho\int \bar{\Omega}\, d\Omega,$$

which is expressed directly in terms of the complex potential $\Omega=\phi+i\psi$ and its conjugate $\bar{\Omega}$.

To illustrate the method of finding the kinetic energy by the use of this formula we shall consider cylinders whose axes are moving with a velocity V in a direction making an angle θ with the x-axis and rotating with an angular velocity ω.

4. *Elliptic Cylinder.*—The cylinder being defined by the transformation

$$z=c\cos(\zeta+i\alpha)\,;\ \eta=0,$$

we have seen in a previous note that the complex velocity potential is given by

$$\Omega=-cVe^{i\zeta}\sinh(\alpha+i\theta)+\tfrac{1}{4}i\omega c^2e^{2i\zeta}.$$

We therefore have

$$\bar{\Omega}=-cVe^{-i\zeta}\sinh(\alpha-i\theta)-\tfrac{1}{4}i\omega c^2e^{-2i\zeta}$$

and

$$d\bar{\Omega}=icVe^{-i\zeta}\sinh(\alpha-i\theta)d\zeta-\tfrac{1}{2}\omega c^2e^{-2i\zeta}d\zeta.$$

In forming $\bar{\Omega}$ and $d\,\bar{\Omega}$ we notice that it is only the values on the cylinder we require, so that we can treat the ζ as real.

Thus the energy is the imaginary part of the integral,

$$-\tfrac{1}{4}\rho\int_0^{2\pi}\left\{-cVe^{i\zeta}\sin(\alpha+i\theta)+\frac{i\omega c^2}{4}e^{2i\zeta}\right\}$$
$$\times\{icVe^{-i\zeta}\sinh(\alpha-i\theta)-\tfrac{1}{2}\omega c^2e^{-2i\zeta}\}d\zeta,$$

and as it is only the constant terms that contribute, this is

$$-\tfrac{1}{2}\pi\rho\left\{-ic^2V^2\sinh(\alpha+i\theta)\sinh(\alpha-i\theta)-\frac{i\omega c^2}{8}\right\},$$

so that the energy is

$$\tfrac{1}{4}\pi\rho\{c^2V^2(\cosh 2\alpha-\cos 2\theta)+\tfrac{1}{4}\omega^2c^2\}.$$

a familiar result.

5. *A General Cylinder.*—The previous case and a number of others of some interest and practical importance are included in the general case where the cylinder is defined by

$$z = ce^{-i\zeta}\left\{ \sum_{n=0}^{\infty} a_n e^{ni\zeta} \right\}; \ \eta = 0,$$

where the a's are complex quantities of such a nature as to ensure convergence when the series in the brackets is extended to infinity.

The complex velocity for a cylinder of this kind moving in the given way and constructed by the method explained in a previous note is

$$\Omega = \sum_{n=0}^{\infty} \Omega_n e^{ni\zeta},$$

where
$$\Omega_0 = a_1 e^{-i\theta} Vc - i\omega c^2 b_0,$$
$$\Omega_1 = Vc(a_2 e^{-i\theta} - \bar{a}_0 e^{i\theta}) - i\omega c^2 b_1,$$
$$\Omega_n = Vc\, a_{n+1} e^{-i\theta} - i\omega c^2 b_n, \quad n > 1$$

where
$$b_n = \sum_{n=r}^{\infty} \bar{a}_{n-r} a_n, \quad r = 1, 2, \ldots$$

and the bar over a letter denotes, as usual, the conjugate complex quantity. The energy will then be the imaginary part of

$$-\tfrac{1}{4}\rho \int \Omega \, d\bar{\Omega}$$

integrated round the cylinder. But this is

$$-\tfrac{1}{4}\rho \int_0^{2\pi} \left(\sum_{n=0}^{\infty} \Omega_n e^{ni\zeta} \right) \left(\sum_{n=1}^{\infty} -in\, \bar{\Omega}_n e^{-ni\zeta} \right) d\zeta.$$

and as all but the constant terms in the integrand give zero on integration, this is simply

$$\tfrac{1}{2}\pi i \rho \sum_{n=1}^{\infty} n \Omega_n \bar{\Omega}_n.$$

We therefore want the values of the products $\Omega_n \bar{\Omega}_n$, ($n = 1, 2, \ldots$), which will be purely real:

$$\Omega_1 = Vc(a_2 e^{-i\theta} - \bar{a}_0 e^{i\theta}) - i\omega c^2 b_1,$$
$$\bar{\Omega}_1 = Vc(\bar{a}_2 e^{i\theta} - a_0 e^{-i\theta}) + i\omega c^2 \bar{b}_1.$$

Therefore

$$\Omega_1 \bar{\Omega}_1 = V^2c^2\{a_2\bar{a}_2 + a_0\bar{a}_0 - a_0a_2e^{-2i\theta} - \bar{a}_0a_2e^{2i\theta}\}$$
$$+ ic^3\omega\{a_2\bar{b}_1e^{-i\theta} - \bar{a}_0b_1e^{i\theta} + a_0b_1e^{-i\theta} - a_2b_1e^{i\theta}\}$$
$$+ \omega^2c^4b_1\bar{b}_1.$$

Similarly when $n > 1$,

$$\Omega_n\bar{\Omega}_n = (Vca_{n-1}e^{-i\theta} - iwc^2b_n)(Vca_{n+1}e^{i\theta} + i\omega c^2\bar{b}_n)$$
$$= V^2c^2a_{n+1}\bar{a}_{n+1} - \omega^2c^4b_n\bar{b}_n + ic^3V\omega(a_{n+1}b_ne^{-i\theta}.$$
$$-b_na_{n+1}e^{+i\theta}).$$

Thus the energy T is given by

$$2\text{T}\,\pi\rho = V^2c^2\{a_0\bar{a}_0 + a_2a_2 - a_0a_2e^{-2i\theta} - \bar{a}_0a_2e^{2i\theta} + \sum_{n=1}^{\infty} na_n\bar{a}_{n+1}\}$$
$$- iVc^3\omega\{\bar{a}_0\bar{b}_1e^{i\theta} - a_0b_1e^{-i\theta} + \sum_{n=1}^{\infty} n(b_na_{n+1}e^{-i\theta}$$
$$-\bar{b}_n\bar{a}_{n+1}e^{i\theta})\} + \omega^2c^4\sum_{n=1}^{\infty} nb_n\bar{b}_n,$$

which can obviously be written in

$$\text{A}w\bar{w} + \text{B}w^2 + \text{B}\bar{w}^2 - i\omega(\text{C}w - \bar{\text{C}}w) + \text{D}\omega^2,$$

where $w = Ve^{i\theta}$, $w = Ve^{-i\theta}$ and the coefficients A, B, C, ... are complex quantities definitely expressible in terms of the coefficients a_n in the transformation defining the cylinder.

6. *Cyclic Motions.*—When the motions of the fluid about the cylinder involve cyclic flow round the cylinder a difficulty is encountered in so far as the energy of such cyclic motions in two dimensions—when the fluid extends to infinity—are infinite. It can, however, be shown that there is no mutual term in the energy of the two motions, and that the energy of the cyclic motion is to be added to that of the acyclic flow. The proof of this is given by Lamb * and depends on the separation of the complex potential into its constituent parts, each satisfying its own appropriate boundary conditions, so that it need not be repeated here. Thus, ignoring the difficulty of the infinite energy of the cyclic flow—which only arises

* H. Lamb, 'Hydrodynamics,' Cambridge, 1906, Chapter VI.

from the two-dimensional picture—we can always say that in the general case the energy of the fluid motion consists of the expression calculated above together with a constant term involving the square of the cyclic constant, so that we have all the information available for determining the forces on the cylinder in motion in the general way we have imagined. We are returning to particular aspects of this calculation in another connexion.

University College, Cardiff.
Feb. 15th, 1937.

V. *Expansion and Pressure Coefficients of Nitrogen, Hydrogen, Helium, and Neon, and the Absolute Temperature of* 0° C. *By* M. Kinoshita *and* J. Oishi *.

With a view of obtaining a possible accuracy of 0·01° for the value of 0° C. on the absolute temperature scale, measurements of expansion and pressure coefficients of N_2, H_2, He, and Ne were undertaken by means of a gas-thermometer.

Description of the Apparatus.

The arrangement of the gas-thermometer is shown in fig. 1.

The main bulb V and the auxiliary bulb V_s are made of Jena glass 1565$^{\text{III}}$. The volume of V up to the mark *a* was measured by filling it with mercury and weighing it on a 10 Kg. balance of the sensitiveness of 5 mg. Its volume V_{tp} when the temperature of the bulb is $t°$, the outside pressure 1 atm., and the inside pressure p m. Hg was

$$V_{tp}=268{\cdot}599\,(1+0{\cdot}972\times10^{-5}t+3{\cdot}5\times10^{-5}p)\text{ c.c.}$$

The volume of V_s was about 140 c.c. When the thermometer was used at a constant volume, the bulb V_s was filled with mercury up to the mark *c* on its capillary so that $V_s=0$. When it was used at a constant pressure, the expansion of volume was measured by weighing the amount of mercury syphoned out of the reservoir R_3 or into the reservoir R_4.

* Communicated by the Authors.

The inner diameter of the capillary tubes to V and V_s was 0·000599 m.c./mm. and 0·000759 c.c./mm. respectively. Each of the platinum capillaries which connect these bulbs to the manometer was 60 cm. in length and 0·3 mm. in inner diameter. The end of the capillary which enters into the manometer was cut sharp to make a fine contact with the lower level of the manometer mercury, the height of which was controlled by an electric triode valve relay with a primary current of the order of 10^{-6} ampere.

Fig. 1.

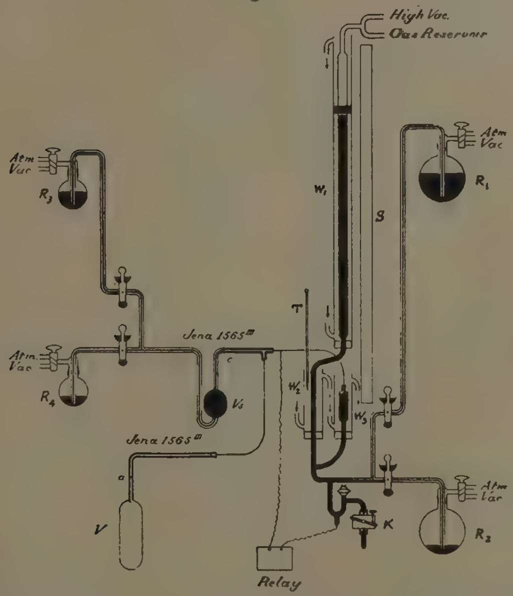

A fine adjustment was made by giving a slight pressure to a piece of rubber tube K connected to the bottom of the manometer.

The manometer tube had 17·35 mm.±0·05 inner diameter.

Accuracy of Measurements.

Accuracies required for all the measurements are as follows :—

For volume measurements : within 0·001 c.c.

For gas-pressure readings : within 0·01 mm. Hg.
Temperature of mercury in manometer to be known : within 0·05° C.
Temperatures of 0° and boiling-point thermostats : within 0·003° C.

To obtain the steam temperature of the boiling-point thermostat within the accuracy of 0·001° C., the following requirements are to be fulfilled :—

Barometer readings : within 0·014 mm.
Temperature of barometer mercury to be known : within 0·1° C.
Water-manometer readings for steam pressure : within 0·2 mm.
Value of the acceleration of gravity to be known : within 0·013 cm./sec.^{2}

To ascertain the exact temperature of the manometer mercury and also that of the dead space, the manometer tubes were jacketed with water which was made to flow through a series of glass tubes exposed to room air and then to enter the jackets in the order W_1, W_2, W_3.

The difference in temperatures of water at the entrance to the first jacket and at the exit from the last jacket was within 0·05°. The temperature of water itself did not vary more than 0·02° during a set of observations.

To obtain an accuracy of 0·01 mm. Hg for the manometer reading of 1500 mm. Hg the temperature of mercury in the manometer should be determined with an accuracy of 0·04°. To obtain an accuracy of 0·001 c.c. in the dead-space volume, which was about 1·6 c.c., the necessary accuracy of temperature reading is 0·1°. The temperature read off on the thermometer T in the second jacket was taken as that of the manometer mercury and also that of the dead space.

The height of mercury was measured on a 1·5 mm. scale S made of super-invar * calibrated to 0·001 mm. against the Japanese standard scale. The pressure was read off by means of a vertical comparator with an accuracy of 0·005 mm. Hg.

* Coefficient of linear expansion $= -2 \times 10^{-8}$. The material was made at the Institute of Metallurgical Research of the Tōhoku Imperial University, Japan. The scale was made at the Institute of Physical and Chemical Research, Tōkyō.

The dead space, which is from the top of the lower level of the manometer to the marks *a* and *c* (fig. 1), had 2·647 c.c. in volume. The deviation from Boyle's law was taken into calculation for the determination of this volume.

Fig. 2 shows the 0° C. thermostat.

Finely shaved ice made from distilled water was kept sunken by means of a perforated nickel plate at the

Fig. 3.

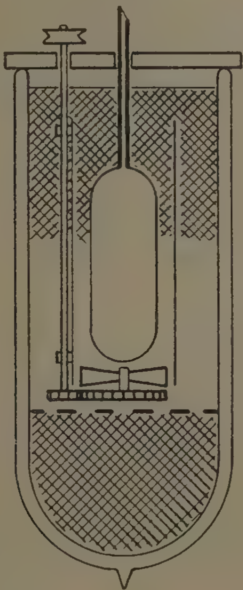

bottom of a large Dewar vessel which contained distilled water. A fair amount of shaved ice filled the top part of the vessel. By slow stirring, the thermostat was kept at 0° C. within the accuracy of 0·001° for over 10 hours.

The effect of heavy water on the ice-point was considered *. In case the content of D_2O in distilled water is 1 in 5000, the ice-point would be 0·00085° higher than that with pure H_2O. The actual content of D_2O

* M. Kinoshita and T. Inai (not yet published).

in water would not be very different from 1 in 5000; a slight variation in the content, therefore, would not affect the required accuracy of the ice-point.

The thermostat for 100° C. was made in the usual manner by using a steam-bath. The over pressure of the steam was read off on a water manometer with an accuracy of 0·1 mm.

The barometric height was measured by a manometer and a scale of similar construction to those shown in fig. 1. Palacios's data * were used for its meniscus corrections. The value of g was calculated as 979·787 cm./sec.^{2} †

The density of mercury was measured by means of a pycnometer of about 90 c.c. capacity made of Jena glass 1565^{III}. Assuming the density of water at 4° C. to be 0·999973 g./cm.^{3}, and using the coefficients of expansion of water and mercury given by Phys.-Techn. Reichsanstalt, that is, for mercury ‡

$$V_t = V_0(1 + 0{\cdot}18182 \times 10^{-3}t + 0{\cdot}78 \times 10^{-8}t^2),$$

the density was determined as shown in Table I.:—

TABLE I.

Date.	Density at 0° C.
July 12, 1935.............	13·5945
„ 15, „	13·5948
„ 16, „	13·5947
Mean.......	13·5947 g./cm.^{3}

The barometer readings were corrected by these values of g and the density to the standard values of g=980·665 cm./sec.^{2} and the density=13·5951 g./cm.^{3} The accuracy of the barometric height was within 0·01 mm. Hg.

* J. Palacios, Landolt-Börnstein, Phys. Chem. Tab. 1st Erg. Bd. p. 11 (1927).

† Ch. Tsuboi, Bull. Earthq. Research Institute, Tōkyō Imp. Univ. xi. pt. 4, p. 637 (1933). The authors are indebted to Dr. Tsuboi for his valuable assistance.

‡ K. Scheel and F. Blankenstein, *Z. f. Phys.* xxxi. p. 202 (1925).

For the boiling-point of water Moser's formula *, that is,

$$t_p = 100{\cdot}000 - 0{\cdot}03687\,(p-760) - 0{\cdot}000022\,(p-760)^2,$$

was used.

The accuracy of the measurement of the boiling-point with the circumstantial conditions described above was within 0·003°.

The Gases used.

(1) *Nitrogen.*—Nitrogen gas obtained by adding saturated solution of $(NH_4)_2SO_4$ drop by drop to heated saturated solution of $NaNO_2$ was made to pass through $FeSO_4$ solution to remove impurities such as N_2O and NO. Traces of CO_2 and H_2O were then removed by soda-lime. Final purification was made in a combustion tube at 600° containing copper gauze to remove oxygen.

(2) *Hydrogen* †.—Electrolytic hydrogen gas of 99·9 per cent. purity was led through an activated charcoal trap at liquid hydrogen temperature.

(3) Helium and neon gases, spectroscopically pure, were supplied by the Ohio Chemical and Manufacturing Co., Cleveland, U.S.A.

In filling the gas-thermometer a trap at liquid-air temperature was used for every gas, which was checked by a Geissler tube connected to the thermometer to ensure its spectroscopical purity.

The Expansion Coefficient α.

Referring back to fig. 1, the gas in the thermometer is subjected to three different temperatures, that is, $t°$ for V, 0° for V_s, and the room-temperature for the dead space v. The latter is reduced to 0° assuming the expansion coefficient to be 0·00367.

At the boiling-point of water t_b and at the pressure p_1 the volume of gas is

$$V_{t_b p_1} + V_{s_1} + v_1.$$

At 0° and at the pressure p_2 it is

$$V_{0 p_2} + V_{s_2} + v_2,$$

where suffixes 1 and 2 refer to t_b and 0° respectively.

* H. Moser, *Ann. d. Phys.* xiv. p. 790 (1932).

† The authors are indebted to Dr. S. Aoyama, of the Cryogenic Laboratory of the Tōhoku Imperial University, Japan, for his kind collaboration in preparing pure hydrogen gas.

In actual measurements p_1 and p_2 were made as near together as possible (see Table IV.), and the mean expansion coefficient α between 0° and t_b is given by the relation

$$1+\alpha t_b=\frac{V_{t_b p_1}}{V_{0p_2}+V\quad+v_2-(V_{s_1}+v_1)Q_0}\frac{p_1}{p_2}\{1-\kappa_{100}(p_1-p_2)\},$$

where

$$Q_0=\frac{p_1}{p_{\cdot}}\{1-\kappa_0(p_1-p_2)\}$$

and

$$\kappa_{100}=\frac{1}{pV}\left(\frac{d(pV)}{dp}\right)_{t=100},\quad \kappa_0=\frac{1}{pV}\left(\frac{d(pV)}{dp}\right)_{t=0}$$

for the gas.

The Pressure Coefficient β.

The mean pressure coefficient β between 0° and t_b is given by the relation

$$1+\beta t_b=\frac{V_{t_b p_1}}{V_{0p_2}+V_{s_2}+v_2-(V_{s_1}+v_1)Q_0}\frac{p_1}{p_2}$$
$$\times\left\{1-p_1\kappa_{100}\left(1-\frac{V_{t_b p_1}}{V_{0p_2}+V_{s_2}+v_2-(V_{s_1}+v_1)Q_0}\right)\right\}.$$

The two volumes, $V_{t_b p_1}$ and $V_{0p_2}+V_{s_2}+v_2-(V_{s_1}+v_1)Q_0$ were made almost equal by controlling the volume V_{s_2}. At t_b, if the mercury in V_s is brought up to the mark c, then $V_{s_1}=0$, and we have

$$1+\beta t_b=\frac{V_{t_b p_1}}{V_{0p_2}+V_{s_2}+v_2-v_1Q_0}\frac{p_1}{p_2}$$
$$\times\left\{1-p_1\kappa_{100}\left(-\frac{V_{t_b p_1}}{V_{0p_2}+V_{s_2}+v_2-v_1Q_0}\right)\right\}.$$

Limiting Values of α and β at the Avogadro State.

For the calculations of γ_α and γ_β, which are the limiting values of α and β respectively at the Avogadro state, the following relations * were employed :

$$100\,(\alpha-\gamma_\alpha)=\frac{p_0}{1-\kappa_0}\{\kappa_{100}-\kappa_0(1+100\,\alpha)\},$$

$$100\,(\beta-\gamma_\beta)=\frac{p_0}{1-\kappa_0}(\kappa_{100}-\kappa_0)(1+100\,\beta),$$

* W. Heuse and J. Otto, *Ann. d. Phys.* ii. p. 1012 (1929).

where p_0 is the pressure at 0°. p_0 and κ are both expressed in m. Hg.

Rewriting the equations, we have

$$\gamma_\alpha \times 10^7 = \alpha \times 10^7 + ap_0,$$

$$\gamma_\beta \times 10^7 = \beta \times 10^7 + bp_0,$$

where

$$a = -\frac{1}{1-\kappa_0}\{\kappa_{100} - \kappa_0(1+100\,\alpha)\} \times 10^5,$$

$$b = -\frac{1}{1-\kappa_0}(\kappa_{100} - \kappa_0)(1+100\beta) \times 10^5.$$

The most reliable values of κ_0 and κ_{100} are those found by Holborn and Otto and others * for the pressure between 20–200 atm. These values are shown in Table II. :—

TABLE II.

	He.	H_2.	Ne.	N_2.	A.
$\kappa_{100} \times 10^5$	67·2	90·7	73·1	38·0	— 24·7
$\kappa_0 \times 10^5$	69·3	82·1	62·8	—61·7	—128·6

According to Heuse and Otto, these values remain practically unaffected at low pressures. Hence, using these values, we have for a and b as shown in Table III. :—

TABLE III.

	N_2.	H_2.	He.	Ne.	A.
a	—122·2	21·4	27·5	12·7	—149·9
b	—136·3	—11·8	2·9	—14·1	—141·8

* L. Holborn and J. Otto, *Z. f. Phys.* xxx. p. 320 (1924); xxxiii. p. 1 (1925); xxxviii. p. 359 (1926). J. Otto, *Z. f. Instrumentenkunde*, xlviii. p. 257 (1928). J. Otto, A. Michels, and H. Wouters, *Phys. Z.* xxxv. p. 97 (1934) (N_2).

The Result of Measurements.

Numerical data obtained are given in Table IV.

TABLE IV.

Gas.	Date.	p_0 m. Hg.	$\alpha\times10^7$.	$\beta\times10^7$.	$\gamma_\alpha\times10^7$.	$\gamma_\beta\times10^7$.
N_2 ..	29. 5. 34	1·00	36730	..	36608	
,, ..	30. 5. 34	1·00	36729	..	36607	
,, ..	31. 5. 34	1·00	36728	..	36606	
,, ..	18. 3. 35	1·08	..	36755	..	36608
,, ..	20. 3. 35	1·08	..	36755	..	36608
,, ..	22. 3. 35	1·08	..	36757	..	36610
,, ..	26. 3. 35	1·08	36739	..	36607	
				Mean ...	36607	36609
H_2 ..	18. 4. 35	1·05	..	36620	..	36607
,, ..	19. 4. 35	1·05	..	36620	..	36607
,, ..	20. 4. 35	1·05	..	36620	..	36608
,, ..	22. 4. 35	1·05	36585	..	36607	
,, ..	23. 4. 35	1·05	36586	..	36609	
,, ..	24. 4. 35	1·05	36585	..	36607	
				Mean ...	36608	36607
He ..	8. 5. 35	1·04	..	36603	..	36606
,, ..	9. 5. 35	1·04	..	36603	..	36606
,, ..	10. 5. 35	1·04	..	36605	..	36608
,, ..	11. 5. 35	1·04	..	36605	..	36608
,, ..	13. 5. 35	1·04	36579	..	36608	
,, ..	14. 5. 35	1·04	36578	..	36607	
,, ..	15. 5. 35	1·04	36580	..	36609	
				Mean ...	36608	36607
Ne ..	28. 5. 35	0·90	..	36612	..	36600
,, ..	29. 5. 35	0·90	..	36614	..	36601
,, ..	12. 6. 35	1·08	36597	..	36611	
,, ..	13. 6. 35	1·08	36598	..	36612	
,, ..	14. 6. 35	1·08	36596	..	36610	
,, ..	20. 6. 35	1·08	..	36618	..	36602
,, ..	21. 6. 35	1·08	..	36618	..	36603
,, ..	22. 6. 35	1·08	..	36616	..	36601
				Mean ...	36611	36601

The values of the expansion coefficient α and the pressure coefficient β between 0° and 100° reduced to $p_0=1$ m. Hg are shown in Table V. :—

TABLE V.

	$\alpha_N \times 10^7$.	$\beta_N \times 10^7$.
N_2	36729	36745
H_2	36586	36619
He	36580	36604
Ne	36598	36616

Table VI. shows the values of γ_α and γ_β for the gases:—

TABLE VI.

	$\gamma_\alpha \times 10^7$.	$\gamma_\beta \times 10^7$.
N_2	36607	36609
H_2	36608	36607
He	36608	36607
Ne	36611	36301

Results on neon gas are inconsistent. Cath and Onnes * found, by using a differential gas thermometer with $p_0=1$ m. Hg, that

$$(\beta_{H_2}-\beta_{Ne})\times 10^7=7,$$

whereas in the present measurements it gives

$$(\beta_{H_2}-\beta_{Ne})\times 10^7=3.$$

Heuse and Otto † give

$$\alpha_N \times 10^7=36601, \quad \beta_N \times 10^7=36623,$$

from which

$$\gamma_\alpha \times 10^7=36614, \quad \gamma_\beta \times 10^7=36509.$$

It is apparent that for neon gas the value of γ_α is considerably larger than that of γ_β. It is safer, therefore, not to include the results on neon for the determination of γ of the ideal gas.

* P. G. Cath and H. Kammerlingh Onnes, Comm. Leiden, No. 156 *a*, 1922.

† W. Heuse and J. Otto, *Ann. d. Phys.* iv. p. 778 (1930).

Argon seems to suit still less for the purpose, as shown by Cath and Onnes *.

The cause of these deviations seems to lie in using the values of κ_0 and κ_{100} measured in high-pressure range. As for Neon, if the values of α_N, β_N, and κ_0 shown in Tables V. and II. respectively are used, we have $\gamma\times 10^7=36635$. Provisional result of measurements in the neighbourhood of 1 m. Hg. pressure gives $\kappa_0=40\times 10^{-5}$, which leads to $\gamma\times 10^7=36604$ which is more in conformity with the rest of the gases.

Results on N_2, H_2, and He are in good agreement with one another. Taking the mean value of twenty data shown in Table IV. for these three gases, it gives

$$\gamma\times 10^7=36607{\cdot}_6\pm 0{\cdot}_7,$$

from which we have

$$T_0=\frac{1}{\gamma}=273{\cdot}16_7\pm 0{\cdot}00_5.$$

Research funds given by the Japan Society for the Promotion of Scientific Research and other public bodies enabled the above measurements to be completed, for which the authors express their appreciation.

Tōkyō Kōgyō Daigaku
(Tōkyo University of Engineering).
May 1936.

VI. *On the Operational Determination of Green's Functions in the Theory of Heat Conduction.* *By* Dr. Arnold N. Lowan †.

THE mathematical theory of heat conduction in solids is concerned with obtaining solutions of the differential equation

$$\frac{dT}{dt}-\kappa\Delta T=0 \quad . \quad . \quad . \quad . \quad . \qquad (1)$$

satisfying prescribed initial and boundary conditions over a given closed surface S. It is a known fact that the desired solution may be obtained with the aid of an

* P. G. Cath and H. Kammerlingh Onnes, *loc. cit.*
† Communicated by the Author.

auxiliary function, the Green's function. For the sake of continuity and since some of the results to be derived are not found in the literature, it is deemed advisable to include in this paper a brief discussion of the significance of the Green's function. Let

$$G=G(x, y, z, \xi, \eta, \zeta, t-\tau) \quad . \quad . \quad . \quad . \quad (2)$$

be a solution of (1) which vanishes everywhere for $t=\tau$ except at the point $P(\xi, \eta, \zeta)$, at which $G=\infty$ in such a manner that

$$\operatorname*{Lim}_{t=\tau} \iiint G(x, y, z, \xi, \eta, \zeta, t-\tau)\, d\xi\, d\eta\, d\zeta=1,$$

where the integration is carried over the volume V bounded by S. The function G satisfying the above conditions and some further boundary conditions to be discussed is called the Green's function of the problem under consideration. To show its usefulness, it may be noticed that considered as a function of τ it must obviously satisfy the differential equation

$$\frac{\partial G}{\partial \tau}+\kappa \Delta G=0 \quad . \quad . \quad . \quad . \quad . \quad (3)$$

If we now rewrite (1) in the form

$$\frac{\partial T}{\partial \tau}-\kappa \Delta T=0, \quad . \quad . \quad . \quad . \quad . \quad . \quad (1')$$

it follows ultimately

$$\iiint\limits_V [TG]_{\tau=0}^{\tau=t}\, d\xi\, d\eta\, d\zeta=\kappa \int_0^t d\tau \iint\limits_S \left(G\frac{\partial T}{\partial n}-T\frac{\partial G}{\partial n}\right) d\sigma,$$

whence

$$T(x, y, z, t)=\iiint\limits_V G_{\tau=0} f(\xi, \eta, \zeta)\, d\xi\, d\eta, d\zeta$$

$$+\kappa \int_0^t d\tau \iint\limits_S \left(G\frac{\partial T}{\partial n}-T\frac{\partial G}{\partial n}\right) d\sigma, \quad (4)$$

where $f(x, y, z)$ is the value of the function T at $t=0$.

The last formula is derived by Carslaw in Art. 80. He applies it to the cases where the boundary condition is either one of the following two :—

(*a*) The surface temperature is a prescribed function, $\phi(x, y, z, t)$; and

(*b*) radiation takes place at the surface into a medium of prescribed temperature, $\psi(x, y, z, t)$.

The general formula (4) may also be used in the case of the more general boundary condition

$$\alpha\frac{dT}{dt}+\beta\frac{\partial T}{\partial n}+\gamma T=\gamma\phi(x, y, z, t). \quad . \quad . \quad . \quad (5)$$

The method of using (4) in connexion with the new boundary condition (5) is not given by Carslaw, and as far as the author is aware is not discussed in the literature. It will therefore be given here in detail.

We operate on (4) with the Laplace operator generally defined for a function $h(t)$ by

$$L\{h(t)\}=\int_0^\infty e^{-pt}h(t)dt=h^*(p),$$

where p is a complex variable the real part of which is positive. Remembering that G and $\frac{\partial G}{\partial n}$ in the second member of (4) are functions of the argument $t-\tau$, and making use of Borel's theorem, we ultimately get

$$T^*(x, y, z, p)=\iiint_V G^*_{\tau=0}(x, y, z, \xi, \eta, \zeta, p)f(\xi, \eta, \zeta)\,d\xi\,d\eta\,d\zeta$$
$$+\kappa\iint_S\left[G^*\frac{\partial T^*}{\partial n}-T^*\frac{\partial G^*}{\partial n}\right]d\sigma. \quad . \quad (6)$$

Similarly, operating on (5) with the Laplace operator, we get

$$(\alpha p+\gamma)T^*+\beta\frac{\partial T^*}{\partial n}=\gamma\phi^*(x, y, z, p). \quad . \quad . \quad (7)$$

In view of (7) the integrand of the surface integral in (6) becomes

$$\frac{\alpha}{\beta}G^*\phi^*-\frac{T^*}{\beta}\left\{(\alpha p+\gamma)G^*+\beta\frac{\partial G^*}{\partial n}\right\}.$$

It is now clear that if the Green's function is so chosen that its Laplace transform satisfies the boundary condition

$$G^*.(\alpha p+\gamma)+\beta\frac{\partial G^*}{\partial n}=0 \text{ on S.} \quad . \quad . \quad (8)$$

equation (6) will reduce to the simpler form

$$\mathrm{T}^*(x, y, z, p) = \iiint\limits_{\mathrm{V}} \mathrm{G}^*_{\tau=0}(x, y, z, \xi, \eta, \zeta, p) f(\xi, \eta, \zeta)\, d\xi\, d\eta\, d\zeta$$

$$+ \frac{\kappa\alpha}{\beta} \iint\limits_{\mathrm{S}} \mathrm{G}^*(x, y, z, \xi, \eta, \zeta, p)\, \phi^*(\xi, \eta, \zeta, p)\, d\sigma, \qquad (9)$$

whence, applying the inverse Laplace transformation in connexion with Borel's theorem, (8) yields

$$\mathrm{T}(x, y, z, t) = \iiint\limits_{\mathrm{V}} \mathrm{G}(x, y, z, \xi, \eta, \zeta, t) \,.\, f(\xi, \eta, \zeta)\, d\xi\, d\eta\, d\zeta$$

$$+ \frac{\kappa\alpha}{\beta} \int_0^t d\tau \iint\limits_{\mathrm{S}} \mathrm{G}(x, y, z, \xi, \eta, \zeta, t-\tau) \,.\, \phi(\xi, \eta, \zeta, t)\, d\sigma. \qquad (10)$$

This is the complete solution of the differential equation (1) satisfying the initial condition

$$\operatorname*{Lim}_{t=0} \mathrm{T}(x, y, z, t) = f(x, y, z) \quad . \quad . \quad . \quad (11)$$

and the boundary condition (5). This solution is expressed in terms of the Green's function whose Laplace transform satisfies (8). The Green's function itself must therefore satisfy the boundary condition

$$\alpha \frac{d\mathrm{G}}{dt} + \beta \frac{\partial \mathrm{G}}{\partial n} + \gamma \mathrm{G} = 0 \text{ on S.} \quad . \quad . \quad (12)$$

Our problem reduces, therefore, to the determination of the Green's function, G. It will be shown that G can be found in specific cases by use of the standard methods of operational calculus. For the sake of simplicity we shall consider the case of a semi-infinite solid extending from $x=0$ to $x=\infty$. Furthermore, we shall treat the special case $\alpha=0$, and will designate $-\frac{\gamma}{\beta}$ by h.

In this case, then, the Green's function must satisfy the differential equation

$$\frac{\partial \mathrm{G}}{\partial t} - \kappa \frac{\partial^2 \mathrm{G}}{\partial x^2} = 0 \quad . \quad . \quad . \quad . \quad . \quad (13)$$

and the boundary condition

$$\frac{\partial \mathrm{G}}{\partial x} - h\mathrm{G} = 0 \quad \text{for } x=0. \quad . \quad . \quad (14)$$

Let us make the substitution

$$G(x,\xi,t-\tau)=\frac{1}{2\sqrt{\pi\kappa t}}\exp\left[\frac{-(x-\zeta)^2}{4\kappa(t-\tau)}\right]+v(x,t). \quad (15)$$

$$=u(x,\xi,t)+v(x,t)\quad\text{(say)}. \quad . \quad . \quad . \quad (16)$$

Since the function u is known to satisfy the first two conditions (postulated for a Green's function)

$$\left.\begin{aligned}u&=0 \quad\text{for}\quad \xi\neq x\\ u&=\infty \quad\text{for}\quad \xi=x\end{aligned}\right\}\text{at } t=\tau, \quad . \quad . \quad . \quad (17)$$

and

$$\operatorname*{Lim}_{t=\tau}\int u\,dx=1, \quad . \quad . \quad . \quad . \quad . \quad . \quad (18)$$

it follows that the unknown function v must be a solution of the differential equation (13) vanishing identically for $t=\tau$, and that, furthermore, we must have

$$\left(\frac{\partial}{\partial x}-h\right)(u+v)=0 \text{ at } x=0. \quad . \quad . \quad . \quad (19)$$

In the subsequent developments it will evidently suffice to make $\tau=0$.

From (19) we have

$$\left(\frac{\partial}{\partial x}-h\right)(u^*+v^*)=0. \quad . \quad . \quad . \quad . \quad (20)$$

Since $v(x,t)$ satisfies (13) its Laplace transform satisfies the equation

$$pv^*-\kappa\frac{\partial^2 v^*}{\partial x^2}=0. \quad . \quad . \quad . \quad . \quad . \quad (21)$$

The general solution of (21) which is finite at $x=\infty$ is

$$v^*(x,p)=\mathrm{A}\exp\left[-x\sqrt{\frac{p}{\kappa}}\right], \quad . \quad . \quad . \quad (22)$$

whence

$$\left[\frac{\partial}{\partial x}-h\right]v^*(o,p)=-\left[\sqrt{\frac{p}{\kappa}}+h\right]\mathrm{A}. \quad . \quad . \quad (23)$$

In the identity

$$\int_0^\infty \exp[-pt]\,.\exp\left[-\frac{\lambda}{t}\right].\frac{1}{\sqrt{\pi t}}dt$$

$$=\frac{1}{\sqrt{p}}\exp[-2\sqrt{\lambda p}] \qquad (\lambda>0), \quad (24)$$

let
$$\lambda = \frac{(x-\xi)^2}{4\kappa},$$

whence
$$\sqrt{\lambda} = \frac{x-\xi}{2\sqrt{\kappa}} \quad \text{for } x<\xi;$$

then (24) becomes

$$\int_0^\infty \exp[-pt] \,.\, \exp\left[-\frac{(x-\xi)^2}{4\kappa t}\right] . \frac{1}{2\sqrt{\pi\kappa t}} dt$$
$$= \frac{1}{2\sqrt{\kappa p}} \exp\left[\frac{(x-\xi)\sqrt{p}}{\sqrt{\kappa}}\right] . \quad (25)$$

Thus
$$v^*(x, p) = \frac{1}{2\sqrt{\kappa p}} \exp\left[(x-\xi)\sqrt{\frac{p}{\kappa}}\right]$$

and

$$\left[\frac{\partial}{\partial x} - h\right] v^*(o, p) = \frac{\left(\sqrt{\frac{p}{\kappa}} - h\right)}{2\sqrt{\kappa p}} \exp\left[-\xi\sqrt{\frac{p}{\kappa}}\right] . \quad (26)$$

In view of (26), (23) ultimately yields

$$A = \frac{\sqrt{\frac{p}{\kappa}} - h}{\sqrt{\frac{p}{\kappa}} + h} \cdot \frac{1}{2\sqrt{\kappa p}} \cdot \exp\left[-\xi\sqrt{\frac{p}{\kappa}}\right],$$

and therefore

$$v^*(x, p) = \frac{\sqrt{\frac{p}{\kappa}} - h}{\sqrt{\frac{p}{\kappa}} + h} \cdot \frac{1}{2\sqrt{\kappa p}} \cdot \exp\left[-(x+\xi)\sqrt{\frac{p}{\kappa}}\right] . \quad (27)$$

The problem now reduces to solving the integral equation

$$\int_0^\infty \exp[-pt]\, v(x, t)\, dt = v^*(x. p) \quad . \quad . \quad . \quad (28)$$

for $v(x, t)$ where $v^*(x, p)$ is given by (27). Clearly,

$$v(x, t) = v_1(x, t) - hv_2(x, t), \quad . \quad . \quad . \quad . \quad (29)$$

where $v_1(x, t)$ and $v_2(x, t)$ are the solutions of equations similar to (27), where v and v^* are replaced by v_1 and $v_1{}^*$, v_2 and $v_2{}^*$.

F 2

Comparison between $u^*(x, p)$ and $v^*(x, p)$ shows clearly that

$$v_1(x, t)=\frac{1}{2\sqrt{\pi\kappa t}}\exp\left[\frac{-(x+\xi)^2}{4\kappa t}\right]. \quad . \quad . \quad (30)$$

In order to get $v_2(x, t)$ we must solve the integral equation

$$\int_0^\infty \exp[-pt] \,.\, v_2(x, t)\, dt=\frac{1}{a+\sqrt{p}} \cdot \frac{1}{\sqrt{p}} \cdot \exp[-b\sqrt{p}], \quad . \quad . \quad . \quad (31)$$

where we have put

$$a=h\sqrt{\kappa} \quad \text{and} \quad b=\frac{x+\xi}{\sqrt{\kappa}}.$$

Let us associate with (31) the new integral equation

$$\int_0^\infty \exp[-pt] \,.\, \mathrm{H}(t)\, dt=\frac{1}{a+p} \cdot \frac{1}{p}\exp[-bp]. \qquad (32)$$

From (31) and (32) it is possible to express $v_2(x, t)$ in terms of $\mathrm{H}(t)$. Indeed, we have

$$v_2(x, t)=\mathrm{L}^{-1}\left\{\frac{1}{a+\sqrt{p}} \cdot \frac{1}{\sqrt{p}} \cdot \exp[-b\sqrt{p}]\right\}. \qquad (33)$$

Since (31) is an identity in p we have

$$\int_0^\infty \exp[-\eta\sqrt{p}] \,.\, \mathrm{H}(\eta)\, d\eta=\frac{1}{a+\sqrt{p}} \cdot \frac{1}{\sqrt{p}} \cdot [\exp(-b\sqrt{p})]. \quad . \quad . \quad . \quad (34)$$

In view of (33), (34) yields

$$v_2(x, t)=\int_0^\infty \mathrm{H}(\eta)\mathrm{L}^{-1}\{\exp[-\eta\sqrt{p}]\}\, d\eta. \quad . \quad (35)$$

In the identity

$$\mathrm{L}^{-1}\{\exp(-2\sqrt{\lambda p})\}=\sqrt{\frac{\lambda}{\pi}} \cdot \frac{1}{t^{3/2}} \cdot \exp\left(\frac{-\lambda}{\tau}\right), \quad . \quad (36)$$

let us put

$$2\sqrt{\lambda}=\eta,$$

whence

$$\lambda=\frac{\eta^2}{4}.$$

Thus

$$\mathrm{L}^{-1}\{\exp(-\eta\sqrt{p})\}=\frac{\eta}{2\sqrt{\pi}} \cdot \frac{1}{t^{3/2}} \cdot \exp\left[\frac{-\eta^2}{4t}\right]. \qquad (37)$$

In view of (37), (35) becomes

$$v_2(x, t) = \frac{1}{2\sqrt{\pi}t^{3/2}}\int_0^\infty H(\eta) \,.\, \eta \,.\, \exp\left[\frac{-\eta^2}{4t}\right] d\eta. \quad (38)$$

Integrating by parts, we get

$$v_2(x, t) = \frac{1}{\sqrt{\pi t}}\left[1 - H(\eta) \,.\, \exp\left(\frac{-\eta^2}{4t}\right)\right]_0^\infty$$

$$+ \int_0^\infty \exp\left[\frac{-\eta^2}{4t}\right] . \frac{\partial}{\partial\eta} H(\eta)\, d\eta. \quad (39)$$

Calculation of H(t).

Let us write (32) in the form

$$\int_0^\infty \exp(-pt) \,.\, H(t)\, dt = \frac{1}{a}\left(\frac{1}{p} - \frac{1}{p+a}\right) \exp(-pb). \quad (40)$$

The solution of

$$\frac{\exp(-pb)}{p} = \int_0^\infty \exp(-pt)\, \kappa(t)\, dt \quad . \quad . \quad (41)$$

is known to be

$$\left.\begin{aligned} \kappa(t) &= 0 \quad \text{for } t < b, \\ \kappa(t) &= 1 \quad \text{for } t > b. \end{aligned}\right\} \quad . \quad . \quad . \quad . \quad . \quad (42)$$

From (41), replacing p by $p+a$, we get

$$\frac{\exp(-pb)}{p+a} = e^{ab}\int_0^\infty \exp(-pt) \,.\, \exp(-at)\, \kappa(t)\, dt. \quad (43)$$

In view of (42) and (43) the inversion of (40) yields

$$H(t) = \frac{1}{a}(1 + \exp\{a(b-t)\})\, \kappa(t), \quad . \quad . \quad . \quad (44)$$

whence

$$\frac{\partial H}{\partial t} = -\exp(ab) \,.\, \exp(-at) \quad \text{for } t > b.$$

Also

$$H(o) = 0. \quad . \quad . \quad . \quad . \quad . \quad . \quad . \quad (45)$$

Thus

$$v_2(x, t) = \frac{-\exp(ab)}{\sqrt{\pi t}}\int_0^\infty \exp\left[\frac{-\eta^2}{4t}\right] . \exp(-a\eta)\, d\eta.$$

Let

$$\eta = b + \frac{\rho}{\sqrt{\kappa}} = \frac{x+\xi+\rho}{\sqrt{\kappa}};$$

therefore

$$a\eta = ab + \frac{a\rho}{\sqrt{\kappa}} = ab + h\rho.$$

Therefore

$$v_2(x, t)=\int_0^\infty \exp(-h\rho) \cdot \exp\left[\frac{-(x+\xi+\rho)^2}{4\kappa t}\right] d\rho. \quad (46)$$

Thus, collecting our results, we have

$$G(x, \xi, t-\tau)=\frac{1}{2\sqrt{\pi\kappa(t-\tau)}}\left\{\exp\left[\frac{-(x-\xi)^2}{4\kappa(t-\tau)}\right]\right.$$
$$\left.+\exp\left[\frac{-(x+\xi)^2}{4\kappa(t-\tau)}\right]\right\}-2h\int_0^\infty \exp[-h\xi]$$
$$\times\exp\left[\frac{(x+\xi+\rho)^2}{4\kappa(t-\tau)}\right] d\xi. \quad . \quad . \quad . \quad (47)$$

Brooklyn College.

VII. *The Dielectric Constant of Mixed Crystals of Sodium Ammonium and Sodium Potassium Tartrates. By* R. C. Evans, *M.A., Ph.D., B.Sc., the Department of Mineralogy and Petrology and the Crystallographic Laboratory, Cambridge* *.

§ 1. *Introduction.*

THE remarkable dielectric properties of Rochelle salt, $C_4H_4O_6NaK \cdot 4H_2O$, have long been known and have been the subject of numerous investigations, but, although many data have been collected, the phenomena observed are so complex that as yet no entirely satisfactory explanation of the anomalous behaviour of this substance has been advanced; nor can we look for any structural explanation until the crystal structure has been elucidated.

So far no parallel to Rochelle salt has been found among the many salts whose dielectric constants have been measured, and it appears to be unique in its remarkable properties, but the salts most closely related to it, namely, the members of the isomorphous series formed by replacing the potassium of Rochelle salt by ammonium, rubidium or cæsium, and mixed crystals of these salts with one another, do not seem to have been systematically investigated. It is the object of this paper to record the results of some measurements of the dielectric constant

*Communicated by the Author.

of $C_4H_4O_6NaNH_4 . 4H_2O$ (which may be conveniently termed ammonium Rochelle salt), and of mixed crystals of this salt with common Rochelle salt. When the experiments were started it was intended to make measurements at both low and high frequencies as well as to investigate the temperature variation of the dielectric constant, since in the case of Rochelle salt the very high values of the dielectric constant (up to 20,000) are observed only at low frequencies, and only in the temperature range $-15°$ C. to $+25°$ C. During the course of the work, however, an account was published by Kourtschatov (1936) of measurements of the dielectric constant of mixed crystals of ammonium and potassium Rochelle salts at low frequencies (up to 20 kc.). The experiments here described were accordingly confined to measurements at high frequencies in the range 50–2000 kc. Although the very high values of the dielectric constant of Rochelle salt are only observed at low frequencies, Errera (1931) has shown that nevertheless, even at frequencies as high as 1000 kc., the value of the dielectric constant is very much larger than that normally found in the solid state, and it is therefore of interest to discover whether these abnormally high values are also observed in the isomorphous salts.

§ 2. *Experimental Details.*

Apparatus.—The apparatus used was essentially the same as that described by Colebrook (1931) as used at the National Physical Laboratory for dielectric constant measurements. It consisted of:

(1) A dynatron oscillator A, the frequency of which could be varied from 50 to 2000 kc. by means of plug-in coils and condensers.

(2) A second similar dynatron oscillator B combined with a rectifier and audio-frequency amplifier.

(3) A dynatron oscillator C with a fixed audio-frequency of 1000 cycles.

The heterodyne audio-frequency note produced by the interference of the two radio-frequencies of A and B was adjusted to the fixed frequency of C by varying the capacity in the oscillating circuits A or B. The condenser containing the crystal of which the dielectric constant

was to be measured was placed in the oscillating circuit B in parallel with a calibrated standard variable condenser.

Fig. 1.

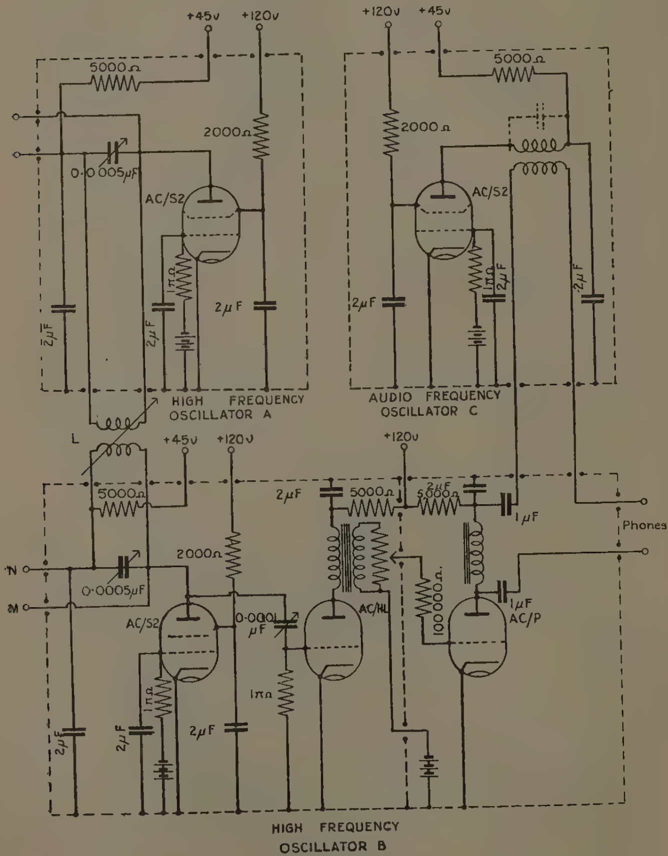

Circuit diagram.

The increase in the capacity of this condenser required to restore the heterodyne frequency to the fixed audio-frequency when the crystal condenser was removed was a measure of the capacity of the latter condenser.

The circuit details and the values of the principal components are shown in fig. 1, which needs little explanation. Each oscillator was enclosed in a separate screened box from which the coils L projected. Only very loose coupling was required between these coils, and normally their separation was about 20 cm. Mazda AC/S2 indirectly heated screened-grid valves were used as the dynatron oscillators. With a potential of about 120 volts on the screen and 45 volts on the anode, the grid potential was adjusted until the screen current was about 5 ma. A large screen current is liable to damage a valve (Scroggie, 1933), but with this particular type of valve 5 ma. appears to be a safe current, for the oscillators have been in use for over 200 hours without suffering harm. The screen current was derived from a mains-operated eliminator, and the anode current from a high tension battery. The purity of the wave-form produced by the oscillator was investigated with a cathode ray oscillograph and, as far as visual observations permitted, was found to be free from appreciable harmonic content provided that L/C in the oscillating circuit was small. Under the conditions employed in the experiments, the peak amplitude of the oscillating potential, as measured with the oscillograph, was found to be 45 volts. The dynatron oscillators proved to be extremely convenient and stable ; without any particular precautions being observed, their frequencies remained constant to within a few cycles per second for considerable periods of time.

Electrodes.—With substances of high dielectric constant any form of solid electrode is unsatisfactory owing to the difficulty of ensuring intimate contact, while the use of a saturated solution of the salt as electrode, as advocated by some authors, has objections in the case of Rochelle salt on account of its very high temperature coefficient of solubility In these experiments mercury electrodes, the details of which are clear from fig. 2, were employed. These electrodes were found to be entirely satisfactory ; reproducible results could be obtained and the crystal sections were not damaged in any way.

The whole electrode system was enclosed in an earthed screen E. The terminals M and N were connected

to the " live " and " earthed " terminals M and N of the oscillator B. Inside the screen M, was connected permanently to one electrode S, while the connexion from N to the other electrode T was made by a brass wire W, which could be withdrawn from the mercury by the thread V. This constituted the switch by means of which the crystal condenser was thrown in and out of circuit. Since all the moving parts of the switch were permanently connected to the earthed side of the oscillating circuit, no spurious changes in capacity could take place on opening or closing the switch. On opening the switch

Fig. 2.

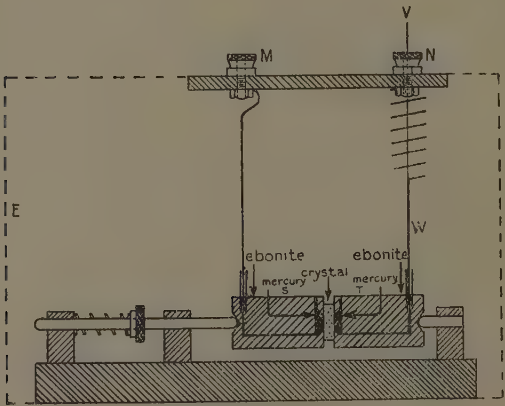

The electrode system.

the wire W was withdrawn sufficiently far from T for the capacity between it and T to be negligible. This was experimentally confirmed by observing that no change occurred in the heterodyne note when W was withdrawn still further. This also served to confirm that the direct capacity between W and S was negligible.

Calibration.—The air capacity of the condenser was determined by direct measurement, using sections of fluorite, quartz and calcite as dielectric. Calibrations were made with sections of each crystal of several thicknesses from 0·04 to 0·4 cm., and within this range the air capacity was found to vary very nearly linearly

with the reciprocal of the distance between the electrodes. The thicknesses of all the Rochelle sections subsequently investigated lay between these limits.

A practical difficulty arises in measuring the dielectric constant of anisotropic crystals in that the air capacity C_0 of the condenser system experimentally determined with an isotropic dielectric, or calculated from the electrode dimensions, is not in general appropriate. Thus with a crystal for which the dielectric constant K in the direction of the field is considerably greater than that in any other direction, the observed capacity will be considerably less than $K . C_0$, and will approximate to K times the geometrical capacity of the condenser system deduced by ignoring edge effects. It is not always made clear in the accounts of experiments with Rochelle salt whether this effect has been taken into account, although some authors use the formula of Kirchhoff for the edge correction in evaluating the capacity of their condenser systems; in these cases the observed dielectric constant must be appreciably too low. In the present experiments the value of the air capacity used was that determined experimentally with nearly isotropic dielectrics. The higher values of the dielectric constant will therefore tend to be too small.

It was necessary to add to all capacity measurements made with the apparatus a small correction due to the capacity between the mercury of electrode T and the screen E, since this capacity, in series with that of the crystal under observation, remained in the oscillating circuit when the switch W was opened. This correction was estimated from the observations on the sections of different thicknesses and dielectric constants used in the calibration; it amounted to not more than 0·03 $\mu\mu$ F. The capacities measured were of the order 3–30 $\mu\mu$ F.

A calibrated variable condenser of capacity 30–300 $\mu\mu$ F., made by Messrs. H. W. Sullivan, was used as standard. This condenser was connected in series with one of three mica condensers of capacities 50, 100, and 1000 $\mu\mu$ F. Changes in the resultant capacity of the combination could be determined to 0·01 $\mu\mu$ F., and measurements could be reproduced with this accuracy.

Preparation of the Crystal Sections.—Ammonium Rochelle salt was prepared by precipitating sodium hydrogen

tartrate from a solution of tartaric acid by the addition of the calculated quantity of sodium carbonate solution. The precipitate was taken up in ammonia, and from the resulting solution ammonium Rochelle salt crystallized out on concentration. Large crystals of this salt, as well as mixed crystals of it and potassium Rochelle salt, were grown by cooling the appropriate saturated solutions in a thermostat from a temperature of about 35° C. to room temperature at a rate of 0·1 to 1° C. per day. In this way very fine crystals with linear dimensions of the order 2–3 cm. were obtained. From these crystals sections were roughly cut with a moist thread (Busch, 1933), and these sections were then accurately ground to the desired orientation and thickness. The preparation of these parallel sections was considerably facilitated by the use of a simple device made for the purpose. This consisted of a brass disk, about 6 cm. in diameter, through which passed three hardened steel screws furnished with locknuts. The rough section, with one surface ground plane and to the desired orientation, was held against the lower surface of the brass disk by suction, the section being placed across a hole in the disk which communicated with a filter pump. The three screws were set to project through the plate a distance equal to the desired thickness of the section, and grinding was carried out on a glass plate, using fine carborundum powder and paraffin, until the screws came into contact with the plate. In this way accurately parallel sections of any predetermined thickness were readily obtained.

In some cases crystals were grown in the form of parallel sections by constraining the growth, from an appropriately orientated seed, to take place between two glass plates.

§ 3. *Results.*

All measurements were made at a temperature between 16° C. and 17° C. on sections cut normal to the X crystallographic axis, this being the only direction in which potassium Rochelle salt exhibits anomalous dielectric properties. Experiments were made with potassium Rochelle salt, ammonium Rochelle salt, and with mixed crystals of these salts of molecular composition 10, 20, 30, 40 and 50 per cent. of the ammonium salt.

In all cases it was found to be impossible to make

significant measurements in the frequency range 50–300 kc. The apparent dielectric constant in this range showed very rapid variations with frequency, and was also dependent on the linear dimensions of the crystal section, so that, although consistent observations could be made with a single section, there was no correlation between the results obtained with different sections. Typical observations in this frequency range, on several sections of each composition, are included in fig. 3. These effects are undoubtedly due to piezoelectric resonances in the crystal section, and may be compared with the observations of Errera (1931) and Busch (1933) on Rochelle salt, where an apparently negative dielectric constant was found due to the same cause. In the present experiments, in fact, an apparent dielectric constant of -60 was observed with one section of potassium Rochelle salt at a frequency of 200 kc., although another section of different dimensions gave a value of $+80$ at the same frequency.

At frequencies above about 300 kc. no disturbing effects due to crystal resonances were observed, except at a few isolated frequencies corresponding to harmonics of the fundamental modes of vibration of the crystal, but in these cases the change in the value of the dielectric constant was quite small. Disregarding these particular frequencies, the dielectric constant of each salt was found to be constant to within the limits of experimental error throughout the frequency range 300–2000 kc. The results of the measurements are shown graphically in fig. 3. In the case of each salt measurements were made on at least two different sections of different thicknesses, but in no case was any change in dielectric constant observed due either to the change in the linear dimensions of the crystal or to the resulting change in the strength of the field in which the measurements were made. Similarly, no change in the dielectric constant was observed in a single section when the field strength was altered by changing the anode potential on the oscillator valves.

Experiments were also made to determine the influence on the observations of the pressure exerted on the crystal section by the electrodes. Normally the electrodes were pressed against the section only sufficiently firmly to prevent the escape of the mercury, but when this pres-

sure was considerably increased no change in the dielectric constant was detected.

The mean values observed for the dielectric constants of the mixed crystals in the frequency range 300–2000 kc. are summarized below :—

Molecular percent. of ammonium salt.	0	10	20	30	40	50	100
Dielectric constant...	114	25·0	15·8	13·0	11·8	9·9	8·2

Fig. 3.

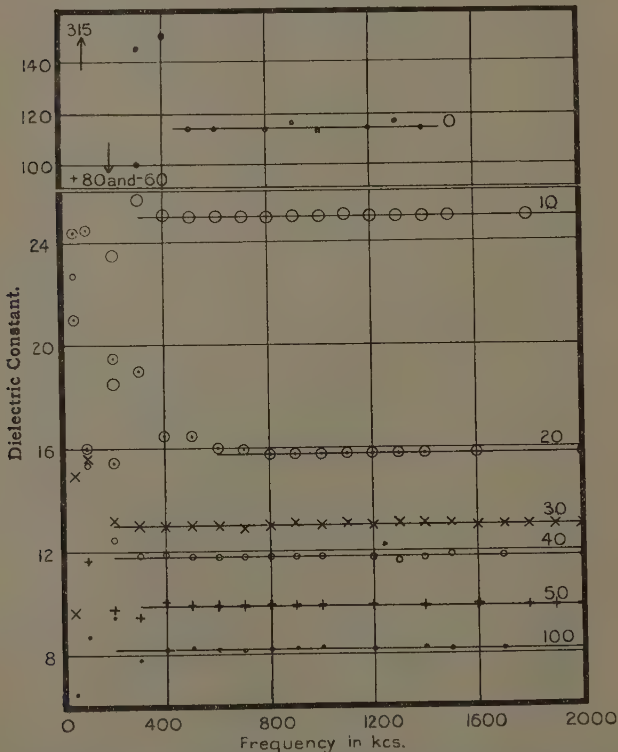

The dielectric constant of mixed crystals of sodium ammonium and sodium potassium tartrates. The number on each curve indicates the molecular percentage of the ammonium salt.

The value of 114 for potassium Rochelle salt may be directly compared with the measurements of Errera (1931) and of Busch (1933), who both found values at 1000 kc. of approximately 100 (as nearly as may be determined from their graphs). In view of the uncertainty in the zero capacity of the condenser, to which allusion has already been made, the agreement is as close as can be expected. The present experiments show that this high value of the dielectric constant of Rochelle salt falls off very rapidly with increasing concentration of the ammonium salt. Ammonium Rochelle salt has a dielectric constant no higher than that found in many solids.

§ 4. *Acknowledgments.*

It is a great pleasure to be able to acknowledge the receipt from the Government Grants Committee of the Royal Society of a grant with which the greater part of the apparatus used in this research was purchased. It is also a pleasure to express my thanks to Mr. J. D. Bernal for many valuable discussions, and to Mr. I. M. Hunter, of Corpus Christi College, Cambridge, for help in various technical matters that arose during the construction of the apparatus.

§ 5. *Summary.*

Measurements have been made of the dielectric constant at high frequencies of mixed crystals of Rochelle salt and ammonium sodium tartrate. It is found that as the proportion of the ammonium salt is increased the dielectric constant falls rapidly from a value of about 114 for Rochelle salt to a value of 8·2 for ammonium sodium tartrate.

References.

Busch, G., *Helv. phys. Acta*, vi. p. 315 (1933).
Colebrook, F. M., Exp. Wireless, viii. p. 639 (1931).
Errera, J., *Phys.* Z. ix. p. 369 (1931).
Kourtschatov, I. V., *Actualités sci.* cccxxxviii. (1936).
Scroggie, M. G., Exp. Wireless, cxxi. p. 527 (1931).

VIII. *Transformations from* γ-FeOOH *and* γ-Fe_2O_3 *to* α-Fe_2O_3 *at Lower Temperatures and the Irreversible Transition* γ-FeOOH *to* α-FeOOH. *By* LARS A. WELO, *Tottenville, Staten Island, New York, and* OSKAR BAUDISCH, *Sarotoga Springs Authority, Saratoga Springs, New York* *.

THIS study originated in the observation † that synthetic γ-ferric oxide monohydrate yielded different products on heating at 240° C. for ten minutes depending on whether the hydrate was in a sealed or in an open tube. After heating, the material in the closed tube gave the X-ray diffraction lines of paramagnetic α-Fe_2O_3 of rhombohedral structure with no admixture of other diffraction lines. The material in the open tube was, as was to be expected, ferromagnetic γ-Fe_2O_3 of cubic structure along with unconverted γ-hydrate. The colour change from yellow-orange to brick-red was rather more advanced in the closed tube than in the open one.

The Observations.

The Transformation Temperature.—Our first interest was to see if the temperature necessary to transform γ-FeOOH in a closed tube might not be much lower than 240° C. as indicated above. Two samples were available. One was prepared in 1936 by a newer method that has been described ‡. This material passed through the whole range of colour from yellow-orange to brick-red in an hour at $136{\cdot}0 \pm 0{\cdot}5°$ C., and became so wet that the previously physically dry powder could not be shaken about in the tube. A second sample prepared in 1933 §, and which had since been kept in a folded piece of paper, did not change when heated in a sealed tube at 180° C. In a tube, however, to which a drop of water had been added before sealing, this γ-hydrate changed to α-Fe_2O_3 in an hour at $147{\cdot}0 < T < 148{\cdot}0°$ C.

* Communicated by the Authors.
† O. Baudisch, *Ber. d. deutsch. Chem. Ges.* lxx. p. 218 (1937).
‡ O. Baudisch, *Svensk Kemisk Tidskrift,* xlvii. p. 115 (1935).
§ L. A. Welo and O. Baudisch, Phil. Mag. (7) xvii. p. 753 (1934).

The Necessity of Water.—These observations on the 1933 sample of γ-hydrate verified our initial assumption that water plays a part in and is necessary to the transformation of γ-FeOOH to α-Fe_2O_3 at lower temperatures. The 1936 sample was analysed for total water, and 14·1 per cent. of dry weight was found. This is 2·9 per cent. above the theoretical requirement in ferric oxide monohydrate. Evidently a sufficient fraction of this "free" water is given off at lower temperatures to maintain saturation at 136° C., the transformation temperature for the 1936 sample for one hour of heating. Weighing of the hydrate that half fills a tube, and use of the steam tables, shows that all of the "free" water in the 1936 sample, if released, is sufficient for saturation up to about 160° C. We may observe that the transformation γ-FeOOH to α-Fe_2O_3 yields free water, so that additional water, if any, is needed only at the start; provided, of course, that the necessary temperature is not too high.

Absence of Intermediate γ-Fe_2O_3.—As is well known, the transformation of γ-FeOOH to α-Fe_2O_3 may be conducted in open tubes in two stages so that one intermediate substance appears. The first stage is dehydration to ferromagnetic γ-Fe_2O_3. This stage is ordinarily completed in an hour at 250° C. At 400° C. γ-Fe_2O_3 undergoes the irreversible transition to α-Fe_2O_3 in an hour. In sealed tubes, on the contrary, intermediate γ-Fe_2O_3 never appears in the end product nor at any stage during the transformation. Sealed tubes which originally contained γ-FeOOH and sufficient water were never visibly attracted when suspended from a long string and approached with a small electromagnet.

Transformation of γFe_2O_3 *at Lower Temperatures in the "Wet" Way.*—The necessity of water for low temperature transformation of γ-FeOOH suggested that γ-Fe_2O_3, derived by dehydration of γ-FeOOH in an open container, might also be transformed to α-Fe_2O_3 at low temperatures in sealed tubes if water were added. It became at once apparent that the transformation γ-Fe_2O_3 to α-Fe_2O_3 occurs at at least approximately the same temperature and rate as the transformation of the parent hydrate to α-Fe_2O_3. That the temperature

and the rate are the same to a high degree of approximation was shown by the following experiment : γ-FeOOH (1936) was sealed in one tube, without extra water. γ-Fe_2O_3, derived from the same γ-hydrate, and water were sealed in another tube. Both tubes were heated together for three hours at $133{\cdot}0 < T < 134{\cdot}0°$ C. At the end of the first hour, γ-FeOOH had changed slightly in colour, but appeared to be a perfectly dry powder. The γ-oxide, which had previously been able to support its own end of the tube in the gap of the magnet, was now no longer able to do so. After the second hour the colour change of the γ-hydrate was nearly complete, but it still appeared to be dry. The tube containing γ-Fe_2O_3, when hung from a string, could still be much deflected by the magnet. At the end of the third hour the red colour in the hydrate tube was noticeably deeper, and the powder had become so wet that part of it adhered to the walls, and the bulk of it could not be shaken about. By this time the γ-Fe_2O_3 had become very nearly non-ferromagnetic. The tube, when suspended from a string, was just barely deflected by the magnet.

Extension to γ-Fe_2O_3 *from Precipitated Magnetite.*— The magnetic behaviour indicates, and the crystallographic investigations by X-ray methods have shown, that the ferric oxide obtained by low temperature oxidation of precipitated magnetite is identical with γ-Fe_2O_3 derived by dehydration of γ-FeOOH. We should expect that γ-Fe_2O_3 derived in this way should show depressed transformation temperatures in the presence of water. This is indeed the case, and such transformations were achieved with two γ-oxides derived from magnetites prepared in different ways. The temperature depression was again of the order 250° C., as in γ-Fe_2O_3 derived from γ-FeOOH. Two other γ-oxides from magnetite did not transform at temperatures close to the critical temperature of water, although saturation up to the critical temperature was assured by having the tube more than one-third full of water previous to sealing. However, these latter oxides were very stable towards the transition γ-$Fe_2O_3 \rightarrow \alpha$-$Fe_2O_3$ in open containers. Temperatures of the order 650° C. to 750° C. were necessary for "dry" transition in one hour. We may say, then, that if γ-Fe_2O_3 is stabilized

against the transition γ-$Fe_2O_3 \rightarrow \alpha$-$Fe_2O_3$ that occurs in open containers, it is also stabilized against transformation to α-Fe_2O_3 in the presence of water in sealed containers, whatever the path of this latter transformation may be.

Our determinations of the transformation temperatures of all the γ-hydrates and γ-oxides studied are assembled in Table I.

TABLE I.

Temperatures for Transformation of Gamma Ferric Oxide Hydrate and Gamma Ferric Oxide to Alpha Ferric Oxide in One Hour. Dry and Wet Processes.

Material.	Temperature, °C.	
	Dry.	Wet.
γ-FeOOH (1936) γ-Fe_2O_3 (from above)	$375 < T < 380$	$136{\cdot}0 \pm 0{\cdot}5$ $133{\cdot}0 < T < 134{\cdot}0$ (3 hours).
γ-FeOOH (1933) γ-Fe_2O_3 (from above)	$400 < T < 410$	$147{\cdot}0 < T < 148{\cdot}0$
γ-Fe_2O_3 from Fe_3O_4 (H)....	$450 < T < 455$	$230 < T < 235$
γ-Fe_2O_3 from Fe_3O_4 (B.&W.)	$460 < T < 465$	$165 < T < 170$
γ-Fe_2O_3 from Fe_3O_4 (S.)....	$650 < T < 675$	$350 < T <$?
γ-Fe_2O_3 from Fe_3O_4 (L.) ...	$720 < T < 750$	$365 < T <$?

References to literature describing the preparation of γ-FeOOH have already been given. Methods for the preparation of the magnetites serving as sources for the four samples of γ-Fe_2O_3 from Fe_3O_4 have also been described *. In the table, H stands for Haber's method, B. & W. stands for our own modification of the Haber method, and L stands for the method of Lefort. S represents a commercial product made by the Lefort method.

The Transformation Scheme.

In a very interesting paper of 12 years ago, Haber † discussed the analogies that exist between the series

* L. A. Welo and O. Baudisch, Phil. Mag. (7) iii. p. 396 (1927).
† F. Haber, *Naturwissenschaften*, xiii. p. 1007 (1925).

of oxides and oxide hydrates of iron and aluminium. It was in this paper that he proposed the extension of the gamma-alpha system of nomenclature already in use for the aluminium series to the analogous series for iron. That proposal has been generally adopted. In this paper the statement was made that, apart from the transition γ-$Fe_2O_3 \rightarrow \alpha$-$Fe_2O_3$, no cross transitions between the two series had ever been observed. We believe that the present study provides the evidence of such a transition, and that it is between γ-FeOOH and α-FeOOH. The necessary condition for its occurrence is that γ-FeOOH shall be wet at the temperature which gives an appreciable rate of transition. This condition is realized in closed tubes; even without added water, in the case of our γ-FeOOH (1936), because the transition temperature is so low, 136° C. It should be stated that when Haber wrote in 1925, γ-FeOOH had not yet been synthesized.

The first step in the transformation of γ-FeOOH in closed tubes with water is then to be regarded as an irreversible transition, γ-FeOOH$\rightarrow\alpha$-FeOOH. This is a natural property of γ-FeOOH just as the irreversible transition γ-$Fe_2O_3 \rightarrow \alpha$-$Fe_2O_3$ is a natural property of γ-Fe_2O_3. The rest of the transformation of γ-FeOOH to α-Fe_2O_3 consists of the shedding of α-Fe_2O_3 to satisfy the equilibrium requirements of the system α-FeOOH, α-Fe_2O_3 and water.

If we start with γ-Fe_2O_3 instead of γ-FeOOH, the transition γ-FeOOH$\rightarrow\alpha$-FeOOH is preceded by hydration of γ-Fe_2O_3 to γ-FeOOH. This hydration continues until all γ-Fe_2O_3 is consumed because γ-FeOOH disappears by irreversible transition.

The fact that intermediate γ-Fe_2O_3 does not appear in the transformation of γ-FeOOH by the wet process shows, it seems to us, that the transformation paths in the wet and the dry processes must be entirely different. The additional fact that γ-Fe_2O_3 transforms by the wet process at the same temperature and at the same rate as the γ-hydrate from which it was derived, clearly indicates that γ-Fe_2O_3 must revert to γ-FeOOH, and that the rest of the transformation proceeds as if we had started with the original hydrate.

The transformation scheme from either γ-FeOOH or γ-Fe_2O_3 for both dry and wet processes is shown

graphically in fig. 1. The temperatures indicated are for the 1936 sample of γ-FeOOH.

Fig. 1.

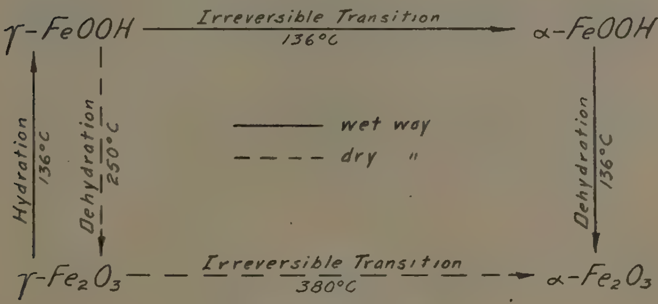

The transformation scheme.

Residual Hydrates.

Analysis of the end products after transformation of γ-FeOOH (1936) with water in sealed tubes, supports the view that the path is by way of α-FeOOH. Transformations were carried out at 134, 137, and 145° C., and the tubes were opened and dried to constant weight at 105° C. The loss of water on heating for an hour at 300° C. was then determined with results as shown in Table II.

TABLE II.

Residual Water after Transformation of γ-FeOOH (1936) in Sealed Tubes.

Transformation temperature, °C.	Residual water. Per cent. (of dry weight).	Per cent. (of water in monohydrate).
134	1·65	14·7
137	1·12	10·0
145	0·28	2·5

This analysis does not distinguish between α-FeOOH and possible unconverted γ-FeOOH. Such a distinction can be made by noting the magnetic behaviour, for,

after heating at 300° in an open container, any residual γ-FeOOH should be dehydrated to ferromagnetic γ-Fe_2O_3. This test was applied to still another portion of γ-FeOOH (1936) that had been heated in a sealed tube for an hour at 136° C. When suspended from a string the containing tube was very feebly drawn aside on approach of the magnet. If the residual hydrate were γ-FeOOH, it should have been present to the extent of over 10 per cent., according to Table II. The magnetic attraction was far less than would correspond to γ-Fe_2O_3 from this

Fig. 2.

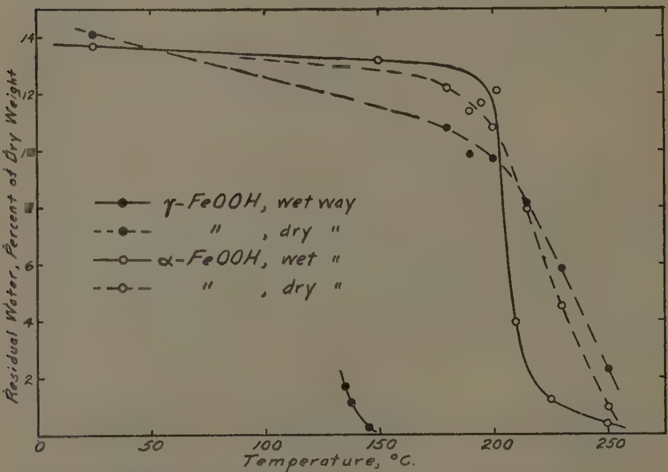

Residual water after heating one hour at each temperature.

amount of γ-FeOOH, and we conclude that the residual hydrate was largely of the alpha modification.

The data of Table II. appear as a short stretch of curve at the bottom of fig. 2, along with other data on residual water from both γ-FeOOH and α-FeOOH. This set of curves is, perhaps, not very instructive, but it does serve to emphasize the unique behaviour of γ-FeOOH when heated with water in sealed tubes. The difference in behaviour of α-FeOOH, for example, as between heating in closed and open tubes, is much less marked, although there seems to be a well-marked critical temperature

for the release of the water of hydration while heating in the closed tube. The curves for γ-FeOOH and α-FeOOH, heated in open tubes, agree with the general experience that γ-FeOOH is less stable towards dehydration than α-FeOOH. The apparent reversal of relative stability at the higher temperatures might not have been observed, if other samples had been used.

This work was, in large part, done in the Research Laboratory of the Consolidated Gas Electric Light and Power Company of Baltimore. We thank the Director, Dr. S. Karrer, for the opportunities and facilities that were provided.

February 15, 1937.

IX. *Change in Water Equilibrium and Hydration in Solutions of some typical Electrolytes.* *By* C. SAMBASIVA RAO, *M.A.*, *D.Sc.*, *Andhra University*, *Waltair* (*India*) *.

1. *Introduction.*

IN two previous papers † an account has been given of a study of the influence of dissolved strong electrolytes on the constitution of water under different experimental conditions, as revealed by the changes in the structure of the Raman water-band in their aqueous solutions. The results obtained have been interpreted on the basis of a change in water equilibrium between the proportions of the single (H_2O), double $(H_2O)_2$, and triple $(H_2O)_3$ molecules that are assumed to be present in water, as also on the basis of a change in hydration of the molecules of the dissolved substance, with variation in concentration and temperature of the solution. A few of the electrolytes previously investigated are now studied with a view to estimate quantitatively the proportions of the three types of water molecules in their aqueous solutions by an analysis of the intensity curves of the water-band in them, and compare the results

* Communicated by I. Ramakrishna Rao, M.A., Ph.D., D.Sc.

† Ind. Jour. Phys. ix. p. 195 (1934); and Proc. Roy. Soc. A, cli. p. 167 (1935).

obtained for each of the solutions with those for the pure solvent.

2. *Experimental.*

The experimental arrangement due to Wood * is employed in the present investigations. For each of the electrolytic solutions studied Raman spectra of both the solution and pure water are taken for purposes of mutual comparison under identical experimental conditions, and the mercury lamp is run under steady terminal voltage and current supply, the maximum variation of the former being less than ± 1 volt in 50 volts and of the latter less than $\pm 0{\cdot}1$ ampere in 4 amperes. These conditions are maintained throughout the exposures for the solution and water taken at one stretch. The strength of the solution is estimated immediately before and after the exposure, and in all the cases studied it has been found to remain unaltered during the course of the exposure. From an exact knowledge of the strength of the solution and its specific gravity the water content in a definite volume of the solution is calculated. Thus, the water content in solutions of hydrochloric acid, 7·65 N, sulphuric acid, 7·81 N, and sodium nitrate, 8 N, is found to be 845 gm., 791 gm., and 687 gm. respectively per litre of the solution. Now for each of the above solutions the times of exposure with the solution and pure water under constant conditions are so chosen that they are inversely proportional to the quantity of water they contain in a definite volume, so that the intensity of the Raman waterband in the pure solvent and in each of the solutions would be exactly of the same order of intensity, and the results obtained under the above conditions would permit of a reliable comparison with one another. Any changes noticed in the structure of the band, as evidenced by the differences in the intensity distribution along the band in the electrolytic solution as compared with that for the pure solvent, should be attributed to the influence of the dissolved electrolyte, and the above study should enable one to quantitatively estimate the changes thus produced in the water equilibrium between the proportions of mono-, di-, and tri-hydrol when the effect due to hydration is inappreciable. When the latter

* Phys. Rev. xxxvii. p. 1022 (1931).

cause is also operative the above study will provide us with information about the combined effect of both and with only a rough idea of the extent and complexity of the former. Hence all the three solutions referred to

Fig. 1.

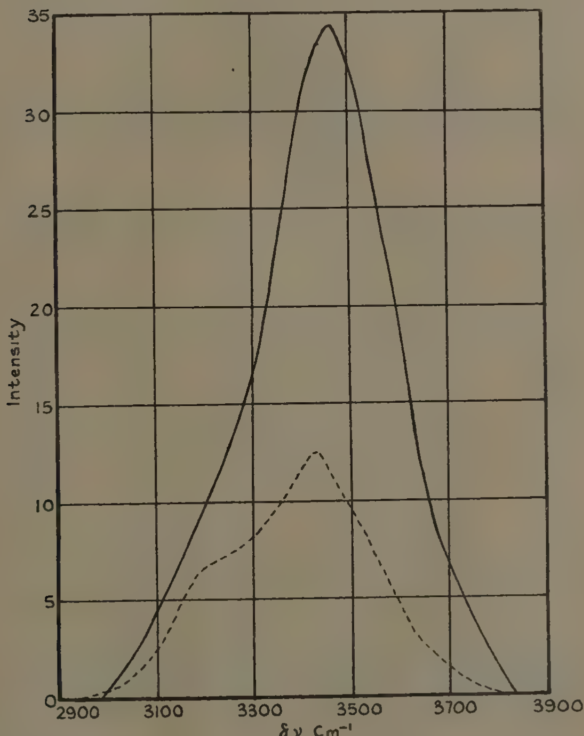

Intensity distribution in the Raman water-band for pure H_2O and $NaNO_3$, 8N solution with times of exposure inversely proportional to their respective water contents.

- - - - - -, curve for pure water. ———, curve for $NaNO_3$, 8N.

before are studied at about the same concentration, viz., 8 N, at the laboratory temperature of 31° C.

As the band excited by the λ3650 group arises out of a group of three lines situated close together, and as the

present investigation is concerned with a quantitative comparison of the intensities of the different components of the water-band in the several cases, this band, although the more intense, has been left out, and the band excited by the $\lambda 4047$ line ($\nu = 24705$ cm.$^{-1}$) is studied on account of its inherent purity, originating as it does in a single exciting line.

3. *Results.*

Fig. 1 gives the intensity curves of the Raman band for water in the pure solvent and in a solution of sodium

Fig. 2.

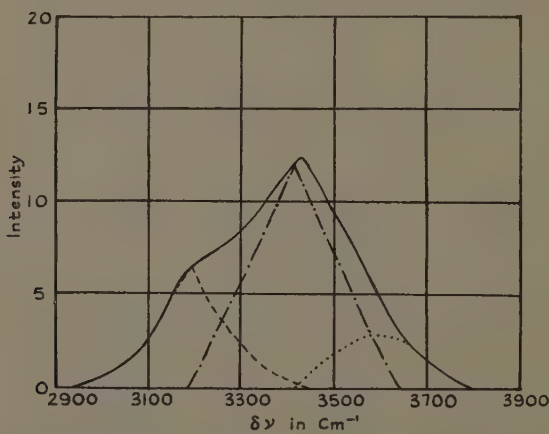

Analysis of the intensity curves of the Raman water-band into its components corresponding to the (H_2O), ($H_2O)_2$, and ($H_2O)_3$ molecules contained in it.
———, resultant curve. - - - - - -, component due to triple molecules. — . — . — ., component due to double molecules. . . . . . ., component due to single molecules.

nitrate at 8 N concentration taken with equivalent times of exposure, as described earlier. These are analyzed on the lines of the analysis made by Ramakrishna Rao *, and the curves so analyzed are represented in figs. 2 and 3 given below. The analysis in the case of the curve for

* Proc. Roy. Soc. A, cxlv. p. 489 (1934).

sodium nitrate solution is made on the assumption that the distribution of intensity along the band in this solution is only due to the existence of the three types of water molecules, and that the effect on the constitution of water in this case is solely to bring about a change in

Fig. 3.

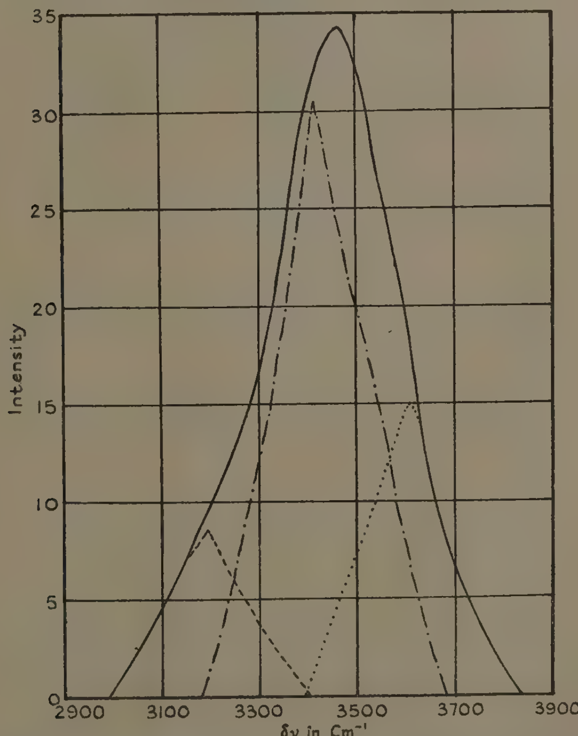

Analysis of the intensity curve of the Raman water-band for $NaNO_3$, 8N solution on the lines of the analysis in fig. 2.

the water equilibrium. That this is so is justified on the ground that the presence of hydration in this case is, at any rate, inappreciable, as was found from the earlier work of the author referred to in the beginning of this paper.

From the above analysis the following values are

obtained for the percentage proportions of the three types of water molecules in the pure solvent and the solution of sodium nitrate at 8N concentration.

TABLE I.

Type of molecules.	Percentage proportion in the Raman water-band for	
	Pure water.	$NaNO_3$, 8N solution.
	Per cent.	Per cent.
1. Triple $(H_2O)_3$ ...	30·45	15·86
2. Double $(H_2O)_2$ ..	56·20	56·40
3. Single $(H_2O)_1$ ...	13·35	27·74

Fig. 4.

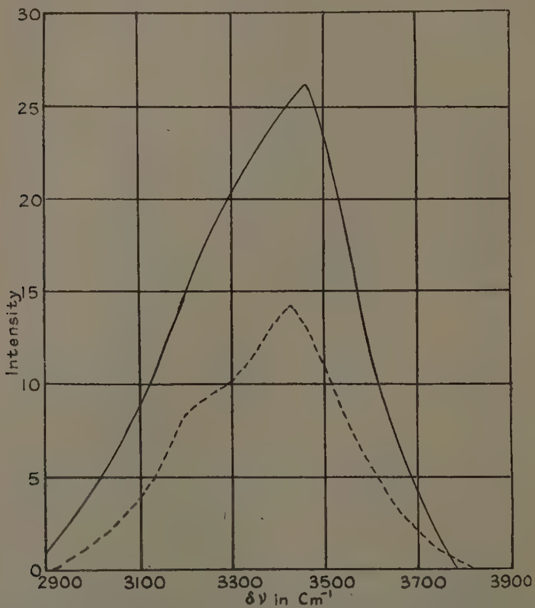

Intensity curves of the Raman water-band in pure water (- - - - -) and H_2SO_4, 7·81 N solution (———), with times of exposure inversely proportional to their respective water contents.

Figs. 4 and 5 represent the intensity curves of the Raman water-band in solutions of sulphuric acid, 7·81 N,

and hydrochloric acid, 7·65 N respectively, each of them being studied along with pure water under equivalent times of exposure. These curves are all also analyzed on the above lines, and the values of the intensities of the three components, as well as the percentage proportions of the three types of water molecules deduced therefrom. are given in Table II.

In the case of hydrochloric and sulphuric acids in addition to the change in water equilibrium with addition

Fig. 5.

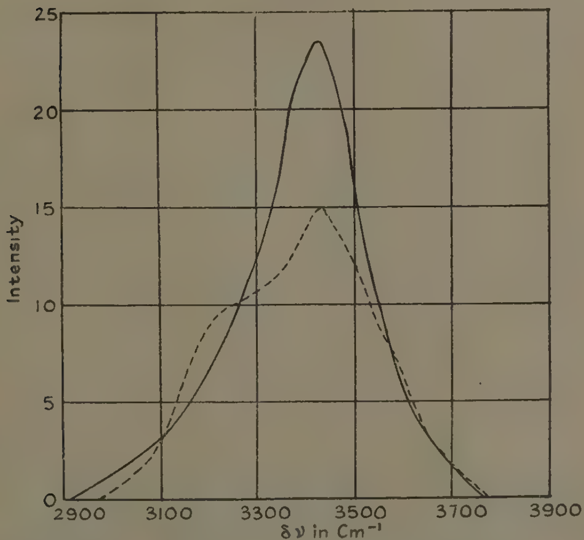

Intensity curves of the Raman band for water in pure H_2O (- - - - -) and HCl, 7·63 N solution (———), taken with times of exposure inversely proportional to their respective water contents.

of the electrolyte there is the complication due to the presence of the hydration of the ions, and it is assumed in these cases that the maxima of intensity due to the hydrates with one, two, and three molecules of water of hydration coincide with the maxima of intensity due to the single, double, and triple water molecules respectively in pure water. That such an assumption is largely justified has been shown by the author in a recent

publication *. The three components of the intensity curves for these two solutions will therefore represent the sum of the effects due to the three types of water molecules and the corresponding hydrates.

4. *Discussion.*

Considering first the case of a solution of 8 N concentration of sodium nitrate, in which it is assumed from the results of the previous investigations by the author that the formation of hydrates is in this case inappreciable, we find that whatever changes are noticed in the structure of its Raman water-band as compared with the band for

TABLE II.

Substance.	Intensity.			Percentage proportion.		
	$(H_2O)_1$.	$(H_2O)_2$.	$(H_2O)_3$.	$(H_2O)_1$.	$(H_2O)_2$.	$(H_2O)_3$.
				Per cent.	Per cent.	Per cent.
I. (*a*) Water	2·85	12·0	6·5	13·35	56·20	30·45
(*b*) $NaNO_3$, 8N	14·95	30·4	8·55	27·74	56·40	15·86
II. (*a*) Water	3·3	13·7	7·4	13·52	56·15	30·33
(*b*) H_2SO_4, 7·81 N ..	7·3	21·7	14·0	16·97	50·50	32·53
III. (*a*) Water	3·6	14·55	8·2	13·70	55·30	31·00
(*b*) HCl, 7·65 N ...	3·5	22·00	6·22	11·04	69·39	19·56

pure water must be due to a change in the proportions of the single (H_2O), double $(H_2O)_2$, and triple $(H_2O)_3$ molecules only. It will be seen from a comparison of the percentage proportions of the three types of water molecules in the solutiou of sodium nitrate and in pure water given in Table I. above that there is a considerable reduction in the number of triple molecules, with a corresponding increase in that of the single molecules, while the percentage proportion of the double molecules remained the same as in the pure solvent. Thus, the addition of sodium nitrate to water results in the simplification of the more complex water molecules into the simplest types, and hence causes a shift in the intensity maximum of the band to the side of higher frequency corresponding

* Proc. Roy. Soc. A, cli. p. 167 (1935).

to single water molecules. The percentage proportions of the triple, double, and single molecules in sodium nitrate solution at 8 N concentration are 15·9, 56·4, and 27·7 respectively, while the corresponding values for water are 30·5, 56·2, and 13·4. The effect of sodium nitrate on the water equilibrium noticed here is in agreement with the qualitative observation of Cabannes and Riols *, as well as with the result deduced by Bancroft and Gould † from their recent work on the Hofmeister series of certain anions including the nitrate ion.

Taking up next the case of the aqueous solution of hydrochloric acid at 7·65 N concentration, the results of the analysis for the percentage values of the intensities of the three components corresponding to triple, double, and single molecules in water are 19·6, 69·4, and 11·0 respectively, while the corresponding values for pure water are 31·0, 55·3, and 13·7. It is thus seen that in this case there is an enhancement of the intensity of the component corresponding to the double water molecules, with a proportionate decrease in that of the component ascribed to the triple molecules, and to a much less degree in that of the single molecules. It, therefore, follows that the effect of the dissolved acid on the constitution of water is to change trihydrol into dihydrol with no appreciable effect on the proportion of monohydrol. This result is in conflict with the observation of Bancroft and Gould, who find, from their work on Hofmeister series referred to before, that the effect of the chloride ion is to change dihydrol into monohydrol with no especial effect on trihydrol. The results obtained by the author from a study of the intensity distribution along the Raman water-band are further in disagreement with those obtained by the above authors, who observe that, for equivalent concentrations, the amount of monohydrol is less with nitrate ion than with chloride ion. As is quantitatively demonstrated here the proportion of monohydrol in nitrate solution is far greater than that in hydrochloric acid at the same concentration. As the method of the Raman effect employed by the author is a more direct one on account of the direct proportionality that exists between the intensities of the Raman band and the numbers

* *Comptes Rendus*, cxcviii. p. 30 (1934).
† Journ. Phys. Chem. xxxviii. p. 197 (1934)

of molecules that give rise to it, the author believes that the results herein obtained are more reliable.

Further, in the case of hydrochloric acid hydration is known to take place, and the increased intensity of the component attributed to the double molecules shows that hydrates with two molecules of water of hydration preponderate at this concentration of the acid, for the maximum of intensity due to hydrates with two associated water molecules more or less conicides with that due to double molecules in pure water.

Finally, the results of the analysis of the intensity curve of the water-band in sulphuric acid at 7·81 N concentration exhibits a slight increase in the intensities of the components attributed to the triple and single molecules, while there is a corresponding decrease in the intensity of the component ascribed to the double molecules. The percentage proportions of the tri-, di-, and monohydrol in the aqueous solution of this acid at 7·81 N concentration are respectively 32·6, 50·5, and 17·0, while those for the pure solvent are 30·3, 56·2, and 13·5. The effect of the acid therefore appears to be to partly change dihydrol into mono- and trihydrol. But sulphuric acid is known to form a large number of hydrates * in its aqueous solutions, and the increased intensity of the component corresponding to triple molecules in water points to the conclusion that at this concentration of the acid there are present hydrates with three and more number of associated molecules of water of hydration, for their maximum of intensity falls in about the same position as that due to this component of the water molecules. Also, the enhanced intensity of the component attributed to monohydrol in water shows that hydrates with one associated molecule of water of hydration are present at this concentration of the acid.

In conclusion, the author desires to express his best thanks to Dr. I. Ramakrishna Rao for his kind interest and advice during the progress of this investigation.

5. *Summary.*

The three strong electrolytes, sodium nitrate, sulphuric and hydrochloric acids, are studied in their aqueous solutions, together with the pure solvent in each case, under

* Mellor, 'Inorganic and Theoretical Chemistry,' x. p. 351 *seq.*

identical experimental conditions, with a view to quantitatively estimating the changes that take place in the constitution of water *as solvent* as compared with that of pure water.

Analysis of the intensity curves of the Raman band for water in the pure solvent and in the solution is done for each of the electrolytes studied, with the following results :—

(i.) Sodium nitrate changes trihydrol into monohydrol, with no especial effect on dihydrol.

(ii.) Sulphuric acid changes dihydrol into mono- and trihydrol : further, at 8N concentration hydrates with one and three molecules of water of hydration seem to preponderate over the other types.

(iii.) Hydrochloric acid exhibits an increase in the component due to the double molecules, with a corresponding decrease in that of the triple molecules, and as such points to the conclusion that it changes trihydrol into dihydrol, and that at 7·65 N concentration hydrates with two associated water molecules are present in greater numbers.

X. *Matrix Theory of Multiconductor Transmission Lines*

By Louis A. Pipes, *Ph.D., Electrical Engineering Department, The Rice Institute, Houston, Texas* *.

Introduction.

THE purpose of this paper is to show how matrix algebra may be used to solve the difficult and unwieldy problem of multiconductor transmission lines with the minimum effort.

The analysis here presented may be compared to that of L. V. Bewley in his 'Travelling Waves on Transmission Systems,' chapter vi. (John Wiley and Sons, publishers). A comparison of the theory here presented and that of Bewley will show the greater power and simplicity of the matrix method. The difficulties encountered in problems of this class may be said to be mechanical

* Communicated by the Author.

rather than mathematical in character, in that the large bulk of equations and terms soon discourages the analyst when proceeding by conventional methods. The analysis here presented is an example of the simplicity effected by the use of matrix methods, and some of the results have been extended.

The Coefficients of Capacity and Induction.

Let us consider a system of n conducting bodies that are situated in air.

Let $(Q_1 \ldots . Q_n)$ represent the charges on the conductors in coulombs.

Let $(V_1 \ldots . V_n)$ be the potentials of the various conductors in volts.

Fig. 1.

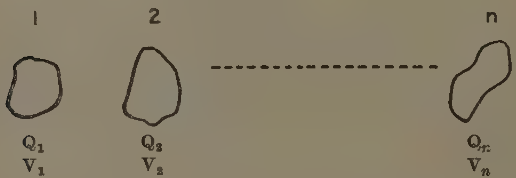

Because of the principle of superposition the effects of the simultaneous charges $(Q_1 \ldots . Q_n)$ on the n conductors gives rise to a system of potentials.

$$V_1 = p_{11}Q_1 + \ldots\ldots\ldots\ldots + p_{1n}Q_n,$$
$$\cdot \quad \cdot \quad \cdot \quad \cdot \quad \cdot \quad \cdot \quad \cdot \quad \cdot \quad \cdot \quad \cdot$$
$$V_n = p_{n1}Q_1 + \ldots\ldots\ldots\ldots + p_{nn}Q_n,$$

where the quantities p_{ij} are known as the coefficients of potential. The value of these constants depends entirely on the geometrical arrangement of the conductors.

Let us introduce the matrices :

$$[V] = \begin{bmatrix} V_1 \\ V_2 \\ \cdot\cdot \\ V_n \end{bmatrix} \qquad [p] = \begin{bmatrix} p_{11} \cdots\cdots p_{1n} \\ p_{21} \cdots\cdots p_{2n} \\ \cdot \quad \cdot \quad \cdot \quad \cdot \quad \cdot \\ p_{n1} \cdots\cdots p_{nn} \end{bmatrix} \qquad [Q] = \begin{bmatrix} Q_1 \\ Q_2 \\ \cdot\cdot \\ Q_n \end{bmatrix}.$$

The above relations may be written as a matrix equation :

$$[V] = [p]\,[Q].$$

We can, however, write the charges in terms of the capacity coefficients as

$$Q_1 = c_{11}V_1 + \dots\dots\dots + c_{1n}V_n,$$
$$\cdot \quad \cdot \quad \cdot \quad \cdot \quad \cdot \quad \cdot \quad \cdot \quad \cdot \quad \cdot$$
$$Q_n = c_{n1}V_1 + \dots\dots\dots + c_{nn}V_n,$$

where the constants c_{ij} are functions of the geometry of the conductor arrangement. The c_{ij} quantities are called coefficients of induction when $i \neq j$ and coefficients of capacity when $i=j$.

If we introduce the matrix

$$[c] = \begin{bmatrix} c_{11} \dots\dots\dots\dots c_{1n} \\ \cdot \quad \cdot \quad \cdot \quad \cdot \quad \cdot \quad \cdot \quad \cdot \\ c_{n1} \dots\dots\dots\dots c_{nn} \end{bmatrix}$$

we may write the matrix relation

$$[Q]=[C]\,[V].$$

From the equations

$$[V]=[p]\,[Q],$$
$$[Q]=[c]\,(V),$$

we may obtain the relation between the p_{ij} quantities and the c_{ij} quantities.

We have, on multiplying the first of these equations by $[p]^{-1}$, the inverse of $[p]$:

$$[p]^{-1}[V]=[p]^{-1}[p][Q]=[Q].$$

Comparing with $\qquad [Q]=[c]\,[V],$

we see that $\qquad [c]=[p]^{-1}.$

It may similarly be shown that $[p]=[c]^{-1}$.

This is the connexion between the two matrices $[c]$ and $[p]$. If we know the elements of one matrix. we may, by finding its inverse, obtain the elements of the other one.

Parallel Cylindrical Conductors.

The above theory holds in general independently of the size or arrangement of the conductors. Following Bewley, let us consider a system of long, parallel, widely separated, cylindrical conductors over an equipotential ground plane.

Let

$\bar{R}_r$=radius of conductor r,

h_r=height of conductor r above the ground plane,

a_{rs}=distance between conductor r and the image of conductor s,

b_{rs}=distance between conductors r and s.

Then, on the assumption that $a_{rs}>>\bar{R}_r$, $b_{rs}>>\bar{R}_r$, or that the distances separating the conductors from each other and from the ground are large compared to the radii of the various conductors, we have

$$p_{rr}=18\log_e 2h_r/\bar{R}_r\times 10^{-11}\text{ darafs/cm.},$$
$$p_{rs}=18\times\log_e a_{rs}/b_{rs}\times 10^{-11}\text{ darafs/cm.}$$

Fig. 2.

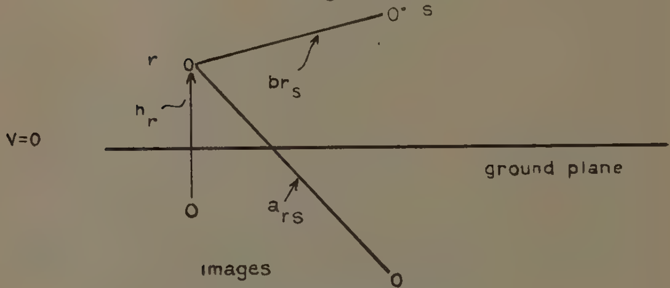

The Electromagnetic Coefficients.

Let us now consider the flux linkages of the various conductors by the flux produced as a result of the current flow in the several conductors. If we let the flux linkage of conductor r due to its own current i_r be $L_{rr}i_r$, then, by the principle of superposition, the total flux linkages of all the conductors are

$$\phi_1=L_{11}i_1+\ldots\ldots\ldots\ldots+L_{1n}i_n,$$
$$\cdots\cdots\cdots\cdots$$
$$\phi_n=L_{n1}i_1+\ldots\ldots\ldots\ldots+L_{nn}i_n.$$

If we introduce the matrix,

and $\begin{bmatrix} L_{11}\ldots\ldots\ldots L_{1n} \\ \cdot\quad\cdot\quad\cdot\quad\cdot\quad\cdot\quad\cdot \\ L_{n1}\ldots\ldots\ldots L_{nn}\end{bmatrix}=[L]$ $\qquad\begin{bmatrix}\phi_1\\ \phi_2\\ \cdot\,\cdot\\ \phi_n\end{bmatrix}=[\phi].$

If we further introduce a vertical columnar matrix $[i]$ whose elements are the currents flowing in the various

conductors, then we may write the flux relation in the matrix form $[\phi]=[L]\,[i]$.

For the system of parallel wires and their images below the ground plane that we are considering we have

$$L_{rr}=\left(\tfrac{1}{2}+2\log_e\frac{2h_r}{R_r}\right)\times 10^{-9}\text{ henry/cm.}$$

$$L_{rs}=2\log\frac{a_{rs}}{b_{rs}}\times 10^{-9}\text{ henry/cm.}$$

The General Differential Equations.

If we let

L_{rr}=self-inductance of conductor r,

L_{rs}=mutual inductance coefficient between conductors r and s,

C_{rr}=self capacitance coefficient between conductors r and s,

C_{rs}=mutual capacitance coefficient between r and s,

R_r=series resistance of conductor r,

g_{rr}=leakage conductance to ground of conductor r,

g_{rs}=leakage conductance between r and s.

If we let $G_{rr}=g_{rn}$,

$G_{rs}=G_{sr}=-g_{rs}=-g_{sr}$,

$Z_{rr}=R_r+pL_{rr}$, where p is the differential operator $p=\delta/\delta t$,

$Z_{rs}=pL_{rs}$,

$Y_{rr}=G_{rr}+pC_{rr}$,

$Y_{rs}=G_{rs}+pC_{rs}$.

It is easy to show (see Bewley, 'Travelling Waves on Transmission Systems,' p. 94) that the differential equations of the system of currents and potentials are

$$-\delta V_1/\delta x=Z_{11}i_1+\dots\dots\dots+Z_{1n}i_n,$$
$$\dots\dots\dots\dots\dots\dots$$
$$-\delta V_n/\delta x=Z_{n1}i_1+\dots\dots\dots+Z_{nn}i_n,$$

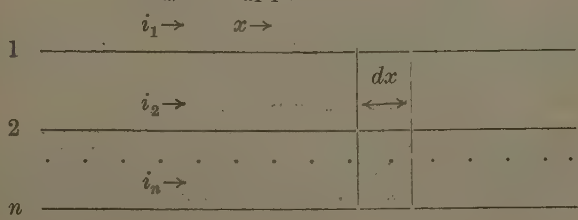

In matrix form: if we let D represent the differential operator $D = \delta/\delta x$,

$$-D[V]=[Z][i].$$

Similarly, the equation for the currents may be written in matrix form as

$$-D[i]=[Y][V],$$

where $[V]$ and $[i]$ are vertical columnar matrices whose elements represent the potentials and currents respectively at a point x of the transmission line, and the matrices $[Z]$ and $[Y]$ are given by

$$\begin{bmatrix} Z_{11} \cdots\cdots Z_{1n} \\ \cdot \quad \cdot \quad \cdot \quad \cdot \\ Z_{n1} \cdots\cdots Z_{nn} \end{bmatrix}=[Z] \qquad \begin{bmatrix} Y_{11} \cdots\cdots Y_{1n} \\ \cdot \quad \cdot \quad \cdot \quad \cdot \\ Y_{n1} \cdots\cdots Y_{nn} \end{bmatrix}=[Y].$$

If we differentiate the first of the above matrices we obtain, on differentiating with respect to x and noting that the $[Z]$ matrix is a matrix of constants as far as x is concerned,

$$D^2[V]=[Z]D[i]=-[Z][Y][V];$$

on substituting from the second of the above equations

$$-D[i]=[Y].[V].$$

Hence $D^2[V]=[Z][Y][V]$ is the equation to be satisfied by the potentials of the several wires along the lines.

Similarly, by differentiating the second of the above equations partially with respect to x we obtain $D^2[i]=[Y][Z][i]$ on making a substitution from the first equation. Now, because $Z_{rs}=Z_{sr}$ and $Y_{rs}=Y_{sr}$, the matrices $[Z]$ and $[Y]$ are symmetric, and hence we may write $[Y][Z]=[Z][Y]$. The fundamental equations of the system reduce to

$$D^2[V]=[Z][Y][V] \quad \text{and} \quad D^2[i]=[Z][Y][i].$$

For simplicity let $[J]=[Z][Y]$.

The equations reduce to

$$D^2[V]=[J][V] \text{ and } D^2[i]=[J][i].$$

If we compare this with the equations arrived at in the conventional manner it would give us a prompt temptation to abandon the problem. The concise matrix equations

may be expanded out to an awful bulk of scalar equations that easily discourages further analytical work.

Because of certain simplifications effected there are three cases which may be considered before discussing the general case.

I. *The No-loss Line*

The no-loss line is characterized by the conditions $R_{ij}=0$ and $G_{ij}=0$. That is, there are no resistances in the lines and no leakages. For this case we have $Z_{ij}=L_{ij}p$ and $Y_{ij}=C_{ij}p$.

Then

$$[J]=[Z][Y]=\begin{bmatrix} L_{11}p & \cdots & L_{1n}p \\ \cdot & & \cdot \\ L_{n1}p & \cdots & L_{nn}p \end{bmatrix}\begin{bmatrix} C_{11}p & \cdots & C_{1n}p \\ \cdot & & \cdot \\ C_{n1}p & \cdots & C_{nn}p \end{bmatrix}.$$

Therefore $[J]=p^2[L][C]$, and the equations become

$$D^2[V]=p^2[L][C][V] \text{ and } D^2[i]=p^2[L][C][i].$$

Let us investigate these equations for a traveling wave solution of the form

$$[V]=[V(z-vt)].$$

Now $\qquad D^2[V]=[D^2V(z-vt)]=[V''(z-vt)]=[V''],$

and $\qquad p^2[V]=[p^2V(z-vt)]=[V''(z-vt)v^2]=v^2[V''],$

therefore $\qquad D^2[V]=p^2[L][C][V]$

becomes by this substitution

$$[V'']=v^2[L][C][V''],$$

or, transposing,

$$([U]-v^2[L][C])[V'']=[0],$$

where $[U]$ is the unit matrix. Let $v^2=1/\mu$, then

$$(\mu[U]-[L][C])[V'']=[0].$$

Now the matrix $(\mu[U]-[L][C])$ is the characteristic matrix of the matrix $[L][C]$. For brevity, let $[K]=[L][C]$, then the various values of μ which satisfy the determinant

$$|\mu[U]-[K]|=0$$

are called the latent roots of the matrix $[K]$. The equation

$$|\mu[U]-[K]|=0$$

is, in general, an equation of the nth degree in μ, where n is the degree of the matrix [K]. Therefore the n values of μ are given by

$$\begin{vmatrix} (\mu-K_{11}) & -K_{12} & \dots & -K_{1n} \\ -K_{21} & (\mu-K_{22}) & \dots & -K_{2n} \\ \cdot & \cdot & \cdot & \cdot \\ -K_{n1} & \dots & \dots & (\mu-K_{nn}) \end{vmatrix} = 0.$$

From the values of μ we compute the velocities of propagation by the equation $v_i=\pm\sqrt{1/\mu_i}$. It is therefore evident that there are $2n$ distinct velocities of propagation in general. The negative values of v correspond to waves travelling in the forward x direction, and positive values of v to waves in the negative x direction. Because of the linearity of the equations this shows that in general there can exist n simultaneous pairs of backward and forward waves of velocities $(v_1, \dots v_n)$. The potential matrix may therefore be written as

$$\begin{bmatrix} V_1 \\ V_2 \\ \cdot\cdot \\ V_n \end{bmatrix} = \begin{bmatrix} f_{11}(x-v_1t)+\dots\dots+f_{1n}(x-v_nt, \\ \cdot\quad\cdot\quad\cdot\quad\cdot\quad\cdot\quad\cdot\quad\cdot \\ \cdot\quad\cdot\quad\cdot\quad\cdot\quad\cdot\quad\cdot\quad\cdot \\ f_{n1}(x-v_1t)+\dots\dots+f_{nn}(x+v_nt) \end{bmatrix}$$

$$+\begin{bmatrix} b_{11}(x+v_1t)+\dots\dots+b_{1n}(x+v_nt) \\ \cdot\quad\cdot\quad\cdot\quad\cdot\quad\cdot\quad\cdot\quad\cdot \\ b_{n1}(x+v_1t)+\dots\dots+b_{nn}(x+v_nt) \end{bmatrix}.$$

Or, more briefly,

$$[V]=[f]+[b],$$

where $[f]$ represents the forward waves and $[b]$ represents the backward waves.

We may most easily obtain the current waves from

$$-D[i]=[Y][V],$$

where $[Y]=[C]p$ in case of the no-loss line. Integrating with respect to x, we obtain

$$-[i]=p[C]\int[V]\,dx+[\phi(t)],$$

where $[\phi(t)]$ represents a vertical columnar matrix whose elements are functions of t. However, if $[V]=[0]$, or in the absence of potentials, then $[i]=[0]$. It therefore follows that $[\phi(t)]=[0]$, and, therefore, we have

$$[i]=-p[C]\int[V]\,dx.$$

But

$$p[V]=\begin{bmatrix} -v_1 f_{11}' \dots -v_n f_{1n}' \\ \cdot \quad \cdot \quad \cdot \quad \cdot \quad \cdot \\ -v_1 f_{n1}' \dots -v_n f_{nn}' \end{bmatrix}+\begin{bmatrix} v_1 b_{11}' + \dots + v_n b_{1n} \\ \cdot \quad \cdot \quad \cdot \quad \cdot \quad \cdot \\ v_1 b_{n1}' + \dots \quad v_n b_{nn}' \end{bmatrix},$$

where the primes indicate differentiation with respect to the various arguments of the functions.

Therefore

$$[i]=-p[C]\int [V]\,dx$$

$$=[C]\begin{bmatrix} v_1(f_{11}-b_{11})+\dots\dots+v_n(f_{1n}-b_{1n}) \\ \cdot \quad \cdot \quad \cdot \quad \cdot \quad \cdot \quad \cdot \quad \cdot \\ v_1(f_{n1}-b_{n1})+\dots\dots+v_n(f_{nn}-b_{nn}) \end{bmatrix}.$$

Therefore

$$i_1=c_{11}\left\{\sum_{r=1}^{n} v_r(f_{1r}-b_{1r})\right\}+\dots\dots+c_{1n}\left\{\sum_{r=1}^{n} v_r(f_{nr}-b_{nr})\right\},$$

etc.

To arrive at these results in the conventional manner requires quite formidable algebraic manipulations.

The Energy of the No-loss Line.

Let $[V]_h=[V_1\dots\dots V_n]$ be a horizontal line matrix representing the potentials of the various wires.

$[Q]_v$ = a columnar matrix whose elements represent the charges per unit length of the wires. Then the electrostatic energy is given by

$$[W]_e=\tfrac{1}{2}\int [V]_h[Q]_v\,dx,$$

where $[W]_e$ represents a single element matrix whose value represents the electric energy.

Now $[Q]=[C]\ [V]_v$, where $[V]_v$ represents a columnar matrix whose elements are the potentials of the various conductors. Therefore, substituting for $[Q]$, we obtain

$$[W]_e=\tfrac{1}{2}\int [V]_h[C]\ [V]_v\,dx.$$

This is a generalization of $W_e=\frac{1}{2}\int C_1V_1^2\,dx$ for a single conductor.

The magnetic energy of the no-loss line is given by

$$[W]_m=\tfrac{1}{2}\int [i]_h[\phi]\,dx,$$

where $[i]_h$ is a horizontal line matrix whose elements represent the various currents flowing in the conductors

and $[\phi]$ is the flux linkage matrix previously discussed. However, we have the equation $[\phi]=[L][i]_v$ discussed in the earlier part of the paper. Accordingly, substituting this relation in the equation above, we obtain

$$[W]_m=\tfrac{1}{2}\int [i]_h[L][i]_v\,dx,$$

and this is analogous to the equation $W_m=\frac{1}{2}\int Li^2\,dx$ for one circuit.

The total energy of the no-loss transmission line is

$$[W]_T=\tfrac{1}{2}\int [i]_h[L][i]_v\,dx+\tfrac{1}{2}\int [V]_h[C][V]_v\,dx,$$

where the integrals must be taken throughout the length of the lines.

II. *The completely Transposed Line.*

If we assume that the n conductors are completely transposed with respect to each other and to the ground, and if we further assume that they have the same leakage and resistance coefficients, then we have the following relations :

$$L_{rr}=L,\qquad C_{rr}=C,\qquad G_{rr}=G,\qquad R_{rr}=R,$$

$$L_{rs}=L_1,\qquad C_{rs}=C_1,\qquad G_{rs}=G_1.$$

Then

$$[J]=[Z][Y]=\begin{bmatrix} Z_{11}\ldots\ldots Z_{1n} \\ \cdot\quad\cdot\quad\cdot\quad\cdot \\ Z_{n1}\ldots\ldots Z_{nn}\end{bmatrix}\begin{bmatrix} Y_{11}\ldots\ldots Y_{1n} \\ \cdot\quad\cdot\quad\cdot\quad\cdot \\ Y_{n1}\ldots\ldots Y_{nn}\end{bmatrix}.$$

In this case

$$Z_{rr}=R_{rr}+pL_{rr}=R+pL=Z_1,\qquad Z_{rs}=pL_1=Z,$$

$$Y_{rr}=G+PC=Y_1,\qquad\qquad Y_{rs}=G_1+pC_1=Y.$$

Let us, for simplicity, consider a three-wire system. The general case may be treated by obvious modifications. In the three-wire case we have

$$[Z]=\begin{bmatrix} Z_1 & Z & Z \\ Z & Z_1 & Z \\ Z & Z & Z_1\end{bmatrix}\quad\text{and}\quad [Y]=\begin{bmatrix} Y_1 & Y & Y \\ Y & Y_1 & Y \\ Y & Y & Y_1\end{bmatrix};$$

therefore

$$[Z]=Z\begin{bmatrix} \beta & 1 & 1 \\ 1 & \beta & 1 \\ 1 & 1 & \beta\end{bmatrix}\quad\text{and}\quad [Y]=Y\begin{bmatrix} \alpha & 1 & 1 \\ 1 & \alpha & 1 \\ 1 & 1 & \alpha\end{bmatrix},$$

where

$$\beta=Z_1/Z=(R+pL)/pL_1, \quad \alpha=Y_1/Y=(G+PC)/(G_1+pC_1).$$

If we further restrict the line to have no losses, then

$$R=G=G_1=0,$$

and in this case

$$\beta=L/L_1, \quad \alpha=C/C_1.$$

Therefore

$$[Z]\,[Y]=p^2L_1C_1\begin{bmatrix}\beta & 1 & 1\\ 1 & \beta & 1\\ 1 & 1 & \beta\end{bmatrix}\begin{bmatrix}\alpha & 1 & 1\\ 1 & \alpha & 1\\ 1 & 1 & \alpha\end{bmatrix}$$

$$=p^2L_1C_1\begin{bmatrix}(\beta\alpha+2) & (\beta+\alpha+1) & (\beta+\alpha+1)\\ (\beta+\alpha+1) & (\beta\alpha+2) & (\beta+\alpha+1)\\ (\beta+\alpha+1) & (\beta+\alpha+1) & (\beta\alpha+2)\end{bmatrix}$$

$$=p^2L_1C_1[K],$$

where

$$[K]=(\beta+\alpha+1)\begin{bmatrix}M & 1 & 1\\ 1 & M & 1\\ 1 & 1 & M\end{bmatrix}\begin{matrix}M=(2+\beta\alpha)/(\beta+\alpha+1),\\ \text{let } s=(\beta+\alpha+1).\end{matrix}$$

The voltage equation then reduces to

$$D^2[V]=p^2L_1C_1[K]\,[V].$$

If, as before, we investigate travelling waves solution of the form $[V]=[V(x+vt)]$, then, on substitution into the above equation, we obtain

$$[V]''=v^2L_1C_1[K]\,[V]'',$$

or

$$(\mu[U]-v^2L_1C_1[K])[V]''=[0],$$

where $v^2=1/\mu$. The various possible values of μ are given by the equation

$$|\,\mu[U]-L_1C_1[K]\,|=0 \quad [U]=\text{unit matrix},$$

or, if we place $\mu_1=\mu/L_1C_1s$, then the equation to be satisfied by μ_1 is

$$\begin{vmatrix}(\mu_1-M) & -1 & -1\\ -1 & (\mu_1-M) & -1\\ -1 & -1 & (\mu_1-M)\end{vmatrix}=0;$$

or, multiplying out $(\mu_1-M+1)^2(\mu_1-M-2)=0$, the two roots for μ_1 are

$$\mu_1=M-1 \quad \text{and} \quad \mu_1=M+2.$$

We obtain the corresponding two values of μ :

$$\mu=\mu_1 s L_1 C_1=(M-1)sL_1C_1=(2+\beta\alpha-s)(L_1C_1)$$
$$=L_1C_1+LC-C_1L-L_1C.$$

Therefore one of the possible values of the forward and backward velocities is

$$v_1=\pm 1/\sqrt{(L_1C_1+LC-C_1L-L_1C)}.$$

The other root gives

$$v_2=\pm 1/\sqrt{4L_1C_1+LC+2(LC_1+LC_1)}.$$

In case of more than three wires there are still only two distinct velocities of propagation in view of the fact that the latent roots in the general case may be written as the solution of

$$\left| \mu_1[U]-\begin{matrix} M & \ldots & \ldots & 1 \\ 1 & M & \ldots & 1 \\ . & . & . & . \\ 1 & \ldots & \ldots & M \end{matrix} \right| = 0 = (\mu-M+1)^{n-1}(\mu-M+1-n).$$

It is therefore evident that in the perfectly transposed no-loss line there are two distinct velocities of propagation.

The Steady State.

Let us investigate the steady state in the general case. We will suppose that the line is operating under the steady state alternating conditions.

We have the equations

(1) $-D[V]=[Z]\,[i].$

(2) $-D[i]=[Z]\,[V].$

(3) $D^2[V]=[Z]\,[Y]\,[V].$

(4) $D^2[i]=[Z]\,[Y]\,[i].$

Let the alternating potentials of the various conductors be given by

$e_1=E_1 \sin(\omega t+\theta_1)=$imaginary part of $E_1 e^{j(\omega t+\theta_1)}$,

. . . . . .

$e_n=E_n \sin(\omega t+\theta_n)=$imaginary part of $E_n e^{j(\omega t+\theta_n)}$, $j=\sqrt{-1}$,

where $E_1 \ldots . E_n$ are functions of x. The analysis will be carried out on the complex voltages, the true

voltage may be obtained from the imaginary part of the complex potentials.

Let

$$[\mathrm{V}] = e^{j\omega t}\begin{bmatrix} \mathrm{E}_1 a_1 \\ \cdot \quad \cdot \\ \cdot \quad \cdot \\ \mathrm{E}_n a_u \end{bmatrix}; \quad \text{where } a_i = e^{j\theta_i}.$$

Let

$$[\mathrm{E}] = \begin{bmatrix} \mathrm{E}_1 a_1 \\ \cdot \quad \cdot \\ \cdot \quad \cdot \\ \mathrm{E}_n a_n \end{bmatrix}.$$

Substituting into equations (3) and (4), we obtain, on cancelling the common factor $e^{j\omega t}$,

$$\mathrm{D}^2[\mathrm{E}] = [\mathrm{J}_1]\,[\mathrm{E}],$$

where $[\mathrm{J}_1] = [\mathrm{J}]_{p=j\omega}$;

$$\mathrm{D}^2[\mathrm{I}] = [\mathrm{J}_1]\,[\mathrm{I}],$$

where

$$[\mathrm{I}] = \begin{bmatrix} b_1 \mathrm{I}_1 \\ \cdot \quad \cdot \\ \cdot \quad \cdot \\ \cdot \quad \cdot \\ b_n \mathrm{I}_n \end{bmatrix}, \quad b_i = e^{j\phi i},$$

where, in the same way as in the case of the voltages, we have assumed a complex form for the currents. The I_i are functions of x analogous to the E_i quantities.

Each of these matrix equations represents a system of n simultaneous ordinary differential equations of the second order; the solution of these equations therefore contains $2n$ arbitrary constants.

Let us assume as a solution

$$[\mathrm{I}] = [\mathrm{A}] \cosh \alpha x + [\mathrm{B}] \sinh \alpha x,$$

$$[\mathrm{E}] = [\mathrm{C}] \cosh \alpha + [\mathrm{D}] \sinh \alpha x.$$

Substituting this into the above equations for [E] and [I], we obtain

$$\mathrm{D}^2[\mathrm{E}] = \alpha^2[\mathrm{C}] \cosh \alpha x + \alpha^2[\mathrm{D}] \sinh \alpha x$$
$$= \alpha^2\,[\mathrm{E}];$$

therefore, substituting into

$$\mathrm{D}^2[\mathrm{E}] = [\mathrm{J}_1]\,[\mathrm{E}],$$

we obtain

$$\alpha^2\,[\mathrm{E}] = [\mathrm{J}_1]\,[\mathrm{E}],$$

or, if we let [U] be the unit matrix, we have

$$[\alpha^2 U - J_1]\,[E] = [0].$$

Now $[\alpha^2 U - J_1]$ is the characteristic matrix of $[J_1]$, and if we let $\alpha = \pm\sqrt{\mu}$ then the equation $0 = |\mu U - J_1|$ gives the characteristic latent roots of $[J_1]\,\mu_1 \ldots \mu_n$. Corresponding to the n values of μ we obtain the $2n$ values of the propagation constants α_n. These are given by the equations

$$\alpha_1 = \pm\sqrt{\mu_1}, \text{ etc.}$$

Because of the linearity of the equations we may write

$$[E] = \begin{bmatrix} C_{11} \ldots\ldots C_{1n} \\ \cdot \quad \cdot \quad \cdot \quad \cdot \\ C_{n1} \ldots\ldots C_{nn} \end{bmatrix} \begin{bmatrix} \cosh \alpha_1 x \\ \cdot \quad \cdot \quad \cdot \\ \cosh \alpha_n x \end{bmatrix} + \begin{bmatrix} D_{11} \ldots\ldots D_{1n} \\ \cdot \quad \cdot \quad \cdot \quad \cdot \\ D_{n1} \ldots\ldots D_{nn} \end{bmatrix} \begin{bmatrix} \sinh \alpha_1 x \\ \cdot \quad \cdot \quad \cdot \\ \sinh \alpha_n x \end{bmatrix}.$$

We are assured that since our equations are ordinary differential equations, with constant coefficients of order 2, that our matrix equation must contain $2n$ arbitrary constants. The C_{ij} above are constants, not capacitance.

In the matrix of constants

$$[C] = \begin{bmatrix} C_{11} \ldots\ldots C_{1n} \\ \cdot \quad \cdot \quad \cdot \quad \cdot \\ C_{n1} \ldots\ldots C_{nn} \end{bmatrix}.$$

(*Note.*—These constants must not be confused with the coefficients of self and mutual capacitance.)

The first subscript in C_{ij} corresponds to the line with which this constant is associated, the second subscript corresponds to the value of the propagation constant α_j for that mode. Since there are in reality only $2n$ arbitrary constants instead of $2n^2$ we must proceed to find the true $2n$ integration constants.

Let

$$\underset{\alpha = \alpha_i}{[\alpha^2 U - J_1]} = [K^{(i)}] = \begin{bmatrix} K^i_{11} \ldots\ldots K^i_{1n} \\ \cdot \quad \cdot \quad \cdot \quad \cdot \\ K^i_{n1} \ldots\ldots K^i_{nn} \end{bmatrix}.$$

We are then able to obtain the ratios of the C_{ij}'s in the same column of [C]. The relation is (see any treatise on modern algebra)

$$C_{s1}/C_{k1} = M^1_{is}/M_{ik},$$

where M^1_{ik} is the minor corresponding to the element K^1_{ik} and the superscript relates to the mode whose propagation constant is α_1. The subscript i relates to a particular row of $[K^1]$ which may be arbitrarily chosen.

We can write $C_{11}=M^1_{11}\bar{C}_1$, and in general $C_{kr}=M^r_{ik}C_r$, where i is an arbitrary interger,

$$k=1,\, 2,\ldots.n, \quad r=1,\, 2,\ldots.n,$$

and the $\bar{C}_i$ are the true integration constants.

Accordingly we can write for the constant matrix [C]

$$[C]=\begin{bmatrix} C_{11}\ldots\ldots C_{1n} \\ \cdot \quad \cdot \quad \cdot \quad \cdot \\ C_{n1}\ldots\ldots C_{nn}\end{bmatrix}=\begin{bmatrix} M^1_{11}\ldots\ldots M^n_{11} \\ \cdot \quad \cdot \quad \cdot \quad \cdot \\ M^1_{1n}\ldots\ldots M^n_{1n}\end{bmatrix}[\bar{C}_1\ldots\ldots\bar{C}_n],$$

where the line matrix $[\bar{C}_1\ldots\ldots\bar{C}_n]$ is the matrix of the true arbitrary constants.

Similarly

$$[D]=\begin{bmatrix} M^1_{11}\ldots\ldots M^n_{11} \\ \cdot \quad \cdot \quad \cdot \quad \cdot \\ M^1_{1n}\ldots\ldots M^n_{1n}\end{bmatrix}[\bar{D}_1\ldots\ldots\bar{D}_n].$$

Let

$$[M]=\begin{bmatrix} M^1_{11}\ldots\ldots M^n_{11} \\ \cdot \quad \cdot \quad \cdot \quad \cdot \\ M^1_{11}\ldots\ldots M^n_{11}\end{bmatrix},$$

and $\qquad [\bar{C}]_h=[\bar{C}_1\ldots\ldots\bar{C}_n], \quad [\bar{D}]_h=[\bar{D}_1\ldots\ldots\bar{D}_n],$

and

$$\begin{bmatrix} \cosh\,\alpha_1 x \\ \cdot \quad \cdot \quad \cdot \\ \cosh\,\alpha_n x\end{bmatrix}=[\cosh\,\alpha x]_v.$$

The solution may be most compactly written as

$$[E]=[M]\,[\bar{C}]_h\,[\cosh\,\alpha x]+[M]\,[\bar{D}]_h\,[\sinh\,\alpha x]_v.$$

In exactly a similar manner we have

$$[I]=[M]\,[\bar{A}]_h\,[\cosh\,\alpha x]_v+[M]\,[\bar{B}]_h\,[\sinh\,\alpha x]_v.$$

We have here exhibited the solution of the equations in terms of the horizontal line matrices $[\bar{A}]_h$, $[\bar{B}]_h$, $[\bar{C}]_h$, $[\bar{D}]_h$, that altogether represent the $4n$ arbitrary constants of the two equations.

The Boundary Conditions.

We will proceed further, and evaluate our constants in terms of the receiver end conditions of the lines :

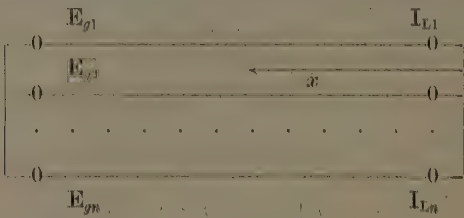

x is measured from the load end.

Let $$[I]_{x=0}=[I_L], \quad [E]_{x=0}=[E_L].$$

Now
$$[I]=[M][\bar{A}]_k[\cosh \alpha x]_n+[M][\bar{B}]_k[\sinh \alpha x]_n,$$

placing $x=0$,

$$[I]_{x=0}=[M][\bar{A}]_k[1]_n=[I]_L.$$

Therefore
$$[\bar{A}]=[M]^{-1}[I_L].$$

where $[M]^{-1}$ is the inverse of $[M]$.

Similarly
$$[\bar{B}]=[M]^{-1}[E_L].$$

To evaluate the other constants we make use of $D[E]=[Z][I]$ and $D[I]=[Y][E]$, where we have measured x from the load end.

Now from

$$[E]=[M][\bar{C}]_k[\cosh \alpha x]+[M][\bar{D}]_k[\sinh \alpha x]$$

$$[I]=[M][\bar{A}]_k[\cosh \alpha x]+[M][\bar{B}]_k[\sinh \alpha x]$$

we obtain

$$D[E]=[M][\bar{C}]_k[\alpha \sinh \alpha x]+[M][\bar{D}]_k[\alpha \cosh \alpha x];$$

now at $x=0$
$$D[E]=[M][\bar{D}]_k[\alpha]_n=[Z][I_L].$$

Therefore

$$\begin{bmatrix} x_1\overline{D}_1 \\ \cdot\ \cdot \\ \cdot\ \cdot \\ x_nD_n \end{bmatrix} = [M]^{-1}[Z]\,[I_L].$$

Similarly

$$\begin{bmatrix} x_1B_1 \\ \cdot\ \cdot \\ \cdot\ \cdot \\ x_nB_n \end{bmatrix} = [M]^{-1}[T]\,[E_L].$$

We have thus succeeded in evaluating all the $4n$ arbitrary constants in terms of the receiver end conditions. It must be remembered that in the matrices [Z] and [Y] p has been placed equal to $j\omega$. Our solution gives the so-called vector or complex solution of the problem. To find the instantaneous solution we multiply our matrices by $\epsilon^{j\omega t}$, and take the imaginary part of the result.

Conclusion.

This simple application of matrix analysis is presented to show the power of the matrix method in the solution of problems that are recalcitrant, not so much in that they are mathematically difficult, but that they are mathematically unwieldy. The short matrix equations parallel the road which the analyst follows in solving the simplest case. It may be mentioned that the straight matrix method in this class of problems has certain advantages over dyadic methods in this class of problem in that one is not confronted with confusing and entirely superfluous unit vectors.

It may be mentioned that while I have not attempted in this discussion to present a numerical example, nevertheless the numerical work is so consistently systematized that a computer would have no trouble in carrying out the computations with a minimum of effort.

References.

Bocher, M., 'Introduction to Higher Algebra.' McMillan.
L. V. Bewley, 'Travelling Waves on Transmission Systems.' J. Wiley.

XI. *On the Variation Calculation of Eigen Values.* By

R. A. NEWING, *Mathematics Department, University College of North Wales* *.

SUMMARY.

THE variation calculation of the eigen values associated with a differential system provides an upper bound for the least eigen value. There is no indication of the error involved in the approximation. An estimate of the accuracy of the approximation may be obtained if a lower bound for the eigen value is also known. An expression for such a lower bound is established and compared with an alternative expression due to D. H. Weinstein. Illustrative calculations are given for two simple problems in wave mechanics. The bound set up in this paper is analogous to, but of wider application than, a result obtained by E. Trefftz for the eigen values associated with integral equations.

---

1. *Introduction.*

THIS paper is concerned with the estimation of the eigen values W_n of W for which the differential equation

$$H\psi-W\psi=0 \quad . \quad . \quad . \quad . \quad . \quad . \quad (1.1)$$

possesses solutions ψ_n which satisfy given boundary conditions, H being a self-adjoint linear differential operator of the second order. It will be assumed here that all the quantities occurring in (1.1) are real, but most of the results to which reference will be made are applicable to a complex equation if the operator H is hermitian. The eigen functions ψ_n may be normalized so that

$$\left.\begin{aligned}\int\psi_n\psi_m d\tau&=0 \text{ if } n\neq m,\\ &=1 \text{ if } n=m,\end{aligned}\right\} \quad . \quad . \quad . \quad (1.2)$$

the integral being throughout configuration space.

The variation calculation of eigen values has been

* Communicated by the Author.

developed from the work of Ritz[1] who proved that, under certain conditions, the integral

$$I = \int \phi \mathrm{H} \phi \, d\tau \quad . \quad . \quad . \quad . \quad . \quad . \quad . \quad (1.3)$$

could be made into an exact solution of (1.1) when ϕ was taken to be a series $\Sigma a_n \theta_n$ of a complete set of normalized orthogonal functions θ_n satisfying the boundary conditions to be imposed on ψ. Eckart[2] proved that if ϕ is a normalized function satisfying the given boundary conditions, but otherwise arbitrary, then the integral I is always less than the greatest eigen value associated with (1.1). It also follows that I is always greater than the least eigen value. The proof usually given of this result depends upon the fact that the function ϕ can be expanded as a convergent series in terms of the functions ψ_n, and it is assumed that the eigen values form a discrete set. In general, there will also be a continuous spectrum of eigen values, and the ψ_n's corresponding to the discrete spectrum will not form a complete set of functions. It will be necessary[3] to modify the normalizing equation (1.2), and, to the summations over the discrete spectrum, must be added integrations over the continuous spectrum. Eckart's result and the results which follow later in this paper may, however, be developed *formally*, without explicit reference to the continuous spectrum, provided that summations over the discrete spectrum are assumed to include integrations over the continuous spectrum. Denote the discrete spectrum by W_n and the continuous spectrum by E, where it is assumed that

$$\mathrm{W}_n \leqslant \mathrm{W}_{n+1} \text{ for all } n,\ \mathrm{E}_1 \leqslant \mathrm{E} \leqslant \mathrm{E}_2,\ \mathrm{E}_1 > \mathrm{W}_1. \quad (1.4)$$

The following cases arise :

A. $\mathrm{W}_1 \geqslant 0$.

B. $\mathrm{W}_n \leqslant 0$ for all n, $\mathrm{E} < 0$.

C. $\mathrm{W}_n \gtrless 0$ according as $n \gtrless k$.

Eckart's result may now be stated as

$$I \geqslant \mathrm{W}_1, \quad . \quad . \quad . \quad . \quad . \quad . \quad . \quad (1.5)$$

where W_1 is the first eigen value. This result is true in all three cases. In cases B and C of course the result may be written $|I| \leqslant |\mathrm{W}_1|$. If ϕ is orthogonal

to the first m eigen functions, then I becomes an upper bound for W_{m+1}. For example, if ψ_1 is known to be symmetrical in the coordinates of configuration space, then a function ϕ antisymmetrical in these coordinates will provide an integral I which is an approximation to the least eigen value consistent with the symmetry of ϕ.

In practical applications of (1.5) ϕ is made to depend on a number of parameters, and the best approximation permitted by the particular form of ϕ is then obtained by minimizing the integral I with respect to these parameters. This method has been highly successful in many investigations, but it has the limitation that it provides only an upper bound. This disadvantage was particularly noticeable, for example, in the wave mechanical calculation of the energy of the ground state of the hydrogen molecule : in 1928, Rosen [(4)] calculated the dissociation energy to be 4·02 v.e., the empirical value being 4·73 v.e., and this remained the best approximation until 1933, when James and Coolidge[(5)] obtained very close agreement with experiment by choosing a very much improved approximation function.

This method of calculating eigen values would obviously be much improved if there were some means of estimating an upper bound for the error $I-W_1$ involved. This is equivalent to finding a *lower* bound for W_1, for if

$$I-W_1<\epsilon, \quad W_1>I-\epsilon.$$

Such a lower bound has been set up by Weinstein[(6)] who has established the general result that if I lies closest to a particular eigen value W_s, then

$$I-\sqrt{(\mu^2-I^2)} \leqslant W_s \leqslant I+\sqrt{(\mu^2-I^2)}, \quad (1.6)$$

where

$$\mu^2=\int(H\phi)^2 d\tau. \quad . \quad . \quad . \quad . \quad . \quad (1.7)$$

It may be proved that this result is applicable to all three cases A, B, C. It will be seen from the illustrative examples of § 3 that in many cases it is not possible to obtain a good lower bound by this method. Weinstein's result has been established and generalized by MacDonald[(7)] who avoids explicit reference to expansion theorems. The corresponding problem in integral equations has been studied by Trefftz[(8)], but his results are not immediately applicable to (1.1) and, in any case,

could be applied only to case A. This latter fact makes it impossible to apply his results to many problems, especially to those occurring in quantum mechanics, which are examples of classes B or C. In § 2, results analogous to those obtained by Trefftz will be established for (1.1), and it will be seen incidentally how Trefftz's results may be modified to cover cases B and C.

2. *A lower bound for the first eigen value.*

Let the function ϕ, satisfying the given boundary conditions, but otherwise arbitrary, be expanded in terms of the functions ψ_n.

$$\phi = \Sigma_n a_n \psi_n, \quad a_n = \int \phi \psi_n d\tau, \quad \Sigma a_n^2 = 1. \quad . \quad (2.1)$$

Then from (1.1), and the definitions of μ and I,

$$I = \Sigma_n a_n^2 \mathrm{W}_n, \quad \mu^2 = \Sigma_n a_n^2 \mathrm{W}_n^2, \quad . \quad . \quad (2.2)$$

and the following identities may be readily established :

$$\mu^2 - I\mathrm{W}_1 = \Sigma_n a_n^2 (\mathrm{W}_n^2 - \mathrm{W}_n \mathrm{W}_1) \quad . \quad . \quad (2.3)$$

$$\mu^2 - I^2 \quad = \Sigma_n a_n^2 (\mathrm{W}_n - I)^2. \quad . \quad . \quad . \quad (2.4)$$

These results, together with (1.4), may be used to establish the following inequalities :

Case A. $\mathrm{W}_1 \leqslant I \leqslant \mu \leqslant \mu^2/I$.

Case B. $|\,\mathrm{W}_1\,| \geqslant |\,\mu^2/I\,| \geqslant |\,\mu\,| \geqslant |\,I\,|$.

Case C. $\mu^2 \leqslant \mathrm{W}_\alpha^2$, W_α being the numerically greatest eigen value.

It is not possible to obtain more definite conclusions in case C unless ϕ is known to be orthogonal, either to the eigen functions associated with positive or with negative eigen values, in which case the conclusions for cases A or B would be relevant. It may be noted that (1.6) follows directly from (2.4), which also shows that $\mu^2 \geqslant I^2$ in all three cases. If μ be taken to have the sign of W_1, then in cases A and B μ^2/I, μ, and I are all upper bounds for W_1, I is the best bound in case A, and μ^2/I in case B. In case C it is possible that μ may be either an upper or a lower bound,

Consider now the function

$$f = \mu^{-1}\mathrm{H}\phi - \phi. \quad . \quad . \quad . \quad . \quad . \quad . \quad (2.5)$$

If ϕ is an exact solution of (1.1), $\mu=W$ and f will be zero, but in general, f will differ from zero.

$$\int f\psi_1\, d\tau=\mu^{-1}\int\psi_1\, H\phi\, d\tau-\int\phi\psi_1\, d\tau.$$

Now, for a self-adjoint operator H,

$$\int\{\psi_i H(\psi_k)-\psi_k H(\psi_i)\}\, d\tau=0,$$

and this result, together with (1.1) and (2.1), will give

$$\frac{W_1-\mu}{\mu}=\frac{1}{a_1}\int f\psi_1\, d\tau. \quad . \quad . \quad . \quad . \quad (2.6)$$

Now a_1 is to be taken as positive ,and it will be seen that $\int f\psi_1\, d\tau$ will be negative in case A and positive in case B. Case C may be subdivided into two classes: C′ and C″, for which $W_1<\mu$ and $W_1>\mu$ respectively. C′ may be classed with B, and C″ with A.

Now, if $a_1\geqslant\alpha$ and $|\int f\psi_1 d\tau|\leqslant\gamma$, then the inequality

$$\left|\frac{W_1-\mu}{\mu}\right|\leqslant\frac{\gamma}{\alpha}. \quad . \quad . \quad . \quad . \quad . \quad . \quad (2.7)$$

is true in all cases, and will provide a *lower* bound for W_1 in cases A, B, and C′. (In case C″ μ may be taken as a lower bound.) Thus, in order to find a lower bound for W_1, it is now necessary to find a lower bound α for a_1 and an upper bound γ for $|\int f\psi_1\, d\tau|$. The result (2.7) is analogous to a result obtained by Trefftz for integral equations, and the quantities α and γ may be estimated in a manner similar to that used by him. It will be necessary, however, to ensure that the results obtained are applicable to the three cases A, B, C.

An upper bound for $|\int f\psi_1\, d\tau|$.

Denote the difference between ψ and ϕ by e, so that

$$e=\psi-\phi.$$

Then

$$\int f\psi_1 d\tau=-g+\int fe\, d\tau, \quad g=1-I/\mu$$

and

$$\int e^2\, d\tau=2(1-a_1)\leqslant 2(1-\alpha).$$

It may be noted that g is positive in all cases and that $\int f^2\,d\tau = 2g$. Now, in cases A and C″, $\int f\psi_1\,d\tau \leqslant 0$, thus

$$\int fe\,d\tau \leqslant g \quad \text{and} \quad |\int f\psi_1 d\tau| \leqslant g + |\int fe\,d\tau|.$$

But by Schwarz's inequality

$$|\int fe\,d\tau| \leqslant \surd\{\int f^2\,d\tau \int e^2\,d\tau\},$$

and it therefore follows that

$$|\int f\psi_1\,d\tau| \leqslant g + 2\surd g\surd(1-\alpha). \quad . \quad . \quad (2.8\ \text{A})$$

In cases B and C′ $\int f\psi_1\,d\tau \geqslant 0$, thus $\int fe\,d\tau \geqslant 0$, and

$$\int f\psi_1 d\tau \leqslant -g + 2\surd g\surd(1-\alpha). \quad . \quad . \quad (2.8\ \text{B})$$

Alternatively, if we put

$$e = \psi_1 - \mu^{-1}\text{H}\phi, \quad \int e^2\,d\tau = 2(1 - a_1\text{W}_1/\mu),$$

and

$$\int f\psi_1\,d\tau = g + \int fe\,d\tau.$$

It may then be shown that

$$|\int f\psi_1\,d\tau| \leqslant -g + 2\surd g\surd(1-\alpha\text{W}_1/\mu). \quad . \quad (2.9\ \text{A})$$

in cases A and C″, and that in cases B and C′

$$|\int f\psi_1\,d\tau| \leqslant g + 2\surd g\surd(1-\alpha\text{W}_1/\mu). \quad . \quad (2.9\ \text{B})$$

It is not possible at this stage to say which of these two sets of results will give the better value for γ in case A. In case B, however, (2.8 B) will give the better value.

Lower bounds for a_1.

From equations (2.1), (2.2), and the inequalities (1.4), it follows that $\mu^2 \geqslant a_1^2(\text{W}_1^2 - \text{W}_2^2) + \text{W}_2^2$ in case A, and that in case B, $\mu^2 \leqslant a_1^2(\text{W}_1^2 - \text{W}_2^2) + \text{W}_2^2$. These inequalities define the lower bounds for a_1:

$$a_1^2 \geqslant \frac{\text{W}_2^2 - \mu^2}{\text{W}_2^2 - \text{W}_1^2} \geqslant \frac{l_2^2 - \mu^2}{l_2^2 - l_1^2} \quad . \quad . \quad . \quad (2.10\ \text{A})$$

and

$$a_1^2 \geqslant \frac{\mu^2 - \text{W}_2^2}{\text{W}_1^2 - \text{W}_2^2} \geqslant \frac{\mu^2 - l_2^2}{l_1^2 - l_2^2}, \quad . \quad . \quad . \quad (2.10\ \text{B})$$

in cases A and B respectively, where $\text{W}_1 \geqslant l_1$, $\text{W}_1 < l_2 \leqslant \text{W}_2$. The lower bounds involving l_1 and l_2 are significant only if $l_2 > \mu$.

An alternative expression for the lower bound may be obtained from the equation

$$\mu^2-IW_2=a_1^2W_1(W_1-W_2)+\sum_{s=3}^{s=\infty} a_s^2W_s(W_s-W_2),$$

which may be used to establish the inequalities

$$a_1^2 \geqslant \frac{IW_2-\mu^2}{W_1(W_2-W_1)}, \quad . \quad . \quad . \quad . \quad (2.11\ A)$$

$$a_1^2 \geqslant \frac{\mu^2-IW_2}{W_1(W_1-W_2)}, \quad . \quad . \quad . \quad . \quad (2.11\ B)$$

in cases A and B respectively.

Now, in case C, it is not possible to obtain results corresponding to (2.10) and (2.11) unless ϕ is known to be orthogonal, either to the eigen functions corresponding to positive eigen values, or to those corresponding to negative eigen values. A lower bound for a_1, *valid in all three cases*, may be derived from the equation

$$W_2-I=a_1^2(W_2-W_1)+\sum_{s=3}^{s=\infty} a_s^2(W_2-W_s),$$

from which follows the inequality

$$a_1^2 \geqslant \frac{W_2-I}{W_2-W_1}. \quad . \quad . \quad . \quad . \quad . \quad (2.12)$$

Now

$$\frac{W_2-I}{W_2-W_1}=1-\frac{I-W_1}{W_2-W_1} \geqslant 1-\frac{I-W_1}{l_2-W_1}=\frac{l_2-I}{l_2-W_1} \geqslant \frac{l_2-I}{l_2-l_1},$$

and therefore

$$a_1^2 \geqslant \frac{l_2-I}{l_2-l_1}. \quad . \quad . \quad . \quad . \quad . \quad (2.12')$$

There will be some difficulty in the application of any of the above three bounds on account of the occurrence of W_2, and a bound not involving W_2 would be a great improvement. To investigate this possiblity consider the equation

$$\mu^2-I^2=a_1^2W_1(W_1-I)+\sum_{s=2}^{s=\infty} a_s^2(W_s-I)W_s.$$

Now, if $I<W_2$, the summation term is positive in case A

and negative in case B. No definite conclusion may be made in case C. In case B it follows that

$$a_1^2 \geqslant \frac{\mu^2 - I^2}{W_1(W_1 - I)} \cdot \quad . \quad . \quad . \quad (2.13\text{ B})$$

No significant result is obtained for case A.

Denote the bounds defined as functions of W_1, W_2, μ, and I in (2.10), (2.11), (2.12), and (2.13), by α_1, α_2, α_3, and α_4 respectively, then it may be established that $\alpha_1 \geqslant \alpha_2$ and $\alpha_3 \geqslant \alpha_1$ in case A, and that in case B $\alpha_1 \leqslant \alpha_2$, $\alpha_3 \leqslant \alpha_1$. In actual applications, however, it will be necessary to replace W_1 and W_2 by their lower bounds, and these inequalities will be valid only if the lower bounds are sufficiently close to W_1 and W_2.

3. *Illustrative Calculations.*

The fundamental inequality (2.7), together with the expressions obtained for γ and α in § 2, will provide upper bounds for the difference $1 \sim W_1/\mu$ and, except in case C″, lower bounds for W_1. For example, taking γ to be given by (2.8 A) and α to be given in terms of l_1 and l_2 by (2.10 A), a result is obtained, valid for case A, which is actually a reproduction of Trefftz's formula as applied to differential equations. If γ be given by (2.8 B) and α is is given by (2.10 B), (2.11 B), or (2.13 B), then a result will be obtained applicable only to case B. (2.8 A) with (2.12′) will give

$$\left| \frac{W_1 - \mu}{\mu} \right| \leqslant \left(\frac{l_2 - l_1}{l_2 - I} \right)^{\frac{1}{2}} \left\{ g + 2\sqrt{g} \sqrt{1 - \left(\frac{l_2 - I}{l_2 - l_1} \right)^{\frac{1}{2}}} \right\}, \quad . \quad . \quad . \quad (3.1)$$

which is applicable to cases A and C″. A similar result, valid for cases B and C′, will be obtained on replacing (2.8 A) by (2.8 B); this will differ from (3.1) only in having the first g on the right-hand side of the inequality replaced by $-g$.

Trefftz's original procedure may be adopted in the application of these results. A rough estimation of l_1 is obtained and inserted in the right-hand side of the inequality, from which a new estimation of l_1 is obtained. This process is repeated and a sequence of numbers is obtained which converges to the best value for l_1 consistent with the values of I and μ and the value chosen

for l_2. The initial value for l_1 may be conveniently found from (1.6), and a value for l_2 may often be found from a knowledge of the physical nature of the problem concerned.

Examples :

(1) *Approximate calculation of* π.

In the notation of §1, $H \equiv -\dfrac{d^2}{dx^2}$, $\psi=0$ at $x=0$ and at $x=1$.

This is an example of case A, and the first eigen function is proportional to $\sin(W_1^{\frac{1}{2}}x)$ where W_1 is π^2. Now, if the approximation function ϕ is taken to be $Nx(x-1)$, N a normalizing factor, then $I=10$, $\mu^2=120$, and from (1.6) $10 \geqslant W_1 \geqslant 5{\cdot}53$. The lower bound 5·53 may be taken as the initial value of l_1 in the successive calculations of § 2. From (2.7), (2.9 A), and (2.12′), it is found that $W_1 \geqslant 9{\cdot}0$, and the percentage error in taking the mean value 9·5 as an approximation to π^2 is less than 5·3 per cent., since $10 \geqslant W_1 \geqslant 9{\cdot}0$.

(2) *The ground state of the hydrogen atom.*

$-H \equiv \nabla^2 + 2B/r$, where B is a positive constant and r is the distance of a point from the origin ; ψ is to be a normalized function, finite and continuous throughout space. This is an example of case C. An exact solution would give $W_1=-B^2$. Take ϕ to be $Ne^{-\alpha r}$, α a constant, then, if $\alpha=B$, ϕ will be the exact solution. Now suppose we had taken $\alpha=kB$, then

$$I=-B^2(2-k)k, \quad \mu^2=k^2B^4(5k^2-12k+8).$$

As an illustrative calculation take $k=1{\cdot}2$, then $I=-0{\cdot}96B^2$, $\mu=-1{\cdot}07B^2$, and from (1.6) $W_1 \geqslant -1{\cdot}44B^2$. We may therefore conclude that $0{\cdot}96 \leqslant -W_1/B^2 \leqslant 1{\cdot}44$. Now consider the results to be obtained from § 2. Take $W_2=-\frac{1}{4}B^2$ and $l_1=-1{\cdot}44B^2$, then (2.7), (2.8 B), and (2.12′) give as a new value for l_1, $-1{\cdot}36B^2$. Starting from this new l_1, a further calculation gives $l_1=-1{\cdot}32B^2$. The process may now be repeated until the limiting value for l_1 is obtained.

This example may be used to study a certain procedure that has been suggested [8], [9] for the application of (1.6). The normal procedure in variation calculations is to minimize I by variation of the parameters occurring in ϕ,

thus obtaining the best upper bound possible with the given ϕ. Now, since $\sqrt{(\mu^2-I^2)}$ provides an upper bound for the difference $I \sim W_s$, it is suggested that an alternative procedure would be to minimize this expression. When $s=1$ this would provide the best lower bound for W_1. Now, in the present example, $\mu^2-I^2=4k^2(k-1)^2B^4$, and this expression is a minimum when $k=0$ and when $k=1$. It will follow from the normalizing condition that $k=0$ corresponds to the trivial solution $\psi\equiv 0$, and it is known that $k=1$ provides an exact solution. It is possible in a general problem that the expression μ^2-I^2 may have several minima, and some difficulty may arise in associating these minima with particular eigen values. It is also possible that the expression may have no minima corresponding to a non-trivial solution of the differential equation. This latter possibility may be illustrated by using the function $\phi=N(R-r)$, $0\leqslant r\leqslant R$; $\phi=0$, $r\leqslant R$; in an estimation of the ground state of the hydrogen atom. In this case $\mu^2-I^2=5(3B^2R^2-4BR+4)/R^4$, and this function decreases from infinity to zero as R increases from zero to infinity. In this case there is no minimum for finite R, and when R is infinite, ϕ becomes the trivial solution $\psi\equiv 0$. In this case it will be necessary to adopt the more usual variation procedure : I is minimum when $BR=4$, and with the help of (1.6) it may be established that $0{\cdot}625 \leqslant -W_1/B^2 \leqslant 1{\cdot}46$. An application of §2 would result in an improved lower bound for W_1.

(3) *The ground state of the ionized hydrogen molecule.*

Neglecting the vibration of the nuclei, this mechanical system may be represented as the motion of an electron in the field of two fixed muclei, A and B, at a distance 2R apart. In the wave mechanical treatment of such a system $-H\equiv\nabla^2+k\left(\frac{1}{r_A}+\frac{1}{r_B}\right)$, r_A, r_B being the distances of the electron from A, B respectively, $k=4K/e^2$, where $-K$ is the energy of the ground state of the hydrogen atom, and e the electronic charge. The boundary conditions imposed on ψ are similar to those of example (2). $W=k\left(\frac{E}{e^2}-\frac{1}{2R}\right)$, E being the total energy of the system.

Two approximation functions will be considered :

(*a*) $\phi = Ne^{-\alpha\xi}$ where $\xi = (r_A + r_B)/2R$.

The integral I is to be minimized with respect to both α and R. A good approximation to the best value for I is obtained by taking $\alpha = 1{\cdot}25$ and $kR = 1{\cdot}836$. The integral μ^2 may be obtained in terms of the functions $F_n(\alpha) = \int_1^\infty \lambda^n e^{-\alpha\lambda} Q_0(\lambda) d\lambda$, which have been tabulated by Rosen[4] for integral values of $n \geqslant 0$. In order to tabulate the functions when n is a negative integer it is necessary to compute the function $F_{-1}(\alpha)$. This may be done by expressing the function as an infinite series involving the functions $A_{-n}(\alpha) = \int_1^\infty \lambda^{-n} e^{-\alpha\lambda} d\lambda$; upper and lower bounds may be obtained for $F_{-1}(\alpha)$, which may be evaluated to any desired degree of accuracy. The values obtained for I and μ are $-0{\cdot}563k^2$ and $-0{\cdot}583k^2$ respectively. Using these results with (1.6), it follows that $0{\cdot}563k^2 \leqslant -W_1 \leqslant 0{\cdot}715k^2$. A much better result may be obtained from § 2. This example is either an example of case C′ or of case C″. In the latter case μ will provide a lower bound for W_1, in the former case a lower bound may be obtained from an application of (2.7) with (2.8 B), and (2.12′). Before calculations may be made it is necessary to obtain some estimation of l_2. Now, in the early days of the application of wave mechanics to molecular problems, Condon[10] developed a very simple graphical method for the construction of energy curves for the hydrogen molecule. Gilbert[11] applied the same method to the molecular ion. He obtained for the dissociation energy D the value 2·97 v.e., the empirical value being 2·78 v.e. Gilbert's results are thus in excess of experiment, and his results may be taken to provide a rough upper bound for the energy magnitudes, and therefore a lower bound for the energies. The value chosen from Gilbert's curves for l_2 was $-0{\cdot}075k^2$, and starting from the value for l_1 obtained from (1.6) a process of successive approximation gives $-0{\cdot}611k^2$ as a limiting value for l_1. If a particular value l_1 gives rise to a new value l_1' on insertion in (2.7)

with (2.8 B) and (2.11′), the latter stages of the calculation may be given in tabular form :

$-l_1/k^2$ ..	0·662	·632	·620	·610	·615	·612	·611	·6108
$-l_1'/k^2$..	0·6319	·6204	·6152	·6104	·6129	·6114	·6109	·6108

It may therefore be concluded that

$$0{\cdot}563 \leqslant -W_1/k^2 \leqslant 0{\cdot}611.$$

(*b*) $\phi = Ne^{-\alpha\xi}(1+\beta\eta^2)$ where $\eta=(r_A+r_B)/2R$ and ξ is as defined in (*a*).

This function involves two parameters α and β, and may be expected to be capable of giving an improved result. In order to use the computational tables set up for (*a*), α was taken to be 1·25, and β and R were adjusted to make I a minimum. The best value of I was found to be given when $\beta=0{\cdot}40$, but for simplicity in calculation β was taken as 0·5 ; the best value for R was found to be $1{\cdot}898/k$. The integral I was evaluated without difficulty and found to be equal to $-0{\cdot}5635k^2$; the integral μ^2, however, presented some difficulty, but after some manipulation, was finally evaluated in terms of the functions mentioned in (*a*). The value obtained for μ was $-0{\cdot}5664k^2$. Using the result (1.6) it now follows that $0{\cdot}5635 \leqslant -W_1/k^2 \leqslant 0{\cdot}6210$. This result is not so good as that obtained from an application of § 2 in (*a*) with a less accurate function ϕ. Applying the results of §2 with ϕ defined as above, the limiting value of l_1 obtained is $-0{\cdot}5707k^2$, and therefore $0{\cdot}5635 \leqslant -W_1/k^2 \leqslant 0{\cdot}5707$. This is a considerable improvement on any of the previous results. The total energy E_1 of the system in the ground state is such that $1{\cdot}2001K \leqslant -E_1 \leqslant 1{\cdot}2291K$, or 16·244 v.e. $\leqslant -E_1 \leqslant$ 16·636 v.e. It follows that the mean value $-16{\cdot}440$ v.e., for E_1 is correct to within about 1·2 per cent. The empirical value is 16·31 v.e. The range of possible values for E_1 is valid whether this problem be an example of case C′ or of case C″ ; for the result has been deduced on the assumption of the former case, and the latter case would give the range of possible values for W_1 as $0{\cdot}5635 \leqslant -W_1/k^2 \leqslant 0{\cdot}5664$, and the range for E_1 would be correspondingly restricted. This restricted range is included in range for E_1 obtained above.

4. *Conclusions.*

The variation method of approximating to the least eigen value of a differential system provides an upper bound. Some idea of the *degree of approximation* may be obtained by finding a *lower* bound for the eigen value. The existing expression (1.6) for the lower bound is applied, in examples 1 and 2, to some simple problems for which the eigen value is known exactly. It is found that functions ϕ giving quite good upper bounds give very poor lower bounds. ϕ must approximate very closely to ψ_1 in order to obtain a good lower bound. The suggested procedure of minimizing the expression $\sqrt{(\mu^2-I^2)}$ instead of I is found to be not reliable in the general case. Another lower bound is established in § 2, and this has been shown to be capable of much better results than (1.6). In example 3 (b), (1.6) gives a range of possible values for W_1 equal to about 10·7 per cent. of the upper bound, while the results of § 2 give a range of less than 2·0 per cent. of the upper bound. The improvement on (1.6) is considerable, but for an approximation function of given accuracy, the lower bound is still much less accurate than the corresponding upper bound. The new lower bound is very sensitive to the nature of the function ϕ, as may be seen by comparing the results of examples 3 (a) and 3 (b). Another defect of the general results established in § 2 is that a rough estimation is required of a lower bound for the second eigen value. A result has been established in § 2 not involving l_2, but this result is found to be applicable only to case B. The results established in this paper would be shown to best advantage in calculating the first eigen value of a differential system involving only negative eigen values (in other words, in calculating an upper bound for the greatest eigen value of a set of positive eigen values), *i. e.*, in application to case B. Case B, however, seems to have little physical significance since problems in mathematical physics fall either in case A (with the greatest eigen value infinite) or in case C.

The results of § 2 are analogous to the results obtained by Trefftz for integral equations. Trefftz's results, however, are applicable only to case A. This is due to the fact that his expressions for α and γ (identical with (2.10 A) and (2.8 A)) are valid only in case A. The results (2.8 B) and (2.12′) may, however, be readily

established for integral equations, and in this way Trefftz's results may be extended. Such an extension is necessary before the results may be applied to problems in quantum mechanics which frequently involve spectra of eigen values having both positive and negative members. Simple examples of such problems are given in §3, examples 2 and 3.

In conclusion, the following procedure may be recommended: (i.) obtain an upper bound by minimizing the integral I; (ii.) obtain an initial lower bound by application of (1.6); (iii.) use l_1 obtained in (ii.) as a starting point in the successive approximations involved in the application of the results of § 2. Stage (iii.) will not be possible unless some estimation of l_2 may be obtained. It must also be noted that the integral μ^2 is often very difficult to evaluate, and thus in many problems stages (ii.) and (iii.) will present considerable difficulty.

References.

(1) Ritz, *J. f. reine und angew. Math.* cxxxv. p. 1 (1909).
(2) C. Eckart, Phys. Rev. xxxvi. p. 879 (1930).
(3) E. Fues, *Ann. d. Phys.* lxxxi. p. 281 (1926). E. Schrödinger, *ibid.* lxxxi. p. 109 (1926). See also Oppenheimer, *Zeits. f. Phys.* xli. p. 268 (1927); Phys. Rev. xxxi. p. 66 (1928); and Kemble, Rev. Mod. Phys. i. p. 157 (1929).
(4) N. Rosen, Phys. Rev. xxxviii. p. 2099 (1931).
(5) H. M. James and A. S. Coolidge, J. Chem. Phys. i. p. 825 (1933).
(6) D. H. Weinstein, Proc. Nat. Acad. Sc. xx. p. 529 (1934).
(7) J. K. L. MacDonald, Phys. Rev. xlvi. p. 828 (1934).
(8) E. Trefftz, *Math. Ann.* cviii. p. 594 (1933).
(9) L. Pauling and E. B. Wilson, 'Introduction to Quantum Mechanics,' p. 190 (McGraw-Hill, 1935).
(10) E. U. Condon, Proc. Nat. Acad. Sc. xiii. p. 466 (1927).
(11) C. Gilbert, Phil. Mag. xvi. p. 929 (1933).

XII. *The Effect of Heat on the Uni-polar Electrical Conductivity of Carborundum.* *By* MANINDRA KUMAR CHAKRAVARTY, *B.Sc., and* S. R. KHASTGIR, *D.Sc.(Edin.), Dacca University* *.

1. *Introduction.*

THE experiments of Khastgir and Das-Gupta † have shown that when carborundum, zincite, or silicon crystal are placed between mercury electrodes giving a

* Communicated by the Authors.

† Khastgir, 'Nature,' vol. cxxxv. p. 148 (Jan. 26, 1935); Khastgir and Das-Gupta, Ind. Jour. Phys. vol. ix. pt. iii. p. 258 (1935).

large contact area there is considerable rectification. Similar experiments with crystals like iron-pyrites, galena, etc., have shown, however, no rectification. This rectification observed in carborundum, etc., can be called *volume rectification*, and is due to uni-polar conductivity, which is quite independent of any point action. Tissot and Pierce * must have detected this volume rectification when they showed that with a certain group of crystals even relatively large polished plates between metallic electrodes made very sensitive detectors. Recently R. Deaglio † has confirmed the existence of volume rectification in the different varieties of the carborundum crystal.

The object of the present investigation has been to study the effect of temperature on the volume rectification of carborundum. It has been established by previous workers ‡ that the contact-point rectification in a crystal generally diminishes with the increase of temperature of the crystal. Experiments have therefore been conducted to ascertain the nature of the heating effect on the volume rectification in carborundum crystal. The results of these experiments are given in this paper, and their interpretation has been attempted in the light of the electronic theory of semi-conductors.

2. *Experimental Arrangements.*

The crystal under examination has been mounted as shown in fig. 1. A four-jawed steel vice fitting into a hole drilled at the bottom of a vertical brass rod EA holds one end of the carborundum crystal, and a brass ring A screwed on to the rod makes the four jaws grip it very tightly. A similar vice with a brass ring B screwed on to the end of a bent brass rod BCD grips the lower end of the crystal. The part CD of the bent rod and the rod AE are held parallel to each other by suitable clamps. The crystal mounted in this way is inserted into an electric furnace. The top of the heater is closed with an asbestos board with two holes for the

* Tissot, *L'Électricien*, vol. xxxix. p. 331 (1910); Pierce, 'Electrician,' vol. lxix. p. 66 (1912).

† Deaglio, *Atti R. Acad. delle Scienze* (*Class. Phys.*), vol. lxx. (1936).

‡ Flowers, Phys. Rev. 1909; Khastgir and Das-Gupta, Phil. Mag vol. xix. p. 557 (March 1935); Sen, Ind. Jour. Phys. vol. x. (1936).

vertical rods to pass through. The ends D and E are fitted with binding screws.

The effect of temperature has been studied in two ways:

(1) The resistance of the crystal for the two opposite directions has been measured by Callendar and Griffith's

Fig. 1.

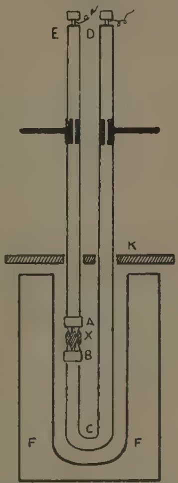

FF. Electric furnace.
K. Asbestos board.
X. Carborundum crystal.

bridge method for various values of the current which heats the furnace; and

(2) a battery of suitable voltage having been connected across the crystal, the current has been measured by a milliammeter for the two opposite directions of current-flow for various values of the heating current.

The temperatures corresponding to the various values of the current which heats the furnace were accurately determined by a separate calibration experiment.

3. *Experimental Results.*

In the first set of experiments the resistance for either direction has been found to decrease in an exponential way with the increase of temperature. The resistance

TABLE I.

Temp. (degree centigrade).	Heating current (amp.).	Resistance in ohms. Direct.	Resistance in ohms. Reverse.	R_2/R_1.
I.				
26° ...	0	16300	12000	1·36
48° ...	·3	11300	8440	1·35
115° ...	·6	7500	5400	1·39
186° ...	·75	5400	3700	1·49
342° ...	1·0	4000	2500	1·60
II.				
24° ...	0	2840	1980	1·43
35° ...	·2	2800	1945	1·44
78° ...	·48	2200	1740	1·26
186° ...	·75	450	760	*·59*
III.				
24° ...	0	3470	1570	2·21
35° ...	·2	3430	1525	2·25
95° ...	·55	3190	1190	2·67
215° ...	·80	2130	690	3·08
342° ...	1·0	950	450	2·11
IV.				
24° ...	0	2040	690	2·95
48° ...	·3	2010	670	3·0
95° ...	·55	1550	490	3·1
186° ...	·75	830	275	3·01
315° ...	·97	410	140	2·93

for one direction has been markedly different from the resistance for the opposite direction. The ratio of the higher value R_2 of the resistance to the lower value R_1 must be equal to the ratio of the larger value I_1 of the current through R_1 to the lower value I_2 of the current through R_2. This ratio can evidently be taken as a

measure of volume rectification. The ratio R_2/R_1 has been determined for various temperatures. Three kinds of variation with temperature have been observed:

Fig. 2.

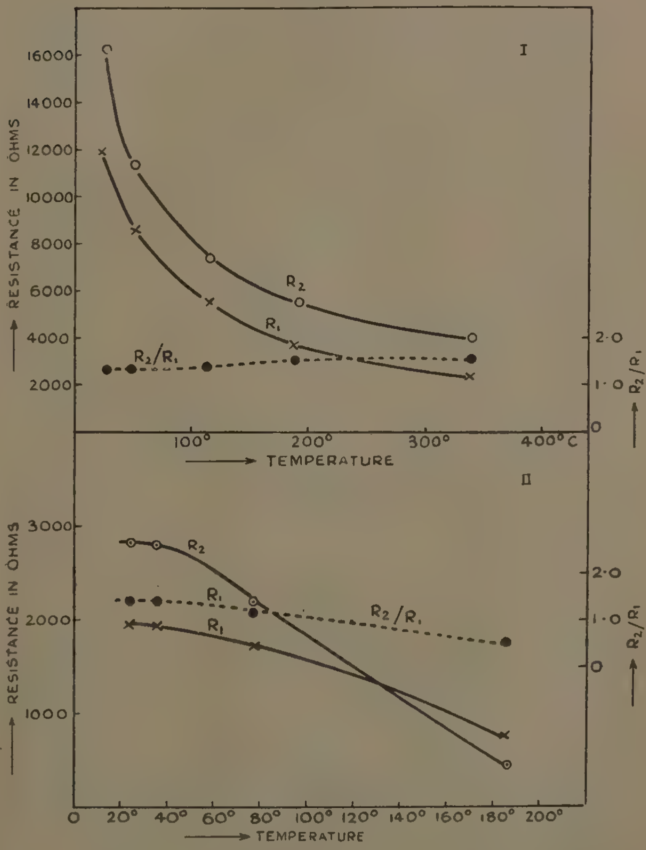

(*a*) a gradual rise; (*b*) a gradual fall; and (*c*) a gradual rise followed by a gradual fall of the ratio. Typical results are given in Table I. These are illustrated in figs. 2 and 3.

It is to be noted that in case II. the ratio R_2/R_1 has fallen below unity, showing change in the sign of rectification. In case IV. the ratio is practically constant.

Fig. 3.

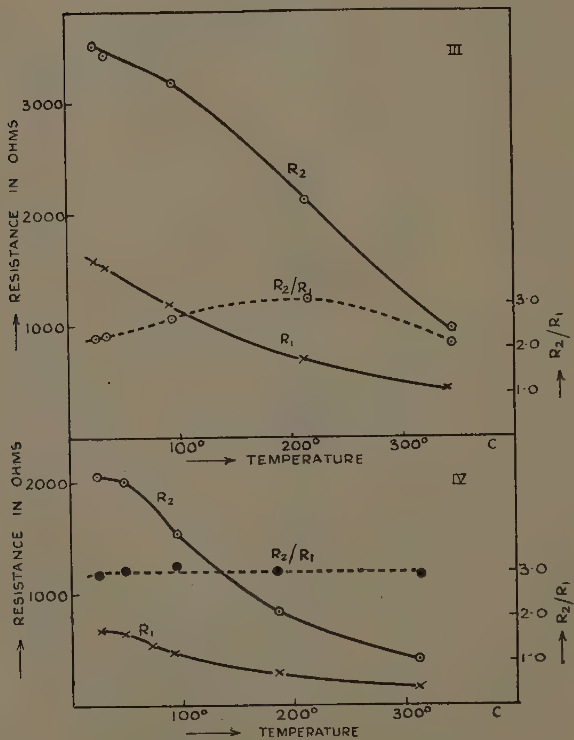

In the second set of experiments the values of the current conductivity have been measured for various temperatures for the two opposite directions. Here also the ratio of the two currents I_1/I_2 (which is equal to R_2/R_1) has been found to vary with temperature

in a similar way. Two typical sets of results are given in Table II. These are graphically shown in fig. 4.

Fig. 4.

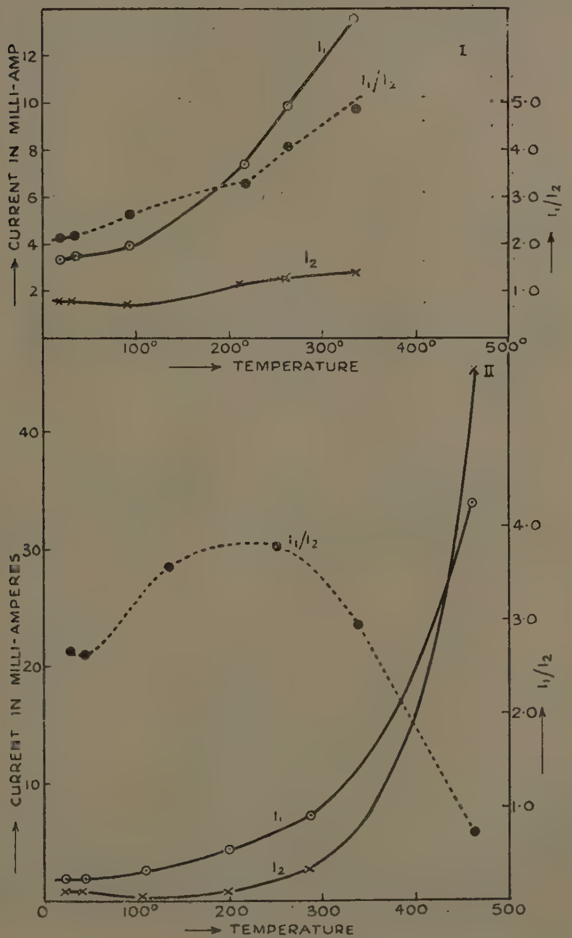

In case II. the ratio has fallen below unity, showing again a change in the sign of rectification.

TABLE II.

Temp. (degree centigrade).	Heating current (amp.).	Current in ma. I_2.	I_1.	I_1/I_2.
I.				
24° ...	0	1·57	3·4	2·16
34° ...	·18	1·58	3·5	2·22
95° ...	·55	1·5	4·0	2·67
215°...	·80	2·22	7·5	3·38
252° ...	·86	2·4	9·9	4·13
337° ...	·98	2·77	13·7	4·94
II.				
28° ...	0	2·01	·75	2·68
48° ...	·3	2·15	·81	2·65
135° ...	·63	2·55	·72	3·54
249° ...	·85	4·4	1·17	3·76
337° ...	·98	7·7	2·6	2·96
511° ...	1·28	34·0	45·0	·76

4. *Interpretation of the Experimental Results.*

The work of Bloch *, Peierls †, Wilson ‡, Fowler § and others has evolved an electron theory of semi-

Fig. 5.

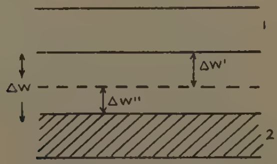

conductors. Our experimental results can be viewed in the light of this theory.

According to this theory, the possible electron levels

* Bloch, *Zeits. f. Phys.* lii. p. 555 (1928).
† Peierls, *Zeits. f. Phys.* liii. p. 265 (1929).
‡ Wilson, Proc. Roy. Soc. A, cxxxiii. p. 158 (1931) and cxxxiv. p. 277 (1931).
§ Fowler, Proc. Roy. Soc. A, cxl. (1933).

of the crystalline lattice of the semi-conductor in question are broken up into bands, of which we are concerned with only two—a lower band (suffix 2) of states exactly full of electrons at the absolute zero, and an upper band (suffix 1) entirely empty at the absolute zero (see fig. 5). At the temperatures at which we are interested, there will be a few electrons in band 1 and a few empty states in band 2 effectively confined to the lowest states of band 1 and the highest states of band 2.

(a) *Semi-conductors without Impurities.*

We shall first consider the case of the semi-conductors without impurities—Fowler calls them "intrinsic semi-conductors." These owe their electrical conductivity and other electrical properties to thermal excitation of electrons from band 2 to band 1.

Fowler shows that the number of electrons N_1 excited to band 1 is related to temperature in the following way :

$$N_1 \propto e^{-\frac{\Delta W}{2kT}},$$

where ΔW is the difference in the energies of the two bands and k the Boltzmann constant. Accepting this relation, the current through the crystal is given by

$$I = N_1 \,.\, e \,.\, v = A \,.\, e \,.\, v \,.\, e^{-\frac{\Delta W}{2kT}},$$

where v is the mobility of the electrons, e the charge on an electron, and A a constant.

Since $v = v_0 \,.\, e^{-\frac{s}{T}}$, where v_0=mobility at absolute zero and s a constant, we get

$$I = A \,.\, e \,.\, v_0 \,.\, e^{-\frac{s}{T}} \,.\, e^{-\frac{\Delta W}{2kT}}$$

We assume here that in carborundum ΔW has different values ΔW_1 and ΔW_2, and s has also different values s_1 and s_2 for currents flowing in the two opposite directions. Thus

$$I_1 = A \,.\, e \,.\, v_0 \,.\, e^{-\frac{s_1}{T}} \,.\, e^{-\frac{\Delta W_1}{2kT}}$$

for one direction and

$$I_2 = B \,.\, e \,.\, v_0 \,.\, e^{\frac{s_2}{T}} \,.\, e^{-\frac{\Delta W_2}{2kT}}$$

for the opposite direction, so that

$$I_1/I_2 = C \, . \, e^{-(\Delta W_1 - \Delta W_2)/2kT} \, . \, e^{-\frac{(s_1 - s_2)}{T}},$$

where A, B, C are constants.

Assuming $\Delta W_2 > \Delta W_1$ and $s_1 > s_2$ when $I_1 > I_2$, and putting

$$\alpha = \frac{\Delta W_2 - \Delta W_1}{2k} \quad \text{and} \quad \beta = (s_1 - s_2),$$

we can write

$$I_1/I_2 = C \, . \, e^{\frac{(\alpha - \beta)}{T}}.$$

When $\alpha > \beta$, the ratio I_1/I_2 falls exponentially with the rise of temperature, and when $\alpha < \beta$ there is exponential increase with the increase of temperature.

Our experimental results have shown both these features.

(b) *Semi-conductors with Impurities.*

Sometimes we have impurities in the crystal, and these impurities, according to Wilson, provide distinct isolated levels for electrons which at low temperatures may normally be either *full* or *empty*, depending on the type of impurities. Semi-conductors with impurity levels *full* of electrons at low temperatures owe their conductivity to the excitation of electrons to band 1 both from the impurity levels and from band 2, the former predominating at ordinary temperatures. Fowler calls these semi-conductors "normal extrinsic semi-conductors." There are also "abnormal extrinsic semi-conductors" with impurity levels *empty* at low temperatures, and their conductivity is due to the excitation of electrons from band 2 both to the impurity levels and to band 1.

In the case of normal extrinsic semi-conductors, if the energy levels of the impurities lie $\Delta W'$ below band 1, then according to Fowler the number of electrons excited to band 1 will be related to temperature as follows :

$$N_1 \propto e^{-\frac{\Delta W'}{2kT}}$$

for low temperatures, so that

$$I_1/I_2 = C \, . \, e^{-\frac{(\alpha' - \beta)}{T}},$$

where

$$\alpha' = \frac{\Delta W_2' - \Delta W_1'}{2k}.$$

Here $\Delta W_1'$ and $\Delta W_2'$ are the values of $\Delta W'$ for currents flowing in the two opposite directions.

For larger values of T where the impurity contribution is swamped by the electrons from the lowest band,

$$N_1 \propto e^{-\frac{\Delta W}{2kT}},$$

and we have again

$$I_1/I_2 = C \, . \, e^{\frac{(\alpha-\beta)}{T}}.$$

In the case of abnormal extrinsic conductors the electrons will be related to temperature as follows:

$$N_2 \propto e^{-\frac{\Delta W''}{2kT}},$$

where the impurity levels lie $\Delta W''$ above band 2. Therefore

$$I_1/I_2 = C \, . \, e^{\frac{(\alpha''-\beta)}{T}},$$

where

$$\alpha'' = \frac{\Delta W_2'' - \Delta W_1''}{2k}.$$

Here, as before, $\Delta W_1''$ and $\Delta W_2''$ are the values of $\Delta W''$ for the two opposite directions of the current-flow. At sufficiently high temperatures we get again

$$I_1/I_2 = C \, . \, e^{\frac{(\alpha-\beta)}{T}}.$$

Without making any distinction between the two types of impurities, we can say that for high temperatures the slope of the conductivity curve increases considerably, since $\Delta W'$ or $\Delta W''$ *increases* to ΔW at high temperatures. Considering conductivity in the two opposite directions, we can also say that the difference $(\Delta W_2' - \Delta W_1')$ or $(\Delta W_2'' - \Delta W_1'')$, i. e., α' or α'' increases to $(\Delta W_2 - \Delta W_1)$, i. e., α at high temperatures.

Joffè * has shown that the value of s in quartz is of the order of 10^3, so that we can take the value of β, i. e., $(s_1 - s_2)$, to be of the same order or less. The value

* Joffè, 'Physics of Crystals.'

of $(\Delta W_2 - \Delta W_1)$ is also of the same order *. We shall now construct a few curves showing the variation of I_1/I_2 with temperature.

I. Let $\beta = 900$, $\alpha' = 1000$ at very low temperatures, and let α' attain gradually the value $\alpha = 2000$ at 200° Å.

Temp. (absolute).	α.	β.	$\alpha - \beta$.	I_1/I_2.
>0<100° ...	1000	900	+ 100	—
100° ...	1500	,,	+ 600	—
200° ...	2000	,,	+1100	—
300° ...	,,	,,	,,	1·0
400° ...	,,	,,	,,	·38
500° ...	,,	,,	,,	·23
600° ...	,,	,,	,,	·15
700° ...	,,	,,	,,	·12
800° ...	,,	,,	,,	·10
900° ...	,,	,,	,,	·085
1000° ...	,,	,,	,,	·075

II. Let $\beta = 2000$, $\alpha' = 1400$ at very low temperatures, and let α' attain gradually the value $\alpha = 1800$ at 200° Å.

Temp. (absolute).	α.	β.	$\alpha - \beta$.	I_1/I_2.
>0<100° ...	1400	2000	−600	—
100° ...	1600	,,	−400	·036
200° ...	1800	,,	−200	·74
300° ...	,,	,,	,,	1·0
400° ...	,,	,,	,,	1·22
500° ...	,,	,,	,,	1·34
600° ...	,,	,,	,,	1·44
700° ...	,,	,,	,,	1·50
800° ...	,,	,,	,,	1·56
900° ...	,,	,,	,,	1·60
1000° ...	,,	,,	,,	1·64

* The classical formula of conductivity is

$$\sigma \propto e^{-\frac{u}{kT}},$$

where u = Work function,
k = Boltzmann constant,
T = Absolute temperature.

Thus $\frac{\Delta W}{2k}$ of the Wilson-Fowler formula corresponds to $\frac{u}{k}$ of the classical formula.

Now $u = \frac{e \cdot V}{300}$, where V is the voltage necessary to liberate the electrons embedded in the crystal lattice. In the case of carborundum the value of this voltage is different for currents flowing in the two opposite directions. Taking the difference in voltage to be ·5 V, the difference in the value of $\frac{u}{k}$ is of the order of 10^3.

III. Let $\beta=500$, $\alpha'=400$ at $100°$ Å., and let α' attain gradually the value of $\alpha=1500$ at $400°$ Å.

Temp. (absolute).	α.	β.	$\alpha-\beta$.	I_1/I_2.
100° ...	400	500	− 100	·04
200° ...	800	,,	+ 300	·45
300° ...	1200	,,	+ 700	1·0
400° ...	1500	,,	+1000	1·22
500° ...	,,	,,	,,	·74
600° ...	,,	,,	,,	·53
700° ...	,,	,,	,,	·42
800° ...	,,	,,	,,	·35
900° ...	,,	,,	,,	·30
1000° ...	,,	,,	,,	·27

IV. Let $\beta=400$, $\alpha'=500$ at $100°$ Å., and let α' attain gradually the value $\alpha=1000$ at $600°$ Å.

Temp. (absolute).	α.	β.	$\alpha-\beta$.	I_1/I_2.
100° ...	500	400	100	1·0
200° ...	600	,,	200	1·0
300° ...	700	,,	300	1·0
400° ...	800	,,	400	1·0
500° ...	900	,,	500	1·0
600° ...	1000	,,	600	1·0
700° ...	,,	,,	,,	·89
800° ...	,,	,,	,,	·78
900° ...	,,	,,	,,	·73
1000° ...	,,	,,	,,	·67

All these computed curves are illustrated in fig. 6.

Fig. 6.

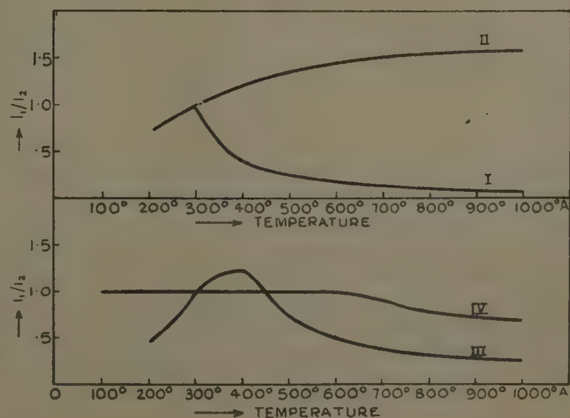

We can thus explain our experimental results on the effect of temperature on the volume rectification observed in carborundum.

5. *Summary and Conclusion.*

The effect of temperature on the uni-polar electrical conductivity of carborundum has been studied between 300° Å. and 800° Å. It has been found that the electrical conductivity in either of the two opposite directions of the current-flow increases continuously with the rise of temperature in an exponential way, and that the ratio of the conductivities in the two opposite directions (which can be taken as a measure of volume rectification) increases in some cases and diminishes in some others with the increase of temperature. In some cases, again, there has been a gradual rise followed by a decrease as the temperature has been increased. The increase or decrease of the relative conductivity depends on the direction of the passage of the current through the crystal, and also on the specimen of the crystal itself. An interpretation of the experimental results has been given in the light of Wilson-Fowler's electron theory of semi-conductors.

It will be interesting if similar experiments to observe the effect of heat on volume rectification be carried out at very low temperatures. For very low as well as for very high temperatures the chief difficulty in these experiments is to keep the contacts between the crystal ends and the electrodes undisturbed. Within the range of temperatures (300° Å. to 800° Å.), however, it has been possible to keep these contacts intact.

Supplementary Note.—When carborundum crystal is used with a metallic point ("whisker"), the observed rectification will comprise volume rectification in addition to contact-point rectification. The effect of heat on rectification by carborundum is therefore a combination of two effects—the effect of heat on contact-point rectification and that on volume rectification. The experiments described in this paper show that volume rectification in carborundum increases or decreases as the crystal is heated. Thus the rectification observed in

carborundum when used with a "whisker" may *either* decrease *or* increase with the increase of temperature of the crystal. We have observed these features, and it seems likely that Sen (Ind. Jour. Physics, vol. x. 1936) has also noticed them.

Physics Laboratory, Dacca University.
Nov. 15th, 1936.

XIII. *The Diffraction of Electromagnetic Waves from an Electrical Point Source round a Finitely Conducting Sphere, with Applications to Radiotelegraphy and the Theory of the Rainbow.*—Part I.

By BALTH. VAN DER POL *and* H. BREMMER, *Natuurkundig Laboratorium der N.V. Philips' Gloeilampenfabrieken, Eindhoven, Holland**.

1. *Introduction.*

THE paper concerns the calculation of the electromagnetic field due to an oscillating electrical dipole placed outside a finitely conducting sphere. This is one of the fundamental problems of radiotelegraphy and has aroused new interest by the coming of television. Here the radiating dipole represents the transmitter antenna, and the absorbing sphere the earth. In our calculations the atmosphere is taken homogeneous and any effects due to the ionosphere are therefore neglected. (The chief contents of Part I. of this investigation have been communicated by Balth. van der Pol in a lecture before the Institute of Radio Engineers in New York in November 1936.)

The rigid solution for a given wave-length, based on the Maxwellian equations with proper boundary conditions, leads to an infinite series of spherical harmonics with coefficients containing twelve Bessel functions, which has been known already for a long time and which is given below as formula (1).

As in all diffraction problems the character of the solution is determined by the ratio of the dimensions of the obstacle to the wave-length λ, in case $2\pi a/\lambda$, where a is the radius of the sphere. When this ratio is small, as, for instance, in the problem of the scattering of light by submicroscopic particles, the series (1) converges so rapidly

* Communicated by Dr. Balth. van der Pol.

that a few terms only give a sufficient numerical approximation. For instance, this approximation led Lord Rayleigh [1] to discover his λ^{-4} law for scattered light, and it also is at the base of Debye's investigation of the light pressure [2].

In the radio application of our problem this ratio is of the order 10^3 to 10^8, while the corresponding ratio in the theory of the rainbow is determined by the dimensions of the raindrops and the wave-length of light, leading to a value of $2\pi a/\lambda$ of the order of 10^4. Under these circumstances the series (1) converges in general extremely slowly, the main contribution being given by the terms where n is of the order $2\pi a/\lambda$. Lord Rayleigh [3] evaluated for an analogous acoustical problem with a similar, but slightly different boundary condition, the field at the surface of the sphere, the point source being also on the surface, by simply adding numerically the important terms for the cases $2\pi a/\lambda=2$ and 10. Later on, A. E. H. Love [4] even undertook the laborious task of evaluating the series (1) for the same case of radiotelegraphy with $2\pi a/\lambda=8000$, by numerical addition of the terms of the series taken in groups. In his paper an historical summary of the problem up to 1915 is also given.

Considerable progress in the present problem was subsequently obtained by G. N. Watson [5], who transformed (1), with the aid of a contour integration, into another much more rapidly converging series (15), which was further considered in more detail with a view to the application to radio by one of us [6]. Also Laporte's [7] investigation uses this series, and a clear exposition by A. Sommerfeld of Watson's method is to be found in Frank-Von Mises, *Differential Gleichungen der Physik*, II, 2. vermehrte Auflage, pp. 964–977. Finally, T. L. Eckersley [8] treated the problem with his method of phase integrals, while P. S. Epstein [9] simplified the treatment by an application of Huygens's principle.

The present investigation attacks the problem in two quite different ways :—

I. The first one, extending Watson's treatment, is more appropriate for investigating the disturbance beyond the optical horizon of the point source and is pushed to considerable numerical details while considering a.o. in the radio case the effect of the height of the trans-

mitter above the earth. *E. g.*, we find that for practical cases of modern television transmission ($\lambda=7$ meter) the attenuation of the radiowaves due to the finite conductivity of the earth dominates *by far* the attenuation due to diffraction. Further, when moving along the surface of the earth, the optical horizon is found not to be a very critical point as regards the amplitude of waves of the order of $\lambda=7$ meter, more or less sharp shadows only occurring for much shorter wave-lengths. Also it is found that for this wave-length the factor by which the field on the surface of the earth and beyond the horizon is increased due to raising the transmitter to a certain height is, as a first approximation, independent of the distance. Moreover, the numerical results show that, as in the analogous problem for a plane boundary, the conductivity of the earth has a very pronounced influence on the attenuation of the waves.

II. The second method also starts with the rigorous harmonic series (1), being a solution of the wave equation. It appeared possible to split up this series uniquely in a series of an infinite number of other series, each of which may be considered to represent the rigorous expression of what can be visualized as rays undergoing successive reflexions at the inner surface of the sphere. An approximation of each of these series clearly shows their ray-character in complete accordance with the classical Airy ray-treatment of the theory of the rainbow. The present investigation therefore provides the link between the exact wave solution and the approximate ray solution of the rainbow extending the latter to the cases of a light source and observer at finite distances.

2. *The Development in Spherical Harmonics.*

Using spherical coordinates, let (fig. 1) the electrical dipole be situated at Q(b, o), the observer at P(r, ϑ), the radius of the sphere being a. The analytical problem consists of finding the function Π, representing the amplitude of the Hertzian vector divided by r, having a radial component only, and satisfying the following differential equations and boundary conditions (where $k^2_{1,2}$ has the usual meaning):

$$(1)\quad (\Delta+k_1{}^2)\Pi=0 \quad (r>a),$$
$$(\Delta+k_2{}^2)\Pi=0 \quad (r<a),$$

(2) $\dfrac{\partial}{\partial r}(r\Pi)$ and $k^2\Pi$ continuous at $r=a$,

(3) a singularity at $Q(b, o)$ of the form $\dfrac{e^{ik_1 R}}{ik_1 R}$ which is further called the "primary field." This means that in the outer space $\Pi=\Pi_{pr}+\Pi_{sec}$, where the "secondary

Fig. 1.

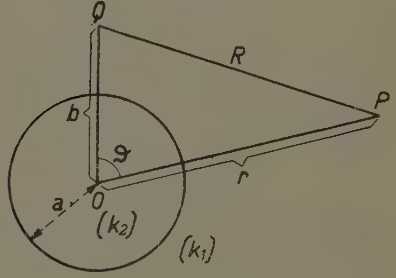

Coordinates used.

field" Π_{sec} has no singularities. The electric and magnetic fields are given by

$$E_r=\left(k^2+\frac{\partial^2}{\partial r^2}\right)(r\Pi)\,;\quad E_\vartheta=\frac{1}{r}\frac{\partial^2}{\partial r\partial\vartheta}(r\Pi)\,;$$

$$E_\phi=0,\ H_r=H_\vartheta=0\,;\quad H_\phi=-\frac{ic}{\omega}k^2\frac{\partial\Pi}{\partial\vartheta}\,;$$

$$k^2_{1,2}=\frac{\epsilon_{1,2}\omega^2+i\sigma_{1,2}\omega}{c^2}.$$

The known solution in the form of harmonic series is :

$$\Pi_{tot}=\Pi_{pr}+\Pi_{sec}=\frac{e^{ik_1 R}}{ik_1 R}$$

$$+\sum_{n=0}^{n=\infty}(2n+1)R_n\frac{\psi_n(k_1 a)}{\zeta_n^{(1)}(k_1 a)}\zeta_n^{(1)}(k_1 b)\zeta_n^{(1)}(k_1 r)P_n(\cos\vartheta)\ (r>a),\quad \ldots\quad (1a)$$

$$\Pi_{\text{tot}}=\frac{k_1^2}{k_2^2}\sum_{n=0}^{n=\infty}(2n+1)(1+\mathrm{R}_n)\frac{\psi_n(k_1a)}{\psi_n(k_2a)}\zeta_n^{(1)}(k_1b)\psi_n(k_2r)\mathrm{P}_n(\cos\vartheta)$$

$$(r<a), \quad . \quad . \quad (1\,b)$$

where the symbols have the following meaning :

$$\zeta_n^{(1)}(x)=\sqrt{\frac{\pi}{2x}}\,\mathrm{H}^{(1)}_{n+\frac{1}{2}}(x)=x^n\left(-\frac{1}{x}\frac{d}{dx}\right)^n\left(\frac{e^{ix}}{ix}\right),$$

$$\zeta_n^{(2)}(x)=\sqrt{\frac{\pi}{2x}}\,\mathrm{H}^{(2)}_{n+\frac{1}{2}}(x)=x^n\left(-\frac{1}{x}\frac{d}{dx}\right)^n\left(\frac{ie^{-ix}}{x}\right),$$

$$\psi_n(x)=\tfrac{1}{2}\{\zeta_n^{(1)}(x)+\zeta_n^{(2)}(x)\}$$

$$=\sqrt{\frac{\pi}{2x}}\,\mathrm{J}_{n+\frac{1}{2}}(x)=x^n\left(-\frac{1}{x}\frac{d}{dx}\right)^n\left(\frac{\sin x}{x}\right),$$

(H = Hankel function), and where

$$\mathrm{R}_n=\frac{-\frac{1}{x}\left[\frac{d}{dx}\log\{x\psi_n(x)\}\right]_{x=k_1a}+\left[\frac{1}{x}\frac{d}{dx}\log\{x\psi_n(x)\}\right]_{x=k_2a}}{\left[\frac{1}{x}\frac{d}{dx}\log\{x\zeta_n^{(1)}(x)\}\right]_{x=k_1a}-\left[\frac{1}{x}\frac{d}{dx}\log\{x\psi_n(x)\}\right]_{x=k_2a}}, \quad . \quad . \quad . \quad (2)$$

It may be remarked that (1 a) is symmetrical in r and b, expressing the well-known property of reciprocity, stating that transmitter and receiver may be interchanged.

3. *Transformation of* (1) *to a Sum of a Series of Residues and an Integral.*

For the derivation of (1) it is necessary to develop first the primary field in a harmonic series. It is well known that two different series are obtained according to whether $r>b$ or $r<b$, viz. :

$$\frac{e^{ik_1\mathrm{R}}}{ik_1\mathrm{R}}=\sum_{n=0}^{n=\infty}(2n+1)\zeta_n^{(1)}(k_1r)\psi_n(k_1b)\mathrm{P}_n(\cos\vartheta) \quad (r>b), \ (3\,a)$$

$$\frac{e^{ik_1\mathrm{R}}}{ik_1\mathrm{R}}=\sum_{n=0}^{n=\infty}(2n+1)\zeta_n^{(1)}(k_1b)\psi_n(k_1r)\mathrm{P}_n(\cos\vartheta) \quad (r<b). \ (3\,b)$$

If we express (1 a) completely as a harmonic series by substitution of (3 b) into (1 a) and considering the

total field at the surface of the sphere only ($r=a$), while making use of the Wronksian :

$$\psi_n(x)\zeta_n^{(1)\prime}(x)-\zeta_n^{(1)}(x)\psi_n{}'(x)=\frac{i}{x^2}, \quad . \quad . \quad . \quad (4)$$

we obtain

$$\Pi_{\text{tot}}=\frac{i}{(k_1a)^3}\sum_{n=0}^{n=\infty}(2n+1)\frac{\zeta_n^{(1)}(k_1b)}{\zeta_n^{(1)}(k_1a)}\frac{1}{\mathrm{N}_n}\mathrm{P}_n(\cos\vartheta), \quad . \quad (5)$$

where

$$\mathrm{N}_n(x,y)=\left[\frac{1}{x}\frac{d}{dx}\log\{x\zeta_n^{(1)}(x)\}\right]_{x=k_1a}$$
$$-\left[\frac{1}{y}\frac{d}{dy}\log\{y\psi_n(y)\}\right]_{y=k_2a}. \quad (6)$$

Following Watson, we transform (5) into a continuous integral over n leading to

$$\Pi_{\text{tot}}=\frac{1}{(k_1a)^3}\int_{\mathrm{L}}\frac{n\,dn}{\cos(n\pi)}\frac{\zeta_{n-1/2}^{(1)}(k_1b)}{\zeta_{n-1/2}^{(1)}(k_1a)}\frac{1}{\mathrm{N}_{n-1/2}}\mathrm{P}_{n-1/2}\{\cos(\pi-\vartheta)\}$$
$$+\frac{1}{(k_1a)^3}\int_0^{i\infty}\frac{n\,dn}{\cos(n\pi)}\frac{\zeta_{n-1/2}^{(1)}(k_1b)}{\zeta_{n-1/2}^{(1)}(k_1a)}\left(\frac{1}{\mathrm{N}_{n-1/2}}-\frac{1}{\mathrm{N}_{-n-1/2}}\right)$$
$$\times\mathrm{P}_{n-1/2}\{\cos(\pi-\vartheta)\}. \quad . \quad (7)$$

Here the contour of integration L in the complex n-plane lies wholly in the first quadrant and encloses all poles lying in that quadrant (see fig. 2 *c*). This path of integration actually makes the sum of the two integrals (7) identical with the series (5), which may be clear by the following transformation:—First the series (5) is transformed into an integral with the path of integration formed by small circles round the poles $n=1/2, 3/2, 5/2 \ldots.$ of the function $1/\cos(n\pi)$ (see fig. 2 *a*, where $n_0, n_1, n_2 \ldots.$ are the poles of the integrand apart from the factor $1/\cos(n\pi)$). Further, this path can be transformed to the loop A of fig. 2 *b*, extending from $\infty-i\epsilon$ to $\infty+i\epsilon$. As the integral becomes exponentially zero when $|n|$ tends to ∞, the integral with integration path A is the difference of the contour integral B of fig. 2 *b* and an integral along the imaginary axis. Further, it appears that the integrand has no poles in the minus first quadrant, so that B may be contracted to the contour L of fig. 2 *c*,

whereas the integral along the imaginary axis may be transformed to the second integral of (7) along the positive imaginary axis.

Fig. 2.

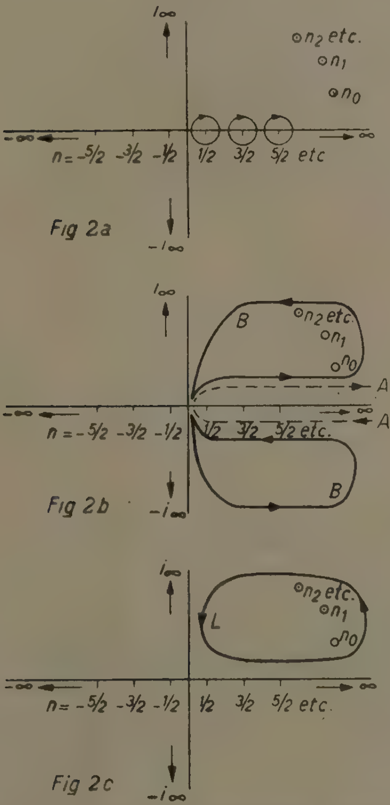

Transformation of the path of integration in the n-plane.

Apparently the second term of (7) vanishes when $N_{n-1\,2}$ is an even function of n. Now the first term of (6) is even in n, whereas the second term, for the case of radiotelegraphy, is to a high approximation equal to

$$\left[\frac{1}{x}\frac{d}{dx}\log\{x\zeta_n^{(2)}(x)\}\right]_{x=k_2a};$$

which is also an even function of n; this approximation is a consequence of the fact that in practice $|e^{2ik_2a}|$ (corresponding to the attenuation of plane waves which have travelled over a distance equal to the diameter of the earth) is very small, due to the great absorption in the earth. Therefore, as a first approximation, we may consider $N_{n-1/2}$ as an even function of n and omit the second term of (7). Watson (*l. c.* p. 99) showed also for a numerical case that this term is negligible compared with the first term, and further on we shall neglect this term.

The first term of (7) enables us to obtain a very physical interpretation of a typical possibility inherent to our spherical problem and which has also been noticed by Watson. For if we develop $1/\cos(n\pi)$ as

$$\frac{1}{\cos(n\pi)} = 2e^{i\pi n} \sum_{m=0}^{m=\infty} e^{i\pi m(2n+1)}, \quad . \quad . \quad . \quad (8)$$

valid over the whole integration path L, we can write (7) as

$$\Pi_{\text{tot}} \sim \sum_{m=0}^{m=\infty} \Pi_m, \quad . \quad . \quad . \quad . \quad . \quad . \quad (9)$$

where

$$\Pi_m = \frac{2e^{i\pi m}}{(k_1a)^3} \int_L n\, dn\, e^{i\pi n(2m+1)} \frac{\zeta^{(1)}_{n-1/2}(k_1b)}{\zeta^{(1)}_{n-1/2}(k_1a)} \frac{1}{N_{n-1/2}} \times P_{n-1/2}\{\cos(\pi-\vartheta)\}. \quad . \quad (10)$$

We are now able to represent this integral as the sum of the residues of all the enclosed poles being the zeros n_s of $N_{n-1/2}$ only, and therefore may write it as

$$\Pi_m = \frac{4\pi i e^{i\pi m}}{(k_1a)^3} \sum_{s=0}^{s=\infty} n_s e^{i\pi n_s(2m+1)} \frac{\zeta^{(1)}_{n_s-1/2}(k_1b)}{\zeta^{(1)}_{n_s-1/2}(k_1a)} \frac{1}{\left(\dfrac{\partial N_{n-1/2}}{\partial n}\right)_{n=n_s}} \times P_{n_s-1/2}\{\cos(\pi-\vartheta)\}. \quad . \quad (11)$$

Further, for all values of ϑ not too near 0 or π, and, as the modulus of all poles n_s is of the order k_1a (as will be shown later on), the well-known asymptotic formula for the spherical harmonics of complex order with positive imaginary part

$$P_{n-1/2}\{\cos(\pi-\vartheta)\} \sim \frac{1}{\sqrt{2\pi n \sin\vartheta}} e^{-in(\pi-\vartheta)+i\pi/4}, \qquad (12)$$

may now be introduced as an approximation in the still rigorous expression (10), yielding

$$\Pi_m \sim \frac{2\sqrt{2\pi}\,.\,e^{i\pi(m+3/4)}}{(k_1a)^3\sqrt{\sin\vartheta}} \sum_{s=0}^{s=\infty} \frac{\zeta^{(1)}_{n_s-1/2}(k_1b)}{\zeta^{(1)}_{n_s-1/2}(k_1a)} \frac{n_s^{1/2}}{\left(\frac{\partial N_{n-1/2}}{\partial n}\right)_{n=n_s}} e^{in_s(\vartheta+2\pi m)}. \quad . \quad (13)$$

The above mentioned physical interpretation is given directly by the last factor of (13), viz. :

$$e^{in_s(\vartheta+2\pi m)} = e^{(i\alpha_s-\beta_s)(\vartheta+2\pi m)}, \quad . \quad . \quad . \quad (14)$$

putting

$$n_s = \alpha_s + i\beta_s \quad (\beta_s > 0).$$

Hence (13) represents a wave travelling round the sphere with a phase velocity and attenuation determined by α_s and β_s respectively. But the presence in the exponent of the combination $\vartheta+2\pi m$ clearly shows that the term Π_m of (9) is representative of a wave which has travelled from the source to the receiver only after having made m complete revolutions round the sphere. This explanation becomes especially vivid for the case of radiotelegraphy, where the transmitter is near the surface of the sphere. It will be clear that the contribution to the field at the surface of the earth by a wave which has travelled several times round the earth, is extremely small compared with the wave coming directly from the transmitter to the receiver ($m=0$). In Watson's analysis the first term Π_0 of the series (9) is retained only, and we will follow the same procedure in Part I. of this paper, so that we will further consider the approximation

$$\Pi_{\text{tot}} \sim \Pi_0 \sim \frac{2\sqrt{2\pi}\,e^{3/4 i\pi}}{(k_1a)^3\sqrt{\sin\vartheta}} \sum_{s=0}^{s=\infty} \frac{\zeta^{(1)}_{n_s-1/2}(k_1b)}{\zeta^{(1)}_{n_s-1/2}(k_1a)} \frac{n_s^{1/2}}{\left(\frac{\partial N_{n-1/2}}{\partial n}\right)_{n=n_s}} e^{in_s\vartheta}. \quad . \quad (15)$$

4. *Approximations for the Bessel Functions.*

It will be clear that for numerical interpretation of (15), a knowledge of the poles n_s and of the residues is necessary. We will therefore make use of *two* approximations :

(*a*) The Debye approximations, as given in full detail in the second edition of Jahnke-Emde, Funktionentafeln, pp. 204–207. These become in our case, where n/z and z lie in the first quadrant :

$$\zeta_n^{(1)}(z)=\sqrt{\frac{\pi}{2z}}\,\mathrm{H}^{(1)}_{n+1/2}(z)$$

$$\sim\frac{2}{i\sqrt{(n+\frac{1}{2})z\sqrt{\dfrac{z^2}{(n+\frac{1}{2})^2}-1}}}$$

$$\times\cos\left\{\frac{\pi}{4}+(n+\tfrac{1}{2})\int_1^{z/(n+1/2)}\sqrt{u^2-1}\,\frac{du}{u}\right\}, \quad . \quad (16\,a)$$

$$\zeta_n^{(2)}(z)=\sqrt{\frac{\pi}{2z}}\,\mathrm{H}^{(2)}_{n+1/2}(z)$$

$$\sim\frac{1}{\sqrt{(n+\frac{1}{2})z\sqrt{\dfrac{z^2}{(n+\frac{1}{2})^2}-1}}}$$

$$\times e^{i\pi/4-i(n+1/2)\int_1^{z/(n+1/2)}\sqrt{u^2-1}\,\frac{du}{u}}, \quad . \quad (16\,b)$$

where the root $\sqrt{\dfrac{z^2}{(n+\frac{1}{2})^2}-1}$ is defined as lying in the same quadrant as $z/(n+\frac{1}{2})$.

(*b*) The approximations reducing the Bessel functions of any order to these functions of order 1/3. For the orders of magnitude obtaining in our problem, these are

$$\mathrm{H}^{(1)}_{(2)\,n}(z)\sim\frac{\sqrt{\dfrac{z^2}{n^2}-1}}{\sqrt{3}}\,e^{\pm i\pi/6\mp in\int_1^{z/n}\frac{du}{u}(u^2-1)^{3/2}}$$

$$\times\mathrm{H}^{(1)}_{(2)\,1/3}\left\{\frac{n}{3}\left(\frac{z^2}{n^2}-1\right)^{3/2}\right\}, \quad . \quad (17)$$

where

$$-\pi/2<\arg\sqrt{\frac{z^2}{n^2}-1}<\pi/2.$$

The formulæ (16) are suitable everywhere except for z near n, while (17), valid only for $n>>1$, is of special use when z is near n. It is further easy to verify that the first term of the asymptotic development of $H_{1/3}$ occurring in (17) leads to (16).

Moreover (16 a) clearly shows the position of the zeros of $\zeta_n^{(1)}(z)$ at constant n, these being determined by the condition that the cosine becomes zero, similar roots not occurring in the quadrant considered in the case of $\zeta_n^{(2)}(z)$. Again, these zeros of $\zeta_n^{(1)}(z)$ separate the two regions where one or the other of the exponential parts of the cosine function dominates, these zeros requiring obviously

$$I_n\left\{\frac{\pi}{4}+(n+\tfrac{1}{2})\int_1^{z/(n+1/2)}\sqrt{u^2-1}\,\frac{du}{u}\right\}=0, \quad . \quad (18)$$

where I denotes the imaginary part of its argument.

The close relationship between (16) and the well-known W.K.B. approximation is at once apparent, remembering that $z\zeta_n(z)$ satisfies the differential equation

$$\frac{d^2}{dz^2}(z\zeta_n)+\left\{1-\frac{n(n+1)}{z^2}\right\}.z\zeta_n=0. \quad . \quad . \quad (19)$$

5. *The Limiting Case of a Plane Boundary* ($a\rightarrow\infty$).

In this paragraph we will show how the well-known solution of the similar problem, but for a plane boundary, can be obtained as a limiting case of the spherical problem. We therefore start with (1 a) in the form

$$\Pi_{sec}=\sum_{n=0}^{n=\infty}(2n+1)R_n\frac{\psi_n(k_1a)}{\zeta_n^{(1)}(k_1a)}\zeta_n^{(1)}(k_1b)\zeta_n^{(1)}(k_1r)P_n(\cos\vartheta)$$

$$(r>a), \quad . \quad (1a)$$

and have to consider the limit of this expression for $a\rightarrow\infty$ while keeping constant the three quantities

$b-a=z_q$ (height of source above boundary),

$z-a=z_p$ (height of receiver above boundary),

$a\vartheta=\rho$ (horizontal distance between source and receiver).

Using the method of § 3 in order to transform (1*a*) into an integral, one finds

$$\Pi_{\text{sec}} = -i \int_{\mathrm{B}} \frac{n\,dn}{\cos(n\pi)} \mathrm{R}_{n-1/2} \zeta^{(1)}_{n-1/2}(k_1 a) \psi_{n-1/2}(k_1 a)$$

$$\times \frac{\zeta^{(1)}_{n-1/2}(k_1 b)\zeta^{(1)}_{n-1/2}(k_1 r)}{\{\zeta^{(1)}_{n-1/2}(k_1 a)\}^2} \mathrm{P}_{n-1/2}\{\cos(\pi-\vartheta)\}. \quad (20)$$

Now putting $n=a\lambda$, and taking the limit for $a\rightarrow\infty$, while keeping λ constant, one finds, for the different factors of the integrand of (19),

(*a*)

$$\lim_{a\rightarrow\infty} \mathrm{R}_{n-1/2} = \frac{k_2{}^2\sqrt{\lambda^2-k_1{}^2}-k_1{}^2\sqrt{\lambda^2-k_2{}^2}}{k_2{}^2\sqrt{\lambda^2-k_1{}^2}+k_1{}^2\sqrt{\lambda^2-k_2{}^2}}. \quad . \quad (21)$$

Here we have used the limits of the logarithmic derivates of (17) in the form

$$\frac{d}{dz}\log\{z\zeta^{\binom{(1)}{(2)}}_n(z)\} \sim \frac{1}{2z} \mp i\frac{n}{z}\left(\frac{z^2}{n^2}-1\right)^{3/2}$$

$$+e^{\pm 2/3 i\pi}\frac{z}{n}\sqrt{\frac{z^2}{n^2}-1}\,\frac{\mathrm{H}^{\binom{(1)}{(2)}}_{2/3}\left\{\frac{n}{3}\left(\frac{z^2}{n^2}-1\right)^{3/2}\right\}}{\mathrm{H}^{\binom{(1)}{(2)}}_{1/3}\left\{\frac{n}{3}\left(\frac{z^2}{n^2}-1\right)^{3/2}\right\}}, \quad (22)$$

where

$$-\frac{\pi}{2} < \arg\sqrt{\frac{z^2}{n^2}-1} < \frac{\pi}{2}.$$

In our limit z/n has the constant value k/λ, but the argument of $\mathrm{H}_{1/3}$ and $\mathrm{H}_{2/3}$ is tending to $+\infty$, and we obtain

$$\lim_{z=ka\rightarrow\infty} \frac{d}{dz}\log\{z\zeta^{\binom{(1)}{(2)}}_{n\lambda}(z)\} = \mp\frac{1}{k}\sqrt{\lambda^2-k^2},$$

where $\sqrt{\lambda^2-k^2}$ has always a positive real part. Further we have

$$\lim_{a\rightarrow\infty} \psi_n(ka) = \tfrac{1}{2}\lim_{a\rightarrow\infty} \zeta^{(2)}_n(ka),$$

because k lies in the first quadrant and therefore the $\zeta^{(1)}_n$ part vanishes, so that

$$\lim_{a\rightarrow\infty} \frac{d}{dz}\log\{z\psi_n(z)\} = \tfrac{1}{2}\lim_{a\rightarrow\infty} \frac{d}{dz}\log\{z\zeta^{(2)}_n(z)\}.$$

The limit of $R_{n-1/2}$ then follows directly from the definition (2) of R_n.

(*b*)

$$\lim_{a\to\infty} \zeta^{(1)}_{n-1/2}(k_1a)\psi_{n-1/2}(k_1a)=\frac{1}{2ik_1a^2\sqrt{\lambda^2-k_1^2}},$$

because, as in (*a*), we first have

$$\lim_{a\to\infty} \zeta^{(1)}_{n-1/2}(k_1a)\psi_{n-1/2}(k_1a)=\tfrac{1}{2}\lim_{a\to\infty} \zeta^{(1)}_{n-1/2}(k_1a)\zeta^{(2)}_{n-1/2}(k_1a),$$

and then can apply (16), using in (16 *a*) only the dominant term of the cos-function.

(*c*)

$$\lim_{\substack{a\to\infty\\ b-a=z_q}} \frac{\zeta^{(1)}_n(k_1b)}{\zeta^{(1)}_n(k_1a)}=e^{-\sqrt{\lambda^2-k_1^2}z_q}.$$

This limit follows directly from the dominant term in (16 *a*), because

$$\frac{\zeta^{(1)}_{n-1/2}(k_1b)}{\zeta^{(1)}_{n-1/2}(k_1a)}\sim\frac{\sqrt{a}}{\sqrt{b}}\,\frac{\sqrt[4]{k_1^2a^2-n^2}}{\sqrt[4]{k_1^2b^2-n^2}}\,e^{ia\lambda\int_{k_1/\lambda}^{(1+z_q/a)k_1/\lambda}\sqrt{u^2-1}\,\frac{du}{u}},$$

and this expression leads at once for $a\to\infty$ to the above limit.

(*d*) Similarly we have

$$\lim_{\substack{a\to\infty\\ b-a=z_p}} \frac{\zeta^{(1)}_n(k_1r)}{\zeta^{(1)}_n(k_1a)}=e^{-\sqrt{\lambda^2-k_1^2}z_p}.$$

(*e*)

$$\lim_{\substack{a\to\infty\\ I(n)>0}} \frac{P_{n-1/2}\{\cos(\pi-\vartheta)\}}{\cos(n\pi)}-\lim_{\substack{a\to\infty\\ I(n)<0}} \frac{P_{n-1/2}\{\cos(\pi-\vartheta)\}}{\cos(n\pi)}$$
$$=2iJ_0(\lambda\rho),$$

where $I(n)$ means the imaginary part of n.

We may prove this by using the relation

$$\frac{P_{n-1/2}\{\cos(\pi-\vartheta)\}}{\cos(n\pi)}=tg(n\pi)P_{n-1/2}(\cos\vartheta)+\frac{2}{\pi}Q_{n-1/2}(\cos\vartheta),$$

which is valid for unrestricted n but real ϑ. For $n=a\lambda$ tending to ∞ the functions $P_{n-1/2}(\cos\vartheta)$ and $Q_{n-1/2}(\cos\vartheta)$ have each the same limit for $I(n)>0$ and $I(n)<0$, but for $tg\,(n\pi)$ we have

$$\lim_{|n|\to\infty} tg(n\pi)=\pm i \text{ resp. for } I(n)\gtrless 0.$$

Therefore

$$\lim_{\substack{a\to\infty \\ I(n)>0}} \frac{P_{n-1/2}\{\cos(\pi-\vartheta)\}}{\cos(n\pi)} - \lim_{\substack{a\to\infty \\ I(n)<0}} \frac{P_{n-1/2}\{\cos(\pi-\vartheta)\}}{\cos(n\pi)}$$
$$=2i \lim_{n\to\infty} P_{n-1/2}(\cos\vartheta)$$
$$=2i \lim_{n\to\infty} P_{n-1/2}\left(\cos\frac{\lambda\rho}{n}\right)=2iJ_0(\lambda\rho).$$

After substitution of the limits $a-d$ in (20), which are valid both for the part of B above and the part below the real axis, we can reduce the path of integration to the real axis after applying (e), and finally obtain

$$\Pi_{\text{sec}}=\frac{1}{ik_1}\int_0^\infty \frac{\lambda d\lambda}{\sqrt{\lambda^2-k_1^2}} \frac{(k_2^2\sqrt{\lambda^2-k_1^2}-k_1^2\sqrt{\lambda^2-k_2^2})}{(k_2^2\sqrt{\lambda^2-k_1^2}+k_1^2\sqrt{\lambda^2-k_2^2})}$$
$$\times e^{-\sqrt{\lambda^2-k_1^2}(z_q+z_p)}.J_0(\lambda\rho).$$

This coincides with the expression given as (1) in a former paper [10], where the primary field was defined as e^{ik_1R}/R instead of e^{ik_1R}/ik_1R as here. Hence a complete agreement is obtained, including a finite height of both point source and receiver and a finite conductivity of the two media.

6. *Development in Characteristic Functions.*

It may be noted that the solution used so far is quite distinct from the well-known method of development in Characteristic Functions, as, *e. g.*, is a standard method for string problems and in wave mechanics.

In our problem we have two differential equations for $r>a$ and $r<a$; before applying the theory of Characteristic Functions, we shall first consider the more general equation of the Sturm-Liouville type

$$\{\Delta+g(x, y, z)\}\Pi'=f(x, y, z).$$

This equation has Characteristic Functions defined by the following properties :

1. $(\Delta+\lambda_j^2 g)\phi_j=0,$

2. ϕ_j finite for $r=0$ and $r=\infty$.

The expansion of the solution in Characteristic Functions as described for instance in chapter v., § 2 of Courant und

Hilbert, *Methoden der Mathematischen Physik*, i., here becomes

$$\Pi'(\mathrm{P})=\Sigma_j\frac{\int\phi_j.f.d\tau}{(1-\lambda_j^2)}\phi_j(\mathrm{P}). \quad . \quad . \quad . \quad . \quad (23)$$

Now let $g(x, y, z)$ degenerate to the discontinuous function $g=k_1^2$ for $r>a$ and $g=k_2^2$ for $r<a$, $g\Pi$ and $\partial/\partial r\ (r\Pi)$ remaining continuous for $r=a$; then the new Characteristic Functions are determined by the conditions

$$\left.\begin{array}{ll} (1) & (\Delta+k_1^2\lambda_j^2)\phi_j=0 \quad (r>a) \\ & (\Delta+k_2^2\lambda_j^2)\phi_j=0 \quad (r<a), \\ (2) & k^2\phi_j \text{ and } \dfrac{\partial}{\partial r}(r\phi_j) \text{ continuous for } r=a, \\ (3) & k_1^2\displaystyle\int_{r=a}^{r=\infty}\phi_j^2\,d\tau+k_2^2\int_{r=0}^{r=a}\phi_j^2\,d\tau=1. \end{array}\right\} . \qquad (24)$$

We now proceed by a method which has been fully expounded by A. Sommerfeld [(11)] in a classical paper, where the primary field is $\cos(k_1\mathrm{R})/(ik_1\mathrm{R})$, belonging to a point source of stationary waves with a singularity at Q; this field leads to a three-dimensional impulsive function $4\pi i\delta(\mathrm{R})/k_1$ at Q for $f(x, y, z)$. Hence substitution in (23) yields

$$\Pi'_{\mathrm{tot}}=-\frac{4\pi}{ik_1}\Sigma_j\frac{\phi_j(\mathrm{Q})\phi_j(\mathrm{P})}{(1-\lambda_j^2)}. \quad . \quad . \quad . \quad (25)$$

As the Characteristic Functions should everywhere be finite and single-valued, they are of the form

$$\phi_{n,j}=\left\{\begin{array}{ll} \mathrm{A}_{n,j}\zeta_n^{(1)}(\lambda_{n,j}k_1r)\mathrm{P}_n(\cos\vartheta) & (r>a), \\ \mathrm{B}_{n,j}\psi_n(\lambda_{n,j}k_2r)\mathrm{P}_n(\cos\vartheta) & (r<a), \end{array}\right\}. \qquad (26)$$

where n is a positive integer.

The boundary conditions further require

$$k_1^2\mathrm{A}_{n,j}\zeta_n^{(1)}(\lambda_{n,j}k_1a)=k_2^2\mathrm{B}_{n,j}\psi_n(\lambda_{n,j}k_2a), \quad . \qquad (27\,a)$$

$$\mathrm{A}_{n,j}\left[\frac{d}{dz}\{z\zeta_n^{(1)}(z)\}\right]_{z=\lambda_{n,j}k_1a}=\mathrm{B}_{n,j}\left[\frac{d}{dz}\{z\psi_n(z)\}\right]_{z=\lambda_{n,j}k_2a}, \quad . \quad . \quad . \quad (27\,b)$$

so that

$$\left|\begin{array}{ll} k_1^2a^2\zeta_n^{(1)}(\lambda_{n,j}k_1a) & k_2^2a^2\psi_n(\lambda_{n,j}k_2a) \\ \left[\dfrac{d}{dz}\{z\zeta_n^{(1)}(z)\}\right]_{z=\lambda_{n,j}k_1a} & \left[\dfrac{d}{dz}\{z\psi_n(z)\}\right]_{z=\lambda_{n,j}k_2a} \end{array}\right|=0,$$

$$\text{or } \mathrm{N}_n(\lambda_{n,j}k_1a,\ \lambda_{n,j}k_2a)=0, \quad (28)$$

(see (6)).

The difference between the method used so far and the present method of Characteristic Functions now becomes very clear by the fact that, although both methods consider the zeros of N,—which is a function of n and the ka's—the first method considers the zeros as a function of n for constant ka's, whereas the method of Characteristic Functions treats the zeros as a function of the ka's, while keeping the integer n constant.

Introducing the normalization condition (3) of (24), and remembering that the integration over all space has to be performed for the inner space and outer space separately, we obtain

$$\frac{A^2_{n,j}}{k_1}\int_{\lambda_{n,j}k_1a}^{\infty}\{\zeta_n^{(1)}(u)\}^2u^2\,du + \frac{B^2_{n,j}}{k_2}\int_0^{\lambda_{n,j}k_2a}\{\psi_n(u)\}^2u^2\,du=\frac{(2n+1)}{4\pi}\lambda^3_{n,j}. \quad (29)$$

(27), (28), and (29) now determine completely $A_{n,j}$ and $B_{n,j}$; after reduction, and making use of well-known integral properties of the Bessel functions, we get

$$A^2_{n,j}=\frac{(2n+1)}{2\pi k_1{}^2a^3\{\zeta_n^{(1)}(x)\}^2\left[\left(\frac{d^2}{dx^2}+\frac{1}{x}\frac{d}{dx}\right)\log\{x\zeta_n^{(1)}(x)\} -\frac{k_1{}^2}{k_2{}^2}\left(\frac{d^2}{dy^2}+\frac{1}{y}\frac{d}{dy}\right)\log\{y\psi_n(y)\}\right]} \quad . \; . \; . \; (30a)$$

$$B^2_{n,j}=\frac{(2n+1)}{2\pi k_2{}^2a^3\{\psi_n(y)\}^2\left[\frac{k_2{}^2}{k_1{}^2}\left(\frac{d^2}{dx^2}+\frac{1}{x}\frac{d}{dx}\right)\log\{x\zeta_n^{(1)}(x)\} -\left(\frac{d^2}{dy^2}+\frac{1}{y}\frac{d}{dy}\right)\log\{y\psi_n(y)\}\right]} \quad . \; . \; . \; (30b)$$

where $x=\lambda_{n,j}k_1a$ and $y=\lambda_{n,j}k_2a$, so that after substitution in (25) we obtain

$$\left.\begin{aligned}\Pi'_{\text{tot}}&=\frac{4\pi i}{k_1}\sum_{n=0}^{n=\infty}\Sigma_j\frac{A^2_{n,j}}{(1-\lambda^2_{n,j})}\zeta_n^{(1)}(\lambda_{n,j}k_1b)\zeta_n^{(1)}(\lambda_{n,j}k_1r)P_n(\cos\vartheta) \\ &\qquad\qquad (r>a), \\ \Pi'_{\text{tot}}&=\frac{4\pi i}{k_1}\sum_{n=0}^{n=\infty}\Sigma_j\frac{A_{n,j}B_{n,j}}{(1-\lambda^2_{n,j})}\zeta_n^{(1)}(\lambda_{n,j}k_1b)\psi_n(\lambda_{nj}k_2r)P_n(\cos\vartheta) \\ &\qquad\qquad (r<a);\end{aligned}\right\} \quad . \; . \; . \; (31)$$

(31) gives the solution of our problem as a double series of Characteristic Functions, the summations to be extended over the integer values of n and over all the j values every time belonging to a given n. It will be clear that (31) must be equal to (1). Further, the orthogonality of the functions $P_n(\cos\vartheta)$ requires that for a fixed n the summation over the corresponding j values must every time lead to the coefficients of $P_n(\cos\vartheta)$ in the harmonic series (1). This idea will further be developed for the special case $|k_2|=\infty$ in paragraph 7 *c*.

7 *a*. *The Harmonic Series for a Perfectly Reflecting Sphere.* ($|k_2|=\infty$).

In this paragraph we will investigate the limiting case for a perfectly reflecting sphere and therefore $|k_2|=\infty$, while basing ourselves on the harmonic series. In the next § 7 *b* we elaborate the residue series and obtain numerical results, showing also the influence of the finite height $b-a=h$ of the transmitter above the surface of the sphere. In § 7 *c* we compare the residue series with the development in Characteristic Functions.

The harmonic series (5) for $a=b=r$ and $|k|_2=\infty$ becomes

$$\Pi_{\text{tot}}=\frac{i}{z^2}\sum_{n=0}^{n=\infty}(2n+1)\frac{1}{zN_n(z)}P_n(\cos\vartheta)_{(z=k_1a)}, \quad . \quad (32)$$

where

$$\frac{1}{zN_n(z)}=\left[\frac{z\zeta_n^{(1)}(z)}{\frac{d}{dz}\{z\zeta_n^{(1)}(z)\}}\right]_{z=k_1a}, \quad . \quad . \quad . \quad (33)$$

and we will now examine the numerical structure of the coefficient $1/zN(z)$ as a function of the positive integer n for $|z|>>1$. To this end we can at once make use of (22), where, as $|z|>>1$, the first term may be neglected. We therefore have

$$zN_n(z)\sim -i\frac{n}{z}\left(\frac{z^2}{n^2}-1\right)^{3/2}$$

$$+e^{2/3i\pi}\frac{z}{n}\sqrt{\frac{z^2}{n^2}-1}\,\frac{H_{2/3}^{(1)}\left\{\frac{n}{3}\left(\frac{z^2}{n^2}-1\right)^{3/2}\right\}}{H_{1/3}^{(1)}\left\{\frac{n}{3}\left(\frac{z^2}{n^2}-1\right)^{3/2}\right\}}, \quad (34)$$

where

$$-\frac{\pi}{2} < \arg\sqrt{\frac{z^2}{n^2}-1} < \frac{\pi}{2}.$$

The square root remains perfectly well defined even for z^2/n^2 real, when this variable is considered as having an infinitesimal positive imaginary part. The approximate expression (34) can, when z is not too near n, be further considerably simplified, for then the argument of the Hankel functions remains so great that the first term of their asymptotic development suffices. Under these circumstances (34) degenerates to the simple form

$$\frac{1}{z\mathrm{N}_n(z)} \approx \frac{1}{i\sqrt{1-\frac{n^2}{z^2}}}, \quad . \quad . \quad . \quad . \quad (35)$$

with the square root in the first quadrant, and this form coincides with the first W.K.B. approximation of the proper solution of (19) Although (34) was developed for $n >> 1$, (35) still gives the right value for $n=0$, viz.

$$\frac{1}{z\mathrm{N}_0(z)} = -i.$$

Further (35) degenerates for $n >>> z$ to

$$\frac{1}{z\mathrm{N}_n(z)} \approx -\frac{z}{n}.$$

Moreover, for the transition case ($n \sim z$) the second term of (34) dominates by far, and when $n=z$ exactly; in the latter case this second term becomes indefinite, but, while taking the first term of the power series of the Hankel functions, it is easy to show that

$$\left\{\frac{1}{z\mathrm{N}_n(z)}\right\}_{n=z} = \frac{2}{6^{1/3}}\frac{\Pi(1/3)}{\Pi(2/3)}e^{-2/3 i\pi}z^{1/3}$$

$$=1{\cdot}0888 \ldots e^{-2/3 i\pi}z^{1/3}.$$

The above approximations enable us to determine numerically $1/z\mathrm{N}_n(z)$ as a function of n in the complex plane. We have chosen $z=k_1a=5{\cdot}72.10^6$ corresponding to waves of 7 meter in the radio case ($2\pi a=4.10^9$ cm.). In fig. 3 we give the result numerically correct. The numbers in this figure refer to the values of $n-z$. It appears from this figure that (a) the modulus of $1/z\mathrm{N}_n(z)$

has a maximum near $n=z$; (*b*) the density along the curve is rather small where the modulus of $1/z\,N_n(z)$ is considerable, whereas nearly all points are lying on the two extreme parts of the curve near the two axes; (*c*) the curve has a horizontal tangent at $n=z$.

Again, figs. 4 and 5 give the modulus and the argument of $1/zN_n(z)$ as a function of $n-z$; a.o. this clearly demonstrates (*b*) above.

Fig. 3.

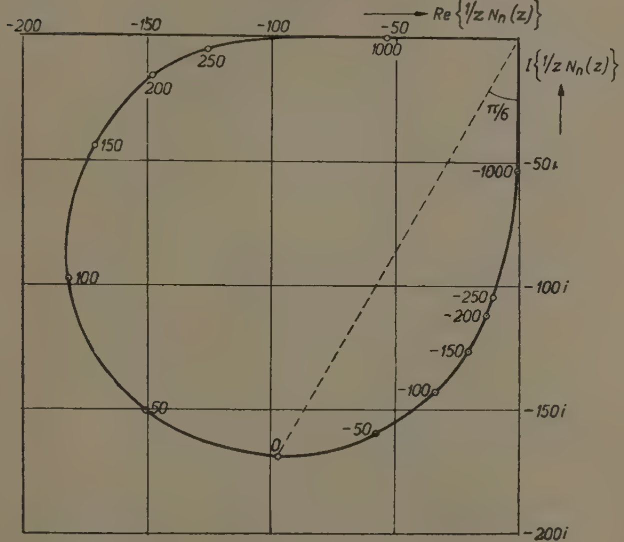

Coefficient of the harmonic series for $|k|=\infty$ and $z=k_1a=5{\cdot}72.10^6$.

A further numerical consideration shows that for all values of n where $1/zN_n(z)$ has an appreciable value, *i. e.*, where $n\sim z$, a good approximation to this function is given by the second term of (34) only; moreover, in this range z^2/n^2-1 may be replaced by $2(z/n-1)$, so that the final approximation for (34) gives $1/zN_n(z)$ as a function of the only variable $\sigma=(n-z)/z^{1/3}$:

$$\frac{1}{zN_n(z)}\approx z^{1/3}e^{-2/3i\pi}\frac{H^{(1)}_{1/3}\{\frac{1}{3}(-2\sigma)^{3/2}\}}{\sqrt{-2\sigma}\,H^{(1)}_{2/3}\{\frac{1}{3}(-2\sigma)^{3/2}\}}. \quad . \quad (36)$$

This shows the universal character of the figures 3, 4, and 5, which retain the same form also for other values of the wave-length than $\lambda=7$ meter.

Returning to the harmonic series (32), the coefficients of which have now been completely investigated, it follows that, when ϑ is not near zero, the oscillatory character of $P_n(\cos\vartheta)$ for fixed ϑ as a function of n causes the series

Fig. 4.

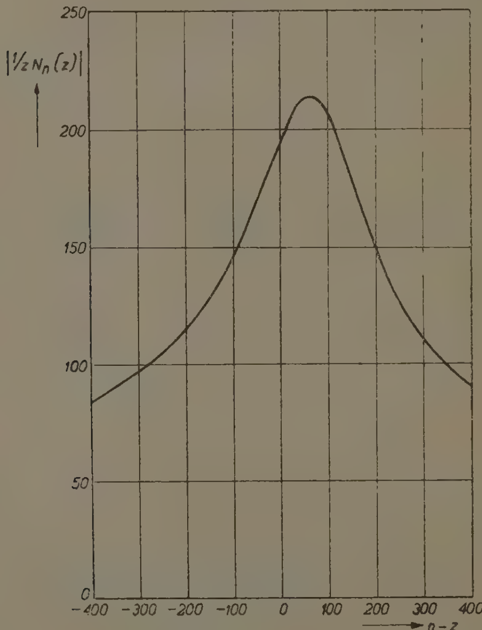

Modulus of the coefficient of fig. 3 as a function of n.

to oscillate very rapidly, so that successive terms nearly cancel each other, which makes the summation of (32) a very intricate process. We will now turn our attention to the much more rapidly convergent residue-series.

7b. *The Series of Residues for* $|k_2|=\infty$.

Consider (7). For $|k_2|=\infty$ the expression $N_{n-1/2}$ is, according to (33), even in n, so that the second term of

(7) is exactly zero. We can therefore further use the series of residues as given by (15) and for numerical applications a knowledge of the zeros of $N_{n-1/2}$, as well as the values of $\frac{\partial N_{n-1/2}}{\partial n}$ at these zeros is necessary. A further investigation shows that for $|z|>>1$, as is the case in the radio application, the zeros n_s of $N_{n-1/2}$ as a function of n for constant z have a modulus at least of

Fig. 5.

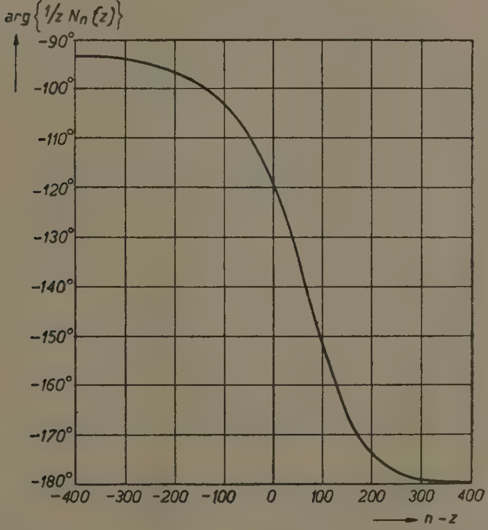

Argument of the coefficient of fig. 3 as a function of n.

the order $|z|$. In order therefore to find the proper approximation for $N_{n-1/2}(z)$ we differentiate (16 *a*) logarithmically, remembering that both $|z|>>1$ and $|n|>>1$. We thus find

$$N_n(z) \sim -\frac{n}{z^2}\sqrt{\frac{z^2}{n^2}-1}\,.\,tg\left\{\frac{\pi}{4}+(n+\tfrac{1}{2})\int_1^{z/n}\sqrt{u^2-1}\,\frac{du}{u}\right\}, \quad . \quad . \quad . \quad (37)$$

so that the zeros n_s of $N_{n-1/2}(z)$ are given by the transcendental equations

$$i(n_s+\tfrac{1}{2})\int_1^{z/n_s}\sqrt{1-u^2}\,\frac{du}{u}=\pi(s+\tfrac{1}{4})\quad(s=0,\,1,\,2,\,\ldots). \quad . \quad . \quad . \quad (38)$$

For real $z=k_1a$ (meaning a non-absorbing atmosphere)

Fig. 6.

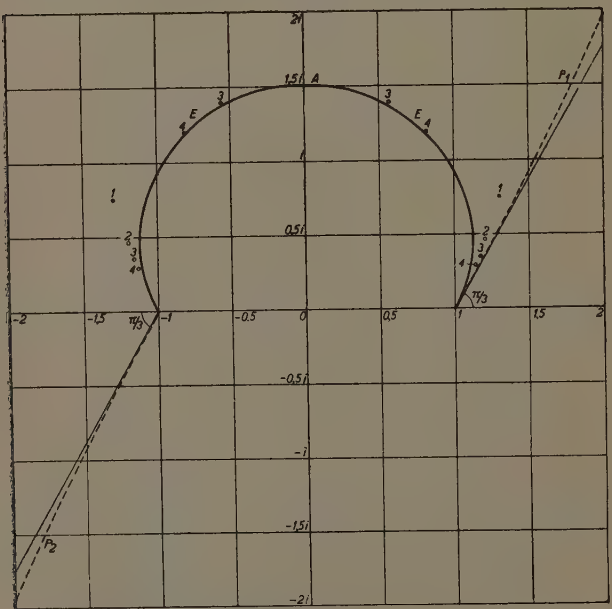

Poles and characteristic frequencies in the n/z plane for $|\,k_2\,|=\infty$.

it follows from (38) that with the approximations used all the zeros n_s are situated on the curves

$$\mathrm{Re}\left\{\frac{n}{z}\int_1^{z/n}\sqrt{1-u^2}\frac{du}{u}\right\}=0 \quad . \quad . \quad . \quad (39)$$

in the n/z plane, which are shown dotted in fig. 6 as P_1 and P_2. The poles n_s nearest the real axis and on the branch P_1, with the exception of the first few, are easily

found from (38), remembering that $|z/n-1|$ is a small quantity. They are given by

$$n_s=z+\tau_s z^{1/3}, \qquad (40)$$

where

$$\tau_s=\tfrac{1}{2}\{3\pi(s+\tfrac{1}{4})\}^{2/3}e^{i\pi/3}. \qquad (40\,a)$$

In order to calculate the first few roots, which lie in the immediate neighbourhood of $n=z$, other authors, *e. g.*, Nicholson [12], Laporte[7], have used approximations with more terms. The difficulty is that especially the first root, which is of predominant influence on the numerical results, lies in the boundary region of the two Debye approximations for the Hankel functions; see, *e. g.*, Jahnke-Emde, 'Funktionentafeln' (1933), pp. 204, 207. In this way they found, in our notation,

Nicholson .. $\tau_0=0{\cdot}804e^{i\pi/3}$.

Laporte.... $\tau_0=0{\cdot}81\ e^{i\pi/3}$.

However, it is of interest to note that the expression (36), which is valid near $n=z$, yields as equation for the first few zero;

$$\mathrm{H}^{(1)}_{2/3}\{\tfrac{1}{3}(-2\sigma)^{3/2}\}=\mathrm{H}^{(1)}_{2/3}\left\{\frac{2^{3/2}}{3\sqrt{z}}(n-z)^{3/2}e^{-3/2i\pi}\right\}=0.$$

Remembering further that

$$\mathrm{H}^{(1)}_{2/3}(\alpha e^{-i\pi})=\frac{e^{-5/6i\pi}}{\sin\pi/3}\{\mathrm{J}_{2/3}(\alpha)-\mathrm{J}_{-2/3}(\alpha)\}, \qquad (41$$

and calling α_s the zeros of (41), which are all positive, and identifying

$$\frac{2^{3/2}}{3\sqrt{z}}(n_s-z)^{3/2}e^{-3/2i\pi}=\alpha_s e^{-i\pi},$$

we again find for the zeros n_s the relation (40), but, instead of (40 *a*),

$$\tau_s=\tfrac{1}{2}(3\alpha_s^{\frac{1}{}})^{2/3}e^{i\pi/3}, \qquad (40\,b)$$

which furnishes a better approximation than (40 *a*).

Summarizing, the equations (40 *a*) and (40 *b*) thus yield for the first three roots

from (40 *a*) :	*from* (40 *b*) :
$\tau_0=0{\cdot}885e^{\pi/3}$,	$\tau_0=0{\cdot}808\,e^{i\pi/3}$,
$\tau_1=2{\cdot}589\,e^{i\pi/3}$,	$\tau_1=2{\cdot}577\,e^{i\pi/3}$,
$\tau_2=3{\cdot}830\,e^{i\pi/3}$,	$\tau_2=3{\cdot}824\,e^{i\pi/3}$,

so that in a relatively simple way we find from (40 b) a value for τ_0 which is very near the accurate values already given by Nicholson and Laporte.

Having thus found the position of the first few poles n_s, the factor of the corresponding residues,

$$\left(\frac{\partial N}{\partial n}\right)_{n=n_s}=-2\tau_s z^{-1/3},$$

may be obtained from (37) and (40). Substitution of the results in (15) yields the final and rapidly converging expression

$$\Pi_{\substack{r=a\\|k_2|=\infty}}\sim 2\frac{e^{iz\vartheta}}{iz\vartheta}\sqrt{\frac{\pi}{2}iz^{1/3}\vartheta}\,.\,\sum_s\frac{\zeta^{(1)}_{z+z^{1/3}\tau_s}(k_1b)}{\zeta^{(1)}_{z+z^{1/3}\tau_s}(k_1a)}\frac{e^{iz^{1/3}\tau_s\vartheta}}{\tau_s}. \quad (42)$$

Taking the special case of the transmitter being placed on the surface of the sphere ($b=a$), (42) simplifies to

$$\Pi_{\substack{r=a=b\\|k_2|=\infty}}\sim 2\frac{e^{iz\vartheta}}{iz\vartheta}F(\eta), \quad . \quad . \quad . \quad . \quad . \quad (43)$$

where

$$F(\eta)=\sqrt[3]{\frac{\pi^2}{2}}\,e^{i\pi/4}\sqrt{\eta}\sum_s\frac{e^{i(2\pi)^{1/3}\tau_s\eta}}{\tau_s}, \quad . \quad . \quad . \quad (43\,a)$$

$$\eta=\sqrt[3]{\frac{k_1a}{2\pi}}\,\vartheta\sim\frac{D}{a^{2/3}\lambda^{1/3}},$$

D being the distance between transmitter and receiver measured along the surface of the sphere.

The structure of (43), which can be written

$$\Pi_{\substack{r=a=b\\|k_2|=\infty}}\sim 2\frac{e^{ik_1D}}{ik_1D}F(\eta), \quad . \quad . \quad . \quad . \quad (44)$$

clearly shows the correction factor $F(\eta)$ (being a function of *one* variable only and which is due to the curvature), which must be added to the solution $2e^{ik_1D}/ik_1D$, which itself belongs to the plane problem ; the factor 2 represents the total reflexion by the infinitely conducting second medium ; (44) confirms the result first obtained by Watson (*l. c.*).

It is of interest to note that the variable η introduced above is closely related with the phase difference ϕ of two beams, one going straight to the receiver through the sphere, the other going along the surface. In fact for

small ϑ this phase difference is given by $\phi = \frac{\eta^3}{24}$, and thus the solution (44) in this respect shows a great analogy with other diffraction problems where also the field near the boundary of the optical shadow is expressible as a function of the corresponding phase difference.

From the expressions (43a) and (44) for the vector Π the normal component of the electric field can simply be calculated with the relations given in § 2.

The result (43 a) is plotted in fig. 7, where the curves

Fig. 7.

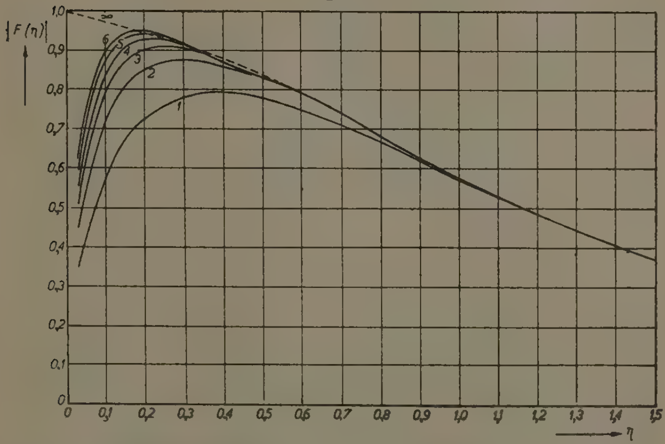

Modulus of the sum of the first few terms of F (η).

marked 1, 2, 3 . . . 6 represent approximations of the modulus of F(η) as a function of η calculated with 1 2, 3 . . . 6 terms respectively, and where due consideration has been given to the phases of the different terms of the series.

Moreover, referring to (42), where the transmitter was not yet lowered to the surface of the earth, this formula has been used to calculate the curve labelled $h=100$ m., $\sigma=\infty$, $\lambda=0{\cdot}7$ metre in fig. 8. As indicated in this figure it was constructed for a wave-length of 70 cm. and for a height of the transmitter above the earth of $h=b-a=$ 100 metre. As a comparison we give in the same figure the curve marked $h=0$ for the same wave-length and which was calculated from (44).

In calculating these curves, as for all following ones, the moment of the transmitter has been assumed to be such that, when placed on an infinitely conducting plane earth, would radiate 1 kw.

7 c. *The Characteristic Functions and Values for* $|k_2| = \infty$.

The results of § 6 become much simpler for the special case $|k_2| = \infty$. The coefficients $B_{n,j}$, and therefore

Fig. 8.

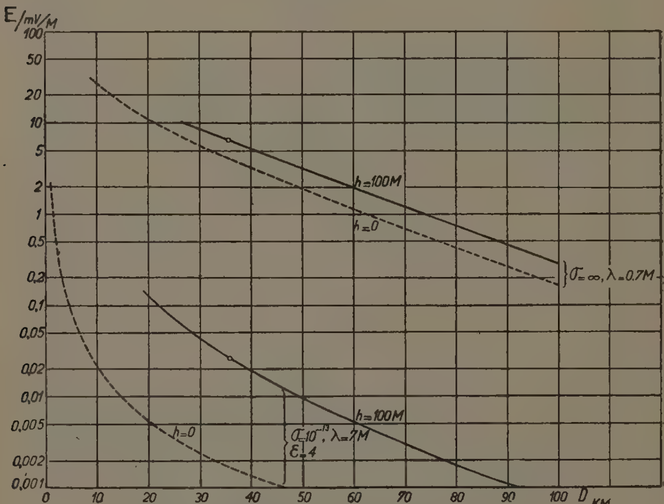

Influence of the height of the transmitter field on the for 1 kw. " radiated."

also the Characteristic Functions $\phi_{n,j}$, then vanish all for $r<a$. Moreover (28), defining the Characteristic Values $\lambda_{n,j}k_1$, then simplifies to

$$\left[\frac{d}{dz}\{z\zeta_n^{(1)}(z)\}\right]_{z=z_{n,j}=\lambda_{n,j}k_1a}=0, \quad . \quad . \quad (45)$$

whose roots, according to the definition of $\zeta_n^{(1)}(z)$, correspond to the zeros of the polynomials

$$e^{-iz}\frac{d}{dz}\left\{z^{n+1}\left(-\frac{1}{z}\frac{d}{dz}\right)^n\left(\frac{e^{iz}}{iz}\right)\right\}=0 ; \quad . \quad (46)$$

hence, remembering that $z\zeta_n^{(1)}(z)$ satisfies (19), the expression (30 a) can be reduced to

$$A_{n,j}^2 = \frac{(2n+1)z_{n,j}^2}{2\pi k_1{}^2 a^3\{\zeta_n^{(1)}(z_{n,j})\}^2\{n(n+1)-z_{n,j}^2\}},$$

and the series (31) for $b=a$ to

$$\Pi'_{\text{tot}} = \frac{i}{2k_1 a}\sum_{n=0}^{n=\infty}(2n+1)P_n(\cos\vartheta)\sum_{j=0}^{j=n}\frac{z_{n,j}}{\{n(n+1)-z_{n,j}^2\}} \times\left\{\frac{1}{k_1 a - z_{n,j}} - \frac{1}{k_1 a + z_{n,j}}\right\}. \quad (47)$$

This series corresponds to a point source $\cos(k_1 R)/(ik_1 R)$, representing stationary waves, while the series (32) corresponds to a point source $e^{ik_1 R}/(ik_1 R)$, representing diverging waves only. In order to transform (32) to a double series analogous to (47) we first write it as

$$\Pi_{\text{tot}} = \frac{i}{k_1 a}\sum_{n=0}^{n=\infty}(2n+1)P_n(\cos\vartheta).\left[\frac{\zeta_n^{(1)}(z)}{\frac{d}{dz}\{z\zeta_n^{(1)}(z)\}}\right]_{z=k_1 a} \quad . \quad . \quad . \quad (48)$$

Now it may be remarked that the definition of $\zeta_n^{(1)}z)$, as given in § 2, implies that $z^{n+1}e^{-iz}\zeta_n^{(1)}(z)$ is a polynomial of degree n, and that therefore the last factor of (48) can be written as a quotient of two polynomials of degree n and $n+1$ respectively. As the denominator is of higher degree than the numerator, this quotient can be split up in partial fractions, which, using the differential equation (19), can be given the form contained in the following series:

$$\Pi_{\text{tot}} = \frac{i}{k_1 a}\sum_{n=0}^{n=\infty}(2n+1)P_n(\cos\vartheta) \times\sum_{j=0}^{j=n}\frac{z_{n,j}}{\{n(n+1)-z_{n,j}^2\}}\,\frac{1}{(k_1 a - z_{n,j})}, \quad (49)$$

which consists of twice the first part of (47), corresponding to the diverging part of the stationary wave represented by this latter equation.

In order to consider (48) in more detail a discussion of the roots $z_{n,j}$ is necessary, to which we will now proceed.

Like in § 7 *b* we therefore have again to consider the roots of (37), but this time considered as a function of z, n being a positive integer. Therefore we now obtain for the equation determining the roots $z_{n,j}$ instead of (38)

$$i(n+\tfrac{1}{2})\int_{1}^{z_{n,j}/n} \sqrt{1-u^2}\,\frac{du}{u} = \pi(j+\tfrac{1}{4}), \quad (j=0, 1, \ldots, n), \quad (50)$$

where, as indicated, j goes from 0 to n, because in this way we cover all the $n+1$ roots of (46). For the same reason the summation over j in (47) and (49) extends also from 0 to n. It will be evident that all the roots of (50) are situated on the curve in the complex n/z plane given by

$$\mathrm{Re}\left\{\int_{1}^{z/n} \sqrt{1-u^2}\,\frac{du}{u}\right\} = 0, \quad . \quad . \quad . \quad (51)$$

instead of (39).

This curve is represented in fig. 6 by the drawn symmetrical curve E, on which therefore all the roots $z_{n,j}$ are situated approximately, whereas, as shown in § 7 *b*, the dotted curves P_1 and P_2 contained all the roots n_s of the equation (38). It is of considerable interest to observe that the curves E and P_1 have in $n/z=1$ a common point and a common tangent making an angle of $\pi/3$ with the real axis, as can be easily shown by comparing (39) and (51).

Further away from the point $n/z=1$ the curve E remains finite, whereas P_1 goes to infinity. In fact, by developing (39) for $|n/z| >> 1$ it can easily be shown that the curve P_1 is asymptotically given by

$$\rho = \tfrac{1}{2} e^{1+\phi\, tg\, \phi},$$

where ρ and ϕ are polar coordinates in the n/z plane.

A further consideration of (51) shows that the curve E cuts the imaginary axis in a point A (fig. 6) situated at $1{\cdot}509\ldots i = \alpha i$, say, where α is the real root of

$$\mathrm{cotgh}\left(\sqrt{1+\frac{1}{\alpha^2}}\right) = \sqrt{1+\frac{1}{\alpha^2}}$$

(see, *e. g.*, Jahnke-Emde, 'Funktionentafeln,' p. 31). It can further be shown that for n even there exist roots $z_{n,j} = z_{n,n/2}$ lying exactly on the imaginary axis corresponding to Characteristic Functions containing a purely aperiodic time function. The n/z values of these

"aperiodic" roots converge rapidly towards the value given above, as could be verified numerically by determining these roots exactly from (46) for small values of n; for these small values, however, it is better to consider $(n+\frac{1}{2})/z$ instead of n/z, according to (16 a). In fact, we obtained the following values:

$$2\tfrac{1}{2}/z_{2,1}=1{\cdot}566\,i,$$
$$4\tfrac{1}{2}/z_{4,2}=1{\cdot}526\,i,$$
$$6\tfrac{1}{2}/z_{6,3}=1{\cdot}517\,i,$$
$$8\tfrac{1}{2}/z_{8,4}=1{\cdot}514\,i,$$
$$\cdot\quad\cdot\quad\cdot\quad\cdot\quad\cdot\quad\cdot$$
$$\lim_{n\to\infty} n/z_{n,n/2}=1{\cdot}509\,i.$$

We also calculated the other roots for $n=1$, 2, 3, and 4 [13], and found

$$\begin{cases} z_{1,0}=0{\cdot}866-0{\cdot}500\,i, \\ z_{1,1}=-0{\cdot}866-0{\cdot}500\,i. \end{cases} \qquad \begin{cases} z_{2,0}=1{\cdot}808-0{\cdot}702\,i, \\ z_{2,1}=\phantom{-1{\cdot}80}0-1{\cdot}596\,i, \\ z_{2,2}=-1{\cdot}808-0{\cdot}702\,i. \end{cases}$$

$$\begin{cases} z_{3,0}=2{\cdot}758-0{\cdot}843\,i, \\ z_{3,1}=0{\cdot}871-2{\cdot}157\,i, \\ z_{3,2}=-0{\cdot}871-2{\cdot}157\,i, \\ z_{3,3}=-2{\cdot}758-0{\cdot}843\,i. \end{cases} \qquad \begin{cases} z_{4,0}=3{\cdot}715-0{\cdot}954\,i, \\ z_{4,1}=1{\cdot}752-2{\cdot}571\,i, \\ z_{4,2}=\phantom{-1{\cdot}75}0-2{\cdot}949\,i, \\ z_{4,3}=-1{\cdot}752-2{\cdot}571\,i, \\ z_{4,4}=-3{\cdot}715-0{\cdot}954\,i. \end{cases}$$

The $(n+\frac{1}{2})/z$ values of all these roots have also been marked with their n value in fig. 6. It is seen that even for these lowest values of n the roots lie already very near the universal E, which was derived for $n>>1$.

Returning to (50), using a similar procedure as in § 7 b, we obtain as a general expression for the roots near the real axis instead of (40)

$$z_{n,j}=n-\tau_j n^{1/3}, \qquad \ldots\ldots \qquad (52)$$

where, as in (40 a),

$$\tau_j=\tfrac{1}{2}\{3\pi(j+\tfrac{1}{4})\}^{2/3}e^{i\pi/3}. \qquad \ldots \qquad (52\,a)$$

Having thus obtained the values of the most important roots $z_{n,j}$, we are now in a position to apply this result to transform (49). We therefore invert in (49) the order

of summation of n and j and substitute the values of the roots $z_{n,j}$ as given by (52). Retaining the first order terms in n, (49) thus becomes

$$\Pi_{\text{tot}} \sim -\frac{i}{2k_1 a} \sum_j \frac{1}{\tau_j} \sum_{n=0}^{n=\infty} \frac{(2n+1)P_n(\cos \vartheta)}{n^{1/3}\{n-k_1 a-(k_1 a)^{1/3}\tau_j\}}. \tag{53}$$

As before, we can transform (53) to an integral over n with a path of integration L as in fig. 2 c, where now the only enclosed pole is

$$n_0 = k_1 a + (k_1 a)^{1/3}\tau_j,$$

so that, taking the residue of this single pole, (53) becomes

$$\Pi_{\text{tot}} \sim -\frac{\pi i}{k_1 a} \sum_j \frac{n_0^{2/3} P_{n_0-1/2}\{\cos(\pi-\vartheta)\}}{\tau_j \cos(n_0 \pi)},$$

and, with the approximation (12) for P_n, we are led again to the series (42), but for $b=a$.

This result means that the s'th term of (42) is the sum of the contributions of the Characteristic Functions $\phi_{n,s}$, where for fixed s the summation extends over all values of n from 0 to ∞—*e. g.*, the first and dominating term of (42) ($s=0$) is obtained by adding all Characteristic Functions $\phi_{n,0}$ which are just those which for fixed n have the smallest damping.

8. *Strongly Absorbing Sphere*

$$\left\{ \left| \frac{k_2^2}{(k_1 a)^{1/3} k_1 \sqrt{k_2^2-k_1^2}} \right| << 1 \right\}.$$

In order to obtain, as in § 7 b, the series of residues, but now for finite k_2, a knowledge of the most important poles, *i. e.*, those in the n/z plane nearest the real axis, is again necessary. In these poles again $N_{n-1/2}=0$, and according to the definition (6) and the approximation (37) we have for $|n/z|$ at least of the order unity

$$N_{n-1/2}(z, z') \sim -\frac{n}{z^2}\sqrt{\frac{z^2}{n^2}-1}\,.\,tg\left\{\frac{\pi}{4}+(n+\tfrac{1}{2})\int_1^{z/n}\sqrt{u^2-1}\,\frac{du}{u}\right\} - \frac{1}{z'}\frac{d}{dz'}\log\{z'\psi_n(z')\}, \tag{54}$$

where

$$z=k_1 a \text{ and } z'=k_2 a.$$

From (54) one can at once deduce the relation which must be satisfied by the zeros n_s:

$$i(n_s+\tfrac{1}{2})\int_1^{z/n_s}\sqrt{1-u^2}\,\frac{du}{u}=\pi(s+\tfrac{3}{4})$$

$$-\operatorname{arc}tg\left[\frac{z}{z'}\,\frac{\sqrt{1-\frac{n_s^2}{z^2}}}{\frac{d}{dz'}\log\{z'\psi_n(z')\}}\right], \qquad (55)$$

$$(s=0,\,1,\,2,\,\ldots)$$

where

$$0<\mathrm{Re}\{\operatorname{arc}tg[\quad]\}<\pi.$$

Now an approximation, derived in the same way as (35), and especially suited when $z'=k_2a$ has a great imaginary part, becomes

$$\frac{d}{dz'}\log\{z'\psi_n(z')\}\sim\frac{d}{dz'}\log\{z'\,.\,\tfrac{1}{2}\zeta_n^{(2)}(z')\}$$

$$\simeq\frac{d}{dz'}\log\{z'\zeta_z^{(2)}(z')\}\approxeq -i\sqrt{1-\frac{k_1{}^2}{k_2{}^2}}, \qquad (56)$$

as the zeros n_s of $N_{n-1/2}$ appear to lie near $z=n$. For strong absorption $|k_2|$ and $|k_1|$ are of the same order of magnitude, and for the zeros near $n/z=1$ the argument of arc tg in (55) is very small, and hence the function arc tg itself, so that as a first approximation this term may be neglected in (55). Thus (55) becomes nearly equal to (38), *i. e.*, the zeros near $n/z=1$ are again on the curve E of fig. 6; but a comparison of (55) and (38) shows that the zeros are now interspaced between the zeros belonging to the case $|k_2|=\infty$. This fact is especially clear when one considers the zeros in the immediate neighbourhood of $n/z=1$, and which are of primary numerical importance. Similarly to (40) and (40 a) these zeros are given by

$$n_s=z+\tau_s' z^{1/3}, \qquad (57)$$

with

$$\tau_s'=\tfrac{1}{2}\{3\pi(s+\tfrac{3}{4})\}^{2/3}e^{i\pi/3}. \qquad (57\,a)$$

As in § 7 b, we again retain in (15) the residues at these poles. In order further to find $\dfrac{\partial N}{\partial n}$ for $n=n_s$

we make use of (54), and derive from it, remembering (57) :

$$\mathrm{N} \sim -\frac{\sqrt{-2\tau'}}{z^{1/3}} \cdot tg\left\{\frac{\pi}{4} + \frac{(-2\tau')^{3/2}}{3}\right\} - \frac{1}{z'}\frac{d}{dz'}\log\{z'\psi_z(z')\}.$$

From this expression we derive $\frac{\partial \mathrm{N}}{\partial n}$ for $n = n_s$, making use of the fact that $\mathrm{N}_{n_s - 1/2} = 0$; thus one obtains three terms, of which one dominates for $|z| >> 1$, so that we are left with

$$\frac{\partial \mathrm{N}}{\partial n} \sim \frac{z}{z'^2}\left[\frac{d}{dz'}\log\{z'\psi_z(z')\}\right]^2.$$

Substitution in (15) gives, after reduction, whereby (57) is used, for our final expression :

$$\Pi_{\mathrm{abs}} \sim 2\frac{e^{iz\vartheta}}{iz\vartheta} \cdot \frac{ik_2^4}{k_1^3(k_2^2 - k_1^2)\mathrm{D}}$$

$$\cdot 2\pi e^{-i\pi/4}\eta^{3/2}\sum_s \frac{\zeta^{(1)}_{z+\tau_s' z^{1/3}}(k_1 b)}{\zeta^{(1)}_{z+\tau_s' z^{1/3}}(k_1 a)} e^{i(2\pi)^{1/3}\tau_s'\eta}. \qquad (58)$$

$$(z = k_1 a)$$

This series shows a great analogy with (42), as $\eta = \mathrm{D}/(a^{2/3}\lambda^{1/3})$ has the same meaning as before.

If we first limit ourselves to a consideration of the case $b = a$, we observe that (58) consists of *three* factors :

(1) the first factor

$$2\frac{e^{iz\vartheta}}{iz\vartheta} = 2\frac{e^{ik_1\mathrm{D}}}{ik_1\mathrm{D}},$$

corresponding to the plane problem and for $|k_2| = \infty$;

(2) the second factor

$$\frac{ik_2^4}{k_1^3(k_2^2 - k_1^2)\mathrm{D}},$$

representing the effect of the absorption already found before for the plane problem ; for, with the primary field as defined in this paper, the plane problem was in a former paper [14] already reduced to the exact result

$$\Pi_{\mathrm{abs},\, a=\infty} = \frac{2k_2^3 i}{(k_2^4 - k_1^4)}\int_{k_1/h'}^{k_2/h'} \frac{e^{ih'\mathrm{D}u}}{\mathrm{D}} \cdot d\left(\frac{1}{\sqrt{u^2 - 1}}\right),$$

$$\left(\frac{1}{h'^2} = \frac{1}{k_1^2} + \frac{1}{k_2^2}\right)$$

and a first approximation for great $k_1\mathrm{D}$ is obtained from this expression by integrating it once by parts and

neglecting the contribution due to the upper limit of integration. We thus obtain exactly the product of the first two factors of (58).

(3) The third factor of (58) we call $G(\eta)$, and, according to the preceding, this factor represents the effect of the curvature of the earth.

Hence, when the transmitter is placed on the surface of the sphere, *i. e.*, for $b=a$, we can write (58) in the elegant form

$$\frac{\Pi_{\text{abs}, a \neq \infty}}{\Pi_{\text{abs}, a=\infty}} \sim G(\eta) = 2\pi e^{-i\pi/4}\eta^{3/2}\sum_s e^{i(2\pi)^{1/3}\tau_s'\eta}. \quad . \quad (59)$$

Fig. 9.

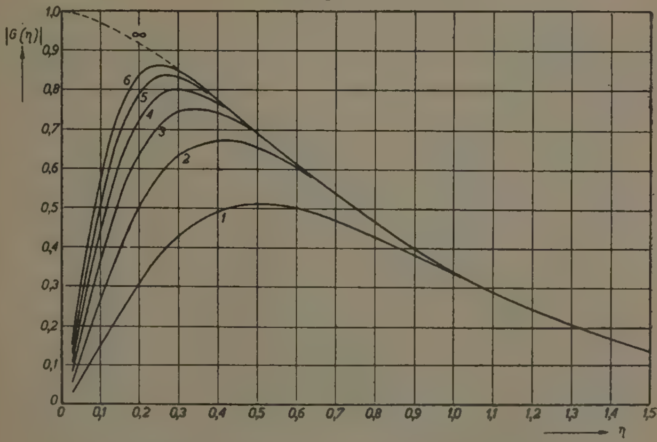

Modulus of the sum of the first few terms of $G(\eta)$.

Thus the functions $F(\eta)$ (of § 7 *b*) and $G(\eta)$ (as given by (59)) give the correction factors due to the curvature of the earth, $F(\eta)$ being valid for $\sigma_2=\infty$ and $G(\eta)$ for strong absorption.

In fig. 9 we have represented by the curves 1, 2, 3 . . . 6 the approximations one finds for $|G(\eta)|$ if 1, 2 . . . 6 terms in (59) are retained; and thus fig. 9 for $G(\eta)$ is analogous to fig. 7 for $F(\eta)$. As our final result we give in fig. 10 the values of the two correction factors $|F(\eta)|$ and $|G(\eta)|$ applicable to the case $\sigma_2=\infty$ and great absorption respectively.

In general, and especially for short waves, not too great values of η are of primary importance: *e. g.*, for

$\lambda=7$ m., D$=50$ km., we have $\eta=0{\cdot}76$. Hence practical values of η are of the order unity, and in this range of values of η the difference of $|F(\eta)|$ and $|G(\eta)|$ is not very great. In practical cases the actual correction factor will be found between these two limiting curves; but, *e. g.*, for $\lambda=7$ m. and sea-water the actual values are already very near the curve $|G(\eta)|$. This results from the fact that then the argument of the arc *tg* function (55) is already very small, as the factor

$$\frac{k_2^{\,2}}{(k_1a)^{1/3}k_1\sqrt{k_2^{\,2}-k_1^{\,2}}}$$

Fig. 10.

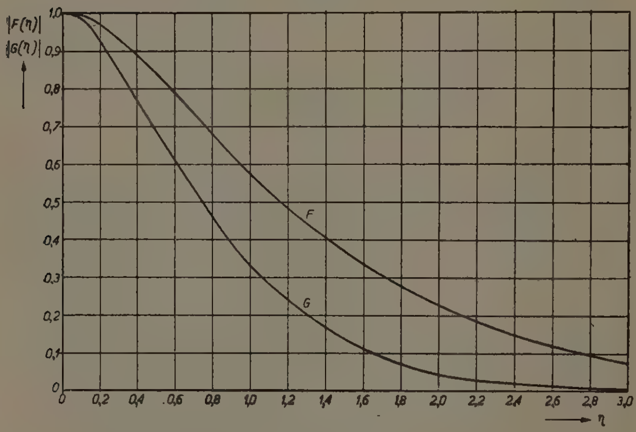

Correction factors for the curvature of the earth.

has a small modulus, and the first term of the arc *tg* development in (55) suffices for the approximation (59).

In this way the curves of fig. 11 (for $\lambda=7$ m.) were calculated. In this figure the drawn curves represent the electric field of an emitter radiating 1 kw. (for definition see § 7 *b*) for $\sigma_2=\infty$, for $\sigma_2=10^{-11}$ and $\epsilon_2=80$ (sea-water), and for $\sigma_2=10^{-13}$, $\epsilon_2=4$ (dry soil) respectively. The dotted lines represent the corresponding fields one would obtain for the same electrical constants of the earth, but for a plane surface. This figure shows very clearly that for $\lambda=7$ m. the influence of the finite conductivity of the soil dominates by far the influence of

the curvature of the earth for the distances considered. This is a general result for short waves.

Finally, it was possible with the aid of (58) to calculate the field of an emitter placed at a height $h=b-a$ above the ground. This was done for $\lambda=7$ m., $h=100$ m., and $\sigma_2=10^{-13}$, $\epsilon_2=4$. The result is given by the two lower curves of fig. 8, where the upper curves gave the result for $\lambda=0{\cdot}7$ m. and $\sigma_2=\infty$. In both cases no apparent effect is seen to occur at the optical horizon of the transmitter, this being situated at D=35·7 km. A further

Fig. 11.

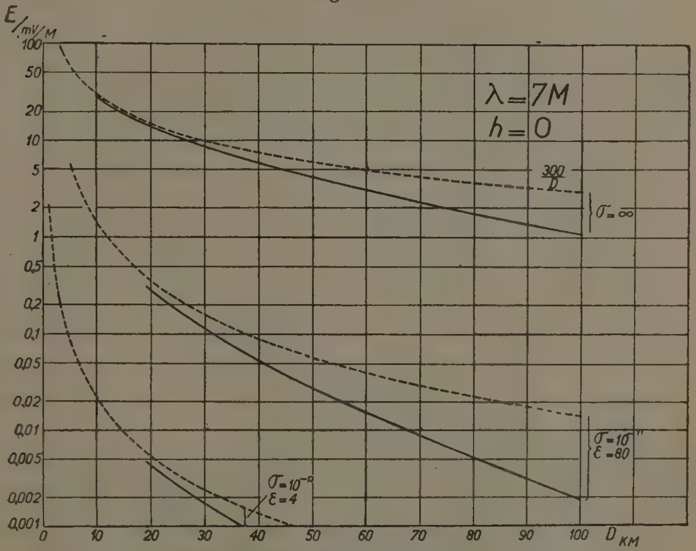

Influence of the conductivity of the soil on the field for 1 kw. " radiated."

investigation showed, however, that for much shorter waves (of the order of 1 mm.) a distinct shadow effect makes its appearance (*cf.* Part II.).

Within a short time we hope to publish Part II. of this paper.

Summary.

The problem of diffraction of electromagnetic waves radiating from a point source outside an absorbing sphere

is treated by several methods. In Part I. an exposition of the method of Watson is given. This method consists in a transformation of the infinite series of spherical harmonics for the Hertzian vector into another series, which is much more rapidly converging for wave-lengths small compared with the dimensions of the sphere. Extensive numerical results are given for the case that the point source is a transmitter of radio waves, which may be situated on the surface of the in general finitely conducting sphere as well as at a small height above it. The former method is compared with that of development in characteristic functions, which is analogous to methods used in string problems and wave mechanics.

In Part II. the original harmonic series for the Hertzian vector is split up into an infinite sum of other harmonic series. Each of them may be considered as the effect of waves (degenerating into rays for extremely high frequencies) which are once or more times reflected at the inner surface of the sphere. These series may be approximated by Kelvin's principle of stationary phase as extended by Debye and Brillouin; this method gives appropriate approximations for the field of a radio transmitter in the region above its optical horizon, whereas, when the point source is at infinity it yields and extends Airy's well-known results for the intensity of the light in a rainbow.

References.

(1) Lord Rayleigh, Phil. Mag. (4) xli. pp. 107, 274, 447 (1871); (5) xii. p. 81 (1881); (5) xlvii. p. 375 (1899).
(2) P. Debye, *Ann. Physik*, xxx. p. 57 (1909).
(3) Lord Rayleigh, Phil. Trans. Roy. Soc. cciii. A, p. 87 (1904); Sci. Pap. V., no. 292.
(4) A. E. H. Love, Phil. Trans. Roy. Soc. ccxv. A, pp. 105–131 (1915).
(5) G. N. Watson, Proc. Roy. Soc. London, A, xcv. p. 83 (1918), and A, xcv. p. 546 (1919).
(6) Balth. van der Pol, Phil. Mag. (6), xxxviii. p. 365 (1919).
(7) O. Laporte, *Ann. Physik*, lxx. p. 595 (1923).
(8) T. L. Eckersley, Proc. Roy. Soc. London, A, cxxxvi. p. 499 (1932).
(9) P. S. Epstein, Proc. Nat. Acad. U.S.A. xxi. p. 62 (1935), nr. 1.
(10) Balth. van der Pol, *Physica*, ii. p. 843 (1935).
(11) A. Sommerfeld, *Jahresbericht d. deutschen Mathematiker-Vereinigung*, xxi. p. 309 (1912).
(12) J. W. Nicholson, Phil. Mag. xxi. p. 64 (1911).
(13) Compare: J. J. Thomson, 'Recent Researches in Electricity and Magnetism,' p. 368 etc.
(14) Balth. van der Pol, *Z. Hochfrequenztechn. u. Elektroakust.* xxxvii. p. 152 (1931).

Eindhoven.
26th October, 1936.

XIV. *The Behaviour of Electrons in Bromine.* *By* J. E. BAILEY, *B.Sc., Demonstrator in Physics, Department of Physics, University of Sydney*, R. E. B. MAKINSON, *B.Sc., and* J. M. SOMERVILLE, *B.Sc.**

Foreword.

THE success of the method developed in Sydney for the study of the behaviour of electrons in chlorine †, in which method are studied, mixtures of chlorine with other gases whose relevant electronic properties are well known, has led to an investigation of bromine along similar lines. This method was used because the rapidity with which pure bromine attacks and is absorbed by the diffusion instrument requires rapidity in observation, and the time occupied in taking a necessary set of readings does not exceed ten minutes.

Fig. 1.

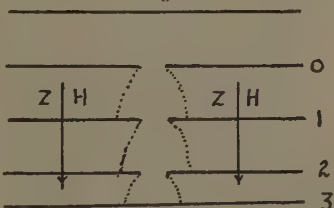

Apparatus.

The diffusion instrument with three successive slits, described previously ‡, was used and is similar to that by means of which chlorine was investigated. Its electrodes are in elevation as illustrated in fig. 2.

Evacuation was produced by means of a mercury pump, backed by a Pfeiffer rotary oil pump, and separated from the apparatus by a liquid-air trap. A spiral Bourdon gauge, similar to those previously described, was used for measuring the pressure of the gas mixture in a small auxiliary volume which was then placed in communication with the diffusion instrument.

* Communicated by Prof. V. A. Bailey, M.A., D.Phil.
† V. A. Bailey and R. H. Healey, Phil. Mag. xix. p. 725 (1935).
‡ V. A. Bailey and J. D. McGee, Phil. Mag. vi. p. 1073 (1928).

The bromine was obtained from Professor J. C. Earl of the Department of Organic Chemistry, University of Sydney, and with the aid of liquid air and CO_2—snow cum ether traps a middle third of a middle third was passed into a storage flask containing P_2O_5; some of this bromine was in liquid form in a side tube attached to the storage flask.

The helium used for making mixtures was obtained from a cylinder supplied by the Matheson Co., and was

Fig. 2.

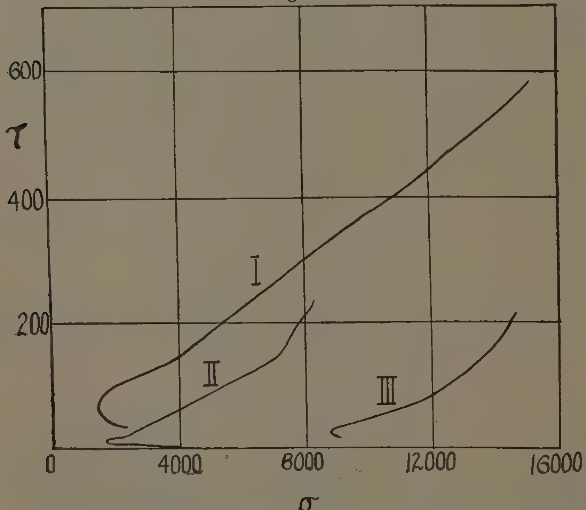

Curve I corresponds to 20 per cent. Br_2 + 80 per cent. CO_2.
Curve II corresponds to 20 per cent. Br_2 + 80 per cent. He.
Curve III corresponds to 100 per cent. Br_2.

purified over charcoal at liquid-air temperature. Carbon dioxide was prepared by heating a tube containing sodium bicarbonate, and was freed from air and moisture by the use of liquid air and CO_2—snow cum ether traps.

The mixtures of bromine with helium and CO_2 were made with the aid of the spiral Bourdon gauge and stored in litre flasks. All the normal observations on mixtures were made within two months after preparation of the

latter, and the constancy of each mixture was tested near the end by repeating some of the early observations.

At all times during the experiments there was an ample emission of photo-electrons from the silver cathode in the instrument under the influence of the ultra-violet light.

Method of Investigation.

In the following description the notation of Table I. is used which is the same as that of the paper on chlorine.

Table I.

p = Pressure of gas, in mm. of mercury.

Z = Electric intensity, in volts/cm.

c = The distance between successive slits of the instrument, namely, 4 cm.

S_1 = Fraction of the stream in the first diffusion chamber which passes out of the chamber, also called the distribution ratio.

S_2 = Corresponding fraction for the second diffusion chamber.

R = The distribution ratio with negative ions in either chamber.

H_0 = The magnetic intensity required to make S_2 (and S_1) equal to R.

k = Mean energy of agitation of an electron in terms of the mean energy of agitation of a molecule at 15° C.

W = The drift velocity of an electron in the direction of Z, in cm./sec.

α = The probability of attachment of an electron to a molecule per unit length of its motion in the direction of Z.

u = The mean velocity of agitation of an electron, in cm./sec.

L = The mean free path of an electron in the gas at 1 mm. pressure, in cm.

λ = The mean proportion of its own energy lost by an electron at a collision with a gas molecule.

h = The probability of an electron becoming attached to the molecule with which it collides.

$\omega = i_0/i_3$.

f_a = The proportion in the mixture of the gas A of known electronic properties.

g_a = The proportion in the mixture of the gas whose electronic properties have to be determined.

$q_a = \rho_a L_a^{-1}$, where $\rho_a = g_a^{-1} - 1$.

$r_a = \lambda_a q_a$.

$s = gk^{-1}(1-k^{-1})^{-\frac{1}{2}}\sigma$.

$t = gk^{-1}(1-k^{-1})^{\frac{1}{2}}\tau$.

$\sigma = 1{\cdot}25\, g^{-1} H_0/p$.

$\tau = 231\, g^{-1} Z^2/pH_0$.

$x = k(1-k^{-1})\,(q_a - q_b)$.

$y = k(1-k^{-1})^{-\frac{1}{2}}(r_a - r_b)$.

Preliminary measurements of H_0 with Z and p known were made in the following mixtures:—10 per cent. bromine and 90 per cent. CO_2; 20 per cent. bromine and 80 per cent. CO_2; 20 per cent. bromine and 80 per cent. helium; 60 per cent. bromine and 40 per cent. helium. It was found that with the method of calculation employed, the most sharply determinate results were obtained from the pair of mixtures of 20 per cent. bromine in CO_2 and 20 per cent. bromine in He, and most of the readings of H_0 were made with these.

The magnitude of H_0 for a given value of Z/p in any gas mixture was found by adjusting the vertical magnetic field until $\omega = i_0/i_3$ was equal to $R^2/(1-R)$ (the value of

Fig. 3.

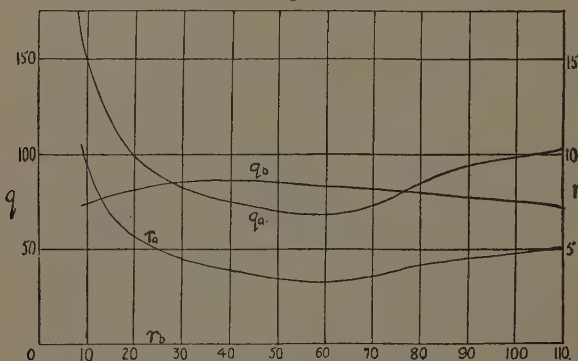

q_a, r_a correspond to 80 per cent. CO_2.
q_b, r_b correspond to 80 per cent. He.

i_0/i_3 for negative ions) which is a known function of Z/c*. The value of H_0 could be found with much precision, since i_0 and i_3 were approximately equal under the conditions of the experiment, and a small change in the magnetic field greatly affected their relative values.

From the experimental values of H_0 in terms of Z and p the curves of fig. 2 were plotted showing σ versus τ for each mixture.

The values of q and r in terms of k for the gases He and CO_2 were plotted as shown in fig. 3, and the following

* V. A. Bailey and W. E. Duncanson, *loc. cit.*

curves were then determined by means of the theory and formulæ of the paper on chlorine * :

For each mixture, k versus Z/p.

For bromine, L, λ, and h versus u, k, α/p, and W versus Z/p.

The method of calculation was briefly as follows :

From the theory *, for a pair of mixtures 1 and 2, we have

$$x=\sigma_1-\sigma_2$$

$$y=\tau_1-\tau_2.$$

By means of the known (x, y) and (k, y) curves shown in figs. 4 and 5 respectively (which depend only on the properties and proportions of CO_2 and He) these equations were solved graphically for k in terms of Z/p for each mixture †. The values of L and λ for bromine were then determined by means of the following formulæ ‡ :

$$L_{Br}=\{k^{-1}(1-k^{-1})^{-\frac{1}{2}}\sigma-q^a\}^{-1},$$

$$\lambda_{Br}=\{k^{-1}(1-k^{-1})^{\frac{1}{2}}\tau-r_a\}.L_{Br}.$$

As a check on the results obtained in this way for bromine some observations were also made of H_0 in pure bromine for different values of Z and p, these being made as rapidly as possible. In general the observations were completed within five minutes of the admission of the gas. Using these values of H_0 and the results for k and Z/p mentioned above from the mixtures 20 per cent. bromine in CO_2 and 20 per cent. bromine in helium, the value of λ in bromine was determined by means of the formula

$$\lambda=186(Z/H_0)^2.(1-k^{-1})^{\frac{1}{2}}$$

and compared with the value given by the diagram in fig. 8.

For example, it was found from the two mixtures that the value $k=77{\cdot}5$ in bromine corresponds to the values $Z/p=18{\cdot}5$ and $\lambda=1{\cdot}08$ per cent. The observations of

* V. A. Bailey and R. H. Healey, *loc. cit.*

† V. A. Bailey and R. H. Healey, *loc. cit.*

‡ (With the lower values of Z/p in the mixture of 20 per cent. Br_2 and 80 per cent. He it was not possible to produce sufficiently strong magnetic fields to determine the values of τ_2 accurately. However, low values of k were determined from observations on 20 per cent. Br_2 and 80 per cent. CO_2 combined with observations made on pure bromine.)

H_0 in pure bromine with $Z=5\cdot37$ and $p=0\cdot290$ mm., that is, $Z/p=18\cdot5$ gave $H_0/Z=130$ and thus $\lambda=1\cdot10$ per cent. This agrees well with the value $\lambda=1\cdot08$ per cent. obtained solely from the mixtures.

Also by regarding pure bromine as a mixture of 100 per cent. Br_2 and 0 per cent. CO_2 or He, and combining its data respectively with those of 20 per cent. Br_2 in He and

Fig. 4.

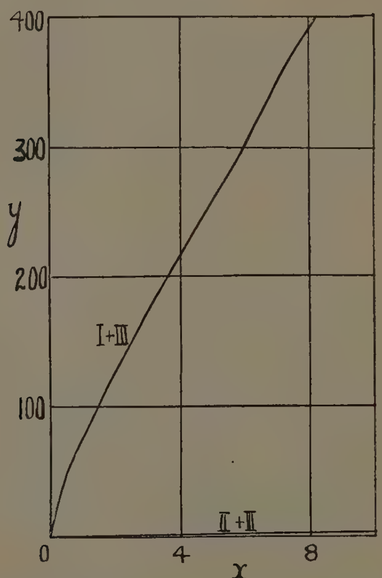

Curve I+III corresponds to mixtures 1 and 3.
Curve II+III corresponds to mixtures 2 and 3.

20 per cent. Br_2 in CO_2, additional points on the $L-u$ and $\lambda-u$ curves were obtained.

In determining h for bromine in terms of u it was found convenient to measure S_1 and S_2 for a mixture in the presence of a vertical magnetic field H less than H_0. In these circumstances the following formulæ are true :

$$\alpha=0\cdot575\{\log_{10}R(Z\sigma/kc)-\log_{10}a\}$$

where

$$a = S_1(R - S_2)/(R - S_1)$$

and

$$(\sigma - 1)/(k - 1) = (H/H_0)^2,$$

and so it follows that the value of h in pure bromine is given by the formula

$$h_{Br} = (8 \cdot 70/g)(\alpha/p)(Z/H_0)(1 - k^{-1})^{\frac{1}{2}} L_{Br}.$$

The values of α/p in this formula were determined by

Fig. 5.

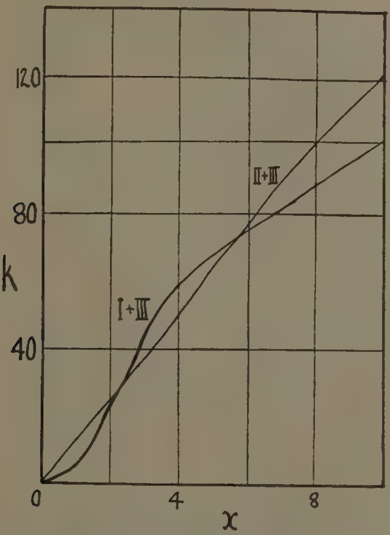

Curve I+III corresponds to mixtures 1 and 3.
Curve II+III corresponds to mixtures 2 and 3.

means of observations made with a mixture of 20 per cent. Br_2 and 80 per cent. CO_2.

Finally, the values of W, k, and α/p for bromine in terms of Z/p were obtained by means of the following formulæ :

$$W = 0 \cdot 64 u \lambda^{\frac{1}{2}},$$

$$k = 0 \cdot 716\, u^2 \times 10^{-14},$$

$$\alpha/p = 1 \cdot 57 h/L\lambda^{\frac{1}{2}},$$

$$Z/p = 4 \cdot 4 \times 10^{-16} u^2 \lambda^{\frac{1}{2}}/L.$$

Experimental Results.

The three principal mixtures studied were the following:

Mixture 1 .... 20 per cent. Br_2 in CO_2.
Mixture 2 .... 20 per cent. Br_2 in He.
Mixture 3* .... 100 per cent. Br_2.

Fig. 6.

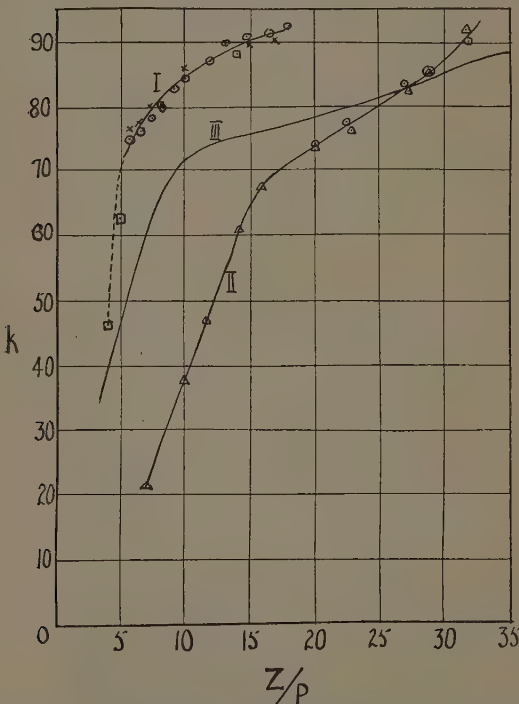

Curve I corresponds to 20 per cent. Br_2+80 per cent. He.
Curve II corresponds to 20 per cent. Br_2+80 per cent. CO_2.
Curve III corresponds to 100 per cent. Br_2.

The method of Bailey and Healey † was applied to them by means of the curves in figs. 2, 3, 4, and 5, and

* This designation of pure Br_2 as a mixture is adopted for the sake of convenience in describing the method for determining k.

† V. A. Bailey and R. H. Healey, *loc. cit.*

combining the observations for these three mixtures in pairs.

In all the experiments free electrons were present in sufficiently large numbers to cause marked variations of the distribution ratios with variations of the applied magnetic field. It will be noticed from the curves in fig. 6, that the values obtained by means of two and often

Fig. 7.

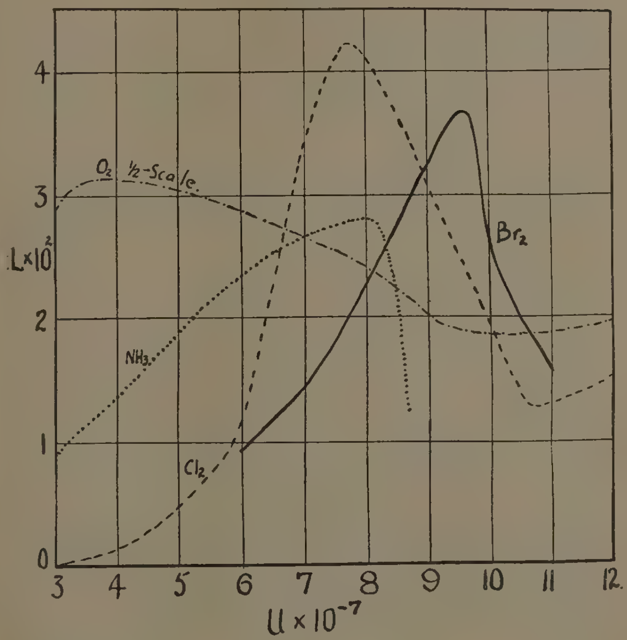

three different methods * for any given value of u are in good agreement with one another, which may be taken as a confirmation of the reliability of the methods used.

For electrons in bromine the values so calculated of L, λ, and h in terms of u are represented by curves in figs. 7, 8, and 9, and the values of k, W, and α/p in terms of Z/p

* As indicated by crosses, triangles, squares, and circles.

are represented by curves in figs. 10 and 11. For comparison the corresponding curves for chlorine are shown dotted.

The Variations of λ, L, *and* h *with* u *in Bromine.*

For comparison with the $\lambda - u$ curve, the optical absorption coefficient * μ for bromine is shown plotted against

Fig. 8.

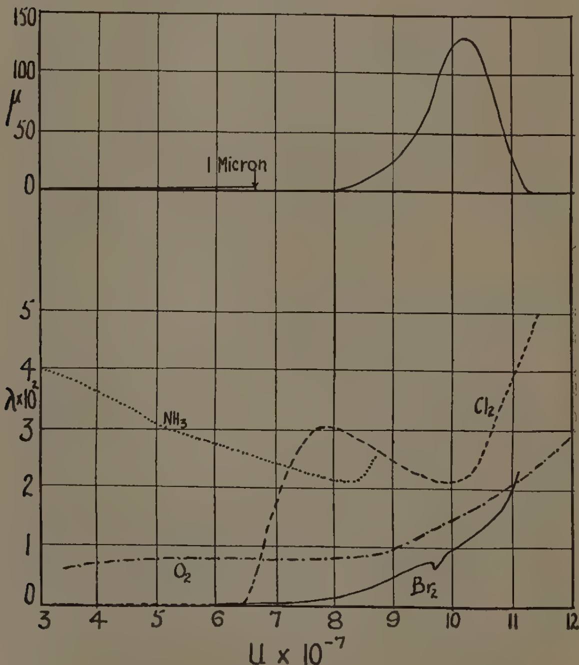

the velocity u of an electron which has the same energy as a light quantum of the frequency at which the absorption was measured.

It is seen that λ is very small when u is less than

* 'International Critical Tables,' vol. 5.

7×10^7 cm. sec.$^{-1}$ and rises sharply as the velocities corresponding to notable absorption are reached. It is interesting to note that these results were predicted in

Fig. 9.

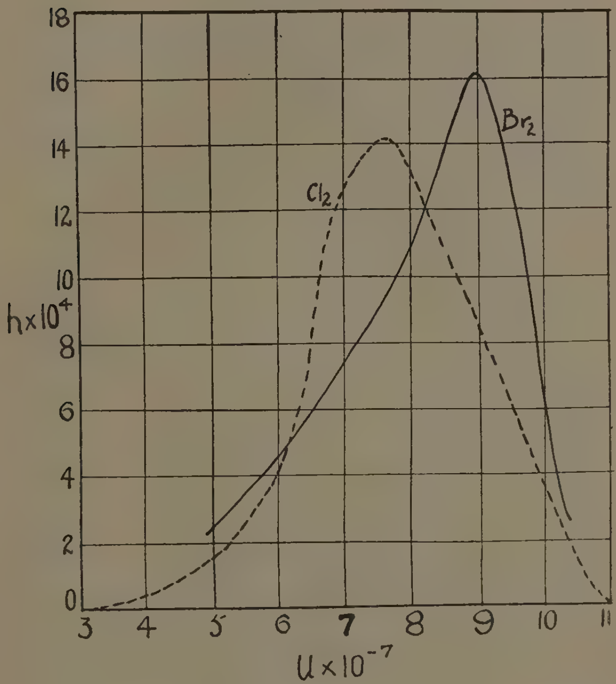

1932 by Professor Bailey *, as is shown by the following quotation :—

" . . . . since, according to Burmeister, Cl_2 and Br_2 are transparent to wave-lengths greater than 1μ, we may expect low values of λ for velocities less than $6 \cdot 6 \times 10^7$. The fact that these gases are coloured makes it probable that large values of λ will be found for velocities between 7×10^7 and 12×10^7."

* V. A. Bailey, Phil. Mag. xiii. p. 998 (1932).

It is also interesting to note that in all sets of readings taken a slight dip in the $\lambda - u$ curve was indicated at approximately $u = 9{\cdot}7$, as is shown in fig. 8. This may perhaps be correlated with the maximum value of the

Fig. 10.

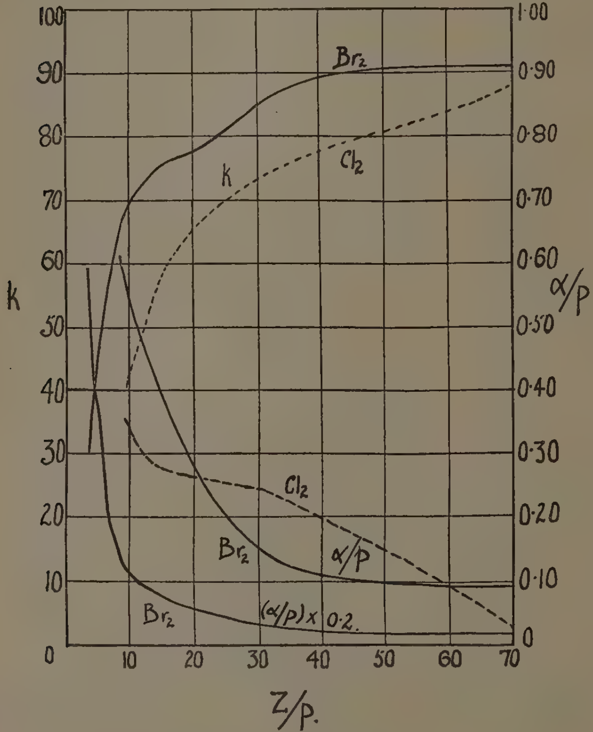

optical absorption coefficient which occurs at $u = 10{\cdot}3$ for bromine.

It is noteworthy that the only critical potentials which have been observed for bromine correspond to much higher values of u than occurred in these experiments.

The value of L in bromine is seen from fig. 7 to vary considerably with u, rising to a prominent maximum at

$u=9{\cdot}6$. The $h-u$ curve of fig. 9 is similar in shape to the $L-u$ curve, supporting the conclusion that the probability of attachment increases as the electron penetrates further into the molecule.

In conclusion, we desire to thank Professor V. A. Bailey of this University for his help and advice during the course of these experiments, and to thank the Colonial Sugar Refining Co. Ltd., and the Commonwealth Oxygen and

Fig. 11.

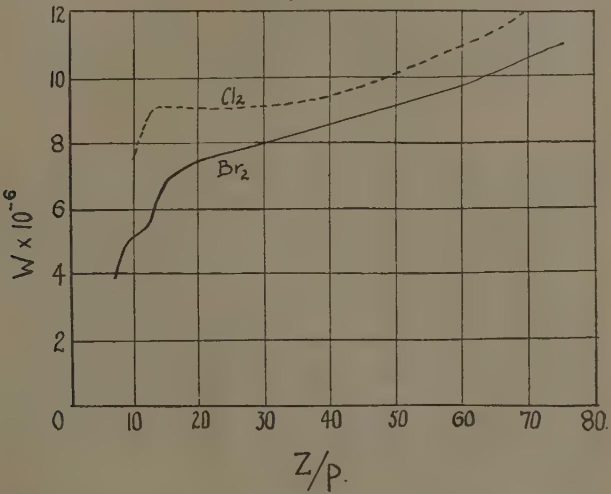

Accessories Co. Ltd., for supplying without cost carbon-dioxide snow and liquid air respectively.

Summary.

The methods developed by Bailey and Healey for the study of the motion of electrons in chlorine have been applied to bromine. The values in bromine of L the mean free path of an electron in the gas at 1 mm. pressure, λ the mean proportion of its own energy lost by an electron at a collision with a gas molecule, and h the probability of an electron becoming attached to the molecule with which it collides, are deduced and represented in terms of the velocity u of the electron, by means of curves. The

following quantities for electrons in bromine are also deduced and represented in terms of Z/p by means of curves: W the drift velocity of an electron in the direction of the electric force Z, k the mean energy of agitation of an electron in terms of the mean energy of agitation of a molecule at 15° C., α/p the probability of attachment of an electron per unit length in the direction of the electric force with the gas at 1 mm. pressure.

XV. *The Lα-Lines of some Nickel Alloys.* By F. C. Chalklin, *D.Sc., Lecturer in Physics, and* S. P. Hillson, *B.Sc., University College, London* *.

Introduction.

MANY researches have been devoted to the study of the effect of chemical combination on the hard X-ray emission lines and absorption edges of the constituent elements. In some cases shifts of several electron-volts have been found for the former, whilst some absorption edges have been found to move by more than 10 volts †. Much less work has been done on the effects produced by the alloying of metals. It is proposed to study this problem for some emission lines in the soft X-ray region. As our first problem we have chosen the study of the Lα-line of nickel in Cu–Ni alloys and in the magnetic alloys Radiometal and Mumetal. For such comparatively short wave-lengths (14·55 Å.) our apparatus does not determine the energy levels with great accuracy, but we have chosen the problem because of its special interest.

It is advantageous that Cu–Ni alloys form a continuous series of solid solutions. Further, for solid nickel, $M_{IV,V}$, the initial level of Lα has a deficiency of 0·6 electrons per atom, and is the source of the ferromagnetism of the metal. The level is at the energy surface of the atom and is overlapped by the valence band (N_I). Addition of copper diminishes the atomic moment of the nickel owing to the filling of the $M_{IV,V}$ level by

* Communicated by Prof. E. N. da Andrade, F.R.S.

† See Lindh, "Röntgenspektroskopie," *Handbuch der Experimentalphysik*, xxiv. pt. 2, pp. 281–323.

N_I electrons from the copper. This process is completed when the atomic percentage of copper reaches 60 *.

Experimental Details.

The experiments were carried out with a plane grating vacuum spectrograph, which has already been described †. A Siegbahn $\frac{1800}{3}$ lines/mm. grating was used at a grazing angle of 32′ and with a collimating slit of width 0·03 mm. The dispersion near Ni Lα was 1·40 Å./mm. The measurements were made with the first order spectrum. The specimens, in sheet form, were soldered to a water-cooled copper anticathode block. The bombarding voltage was approximately 5000.

The following specimens were used ‡ :—

(1) Commercial nickel; (2) commercial copper; (3) alloy, 60 per cent. Ni, 40 per cent. Cu; (4) alloy, 44–45 per cent. Ni, 56–55 per cent. Cu (Ferry); (5) Radiometal, 48 per cent. Ni, 50 per cent. Fe, 2 per cent. Cu; (6) Mumetal, 76 per cent. Ni, 17 per cent. Fe, 5 per cent. Cu, 1·5 per cent. Cr. §.

To remove the surface layer, the surfaces were heavily etched—in the earlier experiments with nitric acid. In the later experiments on Ni, Cu, and the Ni–Cu alloys we etched with 50 per cent. HNO_3+25 per cent. acetic acid+25 per cent. water, as this mixture showed less tendency to oxidize than HNO_3 of any concentration.

It has been shown ‖ that the value of the $M_{IV,V}$ level of a ferromagnetic element does not depend on its temperature or whether the element is above or below its Curie point. Nevertheless, we have usually kept the temperature low. We have made a thermoelectric test of the temperature of the water-cooled anticathode block under running conditions. A specimen value of 0·5 cm. has been obtained for the bombarded area

* See Mott, Proc. Phys. Soc. xlvii. p. 571 (1935).

† F. C. and L. P. Chalklin, Phil. Mag. xvi. p. 363 (1933).

‡ We thank the Mond Nickel Co., Ltd. for the Ferry and the 60/40 Ni–Cu alloy, and the Telegraph Construction and Maintenance Co., Ltd., for the Radiometal and Mumetal.

§ The percentages given for the alloys are by weight.

‖ M. Privault, *Annales de Phys.* v. p. 280 (1936); and F. C. Chalklin, Proc. Roy. Soc. clv. p. 366 (1936).

of the anticathode. The latter test was made by covering the surface with a powder, which, conducting poorly to the metal block, showed the bombarded area as an incandescent patch. For more than half our experiments we estimate the surface temperature of the anticathode to be below 250° C.

Results.

As reference line for our measurements we employ the sharp Mα-line of tungsten, which arises as a result

Fig. 1.

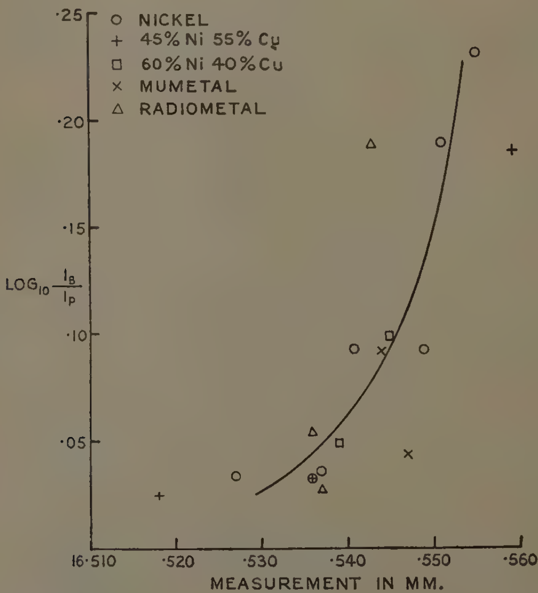

of filament sputtering. The measurement of the Lα-line, made on seven exposures with Ni anticathodes, was found to depend on its intensity. We have therefore plotted (fig. 1) the measurements against the line blackenings, which we have taken as $\log_{10} I_B/I_P$—where I_B and I_P are the microphotometer deflexions for the background and the peak of the lines. The microphotometer response had been found by test to be linear.

The differences between the alloy measures (also plotted in fig. 1) and the measures for the same blackening on the curve drawn through the nickel points are listed in the table.

The mean difference for the five Cu–Ni alloy plates is seen to be zero. The value of Lα for each plate is obtained by taking the mean of four sets of microscope readings. Considering these sets for all the nickel and alloy plates, we calculate the standard error of measurement of the mean value for a plate as $\pm 0{\cdot}003$ mm.

Anticathode.	Plate number.	Measurement—Nickel value.
45%Ni, 55% Cu	H. 6	+0·007 mm.
	H. 29	+0·004 mm.
	H. 36	−0·011 mm.
60% Ni, 40% Cu	H. 23	+0·002 mm.
	H. 27	−0·001 mm.
		Mean.. 0·000 mm.
Radiometal	H. 11	−0·009 mm.
	H. 19	−0·002 mm.
	H. 39	+0·007 mm.
		Mean.. −0·001 mm.
Mumetal	H. 10	−0·001 mm.
	H. 22	+0·011 mm.
		Mean.. +0·005 mm.

(0·01 mm.=0·82 volts). The only Cu–Ni plate showing a serious difference is H. 36 (−0·011 mm.). This plate is the weakest of the whole series and the difference depends on a doubtful extrapolation of the curve.

For Radiometal the mean difference from the nickel curve is again small. For Mumetal we have only two plates. One of these shows the large difference of +0·011 mm., but as the other plate agrees well with the curve, there is no evidence of the shift being real.

We have also measured the Lα-line of copper on the Cu–Ni alloy plates, and have compared it with the line from commercial copper. In addition to some more

intense plates, we have six with line blackenings between 0·034 and 0·076. Their measurements are as follows :—

Cu–Ni alloys, 45% Ni, 55% Cu	15·648 and 15·643 mm.	
60% Ni, 40% Cu	15·653 and 15·657 mm.	Mean 15·650 mm.
Cu	15·650 and 15·655 mm.	Mean 15·653 mm.

(Standard error of measurement $\pm 0{\cdot}004$ mm. Dispersion 0·01 mm. $=0{\cdot}0135$ Å$=0{\cdot}94$ volts.)

The two measurements for 45 per cent. Ni, 55 per cent. Cu, both yield values less than those of copper, but these two plates have the lowest intensity of the six, and, as the nickel curve indicates, low intensity leads to low measurements. For Cu Lα, as for Ni Lα, we thus find no evidence of a shift, but, to obtain a similar precision, a curve for copper similar to that for nickel would be required.

Discussion.

Just as the experiments of Privault * showed that the values of the M-levels of a ferromagnetic element are not affected by the application of a magnetic field, and those of Privault and of Chalklin † show no variation with temperature, so, in the present experiments, is there no evidence of a change of the $M_{IV,V}$ level of nickel when the magnetic condition is altered by alloying with another metal. Further, the experiments of Thoraeus ‡ and of Shearer § on Ni Lα for nickel compounds with the high dispersion and resolution of the crystal spectrograph, show only small effects. On the other hand, the hard X-ray work of Parratt || on the widths at half maximum intensity of $K\alpha_1(L_{III}–K)$ and $K\alpha_2(L_{II}–K)$ for a number of alloys, demonstrates that alloying may affect quite deep levels. His Ni-lines in a Mn-Ni alloy of 60 per cent. (atomic) Mn are widened by 0·06 X.U. (0·27 volts), although the Ni L_{II} and L_{III} levels are at depths of 877 and 859 volts. The Mn lines for various concentrations show a broadening rising to 0·26 X.U. (0/73 volts)

* *Loc. cit.*

† *Loc. cit.*

‡ Phil. Mag. ii. p. 1007 (1926). A splitting of the line is observed for Ni_2O_3.

§ Phil. Mag. xx. p. 504 (1935). The line is found not to shift, but the satellite structure changes.

|| Phys. Rev. xlv. p. 364 (1934).

for α_1 and 0·18 X.U. (0·50 volts) for α_2 for an atomic percentage of 50 of Mn.

There has recently appeared a paper by Saur * in which he describes crystal spectrograph experiments the structure of Lα for Cu and Ni in some compounds and alloys. The satellites † of Cu Lα do not move, but changes are observed in their intensities. For a Cu–Ni alloy he finds the width of Cu Lα to be 0·4 volts greater than for pure copper. For Ni Lα no appreciable change in structure or width is found ‡.

We have been testing a concave grating spectrograph of new design which should increase our dispersion and resolution. It is proposed to employ this in further alloy studies, mainly in the field of longer wave-lengths, in which the voltage accuracy becomes greater and in which the crystal spectrograph cannot be employed.

We wish to thank the Government Grants Committee of the Royal Society for a grant to one of us (F. C. C.) with the aid of which much of our apparatus was constructed. Finally, it is a pleasure to thank Prof. E. N. da C. Andrade for departmental facilities and for his continued interest and encouragement.

XVI. *Transformation Formulæ of Impedances and Admittances in the Method of Symmetrical Coordinates.* *By* S. Koizumi, *Assistant Professor of the Waseda University, Tokyo* §.

§ 1. *Introduction.*

IN the method of symmetrical coordinates, which was first established by Dr. C. L. Fortescue ‖ in 1918, the ordinary current and voltage of a multiphase system are transformed into symmetrical components by the "sequence operator."

* *Zeits. f. Phys.* ciii. p. 421 (1936).

† Not resolved with our apparatus.

‡ Hayasi, in some recent experiments on the K-absorption spectra of nickel and copper (*Sci. Rep. Tohoku Imp. Univ.* xxv. p. 598 and p. 606 (1936), has found the character of the main nickel edge altered in two inter-metallic compounds, but, for two Cu–Ni alloys, has found the Cu and Ni edges unaffected.

§ Communicated by the Author.

‖ C. L. Fortescue: "Method of Symmetrical Coordinates applied to the Solution of Polyphase Networks," Trans. A. I. E. E. vol. xxxvii. pl. ii. pp. 1027–1140 (1918).

Fortescue's idea of this sequence operator is, I think, the same as that of matrix treatment of the problem, in the mathematical point of view, though he did not use the word "matrix." And it may not violate his beautiful results to rewrite them in the matrix forms.

Now let S be the matrix of which rows consist of the sequence operators, that is,

$$S = \begin{bmatrix} S_0 \\ S_{-1} \\ S_{-2} \\ \vdots \\ S_{-(n-1)} \end{bmatrix} = S', \quad . \quad . \quad . \quad . \quad . \quad (1)$$

where S' is the transposed matrix of S.

The S_{-r} is the same as Fortescue's S^r and

$$S_{-r} = (1, a^{-r}, a^{-2r} \ldots, a^{-(n-1)r}), \quad . \quad . \quad . \quad (2)$$

where $$a = e^{j\frac{2\pi}{n}}.$$

Let the ordinary current and voltage of n-phase system be also written in the following matrix forms:

$$I = \begin{bmatrix} I_1 \\ I_2 \\ \vdots \\ I_n \end{bmatrix}; \qquad E = \begin{bmatrix} E_1 \\ E_2 \\ \vdots \\ E_n \end{bmatrix}. \quad . \quad . \quad . \quad (3)$$

Then we have, with Fortescue, as the symmetrical components of the current and voltage,

$$I_s = S^{-1} I; \qquad E_s = S^{-1} E, \quad . \quad . \quad . \quad . \quad (4)$$

and $$I = S I_s; \qquad E = S E_s, \quad . \quad . \quad . \quad . \quad (5)$$

where S^{-1} is the inverse matrix of S, and denoting the conjugate matrix by $\bar{S}$, we obtain readily the following:

$$S^{-1} = \frac{1}{n} \bar{S}, \quad . \quad . \quad . \quad . \quad . \quad . \quad . \quad (6)$$

where $$\bar{S} = \begin{bmatrix} S_0 \\ S_1 \\ S_2 \\ \vdots \\ S_{n-1} \end{bmatrix} \quad . \quad . \quad . \quad . \quad . \quad . \quad . \quad . \quad (7)$$

As the results of (4) or (5), the transformation formulæ of impedances Z_s and admittances Y_s in the symmetrical coordinates will be written in the following forms :

$$\left.\begin{aligned} Z_s &= S^{-1}ZS = \frac{1}{n}\bar{S}ZS, \\ Z &= SZ_sS^{-1} = \frac{1}{n}SZ_s\bar{S}. \end{aligned}\right\} \quad \ldots \ldots \quad (8)$$

$$\left.\begin{aligned} Y_s &= S^{-1}YS = \frac{1}{n}\bar{S}YS, \\ Y &= SY_sS^{-1} = \frac{1}{n}SY_s\bar{S}. \end{aligned}\right\} \quad \ldots \ldots \quad (9)$$

Additionally, the transformation of the power is as follows :

$$\begin{aligned} P &= I'\bar{E} = (SI_s)'(\bar{S}\bar{E}_s) \\ &= nI'_s\bar{E}_s = nP_s. \end{aligned}$$

Now the principal problem of this paper is involved in formulæ (8) or (9). The naive application of matrix multiplication, giving thoroughly satisfactory results in the case of (4) or (5), does not give practically convenient formulæ in the case of (8) or (9). Indeed, we have only the formula

$$n(Z_s)_{rt} = \sum_{k=1}^{n} \sum_{l=1}^{n} a^{(r-1)(k-1)-(l-1)(t-1)} Z_{kl},$$

as for the r-th row, t-th column element of the matrix Z_s.

In the following articles, it is reported that starting from (8) and (9), we can introduce practically convenient transformation formulæ of impedances and admittances, by means of a system of the analytical manipulation of the matrix S and the sequence operator S_r.

§ 2. σ-ρ *Operation of the Matrix* S.

It is evident that when a given permutation of $(1, 2, 3, \ldots., n)$ is impressed on the columns of a matrix P, and the same permutation is impressed on the rows of another matrix Q, then the product PQ remains unchanged under the above permutation.

Let us denote by $\sigma_m P$ the matrix derived from P by subjecting the columns of P to the permutation,

$$\begin{pmatrix} 1, 2 & & n-1, n \\ m+1, m+2\ldots, n, & 1, 2\ldots m \end{pmatrix},$$

and by $\rho_m P$ the matrix derived from P by subjecting the rows of P to the same permutation.

Then we have, from the above,

$$(\sigma_m P)(\rho_m C) = PQ, \quad . \quad . \quad . \quad . \quad . \quad (10)$$

Also it is obvious that

$$(\rho_m P)Q = \rho_m(PQ)\,; \qquad P(\sigma_m Q) = \sigma_m(PQ). \quad . \quad (11)$$

Further, from the definition of the operations,

$$\sigma_l(\sigma_m P) = \sigma_{l+m} P = \sigma_m(\sigma_l P), \quad . \quad . \quad . \quad (12)$$

$$\sigma_n P = \sigma_0 P = P, \quad . \quad . \quad . \quad . \quad . \quad (13)$$

$$\sigma_{m+n} P = \sigma_m P. \quad . \quad . \quad . \quad . \quad . \quad . \quad (14)$$

Also, we have, by (10),

$$(\sigma_l(\sigma_m P))(\rho_l Q) = (\sigma_m P)Q,$$

and so, by (12),

$$(\sigma_{l+m} P)(\rho_l Q) = (\sigma_m P)Q.$$

Hence, if $l = -m$, we get finally, by (13),

$$(\sigma_m P)Q = P(\rho_{-m} Q). \quad . \quad . \quad . \quad . \quad . \quad . \quad (15)$$

The formulæ (12)–(14) hold true when σ is replaced by ρ.

In case the matrix P is a sequence operator, we have, by (2),

$$\begin{aligned} \sigma_1 S_r &= \sigma_1(1, a^r, a^{2r}\ldots, a^{(n-1)r}) \\ &= (a^r, a^{2r}, \ldots, a^{(n-1)r}, 1) \\ &= a^r S_r. \end{aligned}$$

Thus, in general, $\qquad \sigma_m S_r = a^{mr} S_r. \quad . \quad . \quad . \quad . \quad . \quad . \quad . \quad (16)$

§ 3. *Diagonal Form of a Vector.*

Let H be a vector of which components are $h_1, h_2, \ldots, h_n$, that is,

$$H = \begin{bmatrix} h_1 \\ h_2 \\ \vdots \\ h_n \end{bmatrix}.$$

We define the diagonal form of the vector H as the diagonal matrix,

$$\begin{bmatrix} h_1 & 0 & \cdots & 0 \\ 0 & h_2 & & \vdots \\ \vdots & & \ddots & \vdots \\ \vdots & & \ddots & 0 \\ 0 & \cdots & 0 & h_n \end{bmatrix},$$

and denote this by $dg\,\mathrm{H}$.

When B is another vector such that

$$\mathrm{B} = \begin{bmatrix} b_1 \\ b_2 \\ \vdots \\ b_n \end{bmatrix},$$

then we obtain the following relation,

$$dg\,\mathrm{H}\,.\,\mathrm{B} = dg\,\mathrm{B}\,.\,\mathrm{H}, \quad . \quad . \quad . \quad . \quad . \quad (17)$$

since

$$dg\,\mathrm{H}.\mathrm{B} = \begin{bmatrix} h_1\,b_1 \\ h_2\,b_2 \\ \vdots \\ h_n\,b_n \end{bmatrix}.$$

Next, let A be a matrix of which columns consist of vectors $\mathrm{B}_1, \mathrm{B}_2, \ldots, \mathrm{B}_n$,

$$\mathrm{A} = (\mathrm{B}_1, \mathrm{B}_2, \ldots, \mathrm{B}_n),$$

then we define, extending the notion of the diagonal form of a vector, the following:

$$dg\,\mathrm{A} = (dg\,\mathrm{B}_1, dg\,\mathrm{B}_2 \ldots, dg\,\mathrm{B}_n). \quad . \quad . \quad . \quad (18)$$

From this definition and (17), it follows that

$$\begin{aligned} dg\,\mathrm{H}\,.\,\mathrm{A} &= (dg\,\mathrm{H}\,.\,\mathrm{B}_1, dg\,\mathrm{H}\,.\,\mathrm{B}_2 \ldots, dg\,\mathrm{H}\,.\,\mathrm{B}_n), \\ &= (dg\,\mathrm{B}_1.\mathrm{H}, dg\,\mathrm{B}_2.\mathrm{H} \ldots, dg\,\mathrm{B}_n.\mathrm{H}). \quad . \quad (19) \end{aligned}$$

Now, when a matrix P can be partitioned into sub-matrices of l-columns and Q is a matrix of l-rows, we define a new kind of matrix multiplication, denoting it, in order to be distinct from the ordinary matrix product and direct product, by a symbol, $\circ$, such that

$$\begin{aligned} \mathrm{P} \circ \mathrm{Q} &= (\mathrm{P}_1, \mathrm{P}_2 \ldots, \mathrm{P}_n) \circ \mathrm{Q}, \\ &= (\mathrm{P}_1\mathrm{Q}, \mathrm{P}_2\mathrm{Q} \ldots, \mathrm{P}_n\mathrm{Q}), \end{aligned}$$

where each P_r is a matrix of l-columns.

Following this definition, we have, by (19),

$$dg\,\mathrm{H}.\mathrm{A}=(dg\,\mathrm{A})\circ\mathrm{H}=dg\mathrm{A}\circ\mathrm{H}. \quad . \quad . \quad . \quad (20)$$

Moreover, it will be verified readily that there exists the following associative law:

$$\mathrm{T}(\mathrm{P}\circ\mathrm{Q})=(\mathrm{TP})\circ\mathrm{Q},$$

provided that the matrix product TP is not trivial, that is to say the number of columns in T is equal to the number of rows in P.

Hence, if T and A are square matrices of order n and Q is a vector H of n rows, we have

$$\mathrm{T}(dg\,\mathrm{A}\circ\mathrm{H})=(\mathrm{T}\,dg\,\mathrm{A})\circ\mathrm{H} \quad . \quad . \quad . \quad . \quad (21)$$

Further, when we partition T into n-matrices of a single row,

$$\mathrm{T}=\begin{bmatrix}\mathrm{T}_1\\ \vdots\\ \mathrm{T}_n\end{bmatrix},$$

the (rt)th element in $\mathrm{T}\,dg\,\mathrm{A}\circ\mathrm{H}$ will be written as follows:

$$(\mathrm{T}\,dg\,\mathrm{A}\circ\mathrm{H})_{rt}=(\mathrm{T}\,dg\,\mathrm{A})_{(rt)}.\mathrm{H}, \quad . \quad . \quad . \quad (22)$$

where $(\mathrm{T}\,dg\,\mathrm{A})_{(rt)}$ denotes the (rt)th submatrix of $\mathrm{T}\,dg\,\mathrm{A}$ under the above partition, that is,

$$\mathrm{T}_r\,dg\,\mathrm{B}_t.$$

On the other hand, since we have from (1)

$$\mathrm{S}=\mathrm{S}'=(\mathrm{S}'_0,\ \mathrm{S}'_{-1}\ldots,\ \mathrm{S}'_{-(n-1)}),$$

$$dg\,\mathrm{S}=(dg\,\mathrm{S}'_0,\ dg\,\mathrm{S}'_{-1}\ldots,\ dg\,\mathrm{S}'_{-(n-1)}),$$

and by (2),

$$\mathrm{S}_m\,dg\,\mathrm{S}'_l=\mathrm{S}_{m+l}, \quad . \quad . \quad . \quad . \quad . \quad . \quad (23)$$

so we obtain

$$(\bar{\mathrm{S}}\,dg\,\mathrm{S})_{(rt)}=\mathrm{S}_{r-1}\,dg\,\mathrm{S}'_{-(t-1)}=\mathrm{S}_{r-t}. \quad . \quad . \quad (24)$$

Also, since, by (16),
rth row of

$$(\sigma_m\bar{\mathrm{S}})=\sigma_m\mathrm{S}_{r-1}=a^{m(r-1)}\mathrm{S}_{r-1},$$

we see, by (24),

$$(\sigma_m\mathrm{S}.dg\,\mathrm{S})_{(rt)}=a^{m(r-1)}\mathrm{S}_{r-t} \quad . \quad . \quad . \quad (25)$$

§ 4. *Decomposition of the Matrix Z.*

Let the impedance matrix Z be

$$Z = \begin{bmatrix} Z_{11} & Z_{12} \cdots & Z_{1n} \\ Z_{21} & Z_{22} \cdots & Z_{2n} \\ \vdots & & \vdots \\ Z_{n1} & \cdots\cdots & Z_{nn} \end{bmatrix},$$

then we can decompose Z into A_m as follows:

$$Z = \sum_{m=0}^{n-1} A_m, \quad \ldots \ldots \quad (26)$$

where

$$A_m = \begin{bmatrix} 0 & \cdots\cdots & 0 & Z_{1,\,n-m+1} & \cdots & 0 \\ \vdots & & & & \ddots & \vdots \\ 0 & & & & & Z_{m,\,n} \\ Z_{m+1,\,1} & & & & & \vdots \\ \vdots & Z_{m+2,\,2} & & & & \vdots \\ \vdots & & \ddots & & & \vdots \\ 0 & \cdots\cdots & Z_{n,\,n-m} & \cdots\cdots & & 0 \end{bmatrix}.$$

If we impress the operation ρ_m of the article 2 on this A_m, we obtain

$$\rho_m A_m = \begin{bmatrix} Z_{m+1,\,1} & & & & & & \\ & Z_{m+2,\,2} & & & & & \\ & & \ddots & & & & \\ & & & Z_{n,\,n-m} & & & \\ & & & & Z_{1,\,n-m+1} & & \\ & & & & & \ddots & \\ & & & & & & Z_{m,\,n} \end{bmatrix},$$

and so

$$\rho_m A_m = dg\, H_{m+1,\,1}, \quad \ldots \ldots \quad (27)$$

where

$$H_{m+1,\,1} = \begin{bmatrix} Z_{m+1,\,1} \\ Z_{m+2,\,2} \\ \vdots \\ Z_{n,\,n-m} \\ Z_{1,\,n-m+1} \\ \vdots \\ Z_{m,\,n} \end{bmatrix} \quad \ldots \ldots \quad (28)$$

Also, it follows from (28) that

$$\rho_m \mathrm{H}_{r,t} = \mathrm{H}_{r+m,\, t+m}. \quad . \quad . \quad . \quad . \quad (29)$$

N.B.—In Z_{rt} or H_{rt}, when $r=n+l$, l being a positive integer, l should be taken for r; and when $r=-l$, $n-l$ should be taken for r. Also as for t, the same is the case.

§ 5. *Transformation Formulæ of Impedances and Admittances.*

Now the transformation formulæ for impedances and admittances can be given in practical forms, by virtue of the preceding preliminary articles.

We have, by (26),

$$\bar{\mathrm{S}}\mathrm{ZS} = \bar{\mathrm{S}} \sum_{m=0}^{n-1} \mathrm{A}_m \mathrm{S};$$

however, since, by (10), (11), and (27),

$$\begin{aligned} \bar{\mathrm{S}}\mathrm{A}_m \mathrm{S} &= (\sigma_m \bar{\mathrm{S}})(\rho_m \mathrm{A}_m)\mathrm{S} \\ &= (\sigma_m \bar{\mathrm{S}})\, dg\, \mathrm{H}_{m+1,1} . \mathrm{S}, \end{aligned}$$

and so, by (20) and (21),

$$\bar{\mathrm{S}}\mathrm{ZS} = \sum_{m=0}^{n-1} (\sigma_m \bar{\mathrm{S}})\, dg\, \mathrm{S} \circ \mathrm{H}_{m+1,1}.$$

Thus we obtain, by (22) and (25),

$$(\bar{\mathrm{S}}\mathrm{ZS})_{rt} = \sum_{m=0}^{n-1} a^{m(r-1)} \mathrm{S}_{r-t} . \mathrm{H}_{m+1,1}, \quad . \quad . \quad (30)$$

and so we get, by (8), as for the (rt)th symmetrical component of the impedance,

$$(\mathrm{Z}_s)_{rt} = \frac{1}{n} \mathrm{S}_{r-t} \sum_{m=0}^{n-1} a^{m(r-1)} \mathrm{H}_{m+1,1}. \quad . \quad . \quad . \quad (31)$$

Generally in practice, further reduced formulæ, which will be seen in the following lines, may be prevailing; nevertheless, it is considered opportune to introduce the fundamental equation in the steady state of the symmetrical n-phase alternator with uniform air gap, as an example of the application of (31).

Let V and E be respectively the matrices of the terminal voltage and induced voltage of the alternator; and let I be the matrix of the phase current; also, let Z be the impedance matrix of the alternator. Then we have

$$\mathrm{V} = \mathrm{E} - \mathrm{ZI},$$

and so

$$S^{-1}V = S^{-1}E - S^{-1}ZSS^{-1}I\,;$$

thus, by (4) and (8),

$$V_s = E_s - Z_s I_s.$$

However, since elements of A_m of Z are all the same by means of the symmetry of the structure of the alternator, we have

$$S_{r-t}H_{m+1,1}\begin{cases} 0, & \text{if} \quad r \neq t \\ nh_{m+1,1}, & \text{if} \quad r = t \end{cases}$$

and so, by (31),

$$(Z_s)_{rt} = Z_{srt} = 0, \quad \text{if} \quad r \neq t,$$

$$Z_{srr} = \sum_{m=0}^{n-1} a^{m(r-1)} h_{m+1,1}. \quad . \quad . \quad . \quad . \quad (32)$$

On the other hand, since

$$E = \begin{bmatrix} E_a \\ a^{-1}E_a \\ \vdots \\ a^{-(n-1)}E_a \end{bmatrix},$$

and so we have

$$E = \begin{bmatrix} 0 \\ E_a \\ 0 \\ \vdots \\ 0 \end{bmatrix}.$$

Thus we get, finally,

$$V_s = \begin{bmatrix} 0 \\ E_a \\ 0 \\ \vdots \\ 0 \end{bmatrix} - \begin{bmatrix} Z_{s11} & & & \\ & Z_{s22} & & \\ & & \ddots & \\ & & & Z_{snn} \end{bmatrix} I_s. \quad . \quad (33)$$

Now, returning to the main problem, let us consider further reductions of (31).

If n is odd, we have, generally,

$$\sum_{m=1}^{n-1} C_m = \sum_{m=1}^{\frac{n-1}{2}} (C_m + C_{n-m})\,;$$

however, since, in (31),

$$C_m = a^{m(r-1)} S_{r-t} H_{m+1,1},$$

and so

$$C_{n-m} = a^{(n-m)(r-1)} S_{r-t} H_{n-m+1,1}$$
$$= a^{-m(t-1)} a^{-m(r-t)} S_{r-t} H_{-m+1,1}.$$

Then, by (16),

$$C_{n-m} = a^{-m(t-1)} (\sigma_{-m} S_{r-t}) H_{-m+1,1},$$

which will be written, by (15), as

$$C_{n-m} = a^{-m(t-1)} S_{r-t} \rho_m H_{-m+1,1}.$$

Thus we get, by (29),

$$C_{n-m} = a^{-m(t-1)} S_{r-t} H_{1,m+1}.$$

Hence, we have, finally, when n is odd,

$$n(Z_s)_{rt} = S_{r-t} H_{1,1} + S_{r-t} \sum_{m=1}^{\frac{n-1}{2}} \{a^{m(r-1)} H_{m+1,1} + a^{-m(t-1)} H_{1,m+1}\}. \quad (34)$$

Especially, if Z is symmetric, that is $Z' = Z$, since

$$H_{m+1,1} = H_{1,m+1},$$

and so

$$n(Z_s)_{rt} = S_{r-t} H_{1,1} + S_{r-t} \sum_{m=1}^{\frac{n-1}{2}} (a^{m(r-1)} + a^{-m(t-1)}) H_{1,m+1}. \quad (35)$$

E.g., if $n=3$, $r=1$, $t=2$, from (35),

$$3(Z_s)_{12} = S_2 H_{1,1} + S_2(a^0 + a^{-1}) H_{1,2},$$

but, since, by (28),

$$H_{1,1} = \begin{bmatrix} Z_{11} \\ Z_{22} \\ Z_{33} \end{bmatrix} ; \quad H_{1,2} = \begin{bmatrix} Z_{12} \\ Z_{23} \\ Z_{31} \end{bmatrix},$$

we have

$$3(Z_s)_{12} = (Z_{11} + a^2 Z_{22} + a Z_{33}) - a(Z_{12} + a^2 Z_{23} + a Z_{31})$$
$$= (Z_{11} + a^2 Z_{22} + a Z_{33}) - (Z_{23} + a^2 Z_{31} + a Z_{12}).$$

On the other hand, *if n is even*, since

$$\sum_{m=1}^{n-1} C_m = C_{\frac{n}{2}} + \sum_{m=1}^{\frac{n-2}{2}} (C_m + C_{n-m}),$$

we can reduce similarly (31) as follows:

$$n(Z_s)_{rt}=S_{r-t}H_{1,1}+S_{r-t}a^{\frac{n}{2}(r-1)}H_{\frac{n}{2}+1,1}$$
$$+S_{r-t}\sum_{m=1}^{\frac{n-2}{2}}\{a^{m(r-1)}H_{m+1,1}+a^{-m(t-1)}H_{1,m+1}\}. \quad . \quad (36)$$

Moreover, in case $Z'=Z$,

$$n(Z_s)_{rt}=S_{r-t}H_{1,1}+S_{r-t}a^{\frac{n}{2}(r-1)}H_{\frac{n}{2}+1,1}$$
$$+S_{r-t}\sum_{m=1}^{\frac{n-2}{2}}(a^{m(r-1)}+a^{-m(t-1)})H_{1,m+1}. \quad . \quad . \quad . \quad . \quad (37)$$

e.g., if $n=4$, $r=4$, $t=1$, by (37),

$$4(Z_s)_{41}=S_3H_{1,1}+S_3a^{2\cdot 3}H_{3,1}+S_3(a^3+a^0)H_{1,2}$$
$$=S_3H_{11}-S_3H_{31}+S_3(1-j)H_{12}.$$

Now, since

$$S_3=(1,\ a^3,\ a^2,\ a)$$
$$=(1,\ -j,\ -1,\ j),$$

and that

$$H_{11}=\begin{bmatrix}Z_{11}\\Z_{22}\\Z_{33}\\Z_{44}\end{bmatrix};\quad H_{31}=\begin{bmatrix}Z_{31}\\Z_{42}\\Z_{13}\\Z_{24}\end{bmatrix};\quad H_{12}=\begin{bmatrix}Z_{12}\\Z_{23}\\Z_{34}\\Z_{41}\end{bmatrix},$$

so we have

$$4(Z_s)_{41}=(Z_{11}-jZ_{22}-Z_{33}+jZ_{44})-(Z_{31}-jZ_{42}-Z_{13}+jZ_{24})$$
$$+(1-j)(Z_{12}-jZ_{23}-Z_{34}+jZ_{41}).$$

Inversely, since, by (8),

$$n(Z)_{rt}=(SZ_s\bar{S})_{rt},$$

taking the conjugates of S_{r-t} and a^p in (34) and (36), we get readily,

(n: odd)

$$nZ_{rt}=S_{-r+t}H_{(s)1,1}$$
$$+S_{-r+t}\sum_{m=1}^{\frac{n-1}{2}}\{a^{-m(r-1)}H_{(s)m+1,1}+a^{m(t-1)}H_{(s)1,m+1}\},\quad (38)$$

(n: even)

$$nZ_{rt}=S_{-r+t}H_{(s)1,1}+S_{-r+t}a^{-\frac{n}{2}(r-1)}H_{(s)\frac{n}{2}+1,1}$$

$$+S_{-r+t}\sum_{m=1}^{\frac{n-2}{2}}\{a^{-m(r-1)}H_{(s)m+1,1}+a^{m(t-1)}H_{(s)1,m+1}\}, \quad . \quad (39)$$

where $H_{(s)r,t}$ is to Z_s what $H_{r,t}$ is to Z.

Furthermore, comparing (8) with (9), we can see at once that the transformation formulæ for the admittance are entirely similar to the transformation formulæ for the impedance, and so, by virtue of (34)–(39), we can write down readily the transformation formulæ of admittances in the practical forms.

XVII. *On the Determination of an Integral.*

To the Editors of the Philosophical Magazine.

Gentlemen,—

I HAVE determined that the integral

$$\int_0^\infty \frac{\epsilon^{-px^2}}{1+x^2}dx=\frac{\pi}{2}\epsilon^p \operatorname{erfc}(\sqrt{p}),$$

where

$$\operatorname{erfc}(x)=\frac{2}{\sqrt{\pi}}\int_x^\infty \epsilon^{-x^2}dx.$$

Bierens de Haan, however, in table 91, formula 13, gives the value as a complicated expression involving the square root of a double summation. In the 70 years since the publication of the Bierens de Haan tables this simpler result may have been discovered, but, so far as I have been able to determine, there is no way of knowing this. Accordingly I am stating the result and giving the proof, as it should be a matter of record. Of course in the absence of any modern comprehensive compilation of definite integrals this same result may be rediscovered at any later date.

Denoting the integral by J(p), we can define a new function K(p) as

$$K(p)=Je^{-p}=\int_0^\infty \frac{\epsilon^{-p(1+x^2)}}{1+x^2}dx,$$

whence

$$\frac{dK}{dp} = -\epsilon^{-p}\int_0^\infty \epsilon^{-px^2}\,dx = -\frac{\sqrt{\pi}}{2\sqrt{p}}\,\epsilon^{-p}.$$

Since, by inspection,

$$K(\infty)=0,$$

it follows that

$$K = -\int_p^\infty \frac{dK}{dp}\,dp = \frac{\sqrt{\pi}}{2}\int_p^\infty \frac{\epsilon^{-p}dp}{\sqrt{p}} = \frac{\pi}{2}\,\mathrm{erfc}\,(\sqrt{p}),$$

leading immediately to the above-stated result.

Yours faithfully,

LEWI TONKS.

General Electric Company Research Laboratory,
1 River Road, Schenectady, N.Y.
April 7, 1937.

XVIII. *Notices respecting New Books.*

Properties of Matter. By F. C. CHAMPION and N. DAVY. (Vol. III. of 'The Students' Physics.') [Pp. xiv+296.] (Blackie & Sons, 1936.)

IN writing a new text-book on 'Properties of Matter' the authors have been guided in their selection of material by the desire to treat the matters considered from the physical point of view rather than as exercises in applied mathematics. Bearing this in mind, little exception to the authors' choice can be taken. Their clear and concise style has made it possible to deal adequately with most of the topics one would expect to find, within the reasonable compass of 274 pages, although possibly " capillarity " receives rather more than its due share of space.

Recent work is given due prominence, but important classical experimental methods are not omitted on this account. In addition to what may be regarded as standard topics, there are others which should be mentioned. The chapter on the acceleration due to gravity includes an account of the theory and use of the Eötvös torsion balance, and later there is a chapter on seismic waves which concludes with a paragraph on geophysical prospecting. This might well be expanded somewhat.

Surface films receive a chapter and the Debye-Hückel theory of strong electrolytes finds a deserved place in the

account of osmotic pressure. Some description of the production and measurement of low pressure is included in the chapter on kinetic theory.

This is a welcome addition to the 'Students' Physics' Series, and physics students should find it a useful and helpful book.

Relativity Theory of Protons and Electrons. By Sir A. S. EDDINGTON, F.R.S. [Pp. viii+336.] (Cambridge University Press, 1936. Price 21*s*. net.)

SIR A. S. EDDINGTON's unification of quantum theory and general relativity is based on a generalization of quantum mechanics, the development of which at every stage is guided by the assumption that general relativity is true. Quantum theory therefore emerges profoundly modified, whilst general relativity is unaltered. Another fundamental axiom employed is that the "times" of the constituent particles of a system can be amalgamated so as to form a "common-time" whose "axis" is in the direction of the momentum vector of the system as a whole.

The physical consequences of the theory are found in the purely deductive values obtained for one or more of the constants of nature in terms of the others. The constants concerned are the masses and charges of protons and electrons, Planck's constant, the velocity of light, and the constant of gravitation. The guiding principle is that the relations between the constants arise from the possibility of describing the same physical state of affairs in different mathematical ways. Thus, "indistinguishability" of proton and electron in the wave-equation gives the value of the fine-structure constant; the amalgamation of a proton and an electron into a single mathematical system gives the ratio of the masses of these particles, etc. Finally, the comparison of the theory of the universe as worked out by generalized quantum theory and by general relativity, respectively, yields the number of particles in the universe.

In a deductive theory of this type attention is inevitably focussed on the fundamental axioms. These will, perhaps, not be acceptable to every physicist. But, granted Sir Arthur Eddington's premises, the theory is an astonishing feat of reasoning, which gives promise of opening up a whole new branch of physical theory.

[*The Editors do not hold themselves responsible for the views expressed by their correspondents.*]